Cooling for Comfort, Warming the World

Residential and Office Cooling and its Environmental Implications in The Hague

by

Simon N. van Lierde

Student number Leiden University: s2291053

Student number Delft University of Technology: 4986792

A master's thesis

Submitted to the **Institute of Environmental Sciences**

Leiden University

In partial fulfillment of the requirements

For the degree of **Master of Science** in **Industrial Ecology**

January 2024

Supervised by prof.ir. Peter Luscuere and dr. Benjamin Sprecher

Abstract

Despite The Hague's historically mild climate, it is experiencing rising temperatures and more frequent heatwaves, resulting in a growing demand for space cooling. However, there is a significant gap in research and sustainable policies to address this demand in an environmentally and socially responsible manner. While studies have examined the environmental impacts of residential heating, cooling still is understudied, and The Hague lacks sustainable cooling policies.

This study projects cooling demand, energy consumption, material usage, and greenhouse gas emissions in The Hague for the status quo (2020), 2030, and three 2050 scenarios. It uses geospatial analysis of residential and office buildings and uses a thermodynamic model to calculate cooling demand in a bottom-up approach, before evaluating the aggregate environmental impacts. Despite offices accounting for only 13% of floor space, they contribute to 34% of present-day cooling demand and 65% of associated greenhouse gas emissions. Currently, space cooling accounts for 25% of annual office electricity consumption and 5.5% of residential electricity use. Moreover, 77% of cooling demand stays unmet, particularly affecting economically disadvantaged neighborhoods.

The results suggest that adopting stringent climate change adaptation measures may reduce cooling demand and environmental impacts, even in the face of a warming climate. However, a business-as-usual scenario predicts a doubling of cooling demand and a significant rise in associated environmental impacts, challenging the Netherlands' goal of achieving net-zero emissions by 2050.

Sensitivity analyses highlight key areas for The Hague to focus on, including thermal comfort standards, addressing the urban heat island effect, and improving the energy efficiency of cooling technologies. The study further offers recommendations to mitigate environmental impacts, such as minimum energy label standards for building renovations and promoting circular economy practices for cooling equipment.

In conclusion, this study underscores the need to address space cooling in The Hague and the Netherlands. Without action, environmental impacts will worsen the effects of climate change. To tackle this challenge, the study recommends prioritizing energy-efficient cooling technologies, using synergies between sustainable heating and cooling, and incorporating environmental justice into policy measures. This is the path towards securing a sustainable and cooler future for The Hague.

Acknowledgements

I am grateful to my thesis supervisors, Benjamin Sprecher and Peter Luscuere, for their guidance, expertise, and patience. Your support has been fundamental in shaping this work.

A special thanks to Joris, whose mentorship, although not directly connected to my thesis, was crucial in guiding me to the finish line.

To my friends and family, particularly my parents and sister, your love and support have been the bedrock of my strength. You have been integral to my journey, and for that I am deeply grateful.

Finally, to Audrey, my haven of support – your advice, motivation, and love have been the backbone of this journey. Your presence has been the driving force behind this achievement; I truly could not have done this without you. For this, I am forever grateful to you.

Table of Contents

List of Figures

List of Tables

List of Abbreviations

Abbreviation	Description
2050-L	The 2050 low-impact scenario
2050-M	The 2050 medium-impact scenario
2050-H	The 2050 high-impact scenario
AC	Air Conditioning / Air Conditioner
ACH	Air Change per Hour
ADP	Abiotic Resource Depletion
ASHP	Air-Source Heat Pump
ASHRAE	American Society of Heating, Refrigerating and Air Conditioning Engineers
ATES	Aquifer Thermal Energy Storage
ATG	Adaptive Temperature Limits (**A**daptieve **T**emperatuur**g**renswaarden)
BAG	Registry of Addresses and Buildings (Basisregistratie Adressen en Gebouwen)
CBAM	Carbon Border Adjustment Mechanism
CBS	Statistics Netherlands (Centraal Bureau voor de Statistiek)
CDM	Cooling Demand Model
CDD	Cooling Degree Day
CFC	**C**hloro**f**luoro**c**arbon
CML	Institute of Environmental Sciences (**C**entrum voor **Mi**lieuwetenschappen) at Leiden University
COP	Coefficient of Performance
CRM	Critical Raw Material
CSI	Crustal Scarcity Indicator
DSO	Department of Urban Development (Dienst Stedelijke Ontwikkeling) of The Hague
EEA	European Environment Agency
EER	Energy Efficiency Ratio
EIM	Environmental Impact Model
EoL	End-of-Life
ESEER	European Seasonal Energy Efficiency Ratio
ETS	Emissions Trading System
EU	European Union
GDP	Gross Domestic Product
GHG	**G**reen**h**ouse **G**as
GSHP	Ground-Source Heat Pump
GWP	Global Warming Potential
HCFC	**H**ydro**c**hloro**f**luoro**c**arbon
HFC	**H**ydro**f**luoro**c**arbon
HVAC	Heating, Ventilation, and Air Conditioning

IE	Industrial Ecology
IEA	International Energy Agency
IPCC	Intergovernmental Panel on Climate Change
ISSO	Dutch Knowledge Centre for the building and building services sector (**I**nstituut voor **S**tudie en **S**timulering van **O**nderzoek op het gebied van gebouwinstallaties)
KNMI	Royal Netherlands Meteorological Institute (Koninklijk Nederlands Meteorologisch Instituut)
LCA	Life Cycle Assessment
LCI	Life Cycle Inventory
LEED	Leadership in Energy and Environmental Design
MBR	Minimum Bounding Rectangle
MPR	Market Penetration Rate
MEPS	Minimum Energy Performance Standard
MLP	Multi-Level-Perspective
MPR	Market Penetration Rate
NEN	Royal Netherlands Standardization Institute (Nederlands Normalisatie Instituut)
NOS	Dutch Broadcasting Foundation (Nederlandse Omroep Stichting)
NTA	Dutch Technical Agreement (Nederlandse Technische Afspraak)
ODP	Ozone Depletion Potential
OECD	Organization for Economic Co-operation and Development
OEM	Original Equipment Manufacturer
PBL	Netherlands Environmental Assessment Agency (**P**lan**b**ureau voor de **L**eefomgeving)
PCM	Phase Change Material
PDOK	Public Services On the Map (Publieke Dienstverlening Op de Kaart)
PGM	Platinum Group Metal
PPP	Purchasing Power Parity
PRODCOM	European community production (**Prod**uction **Com**munautaire)
PV	**P**hotov**o**ltaic
REE	Rare Earth Element
RIVM	National Institute for Public Health and Environment (Rijksinstituut voor Volksgezondheid en Milieu)
RO	Residential and Office
RQ	Research Question
RVO	The Netherlands Enterprise Agency (Rijksdienst voor Ondernemend Nederland)
SER	Social and Economic Council of the Netherlands (Sociaal-Economische Raad)
SEER	Seasonal Energy Efficiency Ratio
SQ	Status Quo (the 2020 scenario)
SubUHI (effect)	**Sub**surface **U**rban **H**eat **I**sland (effect)

TNO	Netherlands Organization for Applied Scientific Research (Nederlandse organisatie voor **T**oegepast **N**atuurwetenschappelijk **O**nderzoek)
UHI (effect)	Urban Heat Island (effect)
UNEP	United Nations Environment Programme
UNFCCC	United Nations Framework Convention on Climate Change
USGBC	United States Green Building Council
WEEE	Waste from Electrical and Electronic Equipment
WHO	World Health Organization
WMO	World Meteorological Organization
WSHP	Water-Source Heat Pump

1 Introduction

With the last eight years being the hottest on record, the climate crisis is undeniable, and its impacts are becoming increasingly severe (Pörtner, Roberts, Poloczanska, et al., 2022; WMO, 2023). One such impact is the worldwide exponential rise in the demand for air conditioners (ACs) and other cooling equipment in homes and offices (L. W. Davis & Gertler, 2015; IEA, 2018a). This rise has several consequences, most importantly an increasing demand for energy (L. W. Davis & Gertler, 2015; Krayenhoff et al., 2021) and a rise in the amount of refrigerants released into the atmosphere (Calm, 2002; IEA, 2018a), both of which contribute to greenhouse gas (GHG) emissions and exacerbate the climate crisis. Furthermore, the rising demand for space cooling amplifies the global ecological crisis by increasing the need for equipment that uses critical raw materials (CRMs) and other metals, intensifying resource scarcity and causing ecosystem degradation through extensive mining (Heikkilä, 2004).

With operational energy use in buildings making up 40% of final global energy consumption (Nižetić et al., 2019), and space cooling accounting for approximately 20% of electricity use within buildings (Calm, 2002; IEA, 2018a), space cooling already takes up a significant part of the global energy system. The demand for cooling is projected to surge dramatically. By 2050, global energy consumption from space cooling could potentially triple (IEA, 2018a), with some projections suggesting a 20-fold increase (Santamouris & Vasilakopoulou, 2021). Such a rise will strain already vulnerable energy infrastructures globally (T. Peters, 2018). In addition, a rising energy demand is likely to increase local and global GHG emissions or at least inhibit efforts towards a low-carbon built environment. Residential and office (RO) cooling is of particular concern, given that they account for at least 70% of the expected rise in energy use from space cooling (Calm, 2002; IEA, 2018a). These concerns have sparked research into greener and more energy-efficient buildings, although more work is still to be done to curb energy demand from space cooling (Berardi & Jafarpur, 2020).

Besides the issue of energy, refrigerants exacerbate the contribution of active cooling technologies to climate change (Calm, 2002; IEA, 2018a). The most common refrigerants, hydrofluorocarbons (HFCs), have high global warming potentials (GWPs), exacerbating climate change when leaked into the atmosphere (Godwin & Ferenchiak, 2020). In the EU, an estimated 7% of refrigerants used in space cooling leak into the environment

annually (Schwarz & Harnisch, 2003). With the projected rise in space cooling demand, HFCs are anticipated to account for up to one-tenth of global GHG emissions by 2050 (Albà et al., 2021). Some studies even suggest that refrigerant leaks have the potential to exceed the entire 1.5 °C carbon budget unless HFCs are rapidly phased out on a global scale. (Dreyfus et al., 2020; Matthews et al., 2020).

Finally, the rising demand for space cooling has implications for material demand. The size of the global air conditioner stock is projected to more than triple from the current 1.6 billion to 5.6 billion units in 2050 (IEA, 2018b; T. Peters, 2018). This growth not only requires a substantial amount of materials such as steel, iron, and plastics but also raises concerns about CRMs, which are defined as strategically and economically important materials with high-risk supply chains (Ferro & Bonollo, 2019; Heikkilä, 2004). Copper, an instrumental material in air conditioning units, has limited stocks and its mining process has negative social and environmental implications.[1] As of 2017, copper used in cooling equipment was responsible for more than 10% of global copper use, a figure which is only expected to increase with rising cooling demand (DeWit, 2020).

While research has been performed on space cooling demand and its environmental impacts, it predominantly focused on warmer climates with historically higher cooling demands (Eveloy & Ayou, 2019; Lundgren & Kjellstrom, 2013). This leaves a research gap regarding the energy requirements and environmental consequences of cooling in temperate climates, which may become more relevant due to climate change. The climate policies of The Hague, the Netherlands, exemplify this gap. Despite the city's temperate climate, recent heat waves and projected temperature rises warrant consideration of space cooling in policymaking. While The Hague municipality has taken steps towards climate adaptation, energy transition, and Paris Agreement alignment, with an overarching goal to achieve carbon neutrality by 2040, it lacks a strategy for addressing space cooling and its impacts, which is essential for a resilient future (Motie "Vertaling Klimaatakkoord Parijs Naar Haagse Doelstellingen," 2016; 2015 Paris Agreement, 2015; The Hague Municipal Council, 2017). This makes The Hague as a suitable case study to

[1] Although not formally categorized as a critical raw material, copper is acknowledged as a *strategic raw material* by the European Union (EU) (Grohol & Veeh, 2023).

explore the environmental implications of space cooling in temperate cities facing global warming.

1.1 Case Study: The Hague

The Hague, a city in the western Netherlands with around 560,000 residents, has a temperate oceanic climate (type *Cfb* according to Köppen classification), featuring average temperatures of 18 °C in summer and 4 °C in winter (KNMI, 2023a). Due to this temperate climate, research and policy-making in the Netherlands and The Hague has primarily focused on space heating over space cooling (DSO, 2022).

However, the increasing frequency, length, and intensity of heat waves in recent years have raised concerns about heat stress. In response to a 2020 heatwave that caused over 650 deaths in the Netherlands, The Hague municipality introduced the "Haags Hitteplan" in 2021 (The Hague Municipality, 2021a). This plan focuses on safeguarding vulnerable groups during heatwaves, including the elderly, homeless, and those with pre-existing health conditions. While this plan is proactive in informing residents and designating adaptation strategies such as neighborhood cooling stations, there is little mention of the role of indoor space cooling equipment, whether it be as an adaptation strategy or a driver of environmental impacts (The Hague Municipality, 2021a).

Yet, the municipality of The Hague has focused on addressing heat stress through urban greening, as seen through the “Programma Klimaatbestendig”, a strategy for climate-proofing the city (Wijsmuller, 2015b). This strategy acknowledges the urban heat island (UHI) effect and plans for further research into its origins and consequences (Wijsmuller, 2015b). There are also plans to create more urban green spaces, with emphasis on the cooling effect they create (Wijsmuller, 2015a). However, regulations or ambitions on the amount or type of indoor space cooling are not included. In "The Hague Resilience Strategy," which outlines climate change adaptation plans, the need for cooling is mentioned primarily in the context of greening school yards, which are often heavily paved (The Hague Municipality, 2019). Furthermore, homeowners can receive a 50% cost reimbursement for installing green roofs, and future plans for nature-inclusive neighborhood redevelopment outlined in “De Stad Natuurlijk” (Barker, 2020; de Ruiter et al., 2019). While all these efforts are important for climate adaptation and mitigation, greater recognition and preparation for space cooling demand and its impacts is needed for resilience in the face of a changing climate.

In addition, The Hague recently published the "Transitievisie Warmte" and "Stedelijk Energieplan" reports to address environmental footprints of the built environment (DSO, 2022; The Hague Municipality, 2020). These documents outline goals to shift from natural gas to renewable energy in the coming years, primarily through the adoption of improved insulation and sustainable space heating technologies such as heat pumps and neighborhood heat districts (DSO, 2022). Notably, heat pumps have the potential to serve as efficient cooling systems, unlike heating networks that only provide space heating (IEA, 2018a). However, this necessitates the explicit consideration of space cooling in built environment policy and implementation. In contrast, current policies do not explicitly consider space cooling, potentially leading to an overabundance of heating technologies that lack cooling capabilities. This, in turn, may drive the installation of separate cooling devices like portable and split-type air conditioners, which are typically less integrated into the building envelope, resulting in lower energy and material efficiency and increased environmental impact. Given the share of residences with cooling equipment is projected to grow from 14% in 2022 to as much as 60% in 2050, addressing this issue is imperative (Hammingh et al., 2022).

Current plans call for transitioning at least half of all residences to low-carbon heating alternatives, like heat pumps and district heating, by 2030 (The Hague Municipal Council, 2017). Currently, only 7% of residential buildings (17,900 houses) meet this requirement. This leaves approximately 95,500 residences to be retrofitted with sustainable heating systems before 2030.[2]

Besides the ambitions set for residential buildings, all offices need to have at least a C energy label by 2023, according to the 2012 building code (Bouwbesluit, 2012). However, currently, only 69% of offices in The Hague comply with this condition.[3] The remaining 31%—159 offices spanning 31.45 hectares of floor space—require immediate renovation to meet the regulations set by the building code. These large-scale renovations provide a

[2] This does not consider the estimated 26,000–32,500 residences which are to be built in the 2017–2030 period, which already have to adhere to strict energy efficiency standards, including low-carbon heating systems (The Hague Municipal Council, 2017).

[3] Note that the 69% of office buildings that meet the label C or higher requirement are generally the larger, high-rise buildings. When looking at the total floor area, 91% of all office space in The Hague complies with the 2023 energy label regulation.

significant opportunity to incorporate low-carbon cooling technologies and cooling-efficient construction methods.

Nevertheless, although space cooling is mentioned as the second largest energy consumer in buildings after heating, there is little explicit mention of the role of cooling in the "Transitievisie Warmte" (DSO, 2022). In fact, the only reference to cooling is that insulation, a key recommendation, might increase the demand for space cooling.

In summary, while detailed sustainable heating policies and emergency heat wave response plans are in place, space cooling remains under-addressed in policy. This will lead to a missed opportunity for a holistic strategy – combining both space heating and cooling – for a resilient built environment.

1.2 Problem Statement

Considering the escalating global demand for space cooling driven by climate change and other factors, coupled with the associated adverse environmental impacts, there is a pressing need for comprehensive research on the future of space cooling. The projected exponential rise in cooling equipment within residential and office settings has far-reaching consequences including heightened energy consumption, greenhouse gas emissions, and resource depletion.

Despite these impacts, there is a knowledge gap on the extent of the future cooling demand and its environmental impacts, especially in temperate regions such as The Hague. While estimates project a 250% increase in cooling device installations globally and 70% increase in the EU by 2050, extensive research into the future demand and environmental impacts remain underdeveloped (IEA, 2018a). Surprisingly, there has been little comprehensive research on the projected cooling demand in the Netherlands or The Hague, despite the fact that the market penetration of air conditioning in the Netherlands has risen from 1.5% in 2000 to 30% in 2023 (NOS, 2023b; van Kempen, 2000). This highlights the need for targeted investigations to forecast and mitigate the projected rise in cooling demand in the Dutch context.

While studies exist on the environmental impacts of residential heating in the Netherlands, research on the impacts of space cooling is noticeably lacking (Gupta & Gregg, 2018; Nouvel et al., 2017; Verhagen, 2018). This gap is concerning because cooling-related energy consumption is already putting stress on the electricity grid, and the

associated greenhouse gas emissions could jeopardize The Hague's goal of being carbon neutral by 2050 (Motie "Vertaling Klimaatakkoord Parijs Naar Haagse Doelstellingen," 2016; Essent, 2020). Therefore, research into the environmental impacts of cooling demand is highly relevant.

Additionally, this study seeks to address a methodological gap in the existing literature. To date, no studies have utilized a bottom-up modeling approach to estimate cooling demand for individual buildings, which is then aggregated to assess total space cooling demand and its associated environmental impacts.

1.3 Research Questions

This research aims to contribute to the understanding of the current and future demand for cooling in The Hague. Additionally, it investigates the environmental impacts of this demand, and in what way such impacts can be minimized. This leads to the overarching research question:

"How can choices in technology and policy minimize the evolving environmental impacts of residential and office space cooling in The Hague until 2050?"

This overarching research question is split into several sub-questions:

1. What is the current cooling demand in residential and office buildings in The Hague?
2. What are the environmental impacts of the current cooling demand in The Hague?
3. How will the cooling demand in The Hague and its environmental impacts evolve until 2050?
4. What recommendations can be given to minimize the projected environmental impacts of residential and office space cooling in The Hague?

The outcomes of this study hold relevance beyond The Hague, extending to a broader national context within the Netherlands and similar climates. Moreover, these findings offer actionable insights for mitigating adverse environmental effects while shaping strategic cooling approaches for residential and office spaces.

1.4 Report Structure

First, the theoretical context and background of space cooling and its impacts are introduced in Chapter 2. In Chapter 3, the research design is outlined, including the methodologies and modeling framework used. Chapter 4 presents the results of the model, while Chapter 5 discusses its implications and ensuing recommendations. Finally, Chapter 6 provides a concluding overview of the research. For a visual representation of this structure, please refer to Figure 1.

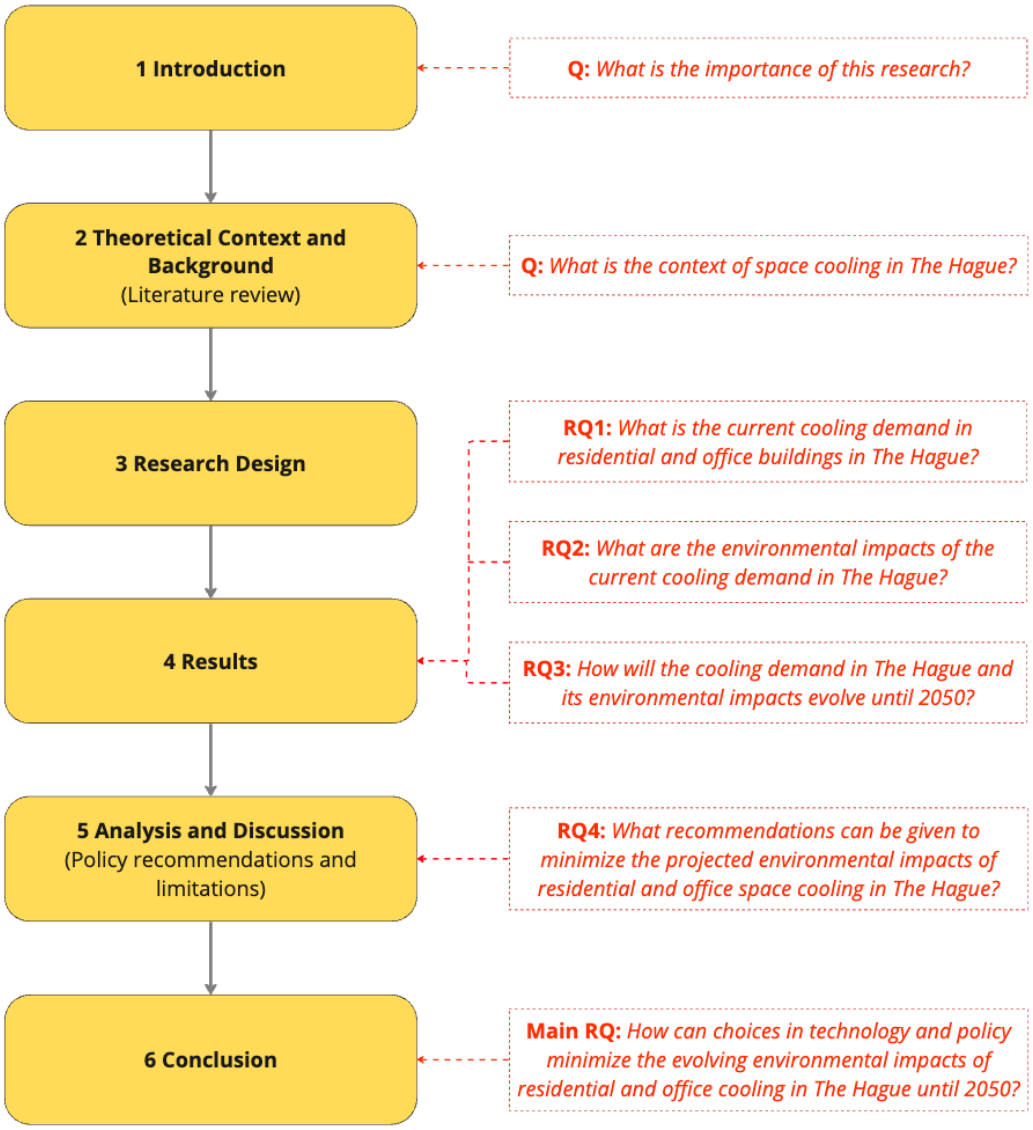

Figure 1: Overview of report structure.

2 Theoretical Context and Background

This section establishes the theoretical framework for understanding The Hague's current and projected cooling demand through a literature review that assesses the drivers of cooling demand, the technical and theoretical background of predominant cooling techniques, and their most important environmental impacts. All relevant terms and concepts necessary to the comprehension of this study are defined in this section.

2.1 The Need for Cooling

Space cooling systems play a vital role in homes and offices by regulating indoor temperatures to maintain thermal comfort—a key factor in occupant well-being and workplace productivity (Kawakubo et al., 2023; Yuan et al., 2022). These systems reduce indoor temperatures to comfortable levels by removing heat from inside and releasing it outdoors.

Thermal comfort is subjective, reflecting personal temperature preferences. Although studies suggest specific optimal temperatures—18.3 °C in one (Fazeli et al., 2016), 22 °C in another (Seppänen & Fisk, 2006), and the EU's use of 24 °C for calculating Cooling Degree Days (Eurostat, 2020)—policies are transitioning towards defining a 'thermal comfort range' instead of a fixed temperature. This range's upper boundary is termed the 'threshold temperature' or 'effective cooling temperature' (de Dear et al., 2020). For more information, refer to Section 2.2.1.

Maintaining thermal comfort is also essential for safeguarding human health against the adverse effects of excessive heat. Heat stress, resulting from the body's inability to sufficiently self-cool, can escalate from mild symptoms like heat rash to life-threatening conditions such as heat stroke (Shindell et al., 2020). It can also exacerbate pre-existing health issues, particularly cardiovascular and respiratory diseases (Gubernot et al., 2015; Kjellstrom et al., 2016).

Heat stress poses a global public health challenge, leading to significant mortality, especially among at-risk groups including the elderly, children, and individuals with chronic diseases. Currently responsible for roughly 12,000 deaths worldwide each year, heat-related fatalities could surge to 260,000 by 2050 without strategic interventions (T. Peters, 2018). This increase can largely be attributed to the projected 25% rise in global

CDDs by 2050, highlighting the increasing need for effective cooling technologies to safeguard both thermal comfort and protect human health (Kennard et al., 2022).

In the Netherlands, climate change is heightening the risks of heat stress, as exemplified by the record-breaking 2019 heatwave which resulted in an additional 400 deaths (CBS, 2019b; Klok, Schaminée, et al., 2012). Research attributes a third of the country's heat-related deaths to climate change, a share which is expected to increase as average summer temperatures rise and heat waves continue to increase in frequency and intensity (Vicedo-Cabrera et al., 2021). Therefore, space cooling is increasingly important for protecting against health risks and deaths.

While space cooling is essential, combating heat stress also involves various other mitigation strategies. Individually, these include hydration, dressing appropriately for the weather, and limiting exposure to the sun during peak heat times. Policy-level interventions include heat-health action plans, urban designs that minimize heat island effects, and public campaigns to raise awareness of heat-related risks (RIVM, 2020; WHO, 2008).

Regarding the benefits of space cooling systems, they serve not only to ensure thermal comfort and reduce heat stress but also play a significant role in improving air quality and preserving sensitive equipment. Many cooling systems incorporate air filtration and ventilation, which improve indoor air quality by reducing pollutants, allergens, and humidity levels. This contributes to a healthier living and working environment that improves occupant well-being (Carlucci et al., 2015). Moreover, by maintaining controlled temperatures and humidity levels, cooling systems help safeguard electronic devices and materials, ensuring their durability and optimal performance—which is particularly important in office environments (ASHRAE, 2021).

In summary, space cooling systems maintain comfortable indoor temperatures, which ensures wellbeing and productivity, protects against heat-related health issues, and preserves sensitive equipment. The escalating impacts of climate change underscore the growing value of these cooling system benefits (De Blois et al., 2015; Seltenrich, 2015).

2.2 Determinants of Cooling Demand

Space cooling demand is influenced by a multitude of factors across societal sectors. Given the interlinked nature of these determinants, this study focuses on the most influential

ones, including thermal comfort ranges, building design, the urban heat island effect, climate change, and other socio-cultural drivers.

2.2.1 Effective Cooling Temperature and Thermal Comfort Range

Thermal comfort, a subjective sensation influenced by cultural and individual preferences, dictates when people decide to use cooling equipment, thereby influencing cooling demand (Esfandiari et al., 2021). The broader the thermal comfort range, the higher the threshold temperature before the space cooling is activated. This not only affects the demand for active cooling systems, such as air conditioning, but also the need for passive cooling strategies, such as natural ventilation or shading.

The static thermal comfort range depends on several factors: air temperature, humidity, airflow, radiant temperature, clothing, and metabolic rates of occupants (de Dear et al., 2020). Furthermore, it is also shaped by gender, age, cultural background, thermal history, and the accustomed climate (Rupp et al., 2015).

These variables lead to the concept of adaptive thermal comfort range, which describes people's ability to adjust their clothing, behavior, and expectations to find comfort across a broader range of temperatures (de Dear & Brager, 1998). While this may provide short-term adaptation in instances such as heat waves, long-term changes in thermal comfort ranges take place through thermal adaptation. Thermal adaptation describes longer-term physiological changes in response to consistent exposure to specific temperature conditions (Zhuang et al., 2022). This results in a lower optimal indoor temperature in summer than in winter, and a higher optimal indoor temperature in consistently warmer climates. Thermal adaptation is considered easier in residences than in offices due to expectations of higher temperatures, the ease of environmental control, and the broader scope for behavioral adjustment, such as changing attire or location within the home (Kurvers et al., 2012). However, the cumulative effect of thermal adaptation on the thermal comfort range is complex and highly context-specific (Ioannou, 2018). Overall, considering the future of the Netherlands under climate change, adaptive thermal comfort and thermal adaptation may allow building occupants to expand their thermal comfort range in a consistently warmer climate.

Thermal comfort ranges directly influence space cooling demand through regulatory policies and consumer behavior, or the purchasing, and frequency and intensity of use of cooling systems. Governments establish standards for "effective cooling temperatures" or

"threshold temperatures" that dictate when active space cooling should be initiated, particularly in new buildings and offices. Over time, policy and personal comfort ranges have trended towards narrower, cooler ranges—partly due to more prevalent air conditioning—with summertime thresholds decreasing by about 1 °C from the 1940s to the 1980s (de Dear et al., 2020). The preference for cooler comfort ranges is generally easier to instill than the acceptance of warmer conditions. As a result, if air conditioning remains the go-to solution to counteract rising temperatures, the market penetration of air conditioners is expected to increase significantly.

However, research indicates a more tolerant and higher temperature range in naturally ventilated structures compared to those with mechanical cooling, sometimes with up to a 4 °C difference (de Dear & Brager, 1998; Hussein et al., 2009). The prevailing thermal comfort standards in the Netherlands, influenced by ASHRAE 55 and EN 15251 and consolidated in ISSO 7,[4] [5] prioritize mechanically cooled environments as the default, positioning natural ventilation as a secondary, less conventional option (Nicol & Wilson, 2011). Yet, the intensifying focus on climate change is driving a pivot in research towards enhancing thermal adaptation and reducing reliance on mechanical cooling. Expectations are mounting for policies to mirror this research, potentially catalyzing a transition towards favoring natural ventilation and adaptive strategies in building regulations, with the potential to widen accepted thermal comfort ranges and reduce active cooling demand and the ensuing environmental impacts (de Dear et al., 2013, 2020; Schellen et al., 2013).

[4] ASHRAE 55 is a standard by the American Society of Heating, Refrigerating, and Air Conditioning Engineers. It guides the assessment of indoor thermal comfort using metrics like Predicted Mean Vote (PMV) and Predicted Percentage of Dissatisfied (PPD). The standard considers factors like air temperature, humidity, air movement, and clothing, while also accounting for adaptive comfort. It is frequently updated to reflect advancements in research and technology related to thermal comfort (ASHRAE, 2020).

[5] EN15251 is a European standard developed by the European Committee for Standardization. It offers guidelines for determining indoor environmental conditions, including thermal comfort, to assess building energy performance. The standard aims to balance occupant comfort with energy efficiency, considering regional differences and building types across Europe, and provides guidelines for maximizing adaptive thermal comfort (NEN, 2007).

Dutch regulations under ISSO 74 use the "Adaptieve Temperatuurgrenswaarden" (ATG, Adaptive Temperature Limits) model for thermal comfort assessments since 2014 (Leitão, 2017). This model classifies buildings into Alpha, with occupant-controlled natural ventilation, and Beta, with mechanical cooling and sealed façades. The ATG model accounts for a wider comfort range in Alpha buildings, as can be seen in Figure 2 (Beek et al., 2007). For Beta buildings, a thermal comfort range of 21–26 °C is set, with the recommended cooling threshold temperature at 24.5 °C (ISSO, 2014). Similarly, other studies on both office and residential buildings recommend a threshold temperature of 25 °C (Boerstra & Leijten, 2003).

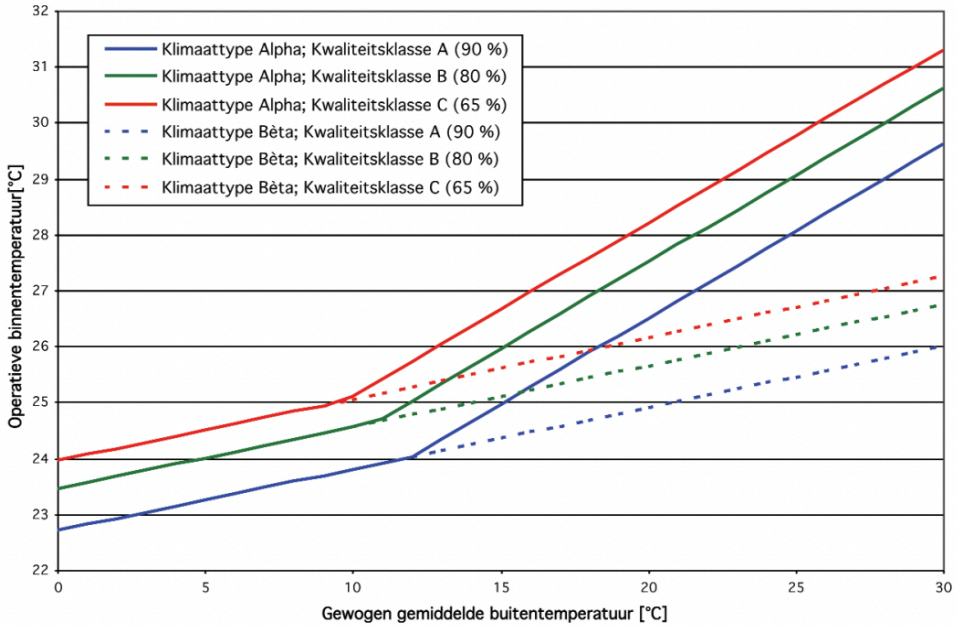

Figure 2: Recommended indoor temperatures for Alpha buildings using natural ventilation (solid lines) and Beta buildings using mechanical ventilation (dashed lines), as determined by the ATG model in accordance with Dutch indoor climate standards. From (Beek et al., 2007)

Despite these standards, actual occupant preferences may vary; a small-scale 2021 Dutch survey indicated a preferred residential temperature of 20 °C, highlighting a discrepancy between prescribed norms and individual comfort levels (Rovers et al., 2021).

In summary, thermal comfort is a personal experience that determines cooling equipment use, affecting energy demand. It varies with individual and environmental factors, with adaptive comfort and thermal adaptation allowing people to tolerate a wider temperature range. Despite guidelines recommending higher thermal comfort ranges for energy conservation, actual user preferences often lean towards cooler conditions.

2.2.2 Building and Urban Design

The interaction between building design and urban planning significantly impacts cooling demand in urban environments. Decisions made during construction and urban layout set the stage for energy consumption and occupant comfort. Building design, and particularly the building envelope, plays a key role. A balance between aesthetics, energy efficiency, and affordability drives design choices. Material choices for components including roofs, ceilings, walls, windows, and doors influence thermal performance. Architectural trends away from traditional shading elements toward all-glass and unshaded facades may increase aesthetic, but also increase the need for cooling within a building. Space-use design, which affects the ratio of interior space to surface area, also impacts heat transfer rates and solar heat gains, with the greater the ratio the lesser the cooling demand (IEA, 2018a).

Technological integration has brought about smart building controls and sensors that enable energy-efficient cooling. Despite their initial costs, these systems offer long-term energy savings and a reduction in cooling demand. The selection of building envelope technologies is influenced by financial considerations and lifecycle costs. High-tech and low-tech solutions implemented during construction or later by building occupants reduce the impact of energy use for cooling, such as materials with high thermal resistance, mechanical and natural ventilation, low thermal mass, and humidity management (IEA, 2018a).

Urban design factors like street orientation, geometry, and landscaping also influence cooling demand. The orientation and geometry of streets dictate heat absorption and airflow, with narrow urban canyons trapping heat and wide streets facilitating ventilation. Street orientation, which determines facade exposure, can have a strong effect on cooling demand, and can vary cooling energy demand by up to 26% annually, with western and southern exposure resulting in the highest energy demand (Ashmawy & Azmy, 2018; Deng et al., 2021). Land use planning also plays a role, as concentrations of heat-generating commercial and industrial spaces can be counteracted through mixed-use zoning and extensive green infrastructure. While urbanization has led to a reduction in green spaces, but efforts such as green roofs, urban greening, and water features are being promoted to lower temperatures in cities and reduce a dependency on active cooling. Roofing choice holds a particularly strong impact, as traditional black roofs only reflect 5–10% of incoming solar radiation, whereas a painted white roof or a green roof reflect 80% (IEA, 2018a).

In summary, the interplay between building design and urban planning is a critical determinant of cooling demand. Material choices, architectural trends, technological integration, and urban layout collectively shape energy consumption and occupant comfort in the built environment.

2.2.3 The Urban Heat Island Effect

The urban heat island (UHI) effect refers to how urban regions typically exhibit higher temperatures than their rural surroundings, a disparity caused by factors like the absorption of radiation by paved surfaces and air pollution, anthropogenic heat generation, and lower evaporative cooling from fewer green and blue spaces (Kleerekoper et al., 2012). These contributing factors lead to an increased need for space cooling in cities, particularly during heatwaves, with temperature differences between urban centers and rural areas averaging 1–3 °C and peaking at around 9 °C (van Hove et al., 2011). For example, The Hague's center was recorded at 8.6 °C warmer than its rural surroundings on a particularly hot summer day (Klok, Shaminee, et al., 2012). The extent of the UHI effect varies based on several interconnected variables (see also Figure 3).

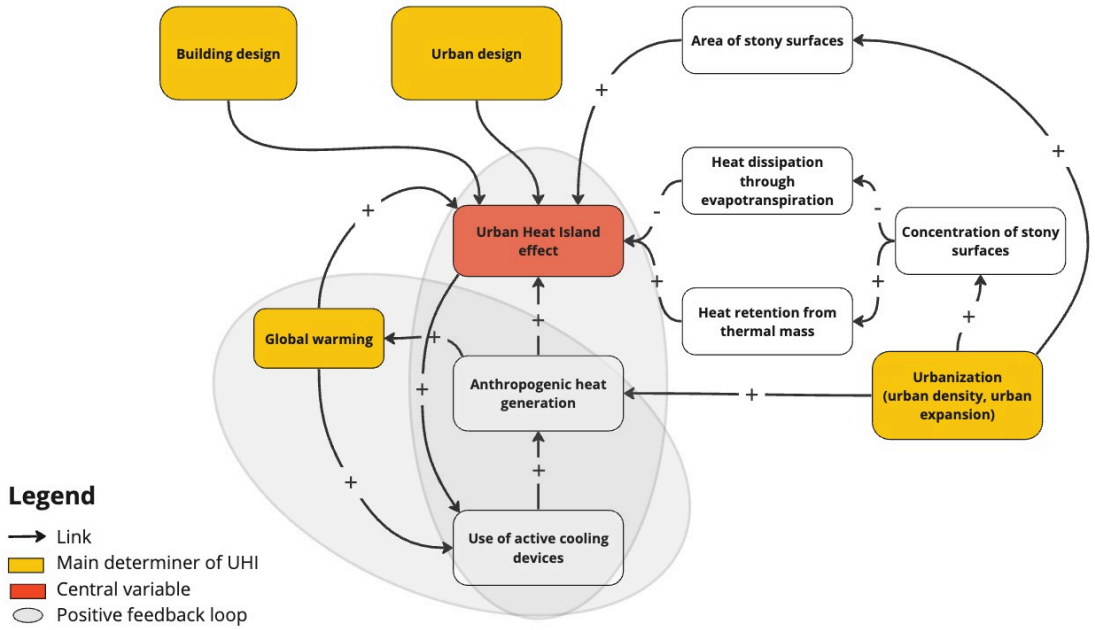

Figure 3: A causal-loop diagram illustrating various factors contributing to the urban heat island effect. Note that the shown factors are representative but not exhaustive.

Firstly, urbanization amplifies the UHI effect by simultaneously increasing the both the overall extent and the concentration of heat-absorbent materials like concrete and asphalt (Salman, 2018). These materials, which make up the roads, roofs, walls, and pavements

of the city, replace natural, evaporative vegetation and soil, thereby reducing the capacity for cooling through evapotranspiration. Furthermore, the thermal mass of urban infrastructure such as roads and buildings absorbs heat throughout the day but radiates it back into the local environment at night, which inhibits nocturnal cooling. As cities expand, they envelop more land with these heat-retentive materials, exacerbating the UHI effect.

Besides urban expansion, the growing urban density also increases the UHI effect (Zhou & Chen, 2018). Within cities, denser neighborhoods often have higher temperatures than less populated areas (Chapman et al., 2017). The push towards urban densification, a global response to population growth and urban sprawl, thus contributes to rising city temperatures. In The Hague, for example, the city's strategy to densify to address a longstanding housing crisis includes the construction of numerous high-rise buildings, increasing urban density, and potentially amplifying the UHI effect (Haagse Hoogbouw, 2023).

Finally, urbanization amplifies the density of anthropogenic heat sources like industry, building heating, air conditioning, and even the human metabolism. In the Randstad, home to The Hague, this type of heat presently contributes to about 10% of the UHI effect (Rovers et al., 2015). With the expected 10% growth of urbanization in the Randstad by 2050, the UHI effect is set to intensify through the interconnected dynamics of increased urban extent, density, and anthropogenic heat production (Manders & Kool, 2015).

Urbanization, however, is not the sole factor in the projected increase of the UHI effect. Climate change serves as a potent multiplier of UHI, through its role in atmospheric heating, altered weather patterns, and feedback loops (Sachindra et al., 2016). As global temperatures rise, urban regions—high on heat-retaining structures and low on greenery—face even higher baseline temperatures compared to their rural surroundings (Chapman et al., 2017). This exacerbated temperature difference is particularly evident during heatwaves, when cities can become hotspots of extreme heat, affecting human health, energy demand, and overall urban comfort. Additionally, climate change can undermine natural cooling mechanisms by diminishing cloud cover and shifting wind patterns, disrupting heat dispersion in cities, and amplifying the UHI effect.

Paradoxically, cities tend to adapt to hotter temperatures with more air conditioning, inadvertently injecting extra anthropogenic heat into the surroundings, exacerbating the UHI effect, a vicious cycle detailed in Figure 3. Waste heat from air conditioner (AC)

systems has been shown to raise local air temperatures by over 1 °C in cities like Phoenix, U.S.A. (Salamanca et al., 2014).

Research of climate change's impact on the UHI effect in the Netherlands is still in early development compared to other countries. Traditionally, the Dutch have enjoyed a moderate climate and only started to confront urban heat issues following a series of intense heatwaves since the early 2000s (van Hove et al., 2011). Nevertheless, recognition of the UHI effect is gaining momentum in Dutch policy discourse (van der Hoeven & Wandl, 2018b). Although concrete predictions are scarce, extrapolations from initial findings and models applied to analogous climates suggest that UHI in Dutch cities could rise by 0–2.3 °C in the coming decades, as summarized in Table 1. When factoring in the compound effects of general warming trends, urban growth, increased heat from cooling systems, and more recurrent heatwaves, the UHI effect emerges as a significant driver for increasing cooling demand.

Table 1: Modeled increases in average UHI from climate change in comparable climates to The Hague.

Time range	Geographic location	UHI effect change (°C)	Source
1971–2000 to 2071–2100	Hamburg, Germany	0 ± 0.02	(Hoffmann & Schlünzen, 2013)
2008 to 2050	Amsterdam, the Netherlands	0.2 ± 0.1	(Koomen & Diogo, 2017)
1961–1990 to 2050	Rostock, Germany	2.3	(Richter, 2016)

On the other hand, strategic urban and building designs offer mitigation potential against UHI severity. Building orientation and the use of selective street geometry to maximize natural shading can help reduce the UHI effect (Salman, 2018). In addition, the presence of green space in the form of urban greening, parks, or water features, cool the surrounding area through evapotranspiration (Rizwan et al., 2008). The construction of green buildings, particularly those adhering to LEED standards, can also diminish UHI; such buildings can reduce urban temperatures by up to 0.48 °C.[6] Material selection plays a role too; for example, the thermal properties of asphalt contribute significantly to UHI

[6] LEED stands for Leadership in Energy and Environmental Design. It is a widely recognized and globally accepted green building certification program and rating system. LEED is developed and administered by the U.S. Green Building Council (USGBC, 2023)

due to its low reflectivity (albedo of 0.05–0.2), whereas materials like brick offer higher albedo values (0.2–0.4) and hence less heat retention (van Hove et al., 2011). In summary, urban design choices pose a promising opportunity for mitigating increasing heat stress from UHI in the coming decades.

2.2.4 Drivers of Increased Cooling Demand

2.2.4.1 Climate Change

The climate is the primary determinant of cooling demand, with higher air temperatures and humidity levels leading to increased space cooling demand (IEA, 2018a). Historically, cooling equipment has been more prevalent in warmer regions, while heating systems have been the focus in cooler regions such as the Netherlands. Climate change, however, has altered these patterns.

Climate change, primarily driven by an increase in atmospheric carbon dioxide and other greenhouse gases (GHGs)—including those used as refrigerants—was hypothesized in the late 19th century and has been acknowledged as a critical global issue since the 1980s (Arrhenius, 1896; Moser, 2010). Global averages temperatures have increased by approximately 1.1 °C from pre-industrial levels, with a more acute rise of 1.6 °C over land. With temperatures projected to increase further to 1.6–2.5 °C by 2050 (see also Figure 4), climate change is commonly referred to as the 'climate crisis' (Archer & Rahmstorf, 2010; Calvin et al., 2023; Hansen et al., 2012).

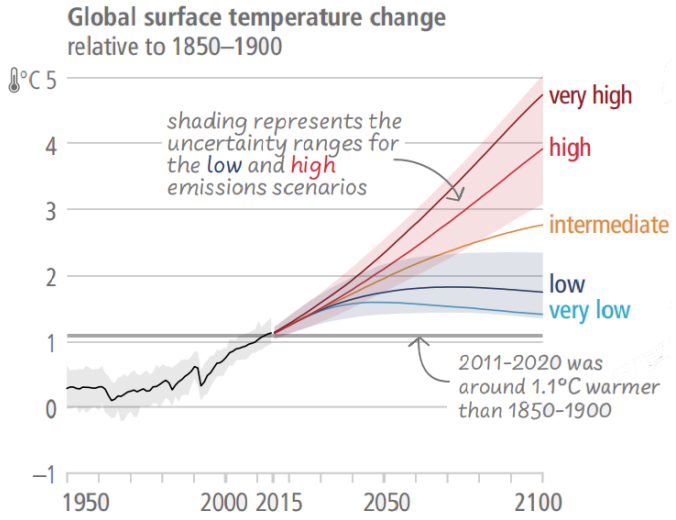

Figure 4: Global surface temperature change relative to pre-industrial levels (1850–1900), adapted from (Calvin et al., 2023).

The mechanics of climate change are rooted in the greenhouse effect, where GHGs trap solar radiation in the atmosphere, leading to global warming. Excessive emissions from activities such as fossil fuel combustion and agriculture have intensified this effect, disrupting climate patterns and elevating temperatures worldwide (Calvin et al., 2023; Pörtner, Roberts, Adams, et al., 2022).

The repercussions of climate change are extensive, as displayed in Figure 5. It drives rising sea levels, worsening air quality, and more frequent extreme weather events like floods, droughts, and particularly heatwaves, which in turn drive up the need for space cooling (Pörtner, Roberts, Adams, et al., 2022). These have secondary effects on biodiversity, human health, resource availability, and socio-economic conditions (Kemp et al., 2022).

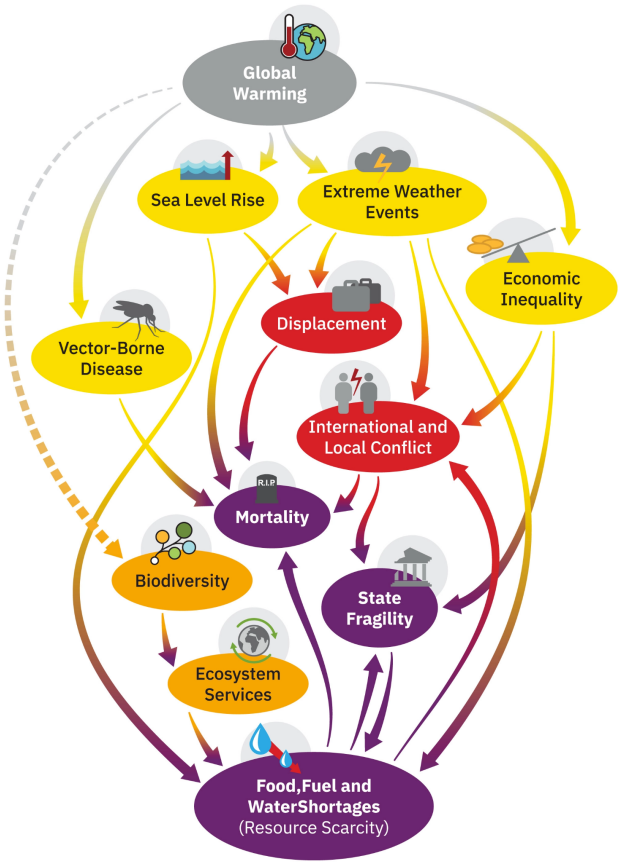

Figure 5: The system dynamics of climate change in a causal loop diagram. A solid line represents amplifying feedback, and a dotted line denotes dampening feedback. From (Kemp et al., 2022).

The complexity of the climate issue is highlighted by the IPCC and underscored by the Paris Agreement, describing it as a 'super wicked problem'. Such problems are marked by their immense complexity, characterized by numerous interdependent factors and

feedback loops (Levin et al., 2012). An example of such a feedback loop is the link between global heating and residential cooling demand, as can be seen in Figure 3. Increased global temperatures boost the demand for air conditioning, which then leads to higher GHG emissions due to energy consumption and refrigerant leaks, exacerbating the warming trend. Refrigerants leaks alone could surpass the entire 1.5 °C carbon budget, unless hydrofluorocarbons (HFCs) are rapidly phased out on a global scale (Dreyfus et al., 2020; Matthews et al., 2020).

In northwestern Europe, climate change raises concerns of coastal and inland flooding, heat waves, water scarcity, and ecosystem disruptions (Pörtner, Roberts, Adams, et al., 2022). In the Netherlands, temperatures have risen at twice the global average rate, exacerbating droughts and heatwaves (KNMI, 2021).

The Royal Netherlands Meteorological Institute (KNMI) forecasts a worrisome acceleration of these trends. Their "Klimaatsignaal '21" (Climate Signal '21) report projects sea-level rise of up to two meters by 2100 along the Dutch coast, increasing the flood threat (KNMI, 2021). Further increasing flood risks is extreme rainfall, which is expected to increase in frequency and intensity. The past three decades have already seen a 10–15% spike in the severity of heavy showers. Moreover, the country has witnessed a doubling of days with high humidity, as indicated by the rise in days with dew points over 18 °C from 1951–2020. In contrast, droughts are also becoming more frequent, both due to rising temperatures and increasing solar radiation, which has risen by 5% over the last 70 years. Together, these climatic shifts are likely to increase cooling demands in the Netherlands.

Quantitatively, the International Energy Agency (IEA) forecasts a 20% global rise in CDDs, a measure of cooling demand, by 2050 (IEA, 2018a). In the Netherlands, a more temperate region, the amount of annual CDDs is expected to rise faster— between 22% and 70% by 2050 (Attema et al., 2014). Such increases are particularly challenging to regions which are traditionally unaccustomed to persistent heat, as their infrastructure, policies, and social behaviors are not well-equipped for such climatic changes.

Within the Dutch context, the national government has recognized the imminent threat of climate change and has implemented several policies to mitigate and adapt to its impacts. The 2019 "Klimaatakkoord" (Climate accord) outlines the country's commitment to reducing GHG emissions and transitioning to a sustainable economy (Klimaatakkoord, 2019). The "Klimaatplan 2021–2030" details concrete actions for the coming decade,

including increasing energy efficiency, promoting renewable energy, and implementing climate adaptation strategies (Ministerie van Algemene Zaken, 2020). However, these plans may not be sufficient to address an increasing demand for space cooling. The Dutch infrastructure and building design are not well-equipped for the expected rise in temperatures. Moreover, the country's social and psychological behavior towards cooling is not yet adapted to the changing climate. For perspective, Spain's recommended activation threshold for air conditioning stands at 27 °C in Spain, much higher than policy standards and common practice temperatures in the Netherlands (Jones, 2022).

In conclusion, climate change, with rising temperatures, increased humidity, intensified solar radiation, and more frequent extreme weather events, is a significant driver of cooling demand. As the world continues to heat, the demand for space cooling is expected to rise, particularly in regions not traditionally accustomed to high heat.

2.2.4.2 Socio-Cultural and Market Drivers

Besides climate change, other factors driving cooling demand include economic prosperity, population growth, an aging demographic and urbanization (as described in Section 2.2.3).

Air conditioners, often considered luxury items with high price-elasticity, tend to see increased purchase rates with rising discretionary income (Bashir et al., 2011). In tropical regions, higher income strongly correlates to higher ownership of air-conditioners (L. Davis et al., 2021). While this correlation is weaker in temperate zones like the Netherlands, global warming is likely to shift cooling equipment from a luxury item to an essential good. The EU's gross domestic product (GDP) is expected to increase by 60% until 2050, with similar expectations for the Netherlands, as shown in Table 2 (Manders & Kool, 2015). As the climate grows hotter, this economic growth is likely to be a significant booster of the acquisition and use of active cooling equipment.

Table 2: Prognosis of GDP per capita, based on total GDP and population growth estimates from (Manders & Kool, 2015).

Scenario	Population growth	GDP growth	GDP per capita growth
2030: Low	2%	20%	18%
2030: High	8%	40%	30%
2050: Low	-2%	45%	48%
2050: High	15%	105%	78%

The market penetration rate (MPR) of cooling equipment is also determined by pricing trends, with air-conditioner prices historically experiencing a slow but steady decline (Rapson, 2014). Looking at recent history, the sale of air-conditioners has increased significantly in the past decade. Consumption of window and wall air conditioning systems in the Netherlands has been analyzed using the Eurostat PRODCOM dataset (Eurostat, 2023).[7] The full analysis can be found in the background research spreadsheet in Appendix A. Figure 6 shows a five-fold rise in the Dutch air conditioner market over the past decade, accompanied by a more than thirty-fold increase in the annual market growth rate. This suggests an imminent exponential growth in the market penetration rates of cooling equipment.

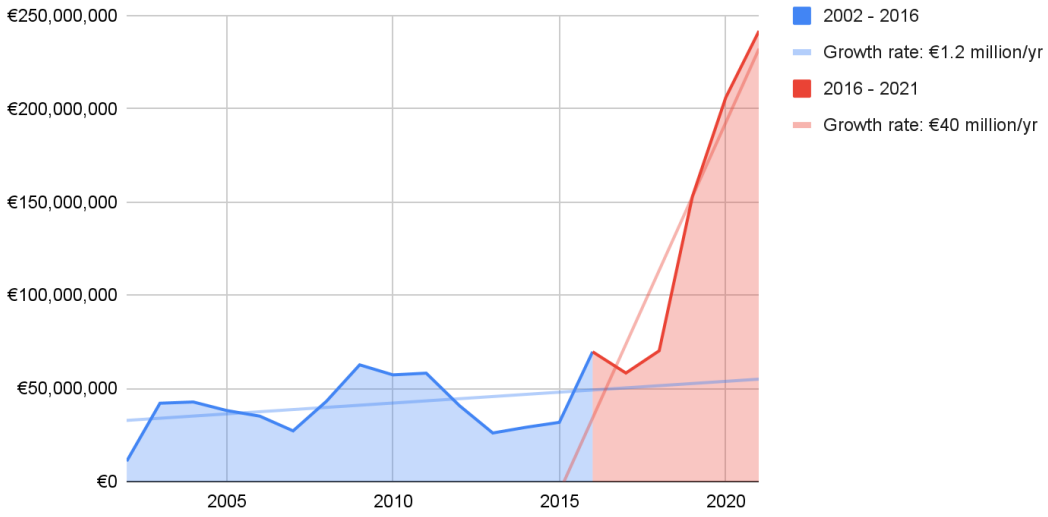

Figure 6: Annual consumption of air conditioners in the Netherlands, 2002–2021. Based on (Eurostat, 2023).

Cooling equipment prices also influence which type of equipment is most commonly purchased. Consumers increasingly prefer energy-efficient cooling systems that promise long-term savings, valuing the Energy Efficiency Ratio (EER) over initial costs, especially as electricity prices rise (Rapson, 2014). Those with the means tend to opt for such cost-effective, high-efficiency options despite higher upfront prices.

Population growth is another important driver of cooling demand, with the world population currently growing an average of 0.9% per year (IEA, 2018a). the Netherlands

[7] Prodcom, short for "PRODuction COMmunautaire" (Community Production), provides statistics on the production, import, and export of manufactured goods within the EU (Eurostat, 2023).

expects a population rise of up to 24% by 2050, mostly due to migration (Beer et al., 2020). This influx of people not only increases the need for cooling to maintain comfort for a larger population, but also could shift cultural expectations regarding thermal comfort.

The aging population further compounds demand; seniors are particularly vulnerable to heat, with those over 75 being the most frequent victims of heatwaves (IEA, 2018a). With the Dutch elderly population projected to grow by 37% by 2050, representing over a quarter of the total population, enhanced space cooling solutions will be needed to ensure public health. (Beer et al., 2020).

Finally, socio-cultural trends and norms also shape cooling technology adoption. Environmental concern has risen significantly within the EU since the 1960s (Tendero, 2021). A survey by the European Commission revealed that 78% of EU citizens viewed climate change as a grave issue in 2021, an increase from 68% in 2011, with 49% citing it as the foremost global challenge (European Commission, 2021). In the Netherlands, public awareness is even greater, with 70% listing climate change as the most pressing global concern and 64% actively trying to reduce their environmental impact.

Such heightened environmental awareness generally leads to more environmentally friendly behavior, such as reduced and more efficient air conditioning use and the adoption of greener cooling strategies (Kondo et al., 2021; Pothitou et al., 2016; Wi & Chang, 2019; Yusliza et al., 2020). As a result, consumer preferences may shift from portable units to more expensive but energy-efficient systems like air conditioners and heat pumps. Supported by targeted policies, this increased environmental awareness could lead to higher and broader thermal comfort ranges in summer, helping to dampen the anticipated rise in cooling demand. Nevertheless, the precise impact of eco-awareness on ownership and use rates of cooling equipment remains unquantified in current research.

2.3 Cooling Technologies

This section outlines the technological foundations of cooling systems, beginning with a historical overview and an explanation of basic air conditioning mechanisms. It then covers key factors such as energy efficiency, refrigerants, and materials, as well as a discussion on the main types of cooling methods, both active and passive.

2.3.1 Historical background

The basic principle behind most space cooling is evaporation: when a liquid evaporates, heat is extracted from the surrounding air. This was already known and utilized by the ancient Egyptians and Mesopotamians, who cooled their houses by hanging moist reeds in their windows (Bahadori, 1978; Tang & Etzion, 2004).

Advancements in phase-change physics during the 17th and 18th century laid the groundwork for artificial refrigeration. Oliver Evans theorized a closed-cycle process using volatile liquids to produce ice in 1805, a concept that didn't materialize into a machine but influenced future pioneers like Richard Trevithick and Jacob Perkins (Evans & Stevens, 1805). Although there is no evidence that he created a functional machine, his theories are likely to have inspired Richard Trevithick and Jacob Perkins. Trevithick conceptualized an air-cycle refrigeration system in 1828, but it was Perkins who successfully demonstrated the vapor-compression method in a prototype that experts now acknowledge as a pivotal moment in refrigeration history. His invention has granted the mechanical vapor-compression process its eponym: the Perkins Cycle (Calm, 2008).

Subsequent innovations culminated in the 1902 invention of the electric air conditioner by Willis H. Carrier, the founder of one of the largest heating, ventilation, and air conditioning (HVAC) companies in the world; the Carrier Corporation (Varrasi, 2022).

2.3.2 Functional design

A simplified diagram of the function of Carrier's AC unit can be seen in Figure 7.

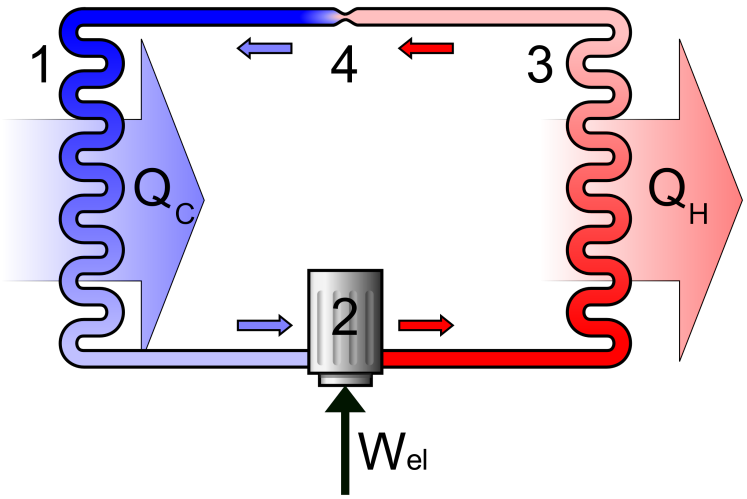

Figure 7: The vapor-compression cycle, with 1) evaporator coil, 2) compressor, 3) condensing coil, 4) expansion valve. Adapted from (Karonen, 2017).

Here, a liquid refrigerant is let to evaporate in a coil, taking in heat from the surrounding air (Q_C). The resulting gas is then compressed, which takes energy, almost always provided by electric work (W_{el}). This compressed gas then condenses in a second coil and releases heat to the external environment (Q_H). After this, the liquid can expand and enter the first evaporator coil again, thus completing the cycle. While this is the basis for active cooling technologies, cooling types and devices vary in their energy efficiencies, refrigerants, and material makeup. Heat pumps work in a similar way, as displayed in Figure 8.

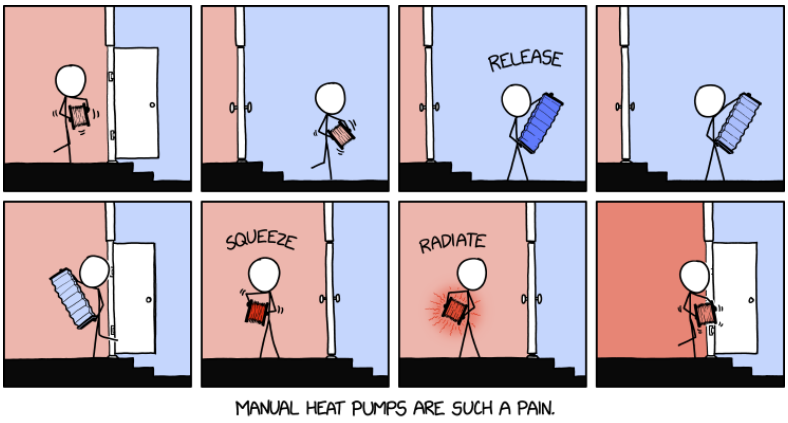

Figure 8: Demonstration of a hypothetical manual heat pump. From (Munroe, 2023).

2.3.3 Energy Efficiency

The coefficient of performance (COP) is the standard measure of an air conditioner's energy efficiency, reflecting the ratio of useful cooling output to the electrical energy input under full-load, steady-state conditions (ASHRAE, 2021). It is mathematically described by Equation 1 (Petrecca, 1993).

$$COP_{cooling} = \frac{Q_C}{Q_H - Q_C} = \frac{Q_C}{E_{el}} \qquad \textit{Equation 1}$$

Here, the COP is defined as the ratio of useful cooling (Q_C) provided to the electric energy consumed by the device (E_{el}). A higher COP indicates a more efficient air conditioner, delivering more cooling per unit of energy consumed.

Real-world usage, however, often deviates from steady-state, full-load conditions, necessitating metrics that account for varied operational states and seasonal changes. The Seasonal Energy Efficiency Ratio (SEER), common in the U.S., measures average system efficiency over the cooling season, offering a more realistic efficiency indicator over diverse conditions (IEA, 2018a). Europe's equivalent, the European Seasonal Energy

Efficiency Ratio (ESEER), incorporates weighted factors for different operational loads to better reflect the fact that cooling equipment more frequently operates at part-load conditions in the more temperature European climate, as described in Equation 2 (Saheb et al., 2006).

$$ESEER = 0.23 \cdot COP_{25\%} + 0.41 \cdot COP_{50\%} + 0.33 \cdot COP_{75\%} + 0.03 \cdot COP_{100\%} \qquad \textit{Equation 2}$$

Both SEER and ESEER enable efficiency comparisons across air conditioning units and inform regulatory standards to promote energy conservation and minimize environmental impacts. Notably, there is a significant discrepancy between the average and top-tier energy efficiencies of cooling devices on the market, as shown in Figure 9. This gap implies that there is significant potential for improvement by promoting the transition from average to of best-in-market cooling devices (IEA, 2018a). This gap indicates a significant opportunity for reducing overall energy demand and related environmental impacts.

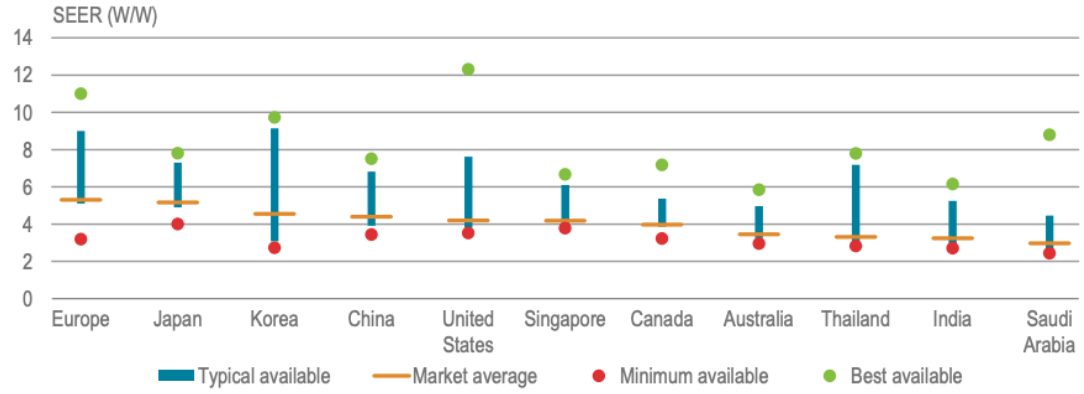

Figure 9: Overview of energy efficiency (SEER) of cooling devices around the world (IEA, 2018a).

2.3.4 Refrigerants

As mentioned above, refrigerants are crucial in cooling equipment, enabling heat exchange. While ancient methods used natural substances like water as refrigerants, technological advancements introduced synthetic refrigerants to enhance cooling efficiency. Now, environmental concerns are driving a return to natural refrigerants for sustainable cooling. This history is detailed in the following section.

2.3.4.1 A History of Refrigerants in four Generations

The evolution of refrigerants is can be divided into four generations, each driven by the need for safer and more environmentally friendly options, as shown in Figure 10 (Calm, 2008). Initially, in the 1830s, Jacob Perkins' vapor-compression machine used hazardous

substances like isoprene, followed by the introduction of efficient but flammable and toxic chemicals such as propane (R-290) and ammonia (R-717).[8]

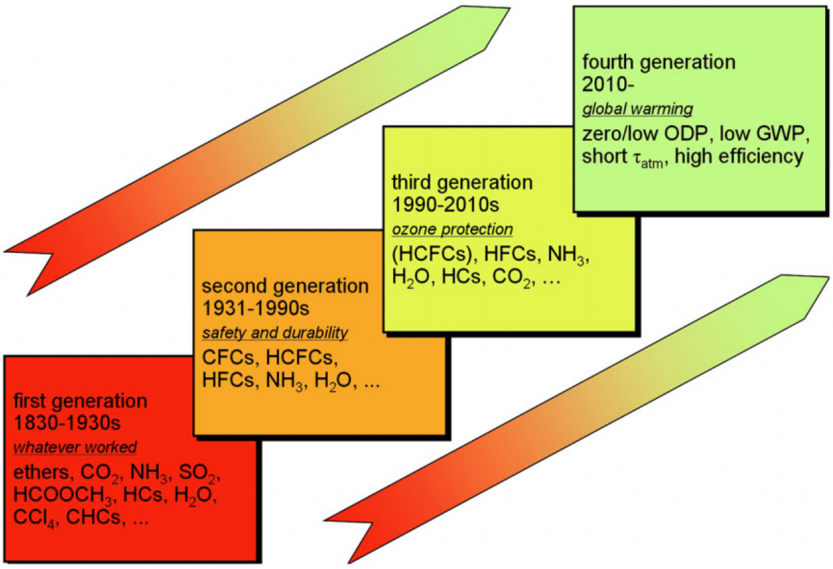

Figure 10: An overview of the four generations of refrigerants, from (Calm, 2008).

The second generation emerged in the late 1920s, when Thomas Midgley Jr. developed chlorofluorocarbons (CFCs), like R-11 and R-12, significantly reducing the risks of toxicity and flammability for household refrigeration. The 1950s saw the rise of hydrochlorofluorocarbons (HCFCs), which further enhanced safety for domestic use (Calm, 2008).

In an effort to preserve the ozone layer, the third generation came into effect post-1985 with global agreements like the Vienna Convention and the Montreal Protocol, facilitating a switch to hydrofluorocarbons (HFCs) (Vienna Convention for the Protection of the Ozone Layer, 1985; Montreal Protocol on Substances That Deplete the Ozone Layer, 1987). This shift successfully curtailed ozone depletion, stabilizing stratospheric ozone levels by the late 1990s (Ritchie et al., 2023).

Today, the focus is on combating climate change. The Kyoto Protocol addressed greenhouse gases but neglected certain ozone-depleting substances that exacerbate global warming (The Kyoto Protocol to the UNFCCC, 1997). This oversight prompted regions to

[8] The R-designation is the ASHRAE standard naming system for classifying refrigerants. It consists of "R-" followed by a unique number (e.g., R-134a). This system helps identify refrigerants based on their properties and chemical composition (ASHRAE, 2019).

enforce stringent measures like the European F-gas directive, leading to the fourth-generation refrigerants with low global warming potential (GWP) (Regulation on Fluorinated Greenhouse Gases, 2014). This directive phased out high-GWP refrigerants in domestic refrigerators by 2015 and will extend the ban to larger air conditioning systems by 2025.

2.3.4.2 The Status Quo of Refrigerant Choices: Tradeoffs Abound

Manufacturers are crafting low-GWP refrigerants to meet the F-gas directive, balancing environmental impact, safety, and efficiency. For instance, R-410a, a substitute for R-22, has zero ozone depletion potential (ODP) but has a higher GWP by 16% as shown in Table 3, and reduces energy efficiency by 6% (Calm, 2008). Fluoro-olefins, like R-1234yf, offer lower ODP and GWP, but they're less stable and more toxic, potentially breaking down into other high-GWP substances, leading to complex interactions and trade-offs among environmental goals.

The European Commission's research into eco-friendly refrigerants highlights R-32's growing use in air conditioners for its lower GWP relative to traditional HFCs like the widely used R-410a (European Commission, 2020). Moreover, natural refrigerants such as CO_2, ammonia, and hydrocarbons like propane are becoming popular in various applications due to their near-zero GWP.

2.3.4.3 Natural Refrigerants

Natural refrigerants are compounds that occur naturally in the environment and can be used as cooling agents in refrigeration systems. They have regained attention as potential alternatives to commonly used HFCs like R-134a and R-22 in recent decades due to their low environmental impact. Commonly investigated natural refrigerants include carbon dioxide propane ammonia and water (Alsouda et al., 2023; Fedele et al., 2023; Singh & Jitendra, 2022).

Carbon dioxide (CO_2 / R-744), is non-flammable and used in industrial cooling and heat pump water heaters in Japan (Hashimoto, 2006). Propane (C_3H_8 / R-290), a flammable hydrocarbon, is commonly employed in domestic refrigerators, freezers, and air conditioning systems (UNEP, 2022). Ammonia (NH_3 / R-717), despite its toxicity and flammability in certain scenarios, has over a century of use, particularly in Northern Europe's industrial refrigeration and food processing sectors (Calm, 2008). Water (H_2O / R-718), serves as a common refrigerant in large absorption chillers.

All of these natural refrigerants have an ozone depletion potential (ODP) of zero and—with the exception of carbon dioxide—also boast a GWP of zero, as shown in Table 3 (Hodnebrog et al., 2020).

Table 3: Global warming potential (GWP) of common and potential future refrigerants. Based on (Hodnebrog et al., 2020).

Refrigerant	GWP (kg CO_2eq/kg)
R-404a	4,985
R-410a	2,376
R-22	2,058
R-407c	2,005
R-134a	1,603
R-32	809
R-152a	172
CO2 (R-744)	1
R-1234yf	1
Ammonia (R-717)	0
Water (R-718)	0
Propane (R-290)	0

2.3.5 Predominant Cooling Technologies

Cooling methods fall into two categories: active and passive. Active cooling employs mechanical systems to actively extract heat, while passive cooling utilizes natural processes and design features to control temperature without mechanical intervention. While active cooling dominates current practice, passive cooling is gaining ground as it aligns better with sustainable building design.

2.3.5.1 Active Cooling

While the basic mechanism of cooling remains the same for most active cooling technologies, its implementation varies per technology. Active cooling can be subdivided into three main types: traditional air conditions, heat pumps, and district cooling (IEA, 2018a). Traditional air conditioners are commonplace in residential and office (RO) sectors in the form of portable air conditioners, split air conditioners, and chillers, as shown in Figure 11. Portable air conditioners are standalone units that are easy to install, typically needing just a venting hose. They operate by drawing indoor air to cool the condenser and venting it outside. Despite their convenience, they are often less energy efficient and slower to cool due to air circulation limitations. However, their ease of

installation and relatively low cost have rendered them popular among homeowners, especially in the U.S.

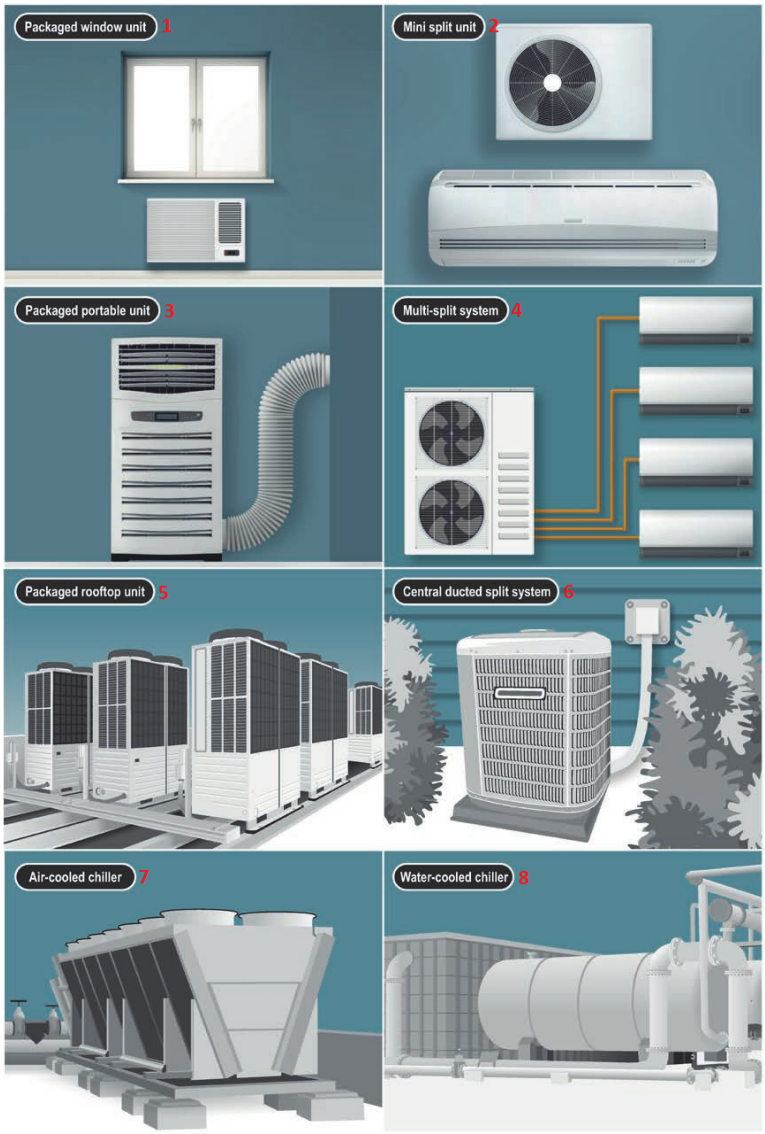

Figure 11: The most common types of cooling devices, from (IEA, 2018a).

Split air conditioners have two components: an outdoor condenser and an indoor evaporator, which allows for improved heat exchange and overall efficiency. They are particularly favored in European households and come in varying configurations from single indoor units to multiple evaporator setups for larger spaces.

Chillers, commonly used for large-scale commercial and industrial cooling, use a secondary loop of water or air to remove heat from their condensers, as shown in Figure 12. This coolant can be sourced naturally and is either released or cycled between the condenser and a cooling tower or heat exchanger. Although more sophisticated and

expensive than standard ACs, chillers are more efficient for larger buildings. They typically achieve lower condensing temperatures, which improves cooling efficiency.

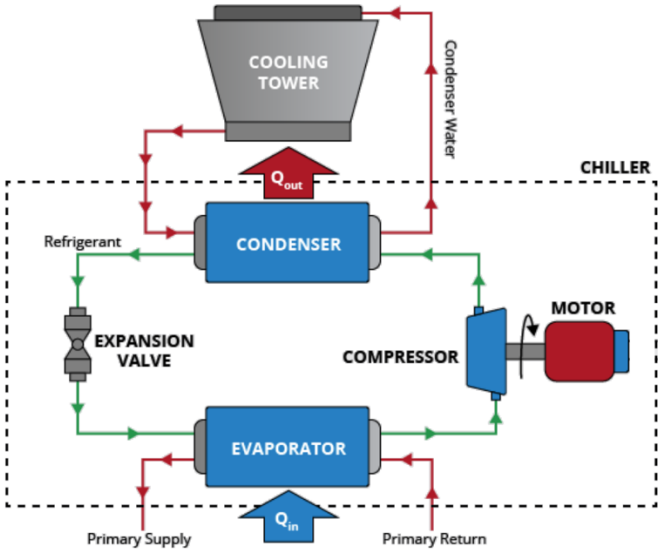

Figure 12: Diagram of water-cooled chiller. Adapted from (HVAC Investigators, 2020).

Reversible heat pumps, as an alternative to conventional air conditioners, serve the dual purpose of heating and cooling environments efficiently (Valancius et al., 2019). Heat pumps use the inverse vapor-compression cycle for heating and, through the actuation of a 'reversing valve'—not present in all models—they can reverse their operation to provide cooling, as depicted in Figure 13. Reversible heat pumps come in packaged systems, which are often used in commercial buildings, or split systems, which are more common in residential settings. Their dual-function capability makes them an energy-efficient choice and lends to their climate resilience, an important feature in an era focused on reducing energy consumption. Reversible heat pumps come in three main types, depending on the external medium they draw exchange heat with: air, ground, or water.

Air source heat pumps are the most akin to traditional air conditioners, drawing or expelling heat from the air outside, depending on the required function. They are the most straightforward to install, compact for residential use, and generally the most cost-effective. However, their efficiency can be less than that of ground or water source pumps. Ground source heat pumps need a network of underground pipes to circulate a fluid, taking advantage of the ground's relatively constant temperature to transfer heat. Their superior efficiency comes at the cost of a higher initial outlay and the need for significant land for installation, making them better suited to large complexes rather than individual

homes. Water source heat pumps, meanwhile, rely on a body of water for their heat exchange, with installation complexity and costs varying based on the site.

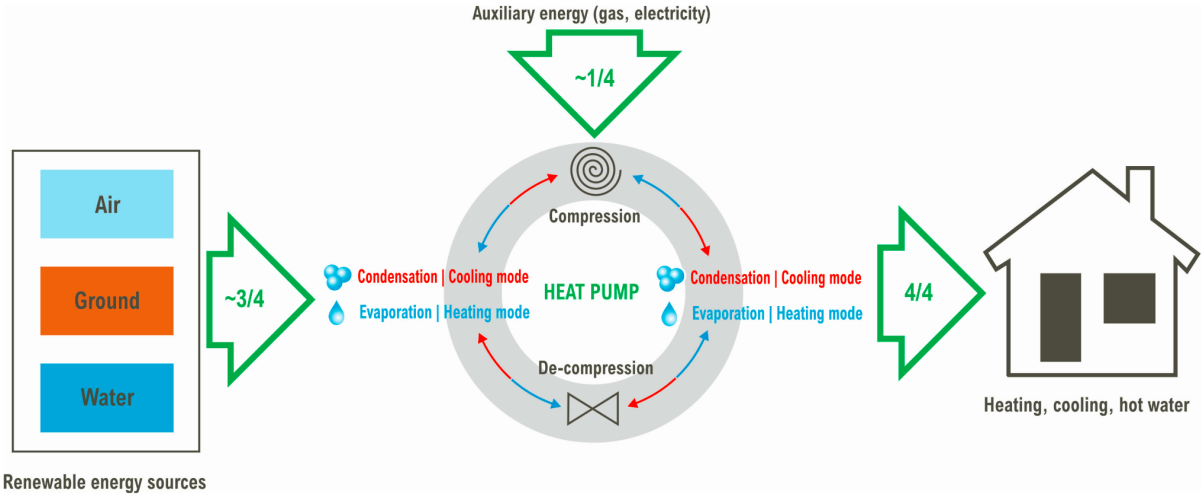

Figure 13: Mechanics of heat pumps used for cooling (in blue) or heating (in red), from (Valancius et al., 2019)

Beyond these, alternative cooling methods like district cooling are emerging as innovative and sustainable solutions for urban areas, functioning via a centralized system that sends chilled water from a large chiller in a central plant to multiple buildings through insulated piping (Inayat & Raza, 2019). The water, after absorbing heat from the buildings, returns to the plant to be re-chilled. This system's centralized nature allows for energy conservation, reduced environmental impact, and ease of maintenance, fitting for densely populated areas.

Though not a direct cooling strategy, mechanical ventilation is pivotal for thermal comfort through proper airflow and indoor air quality management. Active ventilation, including fans and sophisticated systems with sensors and controls, ensures an optimal indoor environment (Zmeureanu & Yu Wu, 2007). Energy recovery ventilators are particularly effective in conserving energy by transferring thermal energy between incoming and outgoing air streams (Kragh et al., 2005). Such active ventilation is essential in modern airtight buildings to maintain healthful indoor air standards while curbing energy use, thereby supporting sustainable and comfortable living spaces.

2.3.5.2 Passive Cooling

Besides using mechanical cooling, buildings can also be cooled in passive ways. Passive cooling uses natural mechanisms and architectural design to cool without the need for energy input or refrigerants. The most common passive cooling method is simply natural

ventilation, letting outside air carry heat away from a room by opening a window. This method is taken a step further by implementing electronic optimization of ventilation rates and duration, as well as night ventilation: mostly ventilating at night as the outside air is cooler at that time (Solgi et al., 2018).

Phase change materials (PCM) are a recent development in passive cooling. Their working is similar to evaporation: a solid material takes up heat from its surroundings by changing to a liquid phase (melting). Using materials with melting temperatures close to room temperature, they can cool a house during the day by melting and solidify again during the night (Farid et al., 2004). PCMs can play an important role in passive cooling systems due to their capability to absorb and release significant amounts of thermal energy during their phase change. PCMs include paraffins, salt hydrates, and fatty acids. However, their production can involve energy-intensive processes and the use of potentially harmful chemicals, raising environmental concerns (Memon, 2014).

In addition, architectural choices such as building orientation, insulation, shading features, and building material selection with regards to thermal mass can also be considered passive cooling (see section 2.2.2 for more detail). Another type of passive cooling is evaporative cooling. Evaporative cooling relies on the natural process of water evaporation to reduce indoor temperatures. In an evaporative cooling system, air is passed over water-saturated pads or media, causing the air to absorb moisture and lower in temperature. The cooled, moist air is then distributed into the indoor space. Evaporative cooling is energy-efficient and environmentally friendly, particularly effective in dry and arid climates. It offers an affordable alternative to traditional air conditioning, but its effectiveness depends on humidity levels, making it less suitable for humid regions.

Passive cooling is integral to sustainability, cutting energy use and aiding climate mitigation. Advances in materials, design, and technology are refining passive cooling for diverse climates. As green building norms and energy efficiency gain traction, passive cooling is set to be key in developing eco-friendly, durable, and comfortable buildings.

2.3.6 Material Makeup

Active space cooling systems are constructed out of an array of materials, with some bearing significant environmental implications and supply chain concerns. An overview of the materials used in air conditioners and their impacts is provided in Table 4.

Table 4: Overview of materials typically present in air conditioners. Based on (Li, 2015).

Material	Description
Copper	Copper is prominently used in heat exchangers and refrigerant lines, especially within split indoor/outdoor HVAC systems. Although it is not classified as a CRM, its unparalleled thermal and electrical conductivity attributes render it critical, especially for a myriad of renewable energy technologies. The demand for copper is anticipated to witness a substantial surge, driven by the increasing adoption of renewable energy sources in the foreseeable future. However, the environmental footprint of copper mining includes land degradation, water contamination, and soil erosion (DeWit, 2020; Elshkaki et al., 2016).
Aluminum	Aluminum finds its primary application in condenser and evaporator coils, as well as in duct systems of HVAC units. Its lightweight nature combined with impressive thermal conductivity makes it an ideal choice not only for HVAC systems but also for electric vehicles and renewable energy apparatuses. As the world leans more towards renewables, the demand for aluminum is projected to rise significantly (DeWit, 2020). However, aluminum production is energy-intensive with significant environmental impacts. It contributes to 1% of human-caused GHG emissions, emitting 0.45-0.5 Gt of CO2 equivalents annually (Brough & Jouhara, 2020).
Refrigerants	Refrigerants, especially Hydrofluorocarbons (HFCs), play a pivotal role in heat transfer in air conditioning systems. These HFCs are synthesized using fluorspar, a CRM predominantly extracted in regions like China, Mexico, and South Africa. The environmental challenges posed by fluorspar mining are considerable, leading to water and soil pollution. Moreover, the geographically concentrated production of fluorspar raises supply chain apprehensions (McCulloch & Lindley, 2003).
Steel	Steel is integral to the structure and function of HVAC systems, being used for casings, frames, and a variety of internal components. The production process of steel is notably resource-intensive, demanding vast energy inputs, predominantly sourced from coal. This results in significant greenhouse gas emissions. Furthermore, the water-intensive nature of steel production and the environmental risks posed by iron ore extraction, a primary ingredient for steelmaking, cannot be overlooked (Olmez et al., 2016)
Plastics	Plastics in HVAC systems are utilized for casings, insulation, and other minor components. Predominantly petrochemical-based, their production contributes to increased fossil fuel demand. Post their lifecycle, plastics present significant waste management challenges, often ending up in landfills or being improperly discarded, leading to severe environmental pollution (Geyer et al., 2017).
Electronic components	Electronic components are vital for the seamless operation of HVAC systems. These components, which include sensors, control units, and printed circuit boards, house a diverse range of metals like gold, silver, copper, silicon, and various CRMs and REEs. The extraction of these materials can lead to habitat destruction, soil and water pollution, and the generation of hazardous waste. Moreover, the low end-of-life recovery and recycling rates for these materials exacerbate resource depletion and waste accumulation challenges (Canal Marques et al., 2013; Robinson, 2009).

Central to these are metals like copper, steel, and aluminum, as well as electronic components which often contain critical raw materials (CRMs) and rare earth elements (REEs). CRMs are a group of raw materials that are considered essential for the economy and whose supply may be at risk due to various factors, including geopolitical instability, supply chain vulnerabilities, or environmental concerns (Baranzelli et al., 2017). However, the exact CRM inventory of ACs is yet unknown, and this is expected to be the case with other cooling technologies as well (Heikkilä, 2008).

Emerging cooling technologies like PCMs offer potential alternatives, yet their environmental impacts remain unclear due a current lack of comprehensive life cycle assessments.

2.3.6.1 Waste Generation

In their end-of-life phase, air conditioners and other space cooling equipment is classified as Waste Electrical and Electronic Equipment (WEEE), such as air conditioners, is a significant concern for various reasons beyond its carbon impact. In 2019, 53.6 million metric tonnes of WEEE, or e-waste, were generated globally, with just 17% formally collected and recycled (Forti et al., 2020). A substantial proportion of the remaining 83% of e-waste, particularly from high-income countries, is illegally exported to informal facilities in Africa and Asia. These facilities typically lack the necessary safety measures, posing severe environmental and health hazards due to the unsafe extraction and disposal of valuable and hazardous substances such as heavy metals and persistent organic pollutants. Secondly, the low recovery rate of valuable materials, such as copper, aluminum, and CRMs, represents a significant economic loss and contributes to resource depletion.

To combat these issues, the Netherlands and the EU at large have committed to circular economy strategies aiming at minimizing waste and maximizing resource efficiency. The European Circular Economy Action Plan identifies electronics as a key product value chain, emphasizing eco-design, repair, reuse, and responsible recycling (A New Circular Economy Action Plan For a Cleaner and More Competitive Europe, 2020). In this context, the management of materials in space cooling equipment and the waste they generate become increasingly significant. The Dutch government's Circular Economy Implementation Program 2019–2023 further promotes circularity in electronics by encouraging business models based on service, sharing, and lease (Rijksoverheid, 2019).

Understanding and improving the material efficiency and waste handling of space cooling equipment aligns directly with these policy goals.

In conclusion, the environmental impacts and supply chain vulnerabilities of space cooling equipment are closely tied to the materials they are composed of. Addressing these issues involves more sustainable material sourcing, improving material efficiency, and promoting R-strategies for cooling devices.

2.3.7 Market Penetration and Cooling Technology Mix

Globally, the residential market penetration rate (MPR) of ACs is currently at 30% of households (IEA, 2018a). This is expected to more than double to 64% by 2050. Consequently, the global air conditioner stock is anticipated to increase from 1.6 billion to 5.6 billion devices, as shown in Figure 14 (IEA, 2018b).

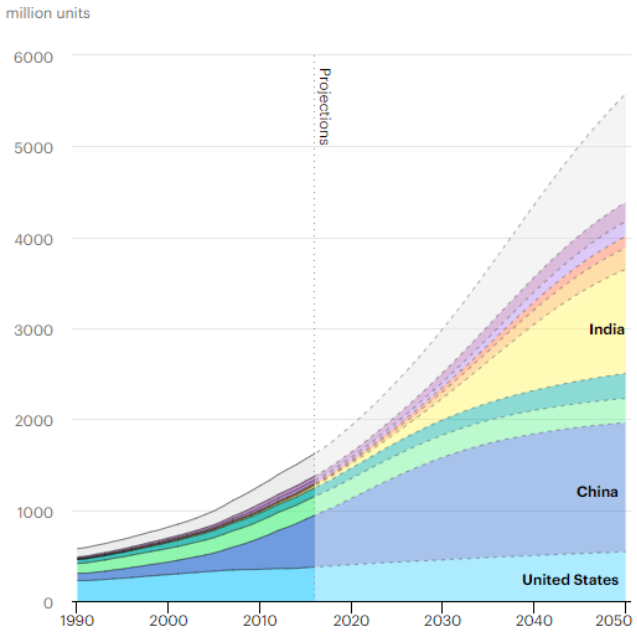

Figure 14: Global air conditioner stock, 1990-2050, from (IEA, 2018b).

However, research on the market penetration of cooling equipment in the Netherlands has been limited. An early study estimated the market penetration of residential cooling systems at 1.5% (van Kempen, 2000). However, more recently, a survey was performed by TNO (Netherlands Organization for Applied Scientific Research) to gauge the MPR for varying cooling technologies in Dutch residences (Rovers et al., 2021). The main results of this survey are presented in Table 5.

The average MPR of cooling equipment in Dutch residences was determined by TNO to be 18%. Besides this, the data point at several noteworthy trends. First is the prevalence of portable air conditioners, constituting half of all cooling equipment installations within the surveyed sample. Large split-type air conditioners make up 39% of the installed cooling systems, while ground source heat pumps and other cooling equipment are less popular, making up the remaining 11%.

Table 5: Survey results on the market penetration rate of cooling equipment, broken down to portable AC, large split AC, and ground-source heat pumps (GSHPs), based on income, location, and building type. Adapted from (Rovers et al., 2021).

		Portable AC	Large split AC	GSHP	Other	Total
Household income	< €15,000	4.4%	0.9%	0.5%	0.0%	5.7%
	€15,000–€30,000	10.3%	4.1%	0.5%	0.5%	15.3%
	€30,000–€60,000	9.1%	6.5%	0.6%	0.0%	16.2%
	> €60,000	12.6%	13.9%	3.0%	0.9%	30.4%
Location	Amsterdam The Hague Rotterdam	7.0%	1.8%	0.5%	0.1%	9.5%
	North-Holland South-Holland Utrecht	6.7%	5.8%	1.2%	0.6%	14.4%
	Friesland Groningen Drenthe	17.2%	6.9%	0.0%	0.0%	24.1%
	Overijssel Gelderland Flevoland	7.5%	7.5%	1.3%	0.0%	16.3%
	Limburg North-Brabant Zeeland	10.0%	12.9%	1.0%	0.0%	23.9%
Building type	Row house (terraced)	6.2%	5.5%	0.5%	0.2%	12.4%
	Row house (corner)	7.2%	8.7%	1.4%	0.0%	17.3%
	Semi-detached	12.9%	17.4%	1.9%	0.7%	32.8%
	Detached house	8.9%	13.7%	3.2%	1.6%	27.4%
	Apartment	11.3%	2.4%	0.9%	0.0%	14.5%

Also worth noting is the strong correlation between household income and the ownership of active cooling equipment, which is supported by a high coefficient of determination (R^2) of 0.91, as shown in Figure 15. From Table 5 it seems that high-income households are not only more likely to have installed active cooling equipment but also that they tend to opt for more advanced and expensive cooling systems such as heat pumps, which come at a higher cost than split-type and portable ACs.

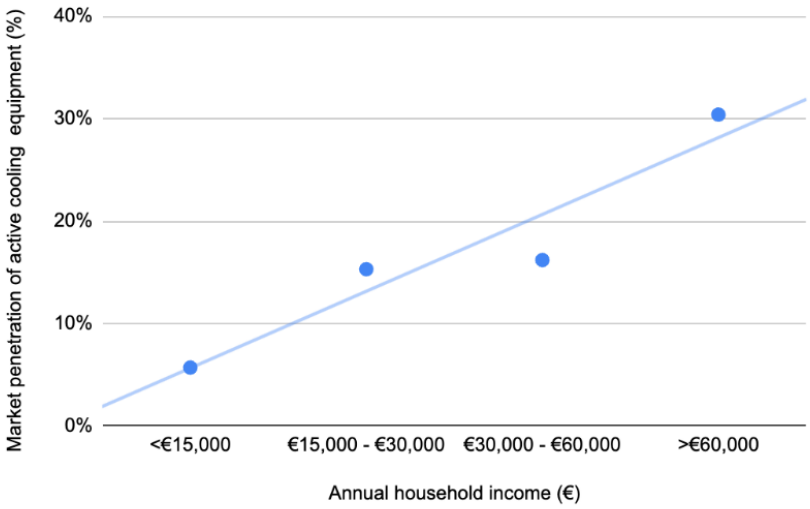

Figure 15: Market penetration rate of active cooling equipment per household income in the Netherlands. Based on (Rovers et al., 2021).

Furthermore, the MPR of cooling equipment varies by region. The MPR in major Dutch cities—including The Hague—is lower at 10% compared to the national average of 18%, likely due to the presence of lower-income neighborhoods in urban areas. In contrast, cities, especially lower-income urban neighborhoods, face more pronounced heat stress challenges due to the UHI effect, introducing a dimension of climate injustice into the equation. This is elaborated upon in section 2.4.2.2.

Lastly, the breakdown of MPR by building type reveals that freestanding houses exhibit a higher prevalence of cooling equipment usage. This trend can also likely be attributed to the generally higher income levels associated with these housing types.

2.4 The Impacts of Cooling

The following section delves in the impacts of the growing demand for space cooling, highlighting environmental issues like rising energy consumption, greenhouse gas emissions, and resource depletion; as well as social issues such as health risks and climate inequality.

2.4.1 Environmental Impacts

The growing demand for space cooling has various environmental impacts. Most notable are GHG emissions from electricity use and refrigerant leaks during the use-phase of cooling equipment. Additionally, the production and end-of-life stages of these devices

contribute to resource depletion and ecotoxicity, as well as accounting for nearly 30% of the associated GHG emissions (Yanagitani & Kawahara, 2000).

2.4.1.1 Electricity Use

Currently, space cooling consumes 2 PWh of electricity annually, equivalent to 10% of global electricity usage (IEA, 2018a; U.S. Energy Information Administration, 2023). By 2050, this is expected to triple to 6 PWh, while some studies suggest even more significant growth to 17 PWh (IEA, 2018a; Santamouris & Vasilakopoulou, 2021; U.S. Energy Information Administration, 2023). There is a broad consensus that space cooling will become the primary component of building-related energy consumption by 2100 (Santamouris & Vasilakopoulou, 2021). In the EU, space cooling is projected to rise by 60%, from 135 to 220 TWh by 2050 (IEA, 2018a). There is limited research on space cooling energy use in the Netherlands, but estimates for residential space cooling range from 0.15 to 0.26 TWh, accounting for 0.14% to 0.26% of total electricity demand (CBS, 2023a; Rovers et al., 2021). These estimates are likely conservative, as they are based on an MPR of cooling equipment below 5% and may underestimate actual space cooling energy consumption.

The anticipated rise in energy demand for space cooling poses a challenge to electricity grids worldwide, including the Netherlands. Many grids are already operating near their limits, and the additional strain from increased cooling needs can lead to grid instability and power shortages (NOS, 2023a; TenneT TSO B.V., 2022).

Energy efficiency of cooling equipment

The energy efficiency of cooling equipment strongly influences electricity consumption from space cooling. Improving energy efficiency is a key strategy to reduce energy consumption and related GHG emissions from space cooling. On a European level Minimum Energy Performance Standards (MEPSs) and energy labeling for household cooling equipment requirements are in place to ensure a sufficient standard of energy efficiency (Ecodesign Requirements for Household Refrigerating Appliances, 2009; Ecodesign Requirements for Air Conditioners and Comfort Fans, 2012; Eurovent Certification, 2022). However, Dutch policy lacks specific energy efficiency requirements for space cooling equipment.

Several key drivers influence the energy efficiency of cooling equipment. Firstly, technological advancements continuously increase energy efficiencies (IEA, 2018a).

Recent EU policies have introduced stricter MEPS for certain equipment types, with revisions anticipated to further improve efficiency (Ecodesign Requirements for Air Heating Products, Cooling Products, High Temperature Process Chillers and Fan Coil Units, 2016). Secondly, socio-cultural factors including environmental awareness drive demand for energy-efficient equipment. Consumers have historically chosen more efficient alternatives as they become available. Finally, economic factors, including GDP per capita and equipment prices, influence the adoption of high-efficiency cooling equipment. Rising electricity costs can encourage consumers to invest in more efficient options. Notably, the energy efficiency often carries more weight than electricity price in determining consumer preferences (Rapson, 2014). With the guide of policy and regulation, these drivers collectively determine average energy efficiency of cooling equipment.

Greenhouse Gas Emissions from Electricity Consumption

GHG emissions from using electricity for space cooling are determined by the carbon intensity of electricity generation. This refers to the emissions produced per unit of generated energy and is commonly measured in g CO_2-eq/kWh or kg CO_2-eq/kWh. This intensity varies based on the mix of energy sources used for electricity generation, or the electricity grid mix. Carbon intensity of electricity depends heavily on geographic location, as displayed in Figure 16. Regions with a high cooling demand also tend to have worse-than-average carbon intensities. For example, in recent years, large heatwaves have plagued regions like the Indian subcontinent and the Arabic Peninsula, which are characterized by carbon inefficient electricity grids. As long as the global electricity mix remains dominated by fossil-fuels, the electricity demand from space cooling will produce significant GHG emissions. Currently, the total estimated carbon footprint of global space cooling-related electricity use being 1.14 Gt CO_2-eq in 2016 (BP p.l.c., 2022; IEA, 2018a).

As for quantifying the carbon intensity of the electricity production mix, two main measures exist: direct GHG emissions and life-cycle GHG emissions. These are also referred to as Scope 1 and Scope 3 emissions, respectively. Scope 1 emissions are direct GHG emissions at the power generation site, primarily from burning fossil fuels. Scope 1 emissions are simpler to calculate and easier to manage in complex scenarios. European and Dutch reporting organizations mainly use Scope 1 emissions data (EEA, 2023), and Statistics Netherlands (CBS) explicitly exclude life-cycle impacts from their reports (CBS, 2015; Harmelink et al., 2012).

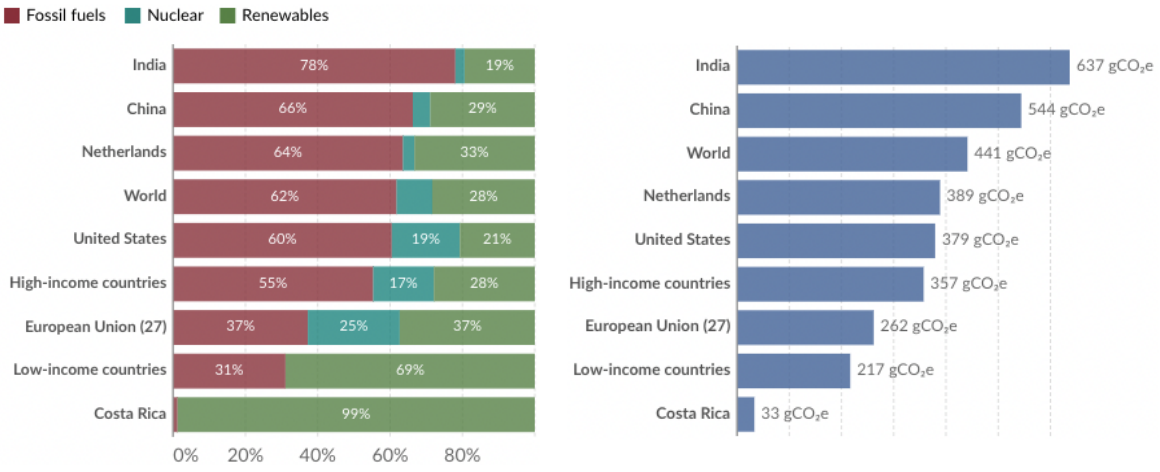

Figure 16: Electricity source mix (left) and carbon intensity, including life-cycle emissions (right), for a selected number of regions, based on (Ritchie et al., 2022).

Scope 3 emissions encompass indirect greenhouse gas emissions throughout the entire life cycle of electricity production, including externalized impacts from, for instance, constructing wind turbines, mining coal, transporting biomass, or decommissioning nuclear power plants. Even when the local electricity grid has a low carbon intensity, upstream and downstream impacts from regions with carbon-intensive grids contribute to Scope 3 emissions.

The differences between these scopes can be significant. For instance, including life-cycle emissions for EU electricity production in 2019 resulted in a 31% higher carbon intensity than commonly reported Scope 1 emissions, as shown in Figure 17.

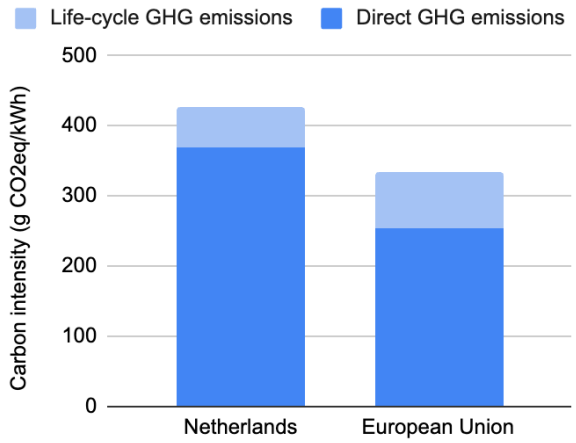

Figure 17: Comparison of direct and life-cycle carbon intensities of the 2019 EU and Dutch electricity grids, based on (EEA, 2023; Scarlat et al., 2022; van der Niet & Bruinsma, 2022).

Evolution of the Global Electricity Grid

While expected to rise, global electricity demand is outpaced by the projected growth in low-carbon energy sources, achieving absolute decoupling of electricity generation and GHG emissions by 2030 across all IEA scenarios, shown in Figure 18 (IEA, 2021b).

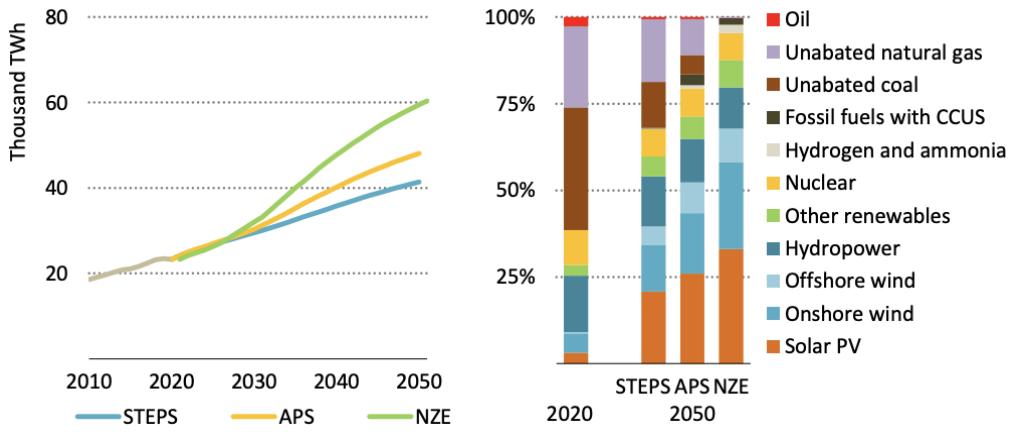

Figure 18: Expected global electricity demand and electricity production mix, for multiple IEA scenarios: the Stated Policies Scenario (STEPS), the Announced Pledges Scenario (APS), and the Net Zero Emission by 2050 scenario (NZE); from (IEA, 2021b).

However, historical progress in expanding renewable electricity generation is not meeting the goals set by the Paris Agreement, which aims for net-zero emissions by 2050 (IEA, 2021b). To achieve this, installation of renewable electricity capacity must occur 80% faster than current rates (IEA, 2021a). While absolute decoupling of global electricity production and GHG emissions is anticipated, the demand for cooling is expected to outpace grid decarbonization rates. The carbon footprint of space-cooling is projected to increase from 1.14 Gt to 2.07 Gt by 2030, or an increase from 8% to 15% of global electricity-related GHG emissions (see Figure 19) (IEA, 2018a).

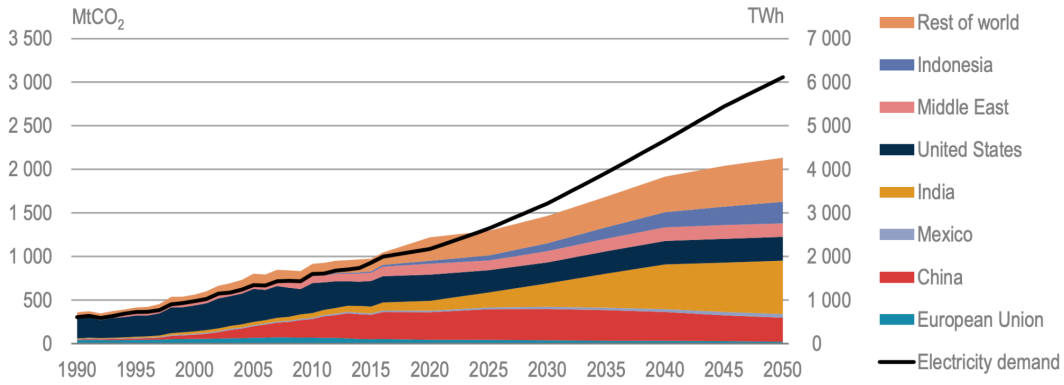

Figure 19: Historical and projected electricity demand and GHG emissions from space cooling, 1990–2050, from (IEA, 2018a).

Evolution of the Dutch Electricity Grid

Figure 20 shows that natural gas currently makes up most of the Dutch electricity production mix (58%). Coals and other fossil fuels make up another 17%, putting the share of low-carbon sources at only 24%. As a result, the Dutch electricity grid has a life-cycle carbon intensity of 427 g CO_2-eq/kWh, one of the highest in the EU, as detailed in Figure 21 (Ritchie et al., 2022; van der Niet & Bruinsma, 2022).

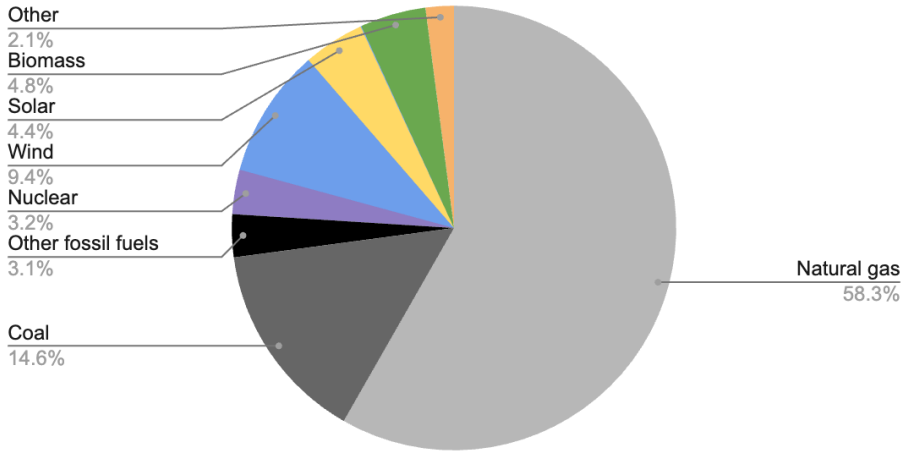

Figure 20: The 2019 Dutch electricity production mix. Based on (van der Niet & Bruinsma, 2022).

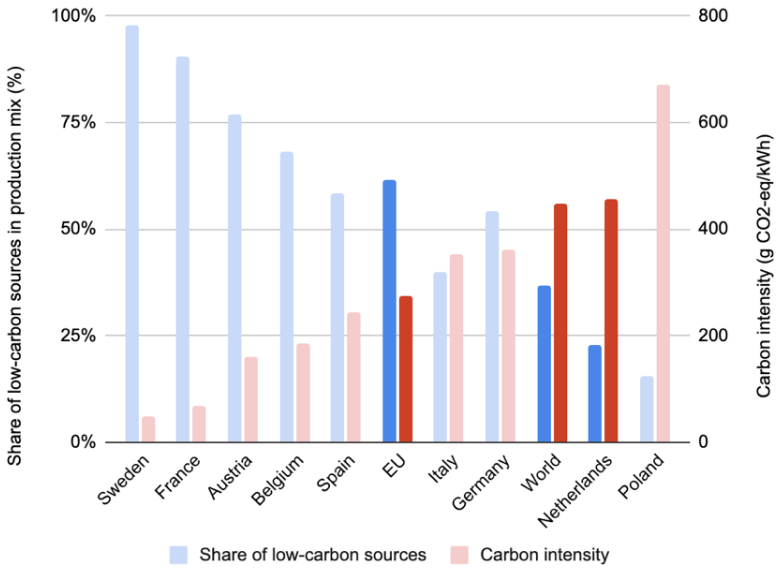

Figure 21: Carbon intensities and shares of low-carbon sources for selected EU electricity grids, 2019, based on (Ritchie et al., 2022).

In 2019, the Dutch Ministry of Economic Affairs and Climate introduced the "Integrated National Energy and Climate Plan 2021–2030," set the target of 26% renewable energy (including electricity, heat, and fuels) in the Dutch energy supply by 2030 (Ministerie van

Economische Zaken en Klimaat, 2019). In addition, the 2019 Climate Agreement ("Klimaatakkoord") set two main targets: a 49% reduction in greenhouse gas emissions by 2030 (compared to 1990 levels) and 100% carbon-neutral electricity generation by 2050 (Klimaatakkoord, 2019). However, declining natural gas availability due to the Russia-Ukraine conflict and the shutdown of the Groningen gas field has led to an increase in coal-based electricity generation in 2021, as depicted in Figure 22. This development jeopardizes the path to full decarbonization by 2050 outlined in the Climate Agreement.

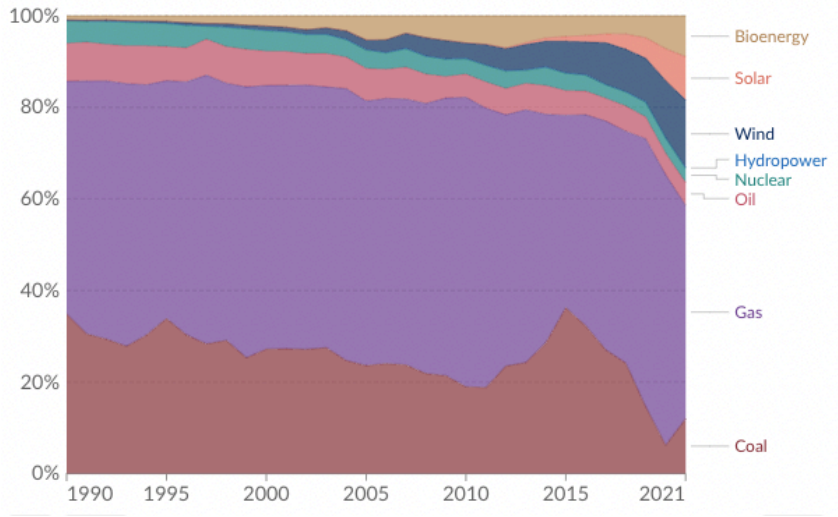

Figure 22: Evolution of Dutch electricity production mix, 1985–2021, based on (Ritchie et al., 2022).

2.4.1.2 Refrigerant Leaks

As mentioned in section 2.3.4, most common refrigerants have a high GWP, which is a concern when they leak through cracks or holes in the coils of air conditioning units. The rate at which these leaks occur is thus an important factor when assessing the climate impacts of space cooling. However, leakage rates vary significantly based on the type of equipment, the specific refrigerant used, and maintenance practices (Purohit et al., 2020). Residential air-conditioning units, for instance, exhibit annual leakage rates of approximately 1–5%, whereas portable air conditioners can exhibit much higher annual leakage rates, ranging from 10–20%, as shown in Table 6 (Penman et al., 2000).

Apart from the annual leakages that occur during the operational lifespan of air conditioners, it is important to acknowledge that leakages can also transpire during the assembly process and the end-of-life treatment of these units. Assembly-related leakages can stem from imperfect connections, faulty components, or human error during installation.

Table 6: Average refrigerant leakage rates, based on (Penman et al., 2000).

Application	Annual Leakage Rate
Domestic Refrigeration	0.1–0.5 %
Stand-Alone Commercial Applications	1–10 %
Medium and Large Commercial refrigeration	10–30 %
Transport Refrigeration	15–50 %
Industrial Refrigeration including Food Processing and Cold Storage	7–25 %
Chillers	2–15 %
Residential and Commercial A/C, including Heat Pumps	1–5 %
Portable Air Conditioners	10–20 %

Conversely, end-of-life treatment involves the disposal or recycling of air conditioners, which can lead to refrigerant leakage if not carried out properly. Refrigerant leaks across the product lifecycle contribute significantly to climate change. As mentioned in section 2.2.4.1, without a swift global phase-out of HFCs, these leaks alone could exceed the 1.5° C carbon budget (Dreyfus et al., 2020; Matthews et al., 2020).

HFC leaks have environmental impacts beyond contributing to global warming. As discussed in section 2.3.4, although they are less harmful to the ozone layer compared to CFCs, they still contribute to ozone depletion in significant quantities (Calm, 2002; Hurwitz et al., 2015). Additionally, some HFCs have shown toxicity to maternal and fetal development in rodent studies, raising concerns about ecotoxicity, which warrants further research (Ema et al., 2010)

Refrigerants also influence the environmental impacts of electricity use (discussed in section 2.4.1.1) because they affect the energy efficiency of cooling equipment. Each type of refrigerant has a particular efficiency in cooling the local environment, meaning gains or losses can be made in terms of energy use from active cooling technologies (IEA, 2018a).

2.4.1.3 Material Demand

Manufacturing the 4 billion cooling devices expected to be newly installed by 2050 puts a large toll on a number of material supply chains (IEA, 2018b; T. Peters, 2018). As mentioned in section 2.3.6, cooling technologies contain many materials, including CRMs and metals like copper, steel, and aluminum, each with considerable environmental and supply chain implications. Key components of air conditioning units, such as compressors, motors, and electronic controls, often contain CRMs, of which the extraction can lead to environmental damage and supply chain vulnerabilities due to geopolitical situations. Copper and aluminum extraction and refining can lead to environmental impacts, such

as land degradation, water pollution, and greenhouse gas emissions (Brough & Jouhara, 2020; Elshkaki et al., 2016). Refrigerants, particularly HFCs produced using fluorspar, are crucial in air conditioning systems but pose significant environmental impacts and supply chain concerns due to geographically concentrated production (McCulloch & Lindley, 2003). Other integral materials in these systems include steel, plastics, and electronic components, which contribute to energy consumption, waste generation, and environmental pollution due to their extraction and production (Canal Marques et al., 2013; Geyer et al., 2017; Olmez et al., 2016; Robinson, 2009). The improper handling of waste electrical and electronic equipment (WEEE) like air conditioners poses additional environmental and health risks and contributes to resource depletion due to low recovery rates of valuable materials (Robinson, 2009).

2.4.2 Social Impacts

In addition to environmental impacts, the widespread use of space cooling in urban areas carries significant social implications. These include concerns about public health, as cooling systems can cause noise pollution and can worsen the UHI effect, with potential health consequences. Furthermore, issues of climate justice emerge as the UHI effect tends to hit poorer areas hardest, and the cost of space cooling can be a burden on vulnerable populations. This section explores these social aspects of space cooling. Although they are important, social impacts are not explicitly modeled in the calculations and are beyond the scope of the research discussed in later chapters.

2.4.2.1 Health Impacts

Cooling systems have become indispensable in many parts of the world, significantly improving indoor comfort and human health during hot weather. However, it is important to recognize that these systems can have multifaceted impacts on human health, beyond their cooling benefits.

One significant concern is noise pollution. The operation of AC units, particularly in densely populated urban areas, can generate substantial noise levels (Claudia et al., 2017; Dandsena et al., 2021; Soeta & Shimokura, 2017). Prolonged exposure to such noise can lead to sleep disturbances, stress, and even adverse cardiovascular effects, impacting the overall well-being of residents (Basner et al., 2014; Geravandi et al., 2015; Jariwala et al., 2017).

Furthermore, the operation of AC units can contribute to the heating of microclimates, as discussed in section 2.2.3. As these systems expel heat into the outdoor environment, they can raise local air temperatures, up to 1 °C, contributing to the UHI effect, which further drives up cooling demand and risk of heat stress (Salamanca et al., 2014). This feedback loop, driven in part by the widespread use of ACs, can have significant health implications, particularly for vulnerable populations such as the elderly and those with preexisting health conditions.

2.4.2.2 Climate Justice and Urban Heat Islands: The Socioeconomic Implications of Space Cooling

Environmental justice encompasses the principles of fairness, equity, and justice, with the aim of rectifying the unequal distribution of environmental burdens and benefits among social groups (Schlosberg, 2013). Climate justice is a prominent example of this, which describes the disproportionate impact of climate change on disadvantaged and vulnerable communities, which bear the least responsibility for climate change (Barrett, 2013). To exacerbate this, these communities historically bear the least responsibility for climate change, with the Global North, comprising more affluent nations, responsible for a substantial 92% of excess GHG emissions (Hickel, 2020a). In contrast, the Global South bears 90% of the costs associated with the climate crisis and experiences 98% of the associated deaths (Hickel, 2020b; McKinnon et al., 2022).

This double inequality is not only present on a global scale, but also within the Netherlands. For example, the wealthiest 1 percent of the Dutch population is responsible for the majority of climate damage, emitting ten times more greenhouse gases than those with lower incomes (Ecorys, 2022). Over the past three decades, emissions from the poorest have fallen by 40 percent, while the wealthiest have reduced emissions by just 3 percent. Ironically, the wealthy receive more subsidies to reduce emissions but make limited progress. In 2017, Dutch households received €750 million in emissions reduction subsidies and tax incentives, with 80% going to rich households and 20% to poor households (Vergeer, 2017). This distribution can be attributed to the nature and eligibility criteria of these subsidies, which often require individuals to have substantial initial capital and ownership of homes or cars. Subsidies generally offer discounts on green investments, which, even with subsidies, often amount to several thousand euros, making them unaffordable for most low-income households.

One manifestation of environmental and climate injustice is the disparate distribution of the UHI effect. Research has shown that individuals of lower socioeconomic status or those living in disadvantaged neighborhoods often reside in areas with a higher density of built environments and fewer green and water spaces, resulting in a higher local UHI (Harlan et al., 2007; Sanchez & Reames, 2019). The increased exposure to UHI effects imposes a higher risk of heat stress and reduced air quality on these populations, with the potential to exacerbate pre-existing health conditions (Hajat et al., 2010).

The increased local temperature heightens the demand for cooling solutions like air conditioning. However, these individuals or communities generally lack the resources needed to afford such cooling equipment. Present and future air conditioning use is primarily concentrated in high-income households (L. Davis et al., 2021). This trend holds true not only on a global scale, where wealthier countries have greater air conditioning prevalence, but also within individual nations. This pattern is particularly pronounced in lower-income countries like Pakistan, where the vast majority of air conditioner adoption through 2050 is expected to occur among the upper-income segment.

In summary, the poorest nations and socioeconomic communities have limited access to cooling equipment. Given the high price elasticity of air conditioners (as discussed in section 2.2.4.2), people will typically choose to purchase more affordable air conditioners when their economic status improves. These cheaper air conditioners are associated with higher environmental impacts due to less energy-efficient design and the use of environmentally harmful materials and refrigerants (Gupta et al., 2021; UNEP, 2017). They typically also have shorter life spans, requiring more frequent replacement and increasing material footprint through greater waste generation and disposal. This leads to further financial strain due to higher electricity costs, and contributes to increased carbon emissions, exacerbating climate-related challenges. This cycle exemplifies cooling inequality, considering that the regions with the highest cooling demand, often in lower-income and tropical areas, typically have fewer resources available to provide efficient and environmentally friendly cooling solutions.

3 Research Design

This chapter provides a detailed overview of the research methodology, segmented into the following sections:

Scope: The temporal, geographical, technological, and environmental boundaries of the study are defined to establish the research context.

Modeling the Status Quo: The determination of present cooling demand in residential and office buildings in The Hague is explained. This process involves Geographic Information System (GIS) analysis to determine the building stock and its characteristics, along with thermodynamic modeling in Python for cooling demand calculations. Additionally, this section sets out the approach for estimating the environmental impacts associated with the calculated cooling demand.

Scenario Modeling: This part explores the drivers affecting cooling demand projections for 2030 and 2050. It explains the method of integrating these drivers into various scenarios, the computation of future cooling demand, and the associated environmental impacts within these scenarios.

Sensitivity Analyses and Extrapolation of Results: The robustness of findings is assessed through sensitivity analyses, and results are extrapolated to derive conclusions for the full residential and office building stock of The Hague.

3.1 Scope

This study focuses on The Hague, Netherlands, aiming to model both the current and future cooling demands of the city's residential and office (RO) buildings and the associated environmental impacts. Conducting a case study is a flexible method for qualitative analysis, particularly effective for in-depth exploration of complex, multi-faceted issues such as the increasing need for cooling and its environmental consequences (Creswell, 2014). This study adopts a bottom-up approach, using individual buildings and cooling devices as foundational elements for quantitative models. This approach allows for detailed analysis of energy consumption at the end-use level, providing a more nuanced understanding of technological options compared to broader top-down methods (Nouvel et al., 2017).

The study used a static thermodynamic model to assess cooling demands over various time frames. For current demand and impact analysis, a five-year period from 2018 to 2022 was selected to minimize weather pattern anomalies and ensure availability of complete yearly data, leading to the exclusion of 2023. The study used geospatial data from the 2023 version of the national Registry of Addresses and Buildings (BAG) to analyze the building stock (PDOK, 2023a). To calculate cooling demand, it relied on Royal Netherlands Meteorological Institute (KNMI) weather data from the Hoek van Holland station, which provides the most accurately available representation of local climate conditions (KNMI, 2023b). These weather series feature an hourly temporal granularity to reflect daily weather variations and the intermittent nature of space cooling needs. Future cooling demands and environmental impacts were modeled using KNMI climate scenarios and the '21 Climate Signal report, predicting weather patterns for 2030 and outlining several scenarios for 2050 (Attema et al., 2014; KNMI, 2021).

The building stock analysis includes residential and office buildings with energy labels, further categorized into eight distinct types by age and height, as shown in Table 7. Six prevalent active cooling technologies were considered in the model, while passive cooling was excluded due to the need for more dynamic modeling of thermal flows. This approach, accounting for the time-lag effects of thermal masses, demands a more complex and specialized modeling technique.

Environmental impacts were assessed across three categories: energy use, material demand, and greenhouse gas (GHG) emissions.

Energy use of space cooling equipment is a significant impact factor in the use-phase of space cooling equipment. Energy use was assessed independently from its climate impact for several reasons. While improving grid carbon efficiency can reduce GHG emissions from energy use, a strongly rising energy demand can still increase reliance on fossil fuels through second-order effects, particularly if the grid isn't fully decarbonized. A heightened energy demand not only contributes to climate change but also strains existing electrical infrastructures. Broader environmental effects of energy use, such as biodiversity loss, land use, air pollution, and resource depletion, are acknowledged but not quantified in this model (Dale et al., 2010; Demirbas, 2009; Tawalbeh et al., 2021; S. Wang & Wang, 2015)

Material demand was determined by estimating the total size of the total cooling equipment stock required to meet cooling demands, providing insights into both the

equipment mass and its impact on abiotic resource depletion (ADP) and the Crustal Scarcity Index (CSI). These impacts were annualized to illustrate the environmental consequences of the continuous introduction of new equipment and the disposal of old equipment.

Climate change impact of space cooling was determined by calculating GHG emissions from four sources across the cooling equipment's life cycle. Primary among these is electricity usage, which carries a carbon footprint due to the use of fossil fuels in power generation. Refrigerants used in cooling technologies, typically with high global warming potential (GWP), contribute to climate change through leaks during the use phase. Lastly, simplified life cycle assessment (LCA) methods were used to quantify GHG emissions associated with the production and disposal of cooling equipment, providing a comprehensive view of the environmental impact of cooling demand.

Table 7: Overview of scope and granularity for the research.

Dimension	Scope	Granularity
Geographic	The Hague municipality	Building-level
Temporal	Status quo: 2018–2022 Scenarios: 2030, 2050	Hourly
Technical: building types	Residential and office buildings Old and new buildings Low rise and high-rise buildings	–
Technical: cooling equipment	Air-Source Heat pump (ASHP) Ground-source heat pump (GSHP) Water-Source Heat pump (WSHP) Chiller Split AC Portable AC	–
Environmental impact	Energy use Material demand Climate change impact	–

3.2 Modeling the Status Quo

This section outlines the methodology used to answer the research questions:

1. *What is the current cooling demand in residential and office buildings in The Hague?*
2. *What are the environmental impacts of the current cooling demand in The Hague?*

The approach begins with the construction of a GIS model to collect detailed data on the current stock of residential and office buildings in The Hague. Following this, a Python-based thermodynamic model was utilized to evaluate the space cooling demand of these buildings over the 2018–2022 period, representing the status quo. Finally, the cooling demand was multiplied with a cooling technology matrix to determine each building's environmental impacts, which were then aggregated to determine the overall impacts. These three main data layers and examples of spatial results are shown in Figure 23.

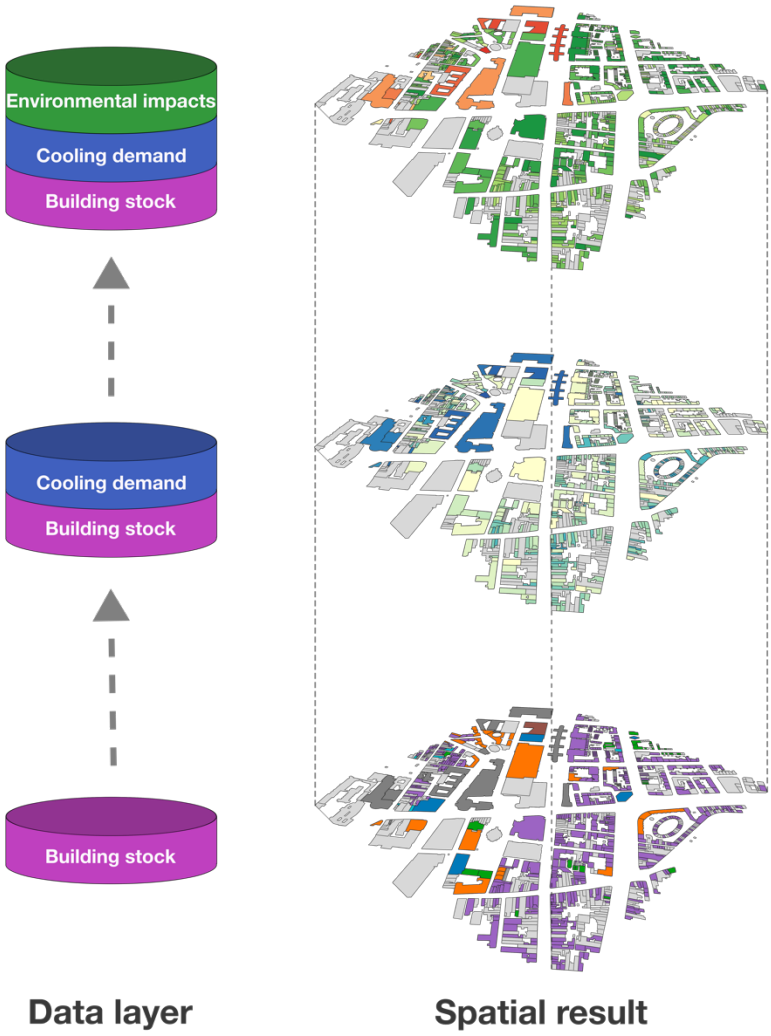

Figure 23: Diagram showing the main data layers used in the research and examples of their spatial results.

3.2.1 Geographic Information System Modeling

To determine the cooling demand of the residential and office building stock of The Hague, the required building characteristics were extracted and pre-processed using a GIS methodology. Specifically, QGIS and the GeoPandas library in Python were used for

spatial data processing (Jordahl et al., 2020; QGIS.org, 2023). For a detailed overview of the steps performed in the GIS software, please refer to Appendix B. For an overview of the raw spatial datasets used in the analysis, see Appendix A. Finally, for the implementation of the data extraction and processing in Python, please refer to the *gis.ipynb* Jupyter Notebook in Appendix C.

Data from the 2023 Registry of Addresses and Buildings (BAG) was used to model the current building stock of The Hague. This registry provides detailed shapefiles of all buildings (*Pand* layer) and point data for all residences (*Verblijfsobjecten* layer) across the Netherlands, including data like building age, end use (residential, office, commercial, etc.), and floor area. The BAG data was first trimmed to fit within The Hague's municipal boundaries using the Administrative Boundaries dataset (PDOK, 2023b).

This process identified a total of 157,784 buildings within The Hague. For thermodynamic modeling purposes, additional building features were derived. Using the shape area of each building, the roof and ground floor areas were determined. Building height was obtained from BAG 3D data, calculated by the height difference between ground and roof (R. Peters et al., 2022).[9][10] The building volume was then computed by multiplying this height with the ground floor area.

To account for building orientation, facade areas in each cardinal and ordinal direction were calculated. Buildings were approximated as rectangles using the Minimum Bounding Geometry function, yielding the width, length, and orientation azimuth φ of each minimum bounding rectangle (MBR). Buildings were classified into one of four main orientations based on this azimuth (see Figure 24 and Table 8). The facade surface area in each direction was determined by multiplying the width of each MBR side with the building height. For residential buildings, an average glazing percentage of **15%** was assumed, considering most row houses lack side windows. Office buildings, typically standalone with higher glazing percentages, were assigned a glazing percentage of **25%**.

[9] The BAG 3D database was not used as the main dataset as it does not include residence-level data or building function.

[10] Building height was calculated by subtracting the ground floor elevation from the 70th percentile of roof elevation, which excludes anomalies like spires and steeply slanted roofs that are not relevant for facade area and building volume calculations.

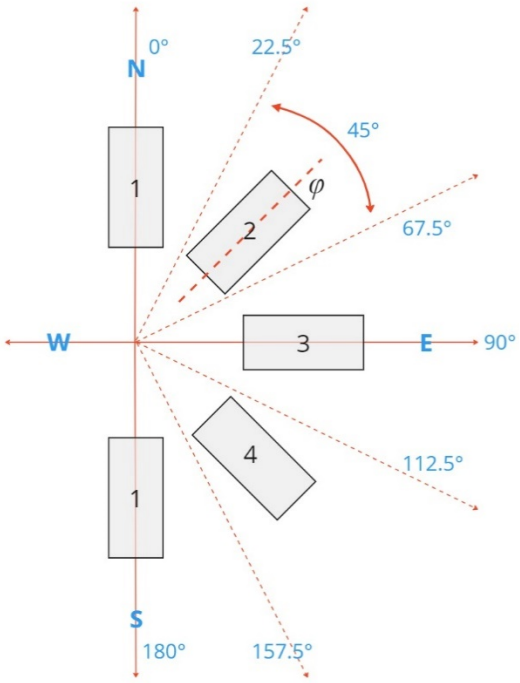

Figure 24: Facade orientation types.

Table 8: Facade orientation types.

#	Building direction	Range of polygon envelope azimuth
1	North–South	[0°, 22.5°], [157.5°, 180°]
2	Northeast –Southwest	[22.5°, 67.5°]
3	East–West	[67.5°, 112.5°]
4	Northwest–Southeast	[112.5°, 157.5°]

Energy label data was obtained from the Energy label registry (*EP-online*) and linked to the Residence layer using the BAG residence identification number (Rijksoverheid, 2023). Energy label data was accessible for 55% of the total floor area across all end uses, with availability rates of 61% and 68% for residential and office floor space, respectively.

As the model calculates cooling demand and impacts on a building-level, a spatial join operation was conducted to link residence-level data to BAG buildings. Firstly, the total floor area of each building was computed by summing the individual residence floor areas. The number of residences in each building was saved as well, to later determine the population size of each building. The primary end use within each building was determined by grouping the constituent residences based on their end use and selecting the end use with the largest floor area; buildings without a residential or office end use were excluded from the cooling demand model. Finally, for each building, the mean energy label was calculated by translating energy labels into numerical values, averaging them

based on residence floor areas, rounding to the nearest integer, and then converting them back into energy labels.

For this study, focusing on residential and office (RO) cooling, buildings were categorized into three end use types: residential, office, or other. This classification resulted in 89,399 RO buildings, accounting for 79% of The Hague's total floor space (see Figure 25). It is noteworthy that about a third of The Hague's buildings lacked a designated end use, necessitating their categorization as 'other.' However, many of these appeared to be non-heated or cooled structures like sheds or garages.

The analysis proceeded with the subset of RO buildings having available energy label data, which included 66% of RO buildings, accounting for 78% of the respective floor space.

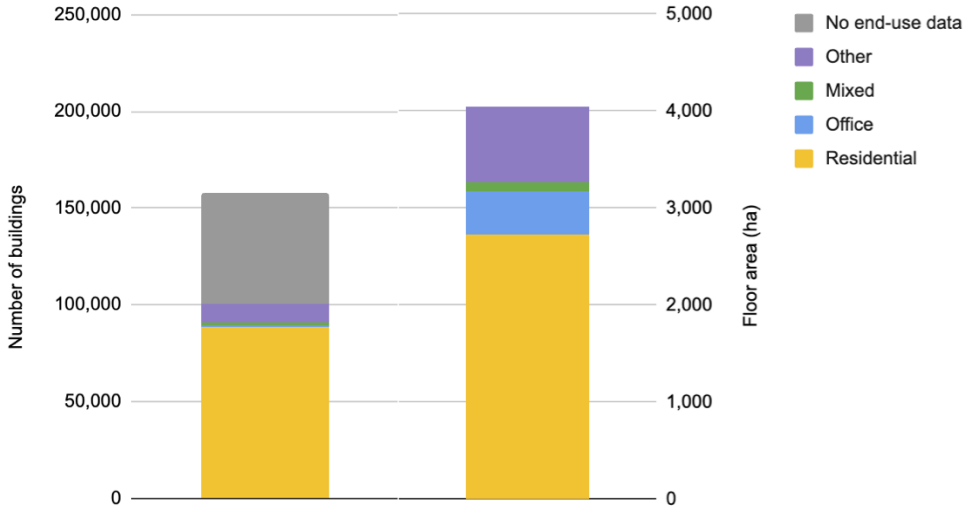

Figure 25: Building count and floor area per end-use in The Hague. Note that buildings without end-use data are not represented in the floor area data, as they do not have any residences registered to them and thus their floor area is not determinable either.

3.2.1.1 Building Types

Due to the lack of detailed, building-specific data on thermodynamic properties and to keep the model's scope within limits, a streamlined approach was adopted for categorizing buildings. This classification was based on end use, height, and construction year, with each building type assigned standard thermodynamic properties.

Buildings were initially divided by their end use as either residential or office. For height classification, the Netherlands defines high-rise buildings as those with five or more stories, averaging 3.5 meters each in height (Blok & Roemers, 2017). Consequently,

buildings standing at least 17.5 meters were classified as high-rise, while those shorter than this threshold were categorized as low-rise.

Table 9: Overview of building types selected for analysis.

Building type	End use	Height	Construction year
1	Residential	≥ 17.5 m	≥ 2003
2	Residential	≥ 17.5 m	<2003
3	Residential	< 17.5 m	≥ 2003
4	Residential	< 17.5 m	<2003
5	Office	≥ 17.5 m	≥ 2003
6	Office	≥ 17.5 m	<2003
7	Office	< 17.5 m	≥ 2003
8	Office	< 17.5 m	<2003

The construction year was the final classification criterion, differentiating between newer and older buildings. Significant changes in building codes occurred in 2012 and 2003 The cutoff year was set at 2003 since buildings constructed post-2012 only accounted for 5% of the total surface area, while those built after 2003 represented 18%. Based on these criteria, eight distinct building types were identified, detailed in Table 9.

3.2.2 Thermodynamic Modeling

After the basic building parameters of each residential and office building in The Hague were identified, the cooling demand for each building was calculated throughout the reference period (2018–2022). This was done with a static thermal balance model, referred to as the cooling demand model (CDM), to calculate the thermal balance for each hour in the reference period per building.[11]

A variety of methods exist for calculating the space cooling demand for a building. A straightforward static cooling demand model as outlined by Laure Itard was used for modeling purposes, through which the thermal energy balance of a building is calculated

[11] The thermodynamic model calculates thermal balances and can therefore also be used to determine heating demand. However, in this study, it will be referred to as a cooling demand model as it is solely used to find cooling demand.

in four main components (van Bueren et al., 2012). An overview of the parameters used in the thermodynamic model can be found in Appendix D to Appendix J.

The thermal energy balance approach determines heat flows in and out of the building to determine whether heating or cooling is needed, based on the first principle of thermodynamics. The building was treated as a single zone with consistent temperature and humidity, analyzing heat transfer through transmission, infiltration, ventilation, solar, and internal gains.

3.2.2.1 Transmission

Thermal energy transfer through the building envelope, caused by the temperature difference between indoor and outdoor air, can be quantified as transmission heat flows (P_{trans}) through a surface. These were calculated using Equation 3 and Equation 4 (van Bueren et al., 2012):

$$P_{trans} = U \cdot A\,(T_o - T_i) \quad [\mathrm{W}] \qquad \textit{Equation 3}$$

$$U = \frac{1}{\frac{1}{\alpha_i} + R_c + \frac{1}{\alpha_o}} \quad [\mathrm{Wm^{-2}K^{-1}}] \qquad \textit{Equation 4}$$

With:

- U: the transmittance of the surface [$\mathrm{Wm^{-2}K^{-1}}$] (see below)
- A: the area of the surface [$\mathrm{m^2}$]
- T_o: the outdoor temperature [K] (see below)
- T_i: the indoor temperature [K] (see below)
- R_c: the thermal resistance of the surface [$\mathrm{m^2KW^{-1}}$] (see below)
- Coefficients α_i and α_o represent the combined indoor and outdoor heat transfer coefficients for convection and radiation, respectively. Typically, α_i is 7.5 $\mathrm{Wm^{-2}K^{-1}}$ and α_o ranges from 25 to 30 $\mathrm{Wm^{-2}K^{-1}}$ (van Bueren et al., 2012). The following values were assumed in the CDM: $\boldsymbol{\alpha_i}$ **= 7.5** $\mathbf{Wm^{-2}K^{-1}}$ and $\boldsymbol{\alpha_o}$ **= 27.5** $\mathbf{Wm^{-2}K^{-1}}$.

Calculating the Outdoor Temperature (T_o)

The outdoor temperature for The Hague (T_o) was retrieved from KNMI weather data for the 2018–2022 period. Among the various meteorological stations operated by KNMI, the Hoek van Holland station is nearest to The Hague. Hourly air temperature and solar radiation flux data were accessed from the Hoek van Holland station via the KNMI API

(KNMI, 2023b). The Python script used to retrieve this weather data, *functions/time_series.py*, is provided in Appendix C.

Quantifying the Urban Heat Island Effect

Although The Hague is only 15 km away from Hoek van Holland, the urban heat island (UHI) effect results in significantly higher temperatures in The Hague compared to the Hoek van Holland weather station. To account for this, UHI effect-induced temperature differences were added to the Hoek van Holland's hourly temperature data to better reflect conditions in The Hague.

Research by the Netherlands Organization for Applied Scientific Research (TNO) estimates that the UHI effect increases average air temperatures by 8.6 °C during the day and 2.4 °C at night on hot summer days in The Hague (Klok, Schaminée, et al., 2012). Similar findings were reported in the "Haagse Hitte" study, which provided a geospatial analysis of The Hague's UHI effect (van der Hoeven & Wandl, 2018a). Given that peak cooling demand occurs on such hot days, these heightened UHI effects were chosen to represent scenarios when cooling is most needed, instead of using annual averages.[12]

However, Hoek van Holland also experiences a UHI effect, being close to the port of Rotterdam and the Westland greenhouse area. Although not included in the TNO study, the National Institute for Public Health and the Environment (RIVM) has mapped an average UHI effect of 0.3 °C for Hoek van Holland (Atlas Natuurlijk Kapitaal, 2017). As specific day and night variations for Hoek van Holland are unavailable, this effect was assumed constant over time.

Table 10: Urban heat island effect correction factors to account for the air temperature difference between The Hague and the Hoek van Holland weather station.

Location	Daytime UHI effect (°C)	Night-time UHI effect (°C)	Source
The Hague	8.6	2.4	(Klok, Schaminée, et al., 2012)
Hoek van Holland	0.3	0.3	(Atlas Natuurlijk Kapitaal, 2017)
ΔUHI	8.3	2.1	-

[12] Take note that incorporating this summertime urban heat island (UHI) effect does not yield accurate simulations for colder months when cooling is not required.

To adjust for the UHI difference between Hoek van Holland and The Hague, the 0.3 °C effect was deducted from The Hague's temperature anomalies. The adjusted UHI effect values are listed in Table 10. The daytime UHI effect value was added to the temperature series for hours between 08:00 and 20:00, while the nighttime UHI effect value was added to temperature from 20:00 onwards.

Determining the Relationship between Economic Status and UHI Effect

Section 2.4.2.2 discusses the unequal impact of the UHI effect as an example of climate injustice, highlighting that lower socioeconomic groups, often in densely built and less green neighborhoods, tend to experience more intense UHI effects. To explore this issue in The Hague, a geospatial analysis was conducted.

Data on the average yearly intensity of the UHI effect was sourced from the Natural Capital Atlas (Atlas Natuurlijk Kapitaal, 2017), while median household income and mean house value per 100m x 100m census block were obtained from Statistics Netherlands (CBS) (PDOK, 2023d). The mean UHI effect for each census block was determined using zonal statistics, after which the Spearman correlation between socioeconomic indicators (household income and house value) and the UHI effect intensity was calculated. For the detailed calculations, see section 2.4 in the *gis.ipynb* Jupyter Notebook in Appendix C.

Calculating the Indoor Temperature (T_i)

In this model, the indoor temperature (T_i) is set at the effective cooling temperature ($T_{effective}$) of **25 °C** for both residential and office buildings, in line with policy guidelines and thermal comfort ranges discussed in section 2.2.1. This temperature is chosen despite being 5 °C higher than the average found in the 2021 TNO survey on residential cooling, due to the survey's limited sample size (Rovers et al., 2021).

Assigning Heat Resistance and Transmission Values by Energy Label

Heat transmittance characteristics such as R_c and U values are dependent on many factors and vary by surface characteristics, as shown in Table 11. Building energy labels were used to approximate these characteristics, with standard R_C and U values for each energy label class presented in Table 12. Finally, the cumulative transmission flows through walls, roofs, windows, and ground floor were computed to determine the total energy flux caused by transmission, as described in Equation 5 and Figure 26.

Table 11: Typical Rc values in buildings. U values are calculated with α_i=7.5 $Wm^{-2}K^{-1}$ and α_o =25 $Wm^{-2}K^{-1}$, adapted from (van Bueren et al., 2012).

Barrier type	R_C (m^2KW^{-1})	U ($Wm^{-2}K^{-1}$)
Single glazing	0.005	5.6
Double glazing	0.16	3
High efficiency glazing	0.38	1.8
Non insulated brick cavity wall	0.35	1.9
Cavity wall with 100 mm insulation	2.68	0.35
Passive house wall	>8	<0.12

Table 12: Assigned heat resistance (R_C) and heat transmission (U) values by energy label.

Energy label	$R_{C,wall}$ (m^2KW^{-1})	$R_{C,roof}$ (m^2KW^{-1})	$R_{C,floor}$ (m^2KW^{-1})	U_{window} ($Wm^{-2}K^{-1}$)
A-A+++++	8	10	6	1
B-C	3	4	2	2
D-E	1	1.5	0.75	3
F-G	0.35	0.5	0.25	6

$$P_{trans} = P_{T,walls} + P_{T,windows} + P_{T,roof} + P_{T,ground}$$
$$= (U_{walls}A_{walls} + U_{roof}A_{roof} + U_{windows}A_{windows})(T_{air} - T_i) \quad [W]$$
$$+ U_{ground}A_{ground}(T_s - T_i)$$

Equation 5

Transmission through the ground floor involves the subsurface temperature (T_s), as the energy transfer is towards the soil instead of the outside air.

Quantifying the Subsurface Temperature

Subsurface temperature data for The Hague was sourced from the KNMI, which records these temperatures at six-hour intervals at only four weather stations. The data from the nearest station, located in De Bilt, was obtained from the KNMI website (KNMI, 2022a). This data provides subsurface temperatures at a depth of one meter.

A sensitivity analysis was conducted to evaluate the impact of using different approaches for subsurface temperatures. The relative difference in calculated cooling demand between using an annual average subsurface temperature and using six-hourly temperature data was minimal, at 0.3%. To simplify the algorithm and reduce computation time, the 2018–2022 average subsurface temperature of **11.8 °C** was

assumed across the reference period**.** In addition, the UHI effect tends to increase urban subsurface temperatures relative to surrounding rural areas. However, due to complexities in estimating the severity of the effect, this was not incorporated in the calculations. More details on this decision can be found in Appendix J.

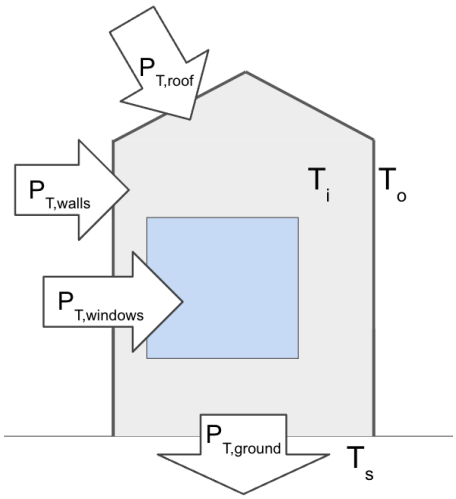

Figure 26: Diagram of heat flows via transmission. In this case, $T_s < T_i < T_o$, simulating a hot summer's day, when space cooling is desired. Based on (van Bueren et al., 2012).

3.2.2.2 Infiltration and Ventilation

Buildings receive fresh air both through controlled ventilation via windows, grilles, or mechanical ventilation systems, as well as through uncontrolled infiltration via construction gaps wall junctions and window frames. Fresh air is crucial for providing oxygen, reducing humidity, and diluting pollutants. The necessary air volume per person varies, usually between 25 to 50 m^3h^{-1}, increasing in high occupancy buildings like offices (van Bueren et al., 2012). While older buildings often use natural infiltration for air exchange, newer buildings may require mechanical ventilation due to their airtight construction. Note that the variability of air humidity or energy use from processes like humidification or dehumidification are out of the scope of this study.[13]

[13] Both outdoor and indoor air are composed of a mix of air and water vapor, known as humid air. In most atmospheric conditions, humidity ratios are small (≤3% of total air mass) and are often not a primary concern (van Bueren et al., 2012). However, activities like humidification or dehumidification within buildings can consume significant amounts of energy. Despite their potential relevance, these processes were not included in the scope of this research.

Infiltration

Thermal flows due to infiltration were estimated using indoor (T_i) and outdoor (T_o) air temperatures, according to Equation 6 (van Bueren et al., 2012):

$$P_{inf} = \dot{m}_{inf} \cdot C_p \, (T_o - T_i) \quad [W] \qquad \textit{Equation 6}$$

With:

- $\dot{m}_{inf}$: the mass flow rate of air by infiltration [kg s^{-1}]
- C_p: the heat capacity of air, which under typical room conditions equals 1,006 $Jkg^{-1}K^{-1}$ (The Engineering Toolbox, 2004b) [14]
- T_o: the outdoor temperature [K]
- T_i: the indoor temperature [K]

In heating, ventilation, and air conditioning (HVAC) literature, volume flow rates are more commonly used than mass flow rates. The mass flow rates were calculated from volume flow rates using Equation 7.

$$\dot{m} = \frac{\rho \cdot \dot{V}}{3600} \quad [kg\ s^{-1}] \qquad \textit{Equation 7}$$

With:

- ρ: the density of air, which under typical room conditions equals 1.2 kgm^{-3} [15]
- $\dot{V}$: the volume flow rate of air [m^3h^{-1}]

Estimating infiltration rates is complex due to its uncontrolled nature and dependency on construction flaws and often very dynamic indoor-outdoor pressure gradients. A common

[14] For this study, typical room conditions were defined as a temperature range of 15 °C to 30 °C at a standard sea-level atmospheric pressure of 1.013 bar. Under these conditions, a constant heat capacity for air (C_p) of 1006 $Jkg^{-1}K^{-1}$ is used throughout the model as a sufficiently accurate approximation. Considering the focus on space cooling, which is not typically needed at outside temperatures below 15 °C, the same heat capacity was assumed for outside air.

[15] As mentioned earlier, typical room conditions were taken to be between 15 °C and 30 °C at a standard sea-level atmospheric pressure of 1.013 bar. In those conditions, the mass density of air ranges between 1.16 and 1.23 kgm^{-3} (The Engineering Toolbox, 2004b).

approach is to use the air change per hour (*ACH*), the rate at which the entire indoor air volume is replaced per hour, as described in Equation 8.

$$ACH = \dot{V}/V_{building} \quad [h^{-1}] \qquad \textit{Equation 8}$$

With:

- $\dot{V}$: the volume flow rate [m^3h^{-1}]
- $V_{building}$: the interior volume of the building [m^3]

In this model, the ACH due to infiltration (ACH_{inf}) was assumed to be **0.5** for older buildings (type 2, 4, 6, 8) and **0.1** for newer buildings (type 1, 3, 5, 7), based on the typical values presented in Table 13.

Table 13: Typical air changes per hour (ACH) from infiltration (van Bueren et al., 2012).

Building type	***ACH* (h^{-1})**
Large modern buildings with a floor area greater than 10,000 m^2	0.1–0.2
Smaller modern buildings	0.2–0.3
Older buildings	0.5–1

Ventilation

Ventilation systems can be divided into three main categories, depicted in Figure 27.

1. **Natural ventilation** occurs via grilles and windows, without a mechanical ventilator.
2. **Mechanical ventilation** uses a single ventilator for the supply or exhaust of air.
3. **Mechanical ventilation with heat recovery** uses two ventilators to enable heat exchange between incoming and outgoing air. In warmer conditions, these systems can cool incoming outdoor air using the cooler indoor exhaust air. Heat recovery efficiency typically ranges from 0.6 to 0.9 (van Bueren et al., 2012).

Thermal flows due to ventilation were calculated using Equation 9. Mechanical ventilation without heat recovery was assumed to be in place for new offices and new high-rise residences (type 1, 5, and 7 buildings). The mass flow rate of air by ventilation, $\dot{m}_{vent}$, was determined using Equation 7, with $\dot{V}$ assumed to be **25 m^3h^{-1}** per person. This rate

aligns with the minimum requirements for new offices and the typical values presented earlier in this section (Hensen Centnerová et al., 2021).[16]

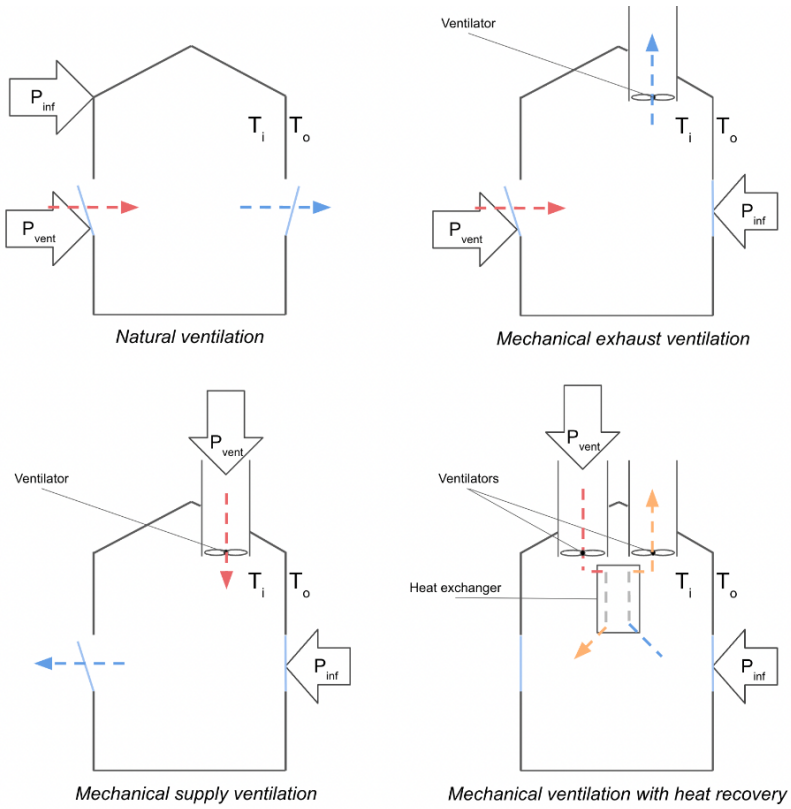

Figure 27: Ventilation system categories. In this case, $T_i < T_o$, simulating a hot summer's day during which space cooling is desired. Based on (van Bueren et al., 2012).

$$P_{vent} = (1 - \eta)\dot{m}_{vent} \cdot C_p\,(T_o - T_i) \quad [\mathrm{W}] \qquad \textit{Equation 9}$$

With:

- η: the heat recovery efficiency, which is zero in cases without heat recovery
- $\dot{m}_{vent}$: the mass flow rate of air by ventilation [kg s^{-1}]
- C_p: the heat capacity of air [$Jkg^{-1}K^{-1}$]
- T_o: the outdoor temperature [K]
- T_i: the indoor temperature [K]

[16] The amount of people per building was estimated from building type and floor area. In residential buildings, the number of residences was multiplied by The Hague's 2020 average household size of 2.01 (The Hague Municipality, 2023). For offices, an occupancy of one person per 15 m_2, or 0.067 people/m^2, was assumed.

3.2.2.3 Solar Radiation

Solar radiation enters buildings mainly through windows and is absorbed by walls and roofs, though the latter can be assumed negligible in well-insulated buildings. The heat buildup in windows themselves is also typically ignored (van Bueren et al., 2012).

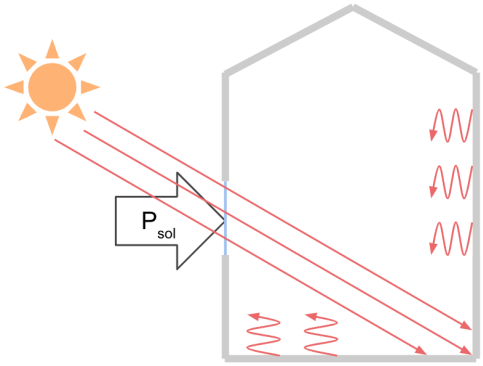

Figure 28: Diagram of heat gain via solar radiation. Based on (van Bueren et al., 2012).

Solar radiation absorbed by a building's structure gradually raises wall temperatures. Once these temperatures exceed the room air temperature, heat is released into the room through convection, as depicted in Figure 28. Although this process can span several hours based on the building's thermal mass, this this study simplifies the approach by not considering such time-lag effects. This reduction in complexity enables the calculation of solar heat gains by evaluating and summing the gains from each direction, as outlined in Equation 10. [17]

$$P_{sol} = \sum_i \; g^i_{window} \cdot A^i_{window} \cdot g^i_{shade} \cdot \Phi^i_{sol,w} \quad [\text{W}] \qquad \textit{Equation 10}$$

With:

- g^i_{window}: the ratio of total solar radiation that passes through windows in direction i and converted into heat. This ratio is commonly known as the g value, solar factor, or solar heat gain coefficient.
- A^i_{window}: the total surface area of windows in direction i [m²]
- g^i_{shade}: the g value of shades (blinds, awnings, etc.) in direction i
- $\Phi^i_{sol,w}$: the incoming direct and diffuse solar radiation flux in direction i [Wm^{-2}]

[17] This research distinguishes between the eight principal winds – north, north-east, east, etc. – when calculating heat gains through solar radiation in different directions.

Calculating Solar Factors

The solar factor (g^i_{window}, g^i_{shade}) depends on many factors and varies by building characteristics. Typical values can be found in Table 14.

Table 14: Typical solar factors for common glazing and shade types, from (van Bueren et al., 2012).

Glazing or shade type	Solar factor
Single glazing	~ 0.8
Double glazing, uncoated	~ 0.7
Triple glazing	0.4–0.6
Double glazing, low-e	0.3–0.6
Double glazing, reflective	~ 0.17
No shade	1
Roller shade	0.6–0.9
Louvre half open	~ 0.7
Louvre closed	~ 0.4
External shade	~ 0.2

In this model, building energy labels served as proxies for specific window characteristics. The solar factor of windows (g^i_{window}) was assumed per energy label class, as detailed in Table 15. Solar factors for shading (g^i_{shade}) were not included in the scope of this research.

Table 15: Assigned solar factor values by energy label.

Energy label	Solar factor
A–A+++	0.4
B–C	0.6
D–E	0.7
F–G	0.8

Calculating Incoming Solar Radiation Flux

Hourly solar radiation data for 2018–2022 was obtained from KNMI to calculate the incoming solar radiation flux ($\phi^i_{sol,\,w}$) for the reference period (KNMI, 2023b). The raw data provided solar radiation density (σ_{sol}) in Jcm^{-2} for each one-hour interval, essentially measuring flux (Φ_{sol}), in $Jcm^{-2}h^{-1}$. Equation 11 was used to convert this flux to the correct unit required for the cooling demand model (Wm^{-2}).

$$\Phi_{sol,Wm^{-2}} = \frac{\Phi_{sol,Jcm^{-2}h^{-1}}}{3{,}600\ s/h}\ 10{,}000\ cm^2/m^2 \quad [Wm^{-2}] \qquad \textit{Equation 11}$$

The solar radiation model requires directional solar radiation data for the eight principal wind directions. However, KNMI's hourly data only provided global radiation values without directional detail. An original Excel model for energy balance, using data from the De Bilt weather station in 1964–1965, provided directional solar radiation (Itard, 2015). This data was normalized to calculate average fractions of solar radiation per direction for each hour in the year.[18] or the 2018–2022 period, KNMI's global radiation values were multiplied by these fractions for each principal wind direction, as detailed in the *functions/time_series.py* Python script in Appendix C.

Using these methods, the solar heat gain for each principal wind direction was calculated and then summed to obtain the total solar heat gain (P_{sol}).

3.2.2.4 Internal Heat Gains

In addition to heat exchange with the external environment, buildings also generate internal heat. These internal heat gains have three primary sources: people, lighting, and other electrical devices, as shown in Figure 29.

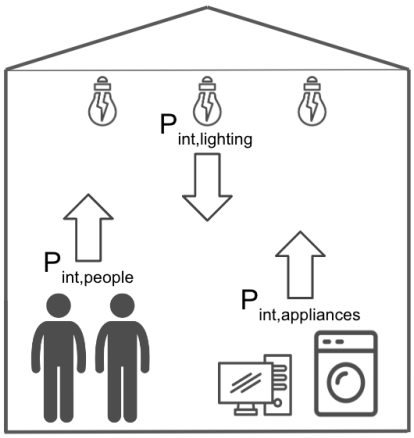

Figure 29: Diagram of internal heat gain sources.

[18] It is important to note a slight inconsistency between the solar ecliptic at the global solar radiation weather station (Hoek van Holland) and the station used to derive directional radiation fractions. This resulted in a few hours each year when directional radiation fractions are zero for all directions, despite Hoek van Holland data showing some global radiation. Consequently, the directional solar radiation values needed to be set to zero for those hours, leading to a minor underestimation of the annual solar radiation in the model. However, this impact is minimal, decreasing the annual total solar radiation in the model weather series by just 1%.

People

The heat generated by the human body, dissipated through breath, perspiration, and convection, contributes to internal heat gains. This was calculated by multiplying the number of occupants (n_{people}) with the average heat generation per person P_M, as shown in Equation 12.[19]

$$P_{int,people} = n_{people} \cdot P_M \quad [W] \qquad \textit{Equation 12}$$

Heat generation rates depend on factors like activity, clothing, and surrounding humidity and temperature, but typically range between 100–120 W for sedentary activities and 180–360 W for physical exercises like walking or dancing (van Bueren et al., 2012). This study assumed an average heat generation P_M of **120 W** to reflect that sedentary activities make up most of the time spent in residences and offices.

Lighting

All electricity used by lighting will eventually dissipate as heat into the building. The electric power use of lighting typically varies based on the used lamp types and the building end use. To limit the complexity of the calculation model, internal heat gains from lighting were estimated using Equation 13:

$$P_{int,lighting} = A_{floor} \cdot \Phi_{lighting} \quad [W] \qquad \textit{Equation 13}$$

With:

- A_{floor}: The floor area of the building [m²]
- $\Phi_{lighting}$: The lighting power flux, i.e., the amount of lighting power per area [Wm^{-2}]

To estimate lighting heat gains, maximum allowable power flux rates can be applied as an upper limit: 10 W/m² for residences and 12 W/m² for office buildings (ASHRAE, 2010). Strategically placing lights and maximizing daylight use can lower power consumption below these limits. Accordingly, the model adopted a moderate power flux rate ($\Phi_{lighting}$) of **6 W/m²** for both residences and offices to account for such energy-saving practices.

[19] For details on the methodology used to calculate the number of occupants per building, please refer to section 3.2.2.2.

Other Electrical Appliances

Other electrical devices like IT equipment and household appliances also dissipate their used electricity into heat. Typical appliance power fluxes ($\Phi_{appliances}$) are **5 Wm^{-2}** for residences and **15 Wm^{-2}** for offices (van Bueren et al., 2012). These values were applied in the model, and the heat gains from these devices were calculated using Equation 14.

$$P_{int,appliances} = A_{floor} \cdot \Phi_{appliances} \quad [W] \qquad \textit{Equation 14}$$

Presence Load Factors

To account for variable internal heat gains, a presence load factor (β) was used. This factor, varying between zero and one, adjusts for the times when people are absent, and lights and appliances are off. For residences, one fifth of occupants was assumed to be home during typical work hours (09:00–17:00), with full lighting and appliance use during mornings (07:00–09:00) and evenings (17:00–21:00). Other times, only a fraction of the lights and appliances (e.g., refrigerators) are assumed to be in use.

In offices, full occupancy was assumed between 09:00 and 17:00, with one fifth of people arrive early or staying late. Lights and appliances were assumed to be fully turned on during extended work hours (07:00–21:00) and turned off for other hours. The resulting load factors (β) per building type can be found in Table 16.

Table 16: Presence load factors for internal heat gains, adapted from (Itard, 2015).

Building type	**Internal heat source**	**Time period**			
		21:00–07:00	*07:00–09:00*	*10:00–17:00*	*17:00–21:00*
Residential	People	1	1	0.2	1
Residential	Lighting	0.2	1	0.2	1
Residential	Appliances	0.2	1	0.2	1
Office	People	0	0.2	1	0.2
Office	Lighting	0	1	1	1
Office	Appliances	0	1	1	1

The total internal heat gains were calculated by summing the heat contributions from these three sources, multiplied by its respective presence load factor, as per Equation 15.

$$P_{int} = \beta_{people} \cdot P_{int,people} + \beta_{lighting} \cdot P_{int,lighting} + \beta_{appliances} \cdot P_{int,appliances} \quad [W] \qquad \textit{Equation 15}$$

3.2.2.5 Calculating Total and Peak Cooling Demand over the Year

To determine the total thermal power (P_{total}) entering or leaving a building, the abovementioned heat flows were calculated and then summed according to Equation 16.

$$P_{total} = P_{trans} + P_{inf} + P_{vent} + P_{sol} + P_{int} \quad [W] \qquad \textit{Equation 16}$$

Since the thermal energy gained or lost over a 1-hour period, measured in watt-hours (Wh), is equivalent in magnitude to the average power in watts (W) during that hour, the total thermal energy (Q_{total}) exchanged with the building in 1 hour was determined by simply multiplying Equation 16 with 1 hour, as per Equation 17.

$$\begin{aligned} Q_{total} &= \left(P_{trans} + P_{inf} + P_{vent} + P_{sol} + P_{int}\right) \cdot 1h \\ &= Q_{trans} + Q_{inf} + Q_{vent} + Q_{sol} + Q_{int} \end{aligned} \quad [Wh] \qquad \textit{Equation 17}$$

In case $Q_{total} > 0$, the internal temperature rises and there is an equally sized demand for cooling: $Q_{cooling} = Q_{total}$.

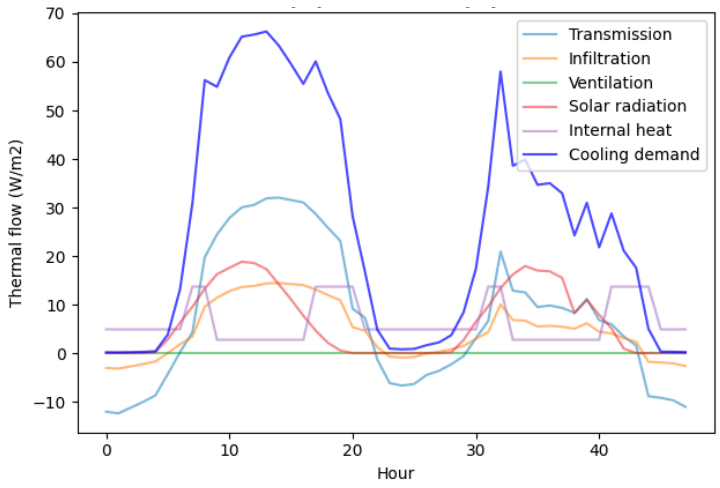

Figure 30: Example thermal flow and cooling demand profiles for an old low rise residential building (type 4) during a heat wave (July 25th–27th, 2019).

These thermal balance calculations were conducted for each hour in the reference period (2018–2022), yielding cooling demands that can be visualized in the form of a cooling demand profile, as exemplified in Figure 30. This data forms the basis for calculating the cumulative cooling demand in kilowatt-hours (kWh) and peak cooling demand in kilowatts (kW). From these, statistical metrics like the 98th percentile of the cooling power demand ($P_{C,98p}$) and the cumulative cooling energy demand capped at the 98th percentile of the cooling power demand ($E_{C,98p}$) were derived. See Figure 31 for a visual representation of these statistical values.

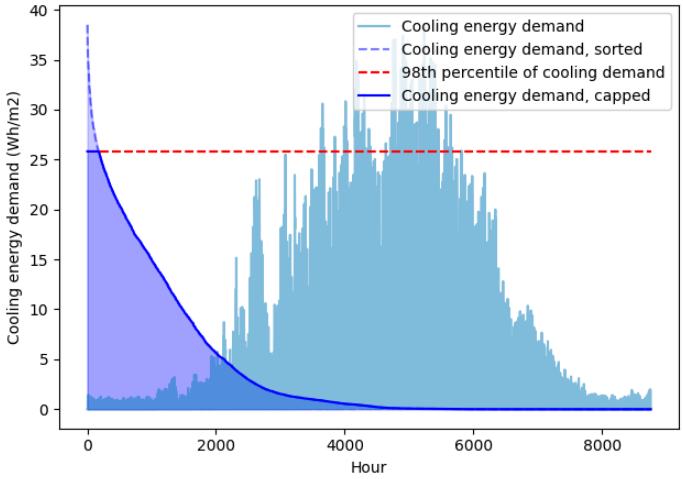

Figure 31: Annual cooling demand load for an old low rise residential building (type 4). Based on average data over the 2018–2022 period.

These statistical measures are commonly used to determine appropriately sized cooling installations for realistic demand fulfillment. The 98th percentile criterion assumes operational leeway for the cooling infrastructure to provide suboptimal heat removal during the hottest 2% of hours throughout the year, aligning with Dutch standards for thermal discomfort exceedance in offices and residences (ISO, 2005).[20]

Designing for the 100th percentile, or peak demand, could lead to an oversized cooling system, as such extreme demand occurs rarely (likely only during the hottest hour of the year). As a result, the system would be oversized and not optimally energy-efficient for most of the time, leading to higher economic, material and energy costs. In this model, it was assumed that cooling equipment installation size and energy consumption are based on the 98th percentile of cooling demand. This implies that people have a tolerance for slight thermal discomfort during 2% of the hottest hours in the summer. Note that henceforth, the 98th percentile of the annual cooling power demand and the cooling energy demand capped at that 98th percentile, is referred to as the "capped cooling power demand" and "capped energy demand", respectively.

[20] The Dutch guidelines for thermal comfort in offices and residential buildings (ISO, 2005; Vabi, 2015) describes guidelines for the maximum amount of thermal discomfort exceedance hours, i.e. the amount of hours per year in which thermal discomfort is acceptable. These values range between 100 and 300 hours per year, or 1.1–3.4% of the hottest hours. An average discomfort tolerance of 2% was assumed, leading to a peak power demand cap at the 98th percentile.

The cooling demand analysis described above was applied to each RO building within The Hague, using the thermodynamic-related attributes from the GIS analysis described in section 3.2.1. The results are presented in section 4.1.

3.2.3 Environmental Impact Modeling

After determining the cooling demand of RO buildings in The Hague as described in the previous section, the environmental impacts of this demand were calculated through an environmental impact model (EIM). This model determines energy use, climate change impact and material impacts, using a life cycle approach that includes production, use, and end-of-life stages.[21] An overview of this methodology is illustrated in Figure 32.

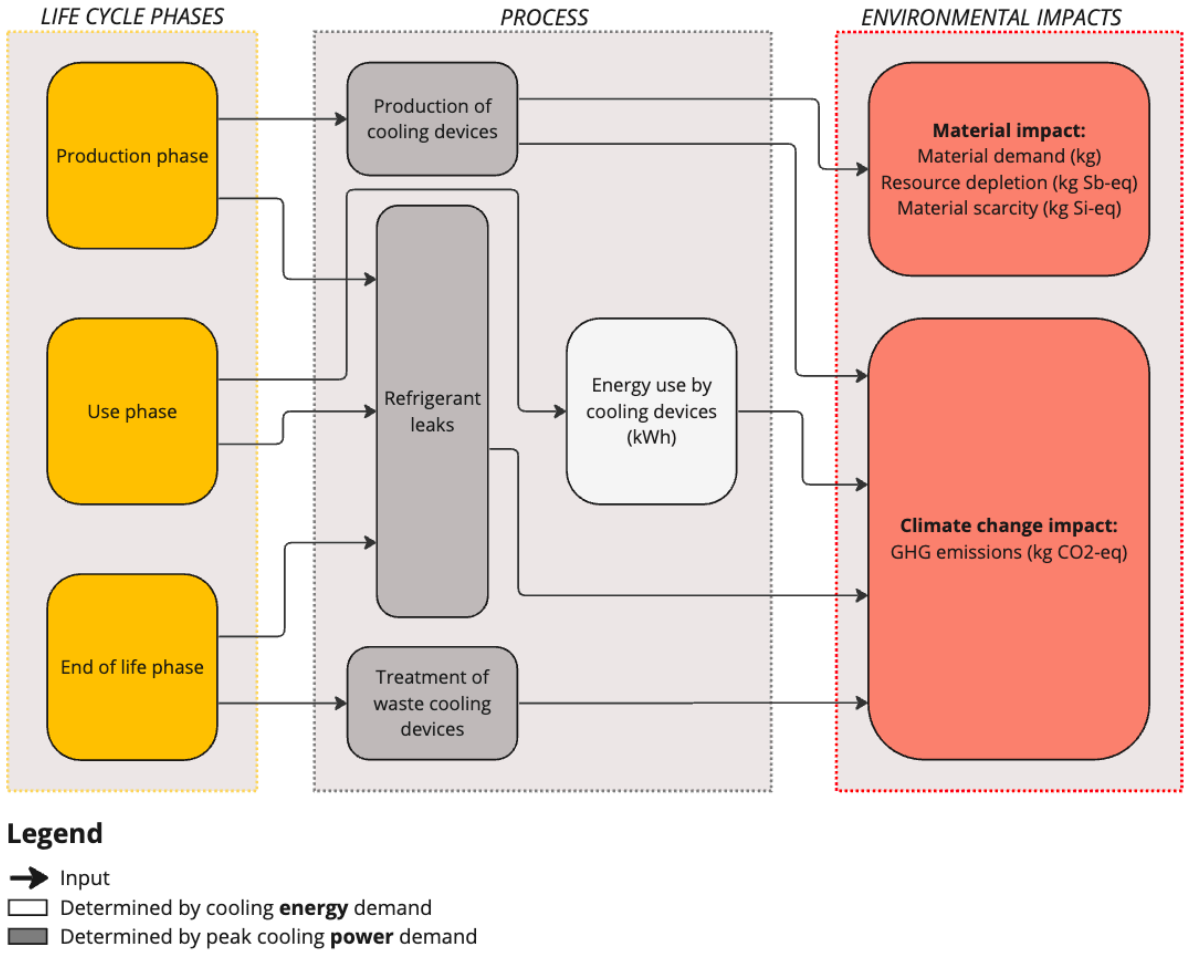

Figure 32: Overview of environmental impact model.

[21] Although energy use is not directly an environmental impact, in this research it was analyzed and discussed independently from climate change and materials impacts, as detailed in section 3.1

3.2.3.1 Electrical Energy Use

To determine the electrical energy (E_{elec}) necessary to fulfil the capped cooling demand ($E_{C,98p}$), the mix of cooling technologies present in each building type was first assessed. Subsequently, energy efficiency estimates were made for each specific cooling technology. The final step involved multiplying the capped cooling energy demand by the effective energy efficiency of each building's cooling system mix, thereby calculating the overall energy usage.

Determining the Cooling Technology Mix per Building Type

The assignment of cooling technology mixes for different building types was informed by market penetration rates (MPR) from previous studies. Six main active cooling systems were considered: **chillers, large split air conditioners, portable air conditioners, air-source heat pumps (ASHP), ground-source heat pumps (GSHP), and water-source heat pumps (WSHP)**. A 2021 TNO study, in particular the survey data presented in Table 5, guided the allocation of these cooling technologies to each building type (Rovers et al., 2021).

For new (type 1) and old (type 2) high-rise residences, the 14.5% total MPR of surveyed apartments was applied.[22] Type 1 buildings were presumed to mainly use chillers and, to a lesser extent, GSHPs, reflecting the low 0.9% MPR found in the survey. Type 2 buildings were assumed to fully rely on portable air conditioners.

For new (type 3) and old (type 4) low-rise residences, MPRs were derived from survey responses for row houses, resulting in a mix of portable (6.2%) and large split air conditioners (5.5%), along with a minor percentage of GSHPs (0.5%).

Lacking specific MPR data for office buildings, a ratio of heat pumps in utility buildings to residential buildings, based on CBS data, was used (CBS, 2022b, 2022c). This ratio was used to scale the overall penetration rate of high-rise (apartment) and low-rise (row house) homes used above to that of office buildings, assuming that the increased presence of heat pumps in office buildings directly translates to an increased presence of overall cooling

[22] A limitation of this approach is that there is likely to be a bias towards the installation rate of cooling equipment being higher than average amongst the respondents of the TNO survey, as people who are interested in space cooling are more likely to have been involved in this survey.

systems. The distribution of cooling technologies within high-rise and low-rise offices was assumed to be similar to that in residential buildings.

The TNO survey focused solely on GSHPs, but CBS data suggests a higher prevalence of ASHPs and WSHPs in the Netherlands (CBS, 2022c). Consequently, the MPRs for these heat pump types were proportionally increased and added to the overall penetration rates.[23] The resulting cooling technology mix per building type is displayed in Figure 33, and the exact percentages used in the model can be found in Appendix I.

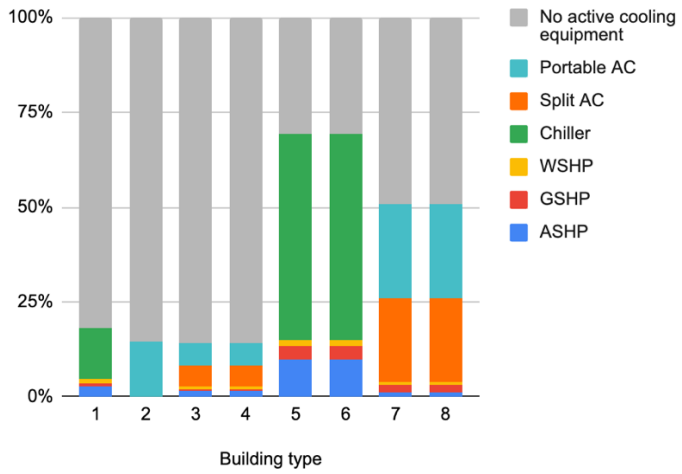

Figure 33: Estimated cooling equipment mix per building type, adapted from (Rovers et al., 2021). WSHP, ASHP, and GSHP stand for water-, air-, and ground-source heat pump, respectively.

Estimating Energy Efficiencies of Cooling Equipment

The energy efficiency of various cooling technologies informed the calculation of the effective seasonal energy efficiency ratio ($SEER_{eff}$) for each building type. The SEER was chosen for its comprehensive representation of annual energy efficiency, as discussed in

[23] Note that this study operates under the assumption that all installed heat pumps are reversible, meaning they can provide both heating and cooling functionalities. However, in practice, achieving this dual capability necessitates the incorporation of supplementary equipment like floor heating systems. As a result, the estimation of cooling-capable heat pumps may potentially be overemphasized. Determining the precise proportion of reversible heat pumps within the existing stock is challenging, however, and has been excluded from the scope of this study.

section 2.3.3.[24] Due to the lack of SEER data for the specific cooling equipment types assessed in this study, generalized figures from the Heat Roadmap Europe project were used (Dittmann et al., 2016).[25] The SEER of portable ACs were assumed to be similar to those of "Movables + Window Units" in the source data. For split ACs and chillers, the study used weighted averages of SEER values for each type, with weights based on the reported EU28 installed capacities in 2015.[26]

Table 17: Assigned SEER per cooling technology in the status quo scenario, based on (Dittmann et al., 2016).

Cooling equipment type	SEER	Assumptions in translation from source data
Chiller	4.1	Average of all chiller types in source data, weighted according to the reported installed capacity in the EU28
Split AC	4.8	Average of all split AC types in source data, weighted according to the reported installed capacity in the EU28
Portable AC	2.5	Assumed values of 'Movables + Window Units' in source data
Air-Source Heat pump (ASHP)	4.8	Assumed air-to-air heat pumps (ASHP) to have similar SEERs as split AC systems, as they are functionally the same.
Ground-source heat pump (GSHP)	6.2	Cooling performance (SEER) of GSHP compared to ASHP: 23% more efficient (Esen et al., 2007), or 37% more efficient (Urchuegia et al., 2008). Averages out to be 30% more efficient.
Water-Source Heat pump (WSHP)	7.5	Assuming the energy efficiency ratio between WSHP and ASHPs to be the same as the ratio between ratio between W/W chillers and A/W chillers, which is 5.5:3.5, i.e. W/W chillers are 57% more efficient than A/W chillers, on average (Dittmann et al., 2016).

[24] Although the European Seasonal Energy Efficiency Ratio (ESEER) could also be suitable metric for assessing seasonal energy efficiency, it was not used in this study due to the unavailability of public, empirical data on ESEER values for the assessed cooling equipment types; they were found only within policy guidelines.

[25] Some of the SEERs used in the modeling of the Status Quo are lower than the market average of 5.3 presented by the IEA and the minimum requirements posed by the EU policy (Ecodesign Requirements for Air Conditioners and Comfort Fans, 2012). This can be explained by the fact that the IEA market average is about recently sold units, not about the total cooling equipment stock. As the average SEER of new equipment increases over time source, the SEER of sold units will generally be higher than the average of the total cooling equipment stock. Additionally, the lack of conformance to EU standards is likely because the minimum energy performance standard (MEPS) is not always followed. IEA estimates that 85% of all space cooling is covered by MEPS-compliant equipment (IEA, 2018a).

[26] EU28 refers to the European Union before the United Kingdom's departure (Brexit) in 2020.

For heat pumps, despite abundant research on the SEER for space heating, there is a lack of such data for space cooling. Therefore, ASHPs were assumed to have similar SEERs as split AC systems, as they function similarly. The increased energy efficiencies of GSHPs and WSHPs over ASHPs were approximated using performance coefficient (COP) ratios. The resulting SEER per cooling technology can be found in Table 17.[27]

To find the effective SEER ($SEER_{eff}$) per building type, the product of the MPR values and the inverse SEER were summed across the cooling technologies i, as shown in Equation 18.[28]

$$SEER_{eff} = \frac{1}{\sum_i \frac{MPR_i}{SEER_i}} \qquad \textit{Equation 18}$$

The cumulative cooling energy demand capped at 98th percentile ($E_{C,98p}$) from the CDM was then divided by the resulting $SEER_{eff}$ values to find the energy demand (E_{elec}) per building, as shown in Equation 19. The building-level energy demands were then summed to find the electrical energy consumption for RO space cooling in The Hague.

$$E_{elec} = \frac{E_{C,98p}}{SEER_{eff}} \quad [\text{kWh}] \qquad \textit{Equation 19}$$

3.2.3.2 Material Demand

A life-cycle assessment (LCA)-based impact analysis was performed to evaluate the environmental footprint of producing and disposing of cooling equipment. LCA is a comprehensive methodology that assesses environmental impacts throughout a product's full life cycle, from raw material extraction to disposal or recycling. This methodology,

[27] W/W and A/W refers to water-to-water and air-to-water, respectively, referring to the source and destination medium of heat transfer used in chillers.

[28] Inverse SEER values were used in the model because energy efficiencies are not additive; only their inverses (electrical energy required per unit of cooling energy demand) are additive. To account for the proportion of buildings without active cooling equipment, an inverse SEER of zero was assigned for that segment, indicating no electrical energy use regardless of cooling demand. Consequently, the resulting effective SEERs per building type may appear unusually high, reflecting the reality that a portion of the cooling energy demand will go unmet and thus will not consume any electrical energy.

developed by the Institute of Environmental Sciences (CML) at Leiden University, quantifies all environmental exchanges associated with a product's life cycle (also referred to as the product system) and translates these into impact indicators such as greenhouse gas emissions and resource depletion (Guinée et al., 2002). By considering every stage of a product's life, LCA offers a holistic perspective on both the direct and indirect environmental effects associated with all phases of a product's existence (ISO, 2005). Previous LCAs on air conditioners are outdated, do not include the desired impact categories, and lack regional specificity for Western Europe (Heikkilä, 2004; Shah et al., 2008; Yanagitani & Kawahara, 2000). To bridge this gap without the complexity of a full LCA, ecoinvent data for processes analogous to active cooling technologies—specifically ventilation systems with heat exchangers—were used as proxies These processes, detailed in Table 18, enable the estimation of production- and EoL-phase impacts of active cooling equipment.

Table 18: Overview of ecoinvent processes used as a proxy for the impact assessment of active cooling technologies.

#	ecoinvent process
1	market for ventilation system production, central, 1 x 720 m3/h, polyethylene ducts, with earth tube heat exchanger
2	market for ventilation system production, central, 1 x 720 m3/h, steel ducts, with earth tube heat exchanger
3	market for ventilation system production, decentralized, 6 x 120 m3/h, polyethylene ducts, with earth tube heat exchanger
4	market for ventilation system production, decentralized, 6 x 120 m3/h, steel ducts, with earth tube heat exchanger

Table 19: Impact categories used in the LCA-based impact assessment of cooling equipment.

Impact category	Impact method	Unit	Source
Climate change (GWP100)	ReCiPe Midpoint (H) V1.13	kg CO_2-eq	(Huijbregts et al., 2017)
Abiotic depletion potential (ADP): elements (ultimate reserves)	CML v4.8 2016	kg Sb-eq	(van Oers et al., 2002; van Oers & Guinée, 2016)
Crustal scarcity indicator (CSI)	Crustal scarcity indicator	kg Si-eq	(Arvidsson et al., 2020)

Environmental impacts were assessed in three impact categories: climate change, abiotic depletion potential (ADP), and the crustal scarcity indicator (CSI), as detailed in Table 19. A 0.1% cutoff rate was applied in the product system analysis to focus on the most significant material inputs and reduce calculation complexity. The openLCA software

facilitated this analysis, which included a contribution analysis to distinguish impacts of the production and end-of-life (EoL) phases (Srocka et al., 2023).

This resulted in the following impact metrics for each of the evaluated product systems:

- Production-phase GHG emissions ($GHG_{product\ system,production-phase}$) [kg CO_2-eq]
- End-of-life-phase GHG emissions ($GHG_{product\ system,EoL-phase}$) [kg CO_2-eq]
- Abiotic resource depletion ($ADP_{product\ system}$) [kg Sb-eq]
- Crustal scarcity index ($CSI_{product\ system}$) [kg Si-eq]

The mass of each product ($m_{product}$) was derived from examining the technological descriptions of the product's economic input flows. The findings are compiled in the background research spreadsheet in Appendix A. Carbon intensity per unit mass (CI_{mass}), measured in kg CO_2-eq per kg of equipment, was then computed using Equation 20. Resource depletion and crustal scarcity intensities were calculated in a similar manner.

$$CI_{mass,production-phase} = \frac{GHG_{product\ system,production-phase}}{m_{product}} \quad [\text{kg } CO_2\text{-eq /kg}] \quad \textit{Equation 20}$$

To evaluate the presence of critical raw materials (CRMs) and other strategic materials, the life-cycle inventories (LCIs) of the four product systems were closely examined, specifically analyzing the concentration of CRMs in their material footprints.

Calculating Material-related Impacts per Cooling Technology

In the absence of comprehensive LCA data for specific cooling technologies, the study used the average impact intensities from the four representative product systems shown in Table 18 as a proxy for the production and EoL impacts of all included active cooling technologies. The typical cooling power capacity (P_{cap}) and mass (m) of each cooling technology was derived from a sample cooling device which was used as a proxy, as detailed in Appendix H. The material density (ρ_{power}) was then calculated for each cooling equipment type using Equation 21.

$$\rho_{power} = \frac{m}{P_{cap}} \quad [\text{kg/kW}] \quad \textit{Equation 21}$$

The average carbon, ADP, and CSI intensities, derived using Equation 20, were then normalized over the life spans (L) of the each cooling equipment type, as informed by IPCC averages (Penman et al., 2000). Further normalization was applied by multiplying with

the material density (ρ_{power}), resulting in impact intensities per installed cooling power capacity. For example, the annualized carbon intensity for the production phase, expressed in kg CO_2-eq per kW of installed cooling power capacity, was calculated using Equation 22.

$$CI_{power,ann.,production-phase} = \frac{CI_{mass,production-phase} \cdot \rho_{power}}{L} \quad [\text{kg } CO_2\text{-eq /kW}] \quad \textit{Equation 22}$$

This method was similarly applied to other impact categories, with the annualized impact metrics—carbon intensity, CSI intensity, and ADP intensity per kilowatt of installed power capacity—detailed in Appendix H.

Determining the Total Material Impact

To determine a buildings' effective density of cooling equipment (ρ_{eff}), in kg per kW of installed cooling capacity, each cooling technology's (i) material density was weighted with its respective market penetration rate, as detailed in Equation 23. This approach was also used to calculate the effective impact metrics, such as the effective production-phase carbon intensity, as shown in Equation 24. The effective ADP, CSI, and EoL-phase carbon intensities were calculated likewise. Note that the market share without active cooling equipment was assigned a material intensity and impact intensity of zero.

$$\rho_{eff} = \sum_i MPR_i \cdot \rho_{power,i} \quad [\text{kg/kW}] \quad \textit{Equation 23}$$

$$CI_{eff,production-phase} = \sum_i MPR_i \cdot CI_{power,ann.,production-phase,i} \quad [\text{kg } CO_2\text{-eq /kW}] \quad \textit{Equation 24}$$

The 98th percentile of cooling power demand ($P_{C,98p}$) from the CDM was then multiplied by the effective material density to calculate the mass of cooling equipment required per building ($m_{equipment}$), as shown in Equation 25. This assumes that cooling systems are sized to meet the demand for 98% of the cooling season. Total impacts per building, such as the GHG emissions from the production phase ($GHG_{production-phase}$), were determined using the effective impact intensities, as per Equation 26. GHG emissions from the EoL-phase and ADP and CSI metrics were calculated in a similar manner.

$$m_{equipment} = P_{C,98p} \cdot \rho_{eff} \quad [\text{kg}] \quad \textit{Equation 25}$$

$$GHG_{production-phase} = P_{C,98p} \cdot CI_{eff,production-phase} \quad [\text{kWh}] \quad \textit{Equation 26}$$

Consequently, the cooling equipment mass, production, and EoL-phase GHG emissions, along with ADP and CSI metrics, were determined for the cooling system mix of each building. These building-level figures were then aggregated to give a comprehensive view of the environmental impact across the entire residential and office building stock in The Hague.

3.2.3.3 Climate Change Impact

Climate change impacts were modeled in terms of the GHG emissions from electricity use, refrigerants leaks, and production and end-of-life treatment of cooling equipment, based on the size of the cooling energy and power demand metrics from the cooling demand model.

Greenhouse gas emissions from electricity use

As elaborated upon in section 2.4.1.1, there is a difference between direct (Scope 1) and life-cycle (Scope 3) carbon intensities. Data availability for life-cycle carbon intensities is generally limited, particularly for future scenarios. Moreover, research has shown that integrating life-cycle emissions has a relatively minor impact on decisions regarding the optimal electricity generation mix (Pehl et al., 2017). In this research, however, the focus is on understanding the full environmental impacts of cooling, not the choice of electricity mixes.

$$GHG_{elec} = CI_{elec} \cdot E_{elec} \quad [\text{kg } CO_2\text{-eq}] \qquad \textit{Equation 27}$$

Therefore, to calculate the emissions from electricity use (GHG_{elec}), the total electricity demand (E_{elec}) was multiplied by the life-cycle carbon intensity (CI_{elec}) of the 2019 Dutch electricity grid in which is **0.427 kg CO_2-eq/kWh** (van der Niet & Bruinsma, 2022), as per Equation 27.[29]

Refrigerant Leaks

The study assessed greenhouse gas emissions from refrigerant leaks by establishing an effective annual leakage rate for each type of cooling technology. This rate reflects the

[29] For the status quo scenario of this analysis, the 2019 electricity grid mix and its associated carbon intensity were used, as this represented the latest year for which comprehensive life-cycle carbon intensity data for the Dutch electricity grid was accessible.

proportion of the refrigerant charge that escapes into the atmosphere annually, incorporating leakages at various stages: assembly, operational use, and end-of-life treatment. Firstly, average leakage rates from assembly ($LR_{assembly}$) and disposal (LR_{EoL}) were annualized by dividing by the lifespan of the cooling device (L), based on typical values documented in Table 20.

Table 20: Leakage rates for various cooling devices, expressed as a percentage of their refrigerant charge, based on lifespans and leakage rates from (Penman et al., 2000).

Cooling equipment type	Average lifetime (year)	Annual leakage rate during operation	Leakage rate during assembly	Leakage rate during end-of-life-treatment	Effective annual leakage rate
Chillers	20	9%	0.6%	13%	9.6%
Large ACs, incl. heat pumps	13	3%	0.6%	25%	5.2%
Portable ACs	12	15%	0.5%	100%	23.4%

It was assumed that leakage during assembly and end-of-life stages, while they are one-time events, effectively contribute to the total refrigerant emissions over the equipment's operational life. These were then added to typical operational leakage rates ($LR_{operation}$) to form an overall annualized leakage rate, relative to the installed refrigerant charge ($LR_{ann.,relative}$), following Equation 28.

$$LR_{ann.,relative} = LR_{operation} + \frac{(LR_{assembly} + LR_{EoL})}{L} \quad [\%/\text{year}] \qquad \textit{Equation 28}$$

To calculate absolute refrigerant emissions, the model defined a standard refrigerant charge for each cooling technology, listed in Table 21. These were based on data on representative proxy models, detailed in Appendix H. For each cooling technology, the refrigerant charge ($m_{refr.}$) was then multiplied by the corresponding relative leakage rates ($LR_{ann.,relative}$) and normalized by the material intensity (ρ_{power}), of that technology. The material intensity is calculated using Equation 21 and shown in Appendix H. This approach yielded the annual mass of refrigerants leaked per kilowatt of installed cooling power, as defined in Equation 29.

$$LR_{ann.,power} = \frac{LR_{ann.,relative} \cdot m_{refr.}}{\rho_{power}} \quad [\text{kg}/(\text{kW}\cdot\text{year})] \qquad \textit{Equation 29}$$

Table 21: Assumed refrigerant charge values for each cooling technology in the model.

Cooling equipment type	Installed refrigerant charge per unit (kg)
Chiller	6.0
Split AC	0.8
Portable AC	0.2
Air-Source Heat pump (ASHP)	1.5
Ground-source heat pump (GSHP)	1.6
Water-Source Heat pump (WSHP)	1.5

The model then calculated the building-level effective leakage rate (LR_{eff}) by aggregating the technology-specific leakage rates ($LR_{ann.,power}$), each weighted by the MPR for each cooling technology (i) within the building's cooling technology mix, as shown in Equation 30.

$$LR_{eff} = \sum_i MPR_i \cdot LR_{ann.,power,i} \qquad \text{[kg/(kW·year)]} \qquad \textit{Equation 30}$$

To determine the global warming potential (GWP) associated with leaked refrigerants, the model selected R-134A as a representative refrigerant due to its widespread usage and relevance within the context of European F-gas regulations (Mota-Babiloni & Makhnatch, 2021). Although R-134A is a hydrofluorocarbon (HFC) with a high GWP of 1,603 kg CO_2-eq/kg, it continues to be used due to its favorable properties and legacy installations. The EU's F-gas regulation aims to significantly reduce R-134A use by 2030, but it's prevalence in existing systems ensure its persistence in the near term. Therefore, a refrigerant global warming potential (GWP_{refr}) of **1,603 kg CO_2-eq/kg** was used in the model.

Similar to the calculation of material impacts described in section 3.2.3.2, the 98th percentile of cooling power demand ($P_{C,98p}$) from was then multiplied by the effective refrigerant leakage rate (LR_{eff}) and the refrigerant GWP (GWP_{refr}) to calculate the global warming potential of refrigerant leaks per building ($m_{equipment}$), as shown in Equation 31.

$$GHG_{refr.} = P_{C,98p} \cdot LR_{eff} \cdot GWP_{refr.} \qquad \text{[kg } CO_2\text{-eq]} \qquad \textit{Equation 31}$$

Greenhouse Gas Emissions of Production and End-of-Life phases

The GHG emissions occurring in the production and EoL phases of the cooling equipment were determined from the LCA-based impact assessment described in section 3.2.3.2.

Determining the Total Climate Change Impact

The total climate change impacts of residential and office cooling in The Hague were determined by adding up the GHG emissions from the four sources mentioned above:

1. Electricity consumption in the use-phase
2. Refrigerant leaks in assembly, use-phase, and EoL treatment of cooling equipment
3. Production of cooling equipment
4. EoL treatment of waste cooling equipment

These impacts were calculated for each residential and office building in The Hague and then aggregated to determine the GHG emissions of the entire building stock.

3.2.4 Integration of Methodology in Python-based Calculation Models

The methodology described above was primarily performed using a repository of Python scripts and input data files. Both the cooling demand and environmental impact calculation models were developed in Python, with the complete code accessible in Appendix C through a GitHub repository. Larger associated data input and output files can be retrieved via Appendix A through a Zenodo repository.

The implementation encompasses nine distinct Python and Jupyter Notebook files, totaling approximately 9,200 lines of code. Notably, simulating the cooling demand for the 59,381 residential and office buildings over the five-year reference period involves processing approximately 21 billion data points.

To account for diverse scenarios, the model incorporates about 190 input parameters, which are adjusted across five distinct scenarios. Detailed information on these input parameters used for the Python-based cooling demand and environmental impact models can be found in Appendix D to Appendix J.

3.3 Scenario Modeling

This section describes the approach used to answer the third research question:

How will the cooling demand in The Hague and its environmental impacts evolve until 2050?

To model the future cooling demand in The Hague and the environmental impacts associated with this cooling demand, four scenarios were selected. One scenario for 2030

was modeled, and three scenarios for 2050. The scenarios were based on climate scenarios published by KNMI in 2014 and updated in 2021 in the Climate Signal report, which aim to assess the potential severity of climate change in the Netherlands and inform appropriate adaptation and mitigation (Attema et al., 2014; KNMI, 2021). The KNMI scenarios are based on changes in two variable characteristics of future climate change: global temperature increase, and changes in air circulation patterns. Using these two axes, KNMI created four 2050 scenarios which include projections for twelve parameters including temperature, wind patterns, precipitation, and sea level rise (see Figure 34).

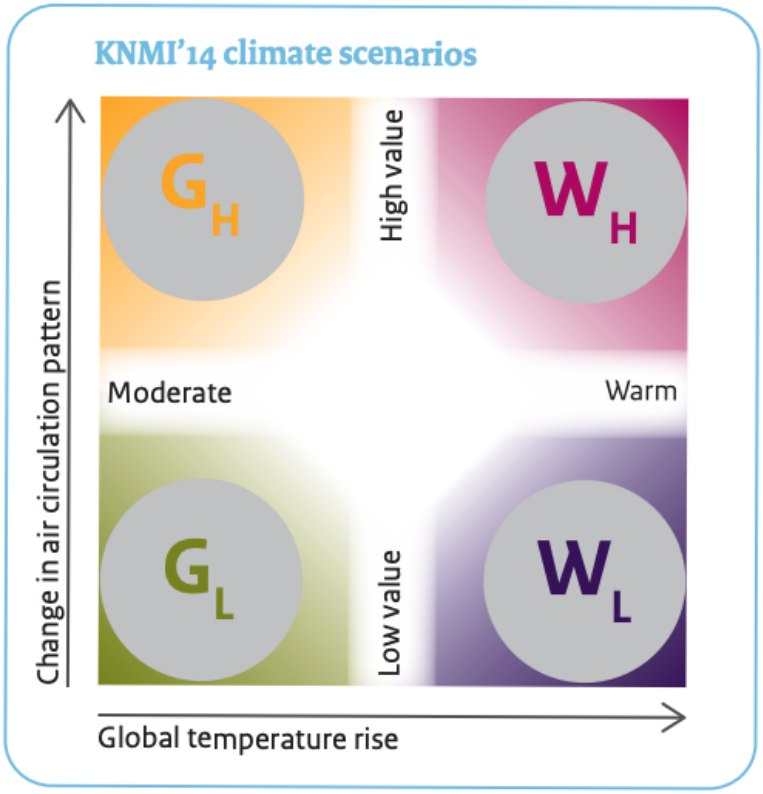

Figure 34: KNMI climate change scenarios, from (Attema et al., 2014).

First, 2030 was modeled to assess near-term changes in cooling demand and impacts and determine the urgency of immediate intervention. Only one scenario was used, given the short time horizon between the status quo reference period (2018–2022) and 2030, leaving a relatively narrow range in climate pattern variation and minimal time for potential interventions to have an impact. The same approach is adopted in the KNMI climate scenarios, which provides one scenario for 2030 due to this reasoning (Attema et al., 2014). Therefore, the KNMI 2030 scenario is used as a guideline in terms of relative temperature and solar radiation increases.

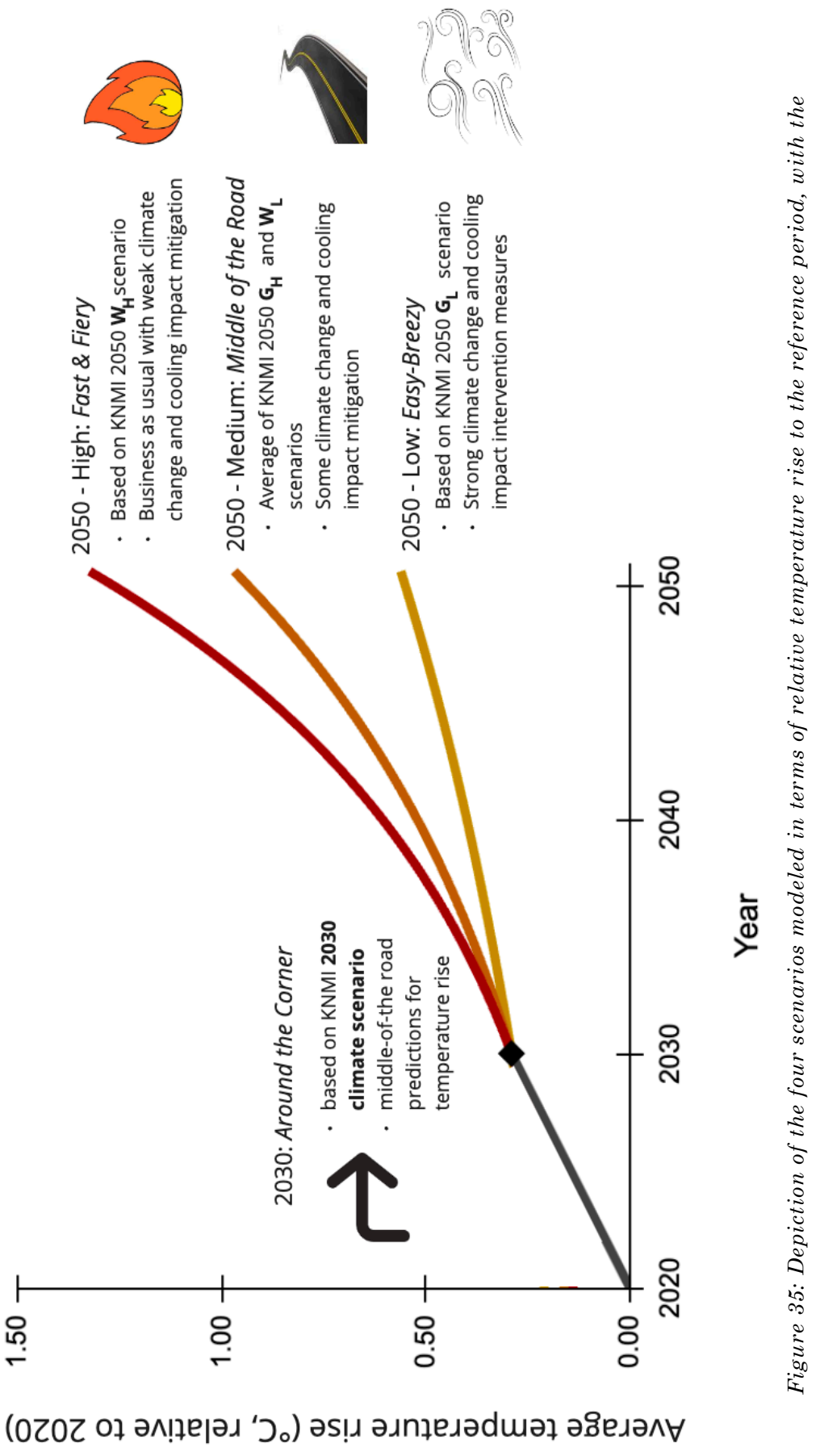

Figure 35: Depiction of the four scenarios modeled in terms of relative temperature rise to the reference period, with the central year of 2020.

For 2050, the four KNMI 2050 scenarios were condensed into three scenarios, which represent low, medium, and high impact trajectories. These scenarios were selected to illustrate a range of climate change severities, as well as intervention efforts (see Figure 35 for an overview). Refer to Appendix L for the KNMI scenario parameters, which underpin the temperature and solar radiation parameters utilized in this research's scenarios.

Adapting the status quo model to future scenarios involved running the cooling demand and environmental impact models (CDM and EIM) with adjusted inputs and parameters. In addition to environmental changes including rising temperatures and intensifying solar radiation, socio-technical changes also affect future cooling demand. The multi-level perspective (MLP) was used as a guiding framework to consider these factors, outlined in section 2.2, and their interdependencies (Geels, 2002). The MLP describes the transition from niche innovations to the socio-technical regime, which consists of five interconnected dimensions, as shown in Figure 36.

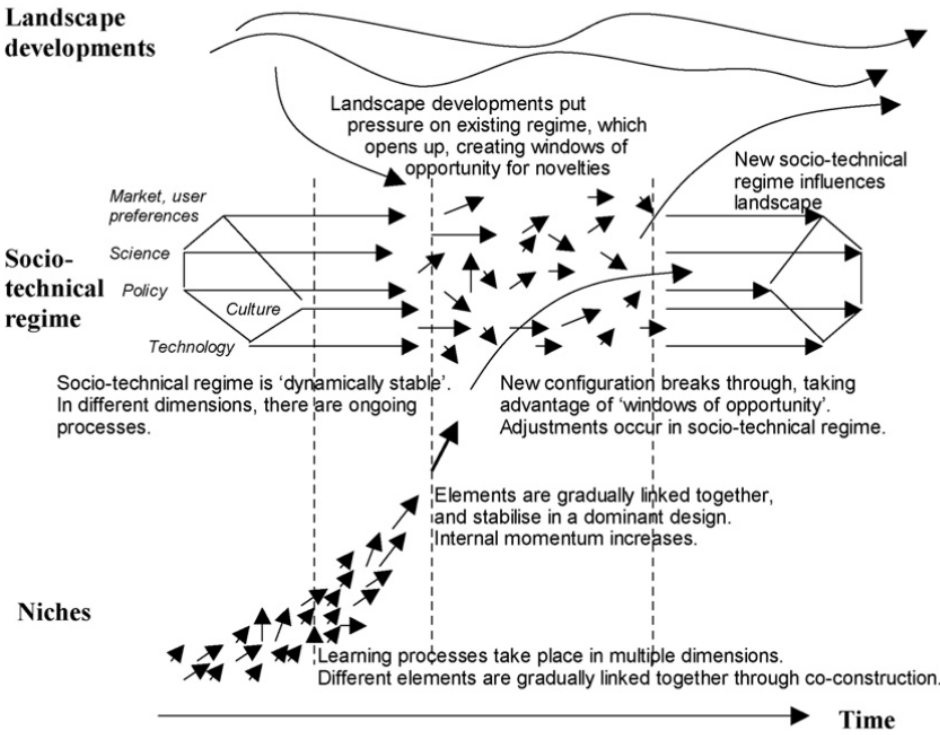

Figure 36: Graphical representation of the multi-level perspective. Adapted from (Geels, 2004).

Although space cooling is not considered a niche innovation on a global scale, its market penetration in residential buildings in The Hague was deemed to be at a niche level for the purpose of this analysis. Thus, the MLP framework was employed to evaluate the

drivers of cooling demand, cooling technologies, and the associated environmental impacts in The Hague.

With these dimensions and the changing climate in mind, specific parameters were selected for consideration, as shown in Figure 37. The following sections outline how these parameters and their expected evolution were incorporated into the building stock analysis, the CDM, and the EIM. A full overview of the input parameters that are varied in future scenarios can be found in Appendix D (global parameters), Appendix I (cooling technology mixes), Appendix J (energy efficiency and refrigerant leakage rates), and Appendix N (electricity grid mixes).

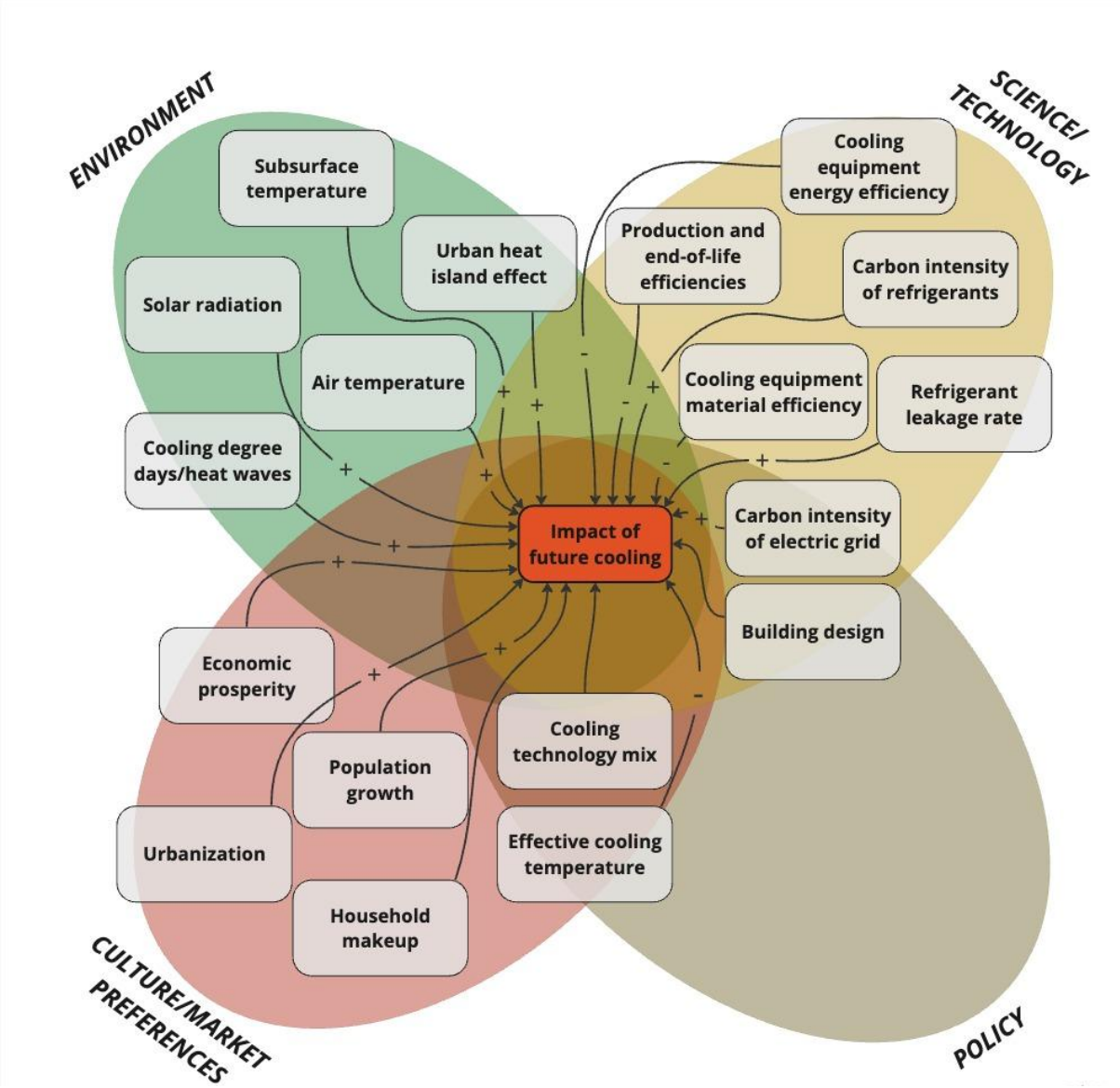

Figure 37: System dynamics map of parameters influencing the impacts of future cooling demand, using the dimensions of the multi-level perspective, with the addition of the environmental dimension.

3.3.1 A Changing Building Stock

Urbanization and population growth are expected to drive an increase in both population and population density in The Hague by 2050, leading to an expanded need for housing, as discussed in section 2.2.4.2. This growth is likely to result in a higher overall cooling demand due to the increased number of residences requiring cooling. On the other hand, office space demand may decrease due to the rise of hybrid working arrangements.

To account for these factors in future cooling demand scenarios, the building stock of The Hague was scaled accordingly. Predicting changes in building stock on a building or neighborhood level was not possible as future projections for the BAG are not available. Therefore, building stock adjustments were made at a city-wide level. Instead of modeling changes at the initial stages of the CDM, the cooling demand resulting from other scenario inputs was scaled according to the expected changes in the building stock. As a result, scenario outcomes can only be interpreted at the granularity of The Hague as a whole.

3.3.1.1 Evolution of the Residential Building Stock

It is assumed that any population growth in The Hague will be matched by an equivalent net increase in the residential building stock.[30] Specifically, this growth will occur in the 'new' residence types (i.e., type 1 and 3), which currently make up 19% of the residential building stock floor space. To consider the higher cooling demand generated by these new residences, the total expected household growth is divided by the share of post-2003 residences, resulting in a building stock growth factor for these newer buildings.

Table 22: Household growth in The Hague: 2020–2050, with lower and upper bounds of a 67% confidence interval. Based on (CBS, 2021; te Riele et al., 2019).

Year	**Building stock size**	*67% confidence interval*	**Building stock growth**	*67% confidence interval*
2020	265,500	261,500–269,700	-	-
2030	286,600	269,500–304,700	7.9%	3.1%–13.0%
2050	306,700	270,400–347,900	15.5%	3.4%–29.0%

[30] Note that this methodology choice is likely to underestimate the growth in the post-2003 building stock, as it assumed that no pre-2003 buildings will be demolished to make way for new buildings. Growth in the post-2003 building stock is likely greater than overall household growth. However, due to a lack of data on demolition rates, this aspect was not explored further in the research.

The total number of households is expected to increase by 15.5% in the 2020–2050 period, as detailed in Table 22 (CBS, 2021; te Riele et al., 2019). Most of this growth is attributed to the substantial increase in single households, projected to rise by over 27% in the next 30 years, as shown in Figure 38.[31]

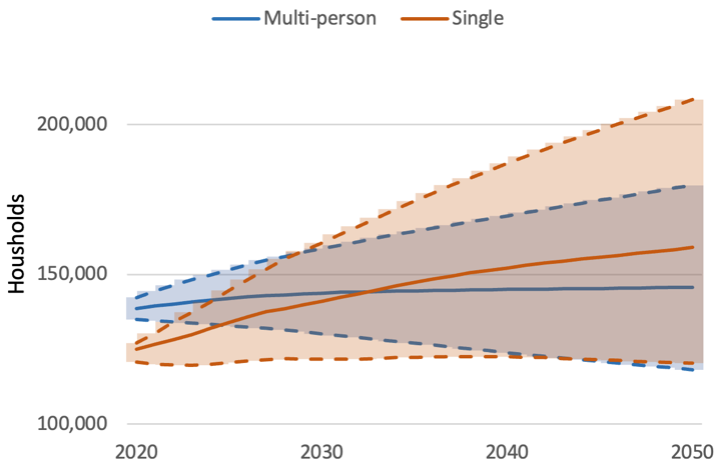

Figure 38: Multi- and single-person household growth in The Hague, 2020–2050. Dashed lines indicate a 67% confidence interval. Based on (CBS, 2021; te Riele et al., 2019).

These considerations inform the final change in building stock for the four scenarios as shown in Table 23. After thermodynamic modeling , the cooling and power demand of post-2003 buildings were multiplied by these growth rates to upscale impacts to the modeled building stock of each scenario, depicted in Figure 39.

Table 23: Modeled residential building stock growth in scenarios.

Scenario	Growth of total building stock	Growth of post-2003 building stock
2030	7.9%	41.8%
2050-L	3.4%	17.9%
2050-M	15.5%	81.7%
2050-H	29.0%	153%

[31] This changing household composition, with an increasing number of single-person households, is expected to influence internal heat gains in buildings and reduce the frequency of occupant presence. This suggests that cooling demand may not increase linearly with the total number of households. However, the precise impact of this shift in household composition falls outside the scope of this research.

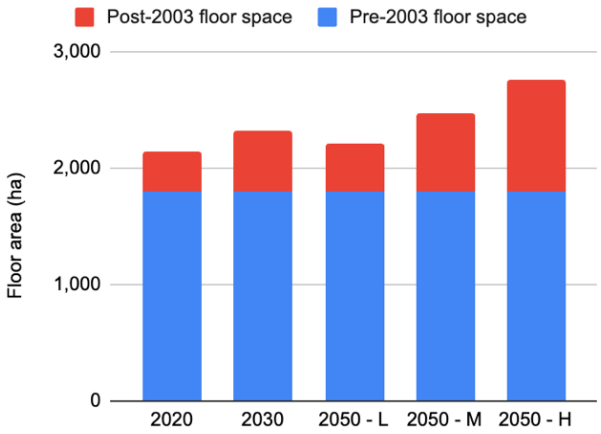

Figure 39: Modeled residential floor space per age class in the four scenarios.

3.3.1.2 Evolution of the Office Building Stock

In contrast to residences, the office building stock in the Netherlands is anticipated to shrink by 2050 according to Netherlands Statistics (CBS), as seen in Figure 40 (Buitelaar et al., 2017). Based on this projection, a reduction in building stock was assumed for pre-2003 office buildings. The assumption is office space demand correlates linearly with the size of the office building stock, allowing the growth factors for office space demand to be considered as the office building stock growth.[32]

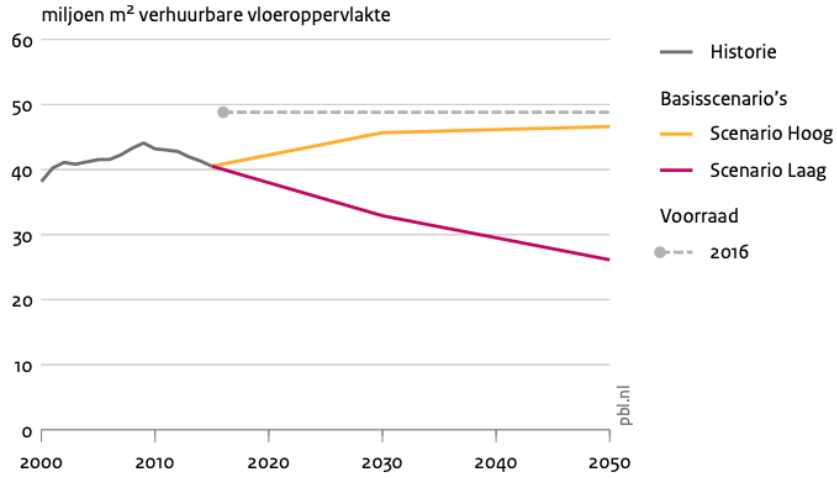

Figure 40: Prognosis of office space demand in the Netherlands, 2000–2050, from (Buitelaar et al., 2017).

[32] In reality, a portion of unused offices may be repurposed or left vacant rather than being demolished. However, for the purposes of this research, the distinction between repurposed, vacant, or demolished offices is not relevant, as their cooling impacts in these states are beyond the scope of this study.

However, this projection is from 2017. Since the onset of the Covid-19 pandemic, many major employers have announced plans to reduce office space (NOS, 2021). The Social and Economic Council of the Netherlands (SER) also assumes that remote working is here to stay (SER, 2022). While a quantitative prognosis is yet to be developed, hybrid working was modeled through assuming lower growth numbers than the 2017 CBS projection, with an additional 10% shrinkage to account for the post-COVID hybrid working culture. The resulting rates of change in the office building stock for the scenarios can be found in Table 24 and are visualized in Figure 41.

Table 24: Modeled change rates for the office building stock, compared to 2020.

Scenario	Change rate	Rationale
2030	-23%	Average of the Low and High 2030 CSB scenarios, with 10% additional reduction to account for post-COVID hybrid working
2050-L	-47%	Low 2050 CBS scenario, with 10% additional reduction to account for post-COVID hybrid working
2050-M	-31%	Average of the Low and High 2050 CBS scenarios, with 10% additional reduction to account for post-COVID hybrid working
2050-H	-14%	High 2050 CBS scenario, with 10% additional reduction to account for post-COVID hybrid working

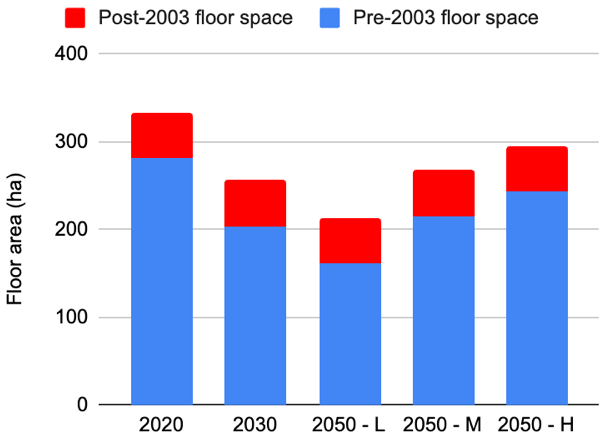

Figure 41: Modeled office floor space per age class in the four scenarios.

3.3.2 Adapting Thermodynamic Modeling Parameters

3.3.2.1 Adjusting the Outdoor Air Temperature

To account for future scenarios, average temperature increases per season were incorporated into the status quo air temperature (T_o) series from the KNMI climate scenarios. Hourly temperature data for 2030 and the three 2050 CDM scenarios were derived by adding the corresponding average temperature increases per season from the

KNMI climate scenarios to the outdoor temperature data from Hoek van Holland for the 2018–2022 status quo period.[33]

It is important to note that the KNMI scenarios project future changes relative to a reference period of 1981–2010, while our status quo modeling is based on the 2018–2022 reference period. To harmonize these reference points, the average temperature change per decade between 1996 (the central year of the KNMI reference period) and the year corresponding to the CDM scenarios (2030 or 2050) was calculated. This average increase was then used to adjust the difference between the CDM status quo (with 2020 as the central year) and the CDM scenario year (2030 or 2050). The background research spreadsheet in Appendix A contains detailed calculations. Table 26 provides the resulting temperature increases used in the scenario models.

In translating air temperatures from Hoek van Holland to The Hague, it was necessary to include the Urban Heat Island (UHI) effect. First, the day and nighttime averages used for the status quo model were added to the hourly temperature data, as described in section 3.2.2.1. Furthermore, considering the expected intensification of the UHI effect due to climate change, incremental increases in the UHI effect were incorporated into each CDM scenario. These increases, derived from study estimates referenced in section 2.2.3, are presented in Table 26.

3.3.2.2 Changes in the Effective Cooling Temperature

In this study, the indoor temperature (T_i) is equivalent to the effective cooling temperature ($T_{effective}$), representing the thermal comfort range's upper limit. Activation of cooling equipment is considered when this threshold is exceeded. The change in effective

[33] Two relevant indicators are provided by KNMI: (1) average temperature increases per season, and (2) the number of summery days with a temperature greater than 25 °C per year, which can be seen as a measure of cooling degree days (CDDs) (Attema et al., 2014). The second data point accounts for the rising frequency of heatwaves, but an analysis was conducted to compare the outcomes of using either data point. Average KNMI temperature increases were added to the status quo weather time series, and the resulting number of additional CDDs was counted. This analysis showed that the increase in CDDs based on a flat temperature increase across the whole time series closely matched the estimated CDD increase provided in the KNMI scenarios. Given that the CDM is based on time series of weather data as input, the first indicator (average temperature increases per season), was considered more suitable for scenario modeling.

cooling temperature is assumed to depend mostly on policy trends concerning adaptive thermal comfort ranges and the environmental impacts of cooling.[34]

For the scenarios, no change in $T_{effective}$ is assumed for 2030 due to the short timeframe. For 2050-L, an increase is presumed to reflect adaptive and environmentally focused policies. In contrast, 2050-M maintains the status quo, and 2050-H models a decrease, assuming historical trends without policy intervention continue, as detailed in section 2.2.1. The $T_{effective}$ values used in the model are shown in Table 26.

3.3.2.3 Development of the Subsurface Temperature

Climate change not only elevates air temperatures but also subsurface temperatures (T_s) (Pollack et al., 1998). Despite the lack of specific projections for subsurface temperature rise in the Netherlands, a strong correlation between air and subsurface temperatures was established using data from the De Bilt weather station for the 1981–2021 period (KNMI, 2022a, 2022b). Detailed calculations and figures are provided in Appendix M. Figure 42 and Table 25 illustrate this correlation, Both temperatures increased by 0.40 ± 0.05 °C over this period, consistent with the 2021 "Climate Signal" (KNMI, 2021).

Table 25: Pearson correlation between air and subsurface temperature, and air and subsurface temperature change in De Bilt, across the 1981–2021 period.

Variable pair	Pearson correlation	p-value
T_{air}, T_s (10-year rolling mean)	0.96	$3 \cdot 10^{-24}$
ΔT_{air}, ΔT_s (10-year rolling mean)	0.85	$1 \cdot 10^{-9}$

Hence, increases in subsurface temperature for each scenario were assumed to match the air temperature rise detailed in section 3.3.2.1, as shown in Table 26. Annual average temperature increases were used, as the subsurface temperature is assumed to be constant over the year (see also section 3.2.2.1).

[34] Contrary to initial expectations, the population's age distribution does not significantly influence the threshold temperature. Despite a forecasted 32% increase in individuals aged 65+ by 2050 (Manders & Kool, 2015), research shows that thermal comfort ranges are relatively consistent across age groups within cultural contexts (Rupp et al., 2015; Z. Wang et al., 2018). While an aging population is more susceptible to heat-related health risks (IEA, 2018a; Kenny et al., 2010), it does not substantially alter the established thermal comfort range. Thus, this aspect is not factored into the model's effective cooling temperature settings.

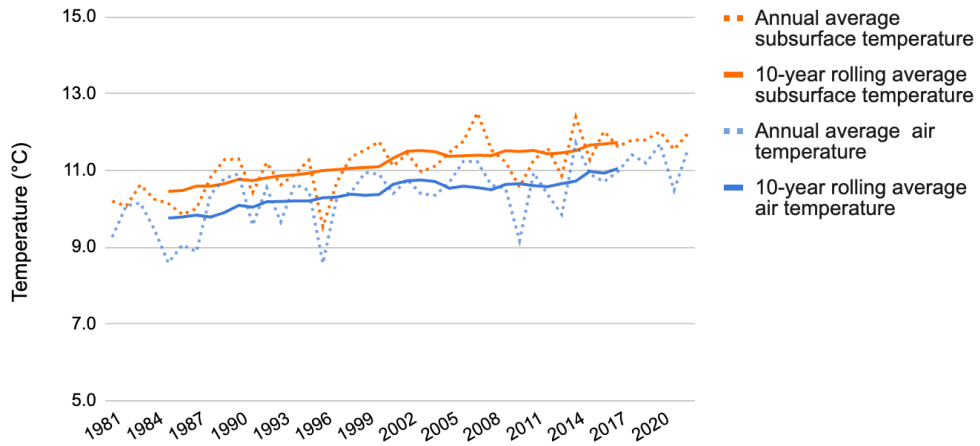

Figure 42: Air and subsurface temperatures in De Bilt (1981–2021), based on (KNMI, 2022a, 2022b).

3.3.2.4 Solar Radiation Projections

KNMI climate scenarios project annual and summer-specific increases in solar radiation as percentages relative to a 1981–2010 reference period (Attema et al., 2014). To align these with the CDM which uses the 2018–2022 reference period, a similar adjustment method to that for air temperature was used. These projections, being percentage-based, necessitated logarithmic calculation of the average per-decade increase, adjusted to fit the 2018–2022 period as reference point. Detailed calculations are available in the background research spreadsheet in Appendix A. The resulting increases in solar radiation were then applied to the existing hourly data to project future solar radiation levels. The summer-specific increase was applied to the summer months, while the annual average increase was used for the other seasons.

Table 26: Scenario values of climate-related parameter inputs in the CDM.

Scenario	Air temperature increase (Δ°C)		UHI effect increase (Δ°C)	Effective cooling temperature (°C)	Subsurface temperature increase (Δ°C)	Solar radiation increase (%)	
2030	Spring	0.23	0.00	25	0.29	Summer	0.53%
	Summer	0.26				Rest of year	0.06%
	Autumn	0.29					
	Winter	0.35					
2050-L	Spring	0.5	0.10	26	0.55	Summer	1.57%
	Summer	0.55				Rest of year	0.45%
	Autumn	0.61					
	Winter	0.61					
2050-M	Spring	0.8	0.30	25	0.94	Summer	2.23%
	Summer	0.85				Rest of year	0.30%
	Autumn	0.96					
	Winter	1.02					
2050-H	Spring	1.16	1.5	23	1.27	Summer	4.80%
	Summer	1.27				Rest of year	0.90%
	Autumn	1.27					
	Winter	1.49					

3.3.2.5 Evolution of Building Design and Energy Label Mix

Energy labels served as a proxy for anticipated changes in building design, reflecting efforts to enhance energy efficiency and reduce the building sector's carbon footprint. The Dutch government has set or proposed requirements for future building standards. For residential buildings, policies proposed to prohibit renting out homes with energy labels E or lower from 2030, impacting around 580,000 rental properties (NOS, 2022). Office buildings face stricter standards, with a requirement for energy label C for offices over 100 square meters by 2023 (Bouwbesluit, 2012; RVO, 2018).

In response to these policies, the energy label distribution for buildings in The Hague was modified in each scenario to mirror future improvements. A study from the Dutch Environmental Assessment Agency (PBL) study provided projections until 2050 for

residential building energy labels under various investment levels—limited (*Investeringspad beperkt*), broad (*Investeringspad breed*), and deep (*Investeringspad diep*)—in climate-neutral buildings, as illustrated in in Figure 43 (van den Wijngaart et al., 2014).

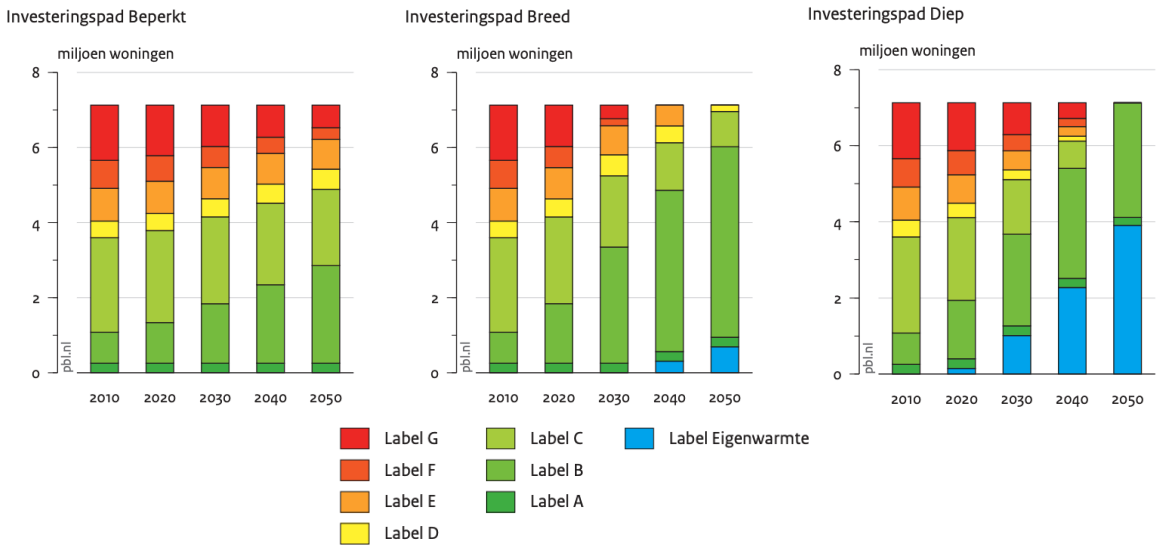

Figure 43: Energy label distributions of residential buildings for PBL 2014 scenarios for limited, broad, and deep investment in climate-neutral buildings, from (van den Wijngaart et al., 2014). Note that "Eigenwarmte" indicates energy-neutral or energy-positive buildings.

Table 27: Energy label conversions assumed between status quo energy label categories and scenarios, based on (van den Wijngaart et al., 2014).

End use	Scenario	Source	Energy label			
	SQ (2020)	2023 building stock	A–A+++++	B–C	D–E	F–G
Residential buildings	2030	PBL 'Breed' 2030	A–A+++++	B–C	D–E	B–C
	2050-L	PBL 'Diep' 2050	A–A+++++	A–A+++++	B–C	B–C
	2050-M	PBL 'Breed' 2050	A–A+++++	B–C	B–C	B–C
	2050-H	PBL 'Beperkt' 2050	A–A+++++	B–C	D–E	B–C
Office buildings	2030	PBL 'Diep' 2030	A–A+++++	B–C	B–C	B–C
	2050-L	PBL 'Diep' 2050	A–A+++++	A–A+++++	B–C	B–C
	2050-M	PBL 'Diep' 2050	A–A+++++	A–A+++++	B–C	B–C
	2050-H	PBL 'Breed' 2050	A–A+++++	B–C	B–C	B–C

These PBL scenarios informed the energy label distribution for this study's scenarios. Adjustments were made at the building level, creating specific 'rules' for each energy label group. For instance, offices with F–G labels are mandated to reach at least C by 2023,

hence are assigned B–C by 2030. For residential buildings, the deep, broad, and limited investment 2050 PBL scenarios were applied as 2050-L, -M, and -H, respectively. The broad PBL scenario for was used for the 2030 scenario in this study. Offices, having higher standards, were assumed to follow the PBL broad scenario for 2050-H and the deep scenario for 2030, 2050-L, and 2050-M. The resulting energy label conversion rules are detailed in Table 27.

Future building energy efficiency and insulation metrics (including R_C, U, and window solar factors) are expected to improve due to stricter building codes and technological advancements. Despite the lack of specific future policies on insulation values, there are policies on energy labels. Therefore, the changing mix of energy labels in the building stock serves as a proxy for these evolving metrics to prevent overlapping calculations. The current R_C, U, and window solar factors values per energy label (see Table 12 and Table 15) were also used in the future scenarios.

3.3.3 Adjusting Environmental Impact Modeling Parameters

After establishing the future cooling demand for residential and office buildings in each scenario, based on the adapted input parameters detailed in the above section, the same Environmental Impact Model (EIM) outlined in section 3.2.3 was used to assess the environmental impacts associated with this demand, tailoring relevant parameters to fit the future scenarios. This section outlines the projection methodology for these parameter inputs for each scenario.

3.3.3.1 Updating the Energy Efficiency of Cooling Equipment

Technological advancements are likely to improve the energy efficiencies of cooling technologies in the future. Therefore, SEER values for these technologies were updated for 2030 and 2050 scenarios, based on projections from the *Heat Roadmap Europe* project (Dittmann et al., 2016).

Table 28: Energy efficiencies (SEER values) by cooling technology used in each scenario, based on (Dittmann et al., 2016).

Scenario	ASHP	GSHP	WSHP	Chiller	Split AC	Portable AC
SQ (2020)	5	6	8	4	5	3
2030	7	9	10	5	7	3
2050-L	9	12	14	7	9	4
2050-M	8	11	13	6	8	4
2050-H	7	10	12	6	7	3

For the 2030 and 2050-M scenarios, the project's projected improvements were adopted. In the 2050-H scenario, only half of the projected improvements in SEER were considered, reflecting potential challenges in environmental initiatives and economic conditions. Conversely, in the 2050-L scenario, an improvement of 50% over the projected SEER values was assumed, driven by effective energy-efficiency policies. The derived SEER values can be found in Appendix J.

3.3.3.2 Evolution of the Carbon Intensity of the Electricity Grid

While specific projections for future carbon intensity are not available, they are influenced by the electricity grid's energy mix. The Netherlands' energy mix is expected to increasingly lean towards renewables and low-carbon sources. To determine carbon intensities for the scenarios, the electricity mix for each was analyzed, and carbon intensities for each energy source were used to calculate an overall figure.

The 2021 "Climate and Energy Outlook" report by PBL projects the penetration of renewables by 2030 based on current climate and energy policy, also shown in Figure 44 (Hammingh et al., 2021). The *Energy Transition Model* offers a detailed breakdown of electricity by source in petajoules (PJ) based on the PBL projection, which was used to determine the precise electricity mix for the 2030 scenario (Zaccagnini et al., 2023).

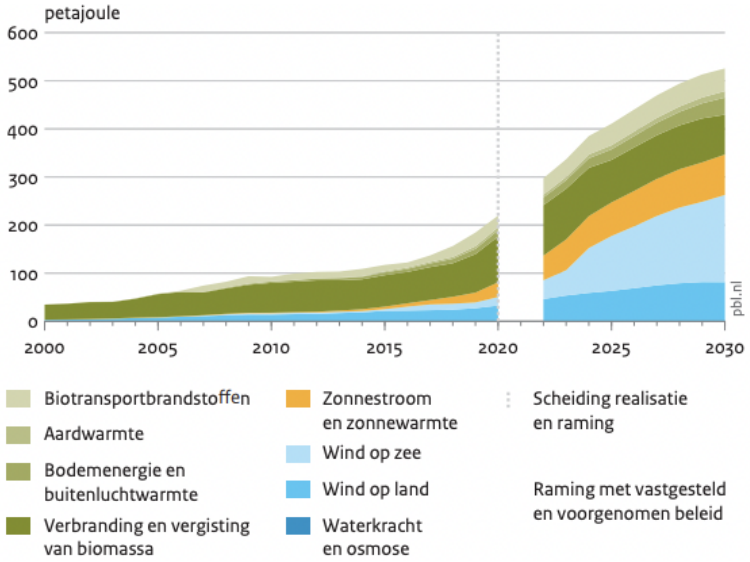

Figure 44: Gross end-use of renewable energy per energy source, 2000–2030 from (Hammingh et al., 2021).

For 2050, the "Klimaatneutrale energiescenario's 2050" (*Climate Neutral Energy Scenarios 2050*) report offered projections for the electricity mix, shown in Figure 45. (Ouden et al., 2020). Given that these scenarios explore carbon-neutral systems, they may

be overly optimistic. Thus, for 2050-H, the 2030 scenario's carbon intensity was retained to consider a less-than-complete grid decarbonization by 2050. The regional scenario informed the 2050-M scenario, and the national scenario was used for 2050-L, reflecting different levels of regional and national efforts. Detailed electricity mixes were again sourced from the *Energy Transition Model* (Zaccagnini et al., 2023).

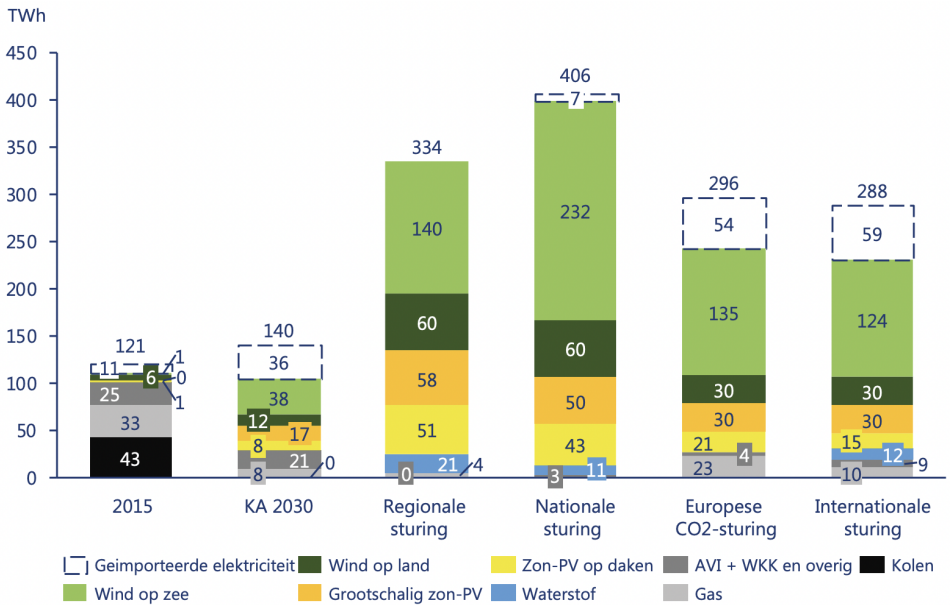

Figure 45: Dutch electricity production mix in 2015, and for several future scenarios, from (Ouden et al., 2020).

Next, these electricity mixes were converted into carbon intensities. The *Energy Transition* Model's provides direct GHG emissions from electricity production. However, a life-cycle perspective, which includes factors like construction and maintenance emissions, reveals that renewable sources have a low but not zero carbon footprint. Thus, life-cycle GHG emission intensities from ecoinvent 3.8 were used in the calculations (Huijbregts et al., 2017; Wernet et al., 2016).[35]

[35] Note that these emission factors are based on LCAs of electricity production facilities from 2020. In reality, these emission factors are likely lower in future scenarios because the infrastructure surrounding electricity production is expected to decarbonize together with the economy, following policy on decarbonization. (e.g., it will likely take less emissions to build a windfarm in 2050 than in 2020). For improved accuracy, one could model the LCAs of all relevant electricity sources using tools like IMAGE and Premise (Sacchi et al., 2022; Stehfest et al., 2014). However, such analysis was left out of the scope of this research.

Due to differences in the categorization of electricity sources in ecoinvent and the *Energy Transition Model* scenarios, assumptions regarding the subdivision of renewable sources were necessary, detailed in Appendix N. These include the emission factors for each electricity source in Table 72, with full calculations available in the background research spreadsheet in Appendix A. The resulting carbon intensities for each scenario can be found in Table 29 and visualized in Figure 46.

Table 29: Modeled carbon intensities of the Dutch grid in each scenario.

Scenario	Carbon intensity (g CO2-eq/kWh)	Source scenario name	Source literature
SQ (2020)	427	-	(van der Niet & Bruinsma, 2022)
2030	159	Climate and Energy Outlook for the Netherlands 2030	(Hammingh et al., 2021)
2050-L	29	2050 International	(Ouden et al., 2020)
2050-M	42	2050 Regional	(Ouden et al., 2020)
2050-H	159	Assumed no progress since 2030	(Ouden et al., 2020)

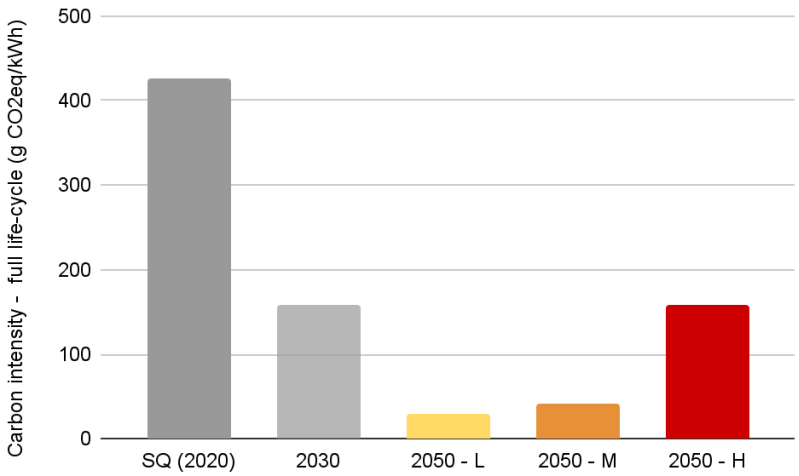

Figure 46: Modeled carbon intensities of the Dutch grid in each scenario.

3.3.3.3 Changes in Refrigerant Leakage Rates

By 2030, with ongoing maintenance practices and moderate new regulations, a slight decrease in refrigerant leakage rates is expected (OzonAction, 2016; Kigali Amendment to the Montreal Protocol, 2016). Hence, the 2030 leakage rates are assumed to align with the lower bound of the leakage rate range estimated by the Intergovernmental Panel on Climate Change (IPCC) (Penman et al., 2000).

For 2050-H, the model anticipates an increase in leakage rates over 2030 levels, attributed to higher cooling demands and inadequate policy and technological measures

to mitigate leakage (UNEP & IEA, 2020). However, overall technological improvements and heightened awareness may moderate this increase, with rates assumed to be on par with the 2018–2022 status quo scenario.

In the 2050-M scenario, significant progress in refrigerant management and equipment maintenance, along with policies favoring low-GWP refrigerants, is expected to further reduce leakage rates by 2050 (OzonAction, 2016). The model translates this to a 50% reduction in leakage rates compared to 2030.

For 2050-L, a substantial decrease in leakage rates is forecasted, based on the widespread implementation of best practices in equipment design, operation, and disposal, alongside aggressive policies to reduce high-GWP refrigerants (Purohit et al., 2020). The model assumes a 75% reduction in leakage rates from 2030 levels.

Table 30 summarizes these modeled refrigerant leakage rates based on the discussed assumptions.

Table 30: Assumed effective annual refrigerant leakage rates, per cooling technology.

	Cooling equipment type					
Scenario	*ASHP*	*GSHP*	*WSHP*	*Chiller*	*Split AC*	*Portable AC*
SQ (2020)	5%	5%	5%	10%	5%	23%
2030	4%	4%	4%	4%	4%	18%
2050-L	1%	1%	1%	2%	1%	6%
2050-M	2%	2%	2%	2%	2%	9%
2050-H	5%	5%	5%	10%	5%	23%

3.3.3.4 Adjusting Refrigerant Global Warming Potentials

The selection of refrigerants for projecting the environmental impacts of space cooling in 2030 and 2050 mirrors changes in regulatory policies and refrigeration technology advancements. Table 31 presents potential future low-GWP refrigerants. For the 2030 scenario, R-32 is chosen for its superior thermodynamic properties and lower GWP compared to R-134A and R-410A, along with growing industry acceptance (Calm, 2008). Despite being an improvement, R-32 still possesses a non-negligible GWP. Under the 2050-H scenario, R-32 remains the preferred refrigerant, assuming no major breakthroughs or regulations prompting a shift to even lower-GWP options. For 2050-M, the model anticipates a move towards lower-GWP refrigerants like CO_2 and R-1234yf, driven by increasing regulatory pressures and industry shifts towards more

environmentally friendly options globally (Mota-Babiloni & Makhnatch, 2021; H. Wang et al., 2021).

Table 31: Candidates for low-GWP refrigerants, adapted from (Calm, 2008)

Candidates	Considerations
"Natural Refrigerants" (NH_3, CO_2, HCs, H_2O, air	Efficiency, for NH3 and HCs also flammability
Low GWP HFCs (R-32, R-152a, R-161 etc.)	Flammability; most suppressants have high GWP
HFEs	Disappointing thus far, still?
HCs, HEs (R-290, R-600, R-E170, etc.)	Flammability
Unsaturates (olefins) (R-1234yf, etc.)	Short atmospheric lifetime and therefore low GWP, flammability? toxicity? compatibility?
HFICs, FICs (R-31I1 (CH_2FI), R-13I1 (CF_3I), etc.)	Expensive, ODP > 0 but not in MP, some are toxic; compatibility?
Fluorinated alcohols (–OH), fluorinated ketones (–(C]O)–)	Efficiency? flammability? toxicity? compatibility?

In 2050-L, the focus shifts to zero-GWP refrigerants such as propane and ammonia, despite their flammability and toxicity challenges. These refrigerants are noted for their minimal climate impact and efficiency under certain conditions (Calm, 2008). The refrigerant choices across these scenarios are summarized in Table 32.

Table 32: Modelled refrigerant choices and their global warming potentials. Based on (Hodnebrog et al., 2020)

Scenario	Refrigerant	GWP (kg CO_2-eq/kg)
SQ (2020)	R-134A	1,603
2030	R-32	809
2050-L	Zero-GWP refrigerants (e.g., ammonia, water)	0
2050-M	Low-GWP refrigerants (e.g., CO_2 and R-1234yf)	1
2050-H	R-32	809

While acknowledging that changing refrigerants can affect the efficiency of cooling devices, this research primarily concentrates on the direct GHG emissions from refrigerants (Nawaz & Ally, 2019). It is assumed that future advancements in device efficiency will lead to an increased proportion of refrigerant emissions in the total environmental impact of cooling systems.

3.3.3.5 Adjusting the Market Penetration Rate of Cooling Equipment

The rate of cooling equipment adoption and the choice of specific cooling technologies are influenced by various factors. These include the demand for cooling, economic prosperity influencing individuals' ability to invest in such equipment, the cost and perceived value

of air conditioners, and policies and regulations at local and global levels. Societal attitudes and cultural norms also play a role in adoption rates, as discussed in section 2.3.

Regarding future market penetration (MPR) of air conditioners in residential buildings in the Netherlands, detailed projections are scarce. One notable study projected annual growth rates of 5% to 15%, but its age limits its applicability to this research (van Kempen, 2000). Broader European studies, like the "Future of Cooling" report by the IEA predict MPR growth rates of 55% by 2030 and 150% by 2050, but don't account for the Dutch context (IEA, 2018a). Therefore, this study relies on the 2021 TNO study, which also informed the status quo MPRs, with findings compared in

Table 33 (Rovers et al., 2021).

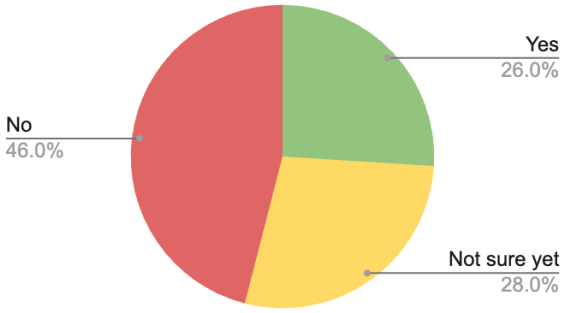

Figure 47: Responses to the question: "Are you considering purchasing cooling equipment in the coming years?". Adapted from (Rovers et al., 2021).

Figure 47 shows survey responses on the intent to purchase cooling systems. These were used to estimate cooling equipment MPRs. For 2030, it was assumed that all respondents who answered 'yes' would purchase an air conditioner. The 2050-L assumed half of the 'I don't know yet' group would buy, the 2050-M scenario assumed all in this group would buy, and the 2050-H scenario included this plus half of the initial 'no' respondents. These projections yield the MPRs in

Table 33, with detailed calculations available in the background research sheet in Appendix A.

Table 33: Comparison of projected residential cooling equipment market penetration rates in The Netherlands, based on several studies.

Scenario	(van Kempen, 2000)	(IEA, 2018a)	(Rovers et al., 2021)
SQ (2020)	15%	15%	**15%**
2030	39%	23%	**37%**
2050-L	65%	30%	**49%**

2050-M	100%	38%	**61%**
2050-H	100%	45%	**80%**

For offices, due to the absence of specific data, residential MPR growth rates were applied. With the MPR already up by 153% from 2020 to 2030, this approach sets a 100% MPR for office cooling equipment in all future scenarios.

3.3.3.6 Projections for the Cooling Technology Mix

The anticipated increase in the total market penetration rate (MPR) of active cooling equipment is clear, yet the specific mix of cooling technologies to be used is uncertain. Influences on the technology mix, including policy, user preferences, and environmental considerations, are detailed in section 2.3.7.

In the Netherlands, there is a notable absence of policies directly targeting specific types of cooling equipment. EU-wide, there are directives like the minimum energy performance standards (MEPSs), but these do not specify preferences for particular cooling technologies. However, policies are significantly promoting heat pumps, with subsidies facilitating their adoption (RVO, 2023). Additionally, the ban on gas connections in new buildings is pushing a shift towards using heat pumps for heating purposes (Wijzigingswet Elektriciteitswet 1998, enz. (voortgang energietransitie), 2021). This policy environment could encourage the move from traditional cooling-only systems to integrated heat pump solutions.

The Netherlands aims to move 20% of its residential buildings off natural gas by 2030 and the entire stock by 2050, with decisions on heat pumps or heat districts being made at the municipal level (Klimaatakkoord, 2019). The Hague places a notable emphasis on heat districts (DSO, 2022), as highlighted in Table 34.

Table 34: Proposed heating solutions and population sizes for The Hague neighborhoods, based on (DSO, 2022; The Hague Municipality, 2023).

Proposed heating solution	Number of neighborhoods	Number of residents (2022)	Share of population (2022)
Heat district	43	271,030	49%
Heat pumps	20	46,360	8%
Mix of heat pumps and heat district, or heating solution yet to be determined	43	235,916	43%

Considering these factors, the following assumptions were made for market penetration rates (MPR) and technology mixes for residential and buildings:

- **2030**: 8% of The Hague's residential buildings use heat pumps.[36] The remaining MPR (29%) is met by large split AC systems, chillers, and portable AC units in the same ratio as the status quo.
- **2050-L**: 51% of residential housing uses reversible heat pumps, covering the total MPR of 49%, eliminating the need for separate cooling equipment.
- **2050-M**: 30% of residential housing uses heat pumps, with the remaining MPR (31%) met by the same mix as in 2030.
- **2050-H:** 8% of residential housing uses heat pumps for heating, with most heat provided by heat districts, necessitating separate cooling equipment. Additional installations compared to 2030 are assumed to be portable AC units.

For office buildings, due to the absence of specific data, the assumptions mirror those for residential settings,[37] except for the portable AC MPR which was assumed to remain constant from the status quo. The details of the resulting cooling technology mixes are available in Appendix I, with Figure 48 illustrating the assumed mix for the 2030 scenario.

[36] This research operates under the assumption that all installed heat pumps are reversible and capable of providing cooling. However, it's important to recognize that in practice, not all heat pump systems may offer cooling functionality due to limitations in the heat pumps or specific building constraints. Determining the exact proportion of reversible heat pumps is challenging and was not addressed in this study's scope.

[37] This research assumes that large-scale heat pumps in offices have similar characteristics to residential ones, due to the lack of specific data on their differences.

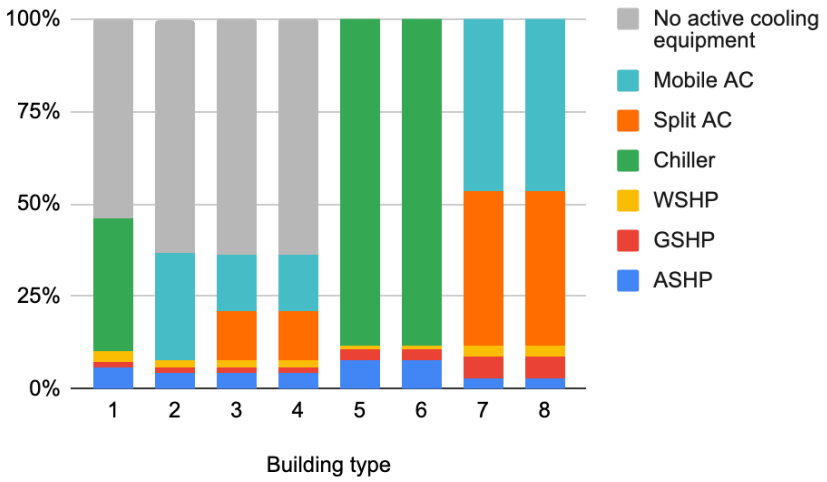

Figure 48: Cooling technology mix choices per building type, for the 2030 scenario.

3.3.3.7 Adjusting Material Efficiency and Production- and EoL-phase impacts of Cooling Equipment

Both the material impacts and production- and EoL-phase GHG emissions of cooling equipment are expected to decrease in the future due to stricter policy and technological optimizations. Predicting changes in cooling devices' material composition is challenging due to data scarcity and uncertainties in technological innovation. Thus, this research assumes no changes in their material makeup across both current and future scenarios. While production and EoL-phase GHG emissions are expected to decline with grid decarbonization and enhanced production and e-waste regulations, detailed modeling of these aspects was not conducted due to their complexity. Thus, these emissions were assumed to stay constant across scenarios in this study.

3.4 Sensitivity Analyses and Extrapolation of Results

3.4.1 Sensitivity Analysis

Sensitivity analyses for key input parameters like the UHI effect, effective cooling temperature, and the cooling demand cap percentile were performed, see the full list in Table 35, using the Status Quo (SQ) scenario input parameter configuration.

The analyses involved running the cooling demand model 100 times on a representative sample of 314 buildings, reflecting the characteristics of the larger stock of 59,381 buildings used in the main model. Each parameter was linearly adjusted within specified ranges to understand its influence on the five main impact metrics: cooling energy demand, cooling power demand, electricity consumption, GHG emissions, and material

requirements. Elasticities (*El*) were calculated using Equation 32, with x as the input parameter, y as the impact metric, and Δx and Δy as their respective changes.

$$El = \frac{\Delta y / y}{\Delta x / x} = \frac{\Delta y}{\Delta x} \cdot \frac{x}{y} \qquad \textit{Equation 32}$$

Key findings from these analyses are detailed in section 4.3.1, with a comprehensive table of elasticities and detailed graphs in Appendix O.

A second set of sensitivity analyses evaluated the environmental impact of different cooling technologies. Here, the SQ scenario was modified to simulate 100% market penetration of one cooling technology (e.g., heat pumps), then incrementally shifted 1% at a time to another technology (e.g., large split AC systems). This gradual transition recorded the average changes in environmental impacts for all possible pairs of cooling technologies. The results of these assessments are documented in section 4.3.1.7.

Table 35: The input parameters for which sensitivity analysis were performed.

Input parameter	Reference value	Unit	Analyzed range	Range description
Peak cooling power demand percentile	98%	%	80–100	This corresponds with a range between 870 and 0 hours of indoor temperatures above the thermal comfort range
Effective cooling temperature	25	°C	15–30	This range corresponds with the outer limits of thermal comfort ranges found in the literature.
Summertime temperature	18.2	°C	16.2–26.2	This range corresponds with a -2 °C to +6 °C degree scenario
Total market penetration rate of cooling equipment	12	% of the market	0–100	
Daytime UHI effect	8.3	°C	0–15	This corresponds with a range between no UHI effect and an extreme UHI effect as seen on the hottest days in cities like Phoenix
Energy efficiency of cooling technologies (SEER)	5	kWh cooling / kWh electricity	1–20	
Summertime solar radiation	229	W / m²	227–252	This range corresponds with a -1% to 10% increase of the solar radiation.
Carbon intensity of electricity grid	0.427	kg CO_2-eq / kWh	0–0.5	This corresponds with a range between carbon-neutral and 100% hard coal-based electricity
Internal heat gains	6	W / m²	0.5–15	This corresponds with a range between efficient LED and old-fashioned Incandescent light bulbs
Density of people in offices	0.067	-	0.04–0.2	This corresponds with a range between 25 m² (large private offices) and 5 m² per

				person (slightly under the minimum requirement set by the NEN norm)
Average amount of people per household	2.01	-	1–6	This corresponds with a range between single households and large families
Refrigerant leakage	9	% of charge per year	0.5–18	
Global warming potential of refrigerant	1603	kg CO_2-eq / kg	0–20,000	Between water or propane as a refrigerant and R-13.
Nighttime UHI effect	2.1	°C	0–15	This corresponds with a range between no UHI effect and an extreme UHI effect as seen on the hottest days in cities like Phoenix

3.4.2 Extrapolation of Impacts

In the CDM, about 30% of the residential and office building stock was excluded due to missing energy labels, as detailed in Table 36. Energy labels are crucial for estimating a building's thermal insulation properties, which are key to calculating cooling demand and associated environmental impacts. Consequently, these buildings were not directly included in the primary model.

Table 36: Overview of energy label data availability of the residential and office building stock of The Hague. Based on GIS analysis of the BAG and EP-online data (PDOK, 2023a; RVO, 2019).

Building stock	Building count	Floor space (ha)
Residential and office buildings without energy label data	30,018	694
Residential and office buildings with energy labels	59,381	2,478
Total residential and office building stock of The Hague	89,399	3,172

To address this data gap, an extrapolation method based on the total floor area of each building type was employed. The floor area for each type within the unlabeled stock was first identified using the GIS model. Then, impact intensities from the primary model were applied to these building types, multiplied by their respective floor areas.

This building-type specific extrapolation was necessary because the mix of building types without energy labels differs significantly from those in the primary model's dataset.[38] Appendix P provides a detailed analysis of building type distributions within this subset.

3.5 Policy Recommendations

The literature review presented in the theoretical background (Chapter 2), combined with the results from the status quo and scenario models, and insights from the sensitivity analyses, were used to inform policy recommendations. These recommendations, outlined in section 5.4, are specifically tailored for the municipality of The Hague, aiming to guide policy changes that effectively mitigate the projected environmental impacts of cooling.

[38] Note that, for future scenarios, it is assumed that the size of the subset of buildings being extrapolated over will increase proportionally with that of the subset of buildings analyzed in the main results.

4 Results

This chapter presents the results from the research and modeling performed according to the methodology described in Chapter 3. Note that throughout this chapter, all figures and statistics represent annualized impacts, unless stated otherwise. It is structured as follows:

Status Quo (2020) Cooling Demand and Environmental Impacts

This section provides an overview of the residential and office building stock in The Hague, highlighting its key characteristics. Then, an exploration is undertaken into the cooling demand in The Hague's residential and office buildings for the year 2020. Additionally, it examines the current environmental impacts resulting from the use of cooling technologies and their cooling demand.

Exploring Future Cooling Scenarios

This section explores the anticipated cooling demand for the residential and office building stock in The Hague for the years 2030 and 2050, along with the expected changes in environmental impacts.

Supplementary Results

This section presents the sensitivity analyses and extrapolation of findings. First, the impact of key parameters on the cooling demand and related environmental impacts is assessed by varying factors like weather data and technology choices. This helps gauge result robustness and potential variability of the environmental impacts. Lastly, the cooling demand and environmental impacts are extrapolated to estimate the cooling demand and related environmental impacts of the full residential and office building stock, including buildings without energy label data.

4.1 Status Quo (2020) Cooling Demand and Environmental Impacts

4.1.1 What are the Characteristics of the Residential and Office Building Stock of The Hague?

In this section, the results of the geographic information system (GIS) -based extraction and processing of Registry of Addresses and Buildings (BAG) data are presented. The building stock of The Hague is analyzed regarding building end use, height, and age. Subsequently, the building stock is divided into eight building types, which are used to inform their thermodynamic properties in the cooling demand model. Finally, the distribution of energy labels, its correlation with building age, and its implications for the office building stock adhering to regulations on energy performance are also examined. It should be noted that the following results are derived from the analysis conducted on the subset of The Hague building stock that possesses a residential or office end use and registered energy label data, as detailed in section 3.2.1.

4.1.1.1 Building End Use, Height, and Construction Year

The residential and office (RO) building stock of The Hague is dominated by residential buildings in both building count and floor space, with residential buildings making up 99% and 87%, respectively (see Table 37). As office buildings are on average larger than residential buildings and hence make up 13% of floor space, they still play a significant role in the building stock makeup of The Hague. In terms of building height, there is a strong prevalence of buildings between 10 and 15 meters tall, or approximately three to five stories (Figure 49). High-rise buildings (>17.5 meters) make up a small portion (2.1%) of buildings in The Hague, yet represent 26% of total RO floor space, emphasizing their importance in the building stock makeup. As for building age, most buildings in The Hague were constructed in the 20th century, with a construction boom post World War 2 and around the turn of the 21st century. Approximately 16% of buildings have been built post-2003, when a major building code update was implemented.

Table 37: End use distribution of residential and office buildings in The Hague, 2023.

End use	Building count	Floor space (ha)	Share of floor space
Residential	58,865	2,144	87%
Office	516	334	13%
Total	59,381	2,478	100%

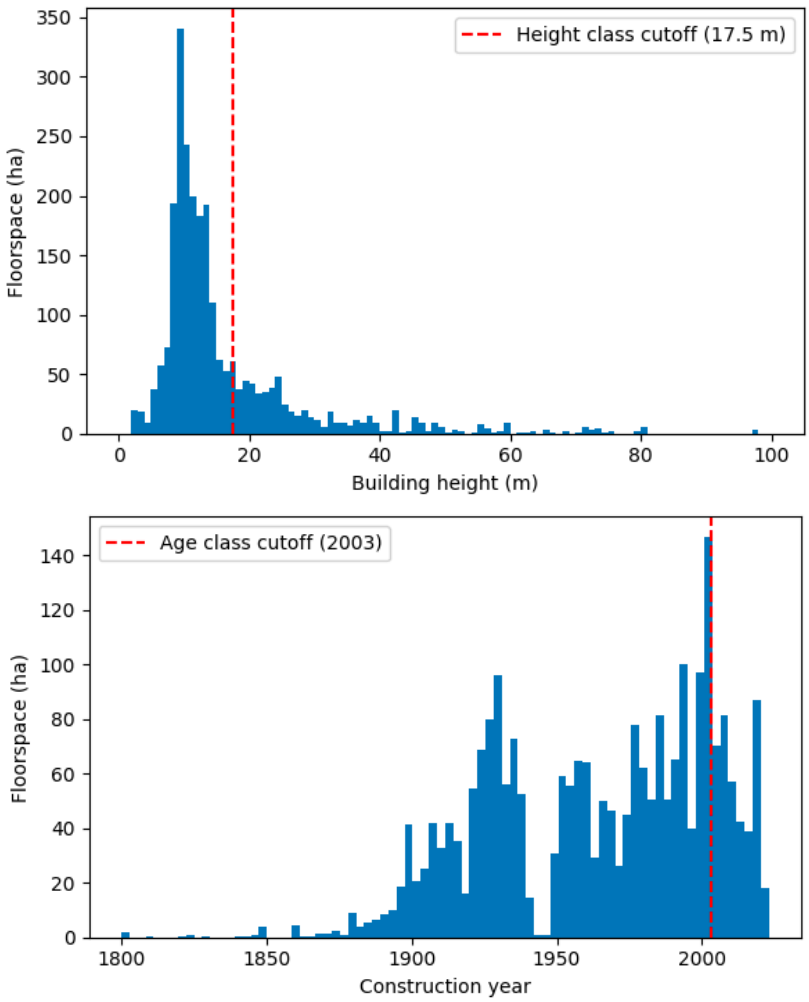

Figure 49: Building height (top) and construction year (bottom) distribution by floorspace in The Hague. The height and age class cutoffs used for modeling building types shown in red.

4.1.1.2 Building Types

Three characteristics - end use, building height, and construction year - were used to divide the building stock into eight building types, whose distribution can be found in Table 38. Old (pre-2003) low rise residential buildings make up most of the RO building stock, both in terms of floor space and building count. Old high-rise residential, which makes up the second largest share, comprises only one sixth of the floor space in

comparison. In terms of the office building stock, old offices dominate, with old low-rise offices holding the highest building count, and old high-rise offices the highest share of floor space. Figure 50 shows the spatial distribution of building types, which reaffirms the ubiquity of old low rise residential buildings. Offices are concentrated in the city-center and business district (center-top), with clusters of old high-rise offices peppered with newer high-rises. Old low-rise offices can also be seen in certain pockets of business parks outside the city center. New low rise residential is concentrated on the outskirts of the municipality, where new developments have likely been built to satisfy urbanization. High rise residential buildings do not follow a clear pattern but are distributed throughout The Hague, although they generally run in strips along main roads.

Table 38: Distribution of building types in The Hague, 2023. Extracted from the BAG (PDOK, 2023a).

Building type	Building count	Floor space (ha)	Share of floor space
1: New high rise residential	158	116	5%
2: Old high rise residential	958	284	11%
3: New low rise residential	8,162	226	9%
4: Old low-rise residential	49,587	1,518	61%
5: New high-rise office	16	39	2%
6: Old high-rise office	140	213	9%
7: New low-rise office	26	14	1%
8: Old low-rise office	334	68	3%
Total	59,381	2,478	100%

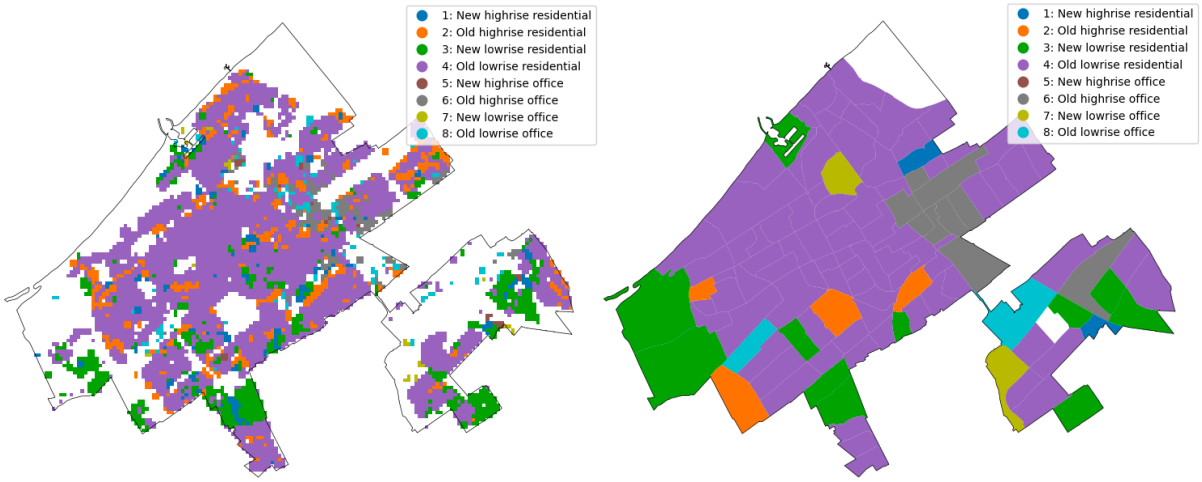

Figure 50: Spatial distribution of building types in The Hague by 100x100m grid cell (left) and neighborhood (right).

4.1.1.3 Energy Labels

Figure 51 displays the distribution of energy labels for RO buildings in The Hague which have been assigned an energy label. Energy label A is most prevalent (28% of floor space), with labels B through E representing most of the remaining floor space. In contrast, labels A+—A+++++ remain relatively underrepresented, likely because they are newer additions to the energy label system, and hence are mainly achieved by recently constructed buildings. As shown in Table 39, energy label classes are divided relatively evenly (in terms of floor space) between A–A+++++, B–C, and D–E, while F–G is the minority as only 8% of buildings have these labels.

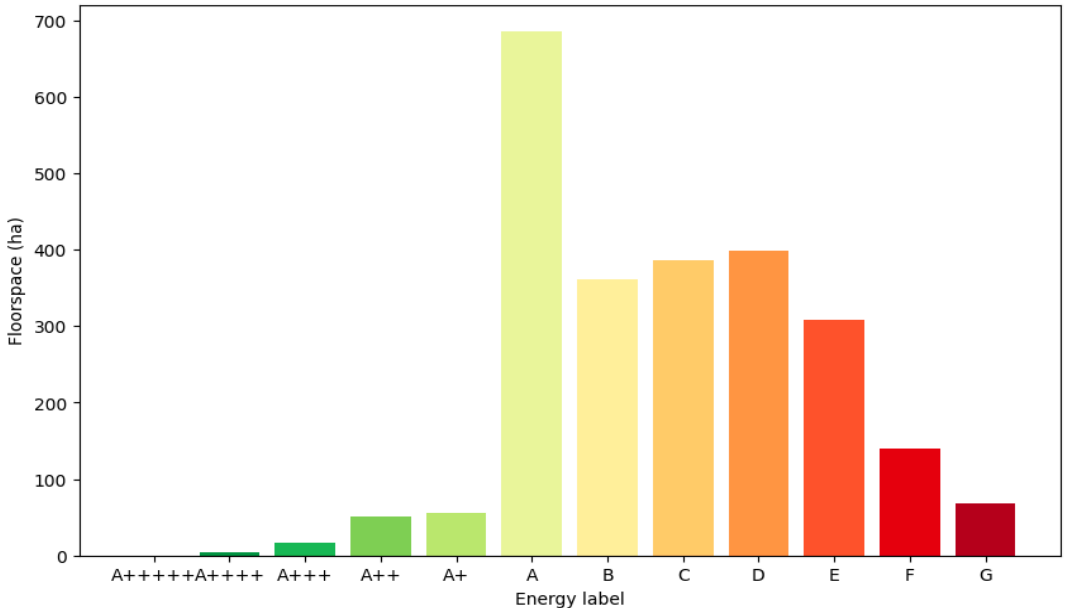

Figure 51: Distribution of energy labels within the RO building stock of The Hague, by floor space.

Table 39: Overview of energy label classes and their distribution across the RO building stock of The Hague.

Energy class	Building count	Floor space (ha)	Share of total space
A–A+++++	18,176	814	33%
B–C	16,819	749	30%
D–E	17,388	706	28%
F–G	6,998	209	8%
Total	59,381	2,478	100%

An analysis was performed to investigate the correspondence of energy labels with building characteristics, including building type and construction year. As seen in Figure 52, a stark divide in building types exists between energy labels of old and new building types, with old building types (2,4,5,8) corresponding to lower energy labels, and new building types (1,3,5,7) mainly consisting of energy labels above C. Old low rise residential buildings, which make up the majority of the building stock, are the building type with the worst energy labels overall, while high rise offices (type 5 and 7) have the best. Offices have better energy labels overall, with a higher prevalence of labels A–A+++++. As for the spatial distribution of energy labels, the city center and outskirts of the city have better energy labels (see Figure 53).

Figure 54 shows the construction year of buildings per neighborhood. Comparing these figures, older neighborhoods often have a lower energy label, although this is not always the case, likely due to building renovations. Neighborhoods on the outskirts of the city are mainly recent developments, which likely explains their higher energy label. In contrast, historic neighborhoods surrounding the city center have a concentration of lower energy labels, such as E, F, and G. Figure 55 provides further insight into the degree of correspondence between energy class and construction year. Overall, the lower the energy class, the older its construction year, with energy label A–A+++++ most assigned to buildings constructed after the building code update in 2003, label B–C in the 1980s and 1990s, D–E around 1930 and 1960, and E–F during the first half of the 20th century. This demonstrates that of the characteristics analyzed: building age, building height, and end use, building age has the strongest correlation with energy labels.

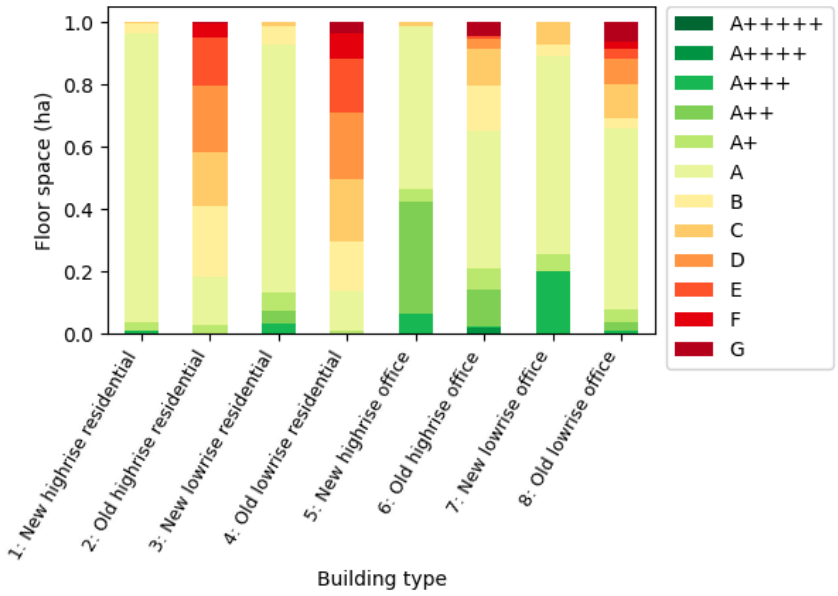

Figure 52: Distribution of energy labels per building type (by floor space).

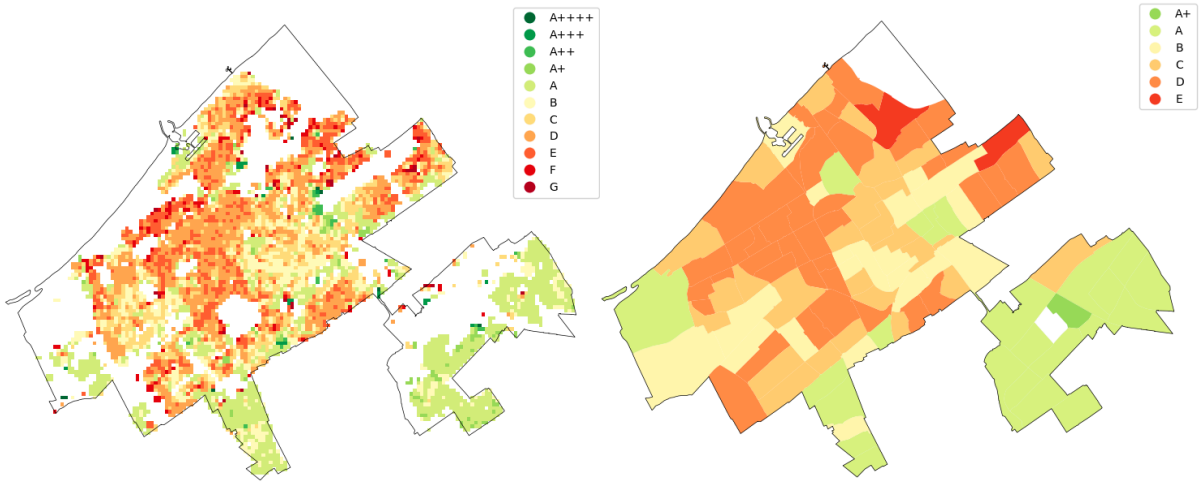

Figure 53: Spatial distribution of energy labels in The Hague by 100x100m grid cell (left) and neighborhood (right).

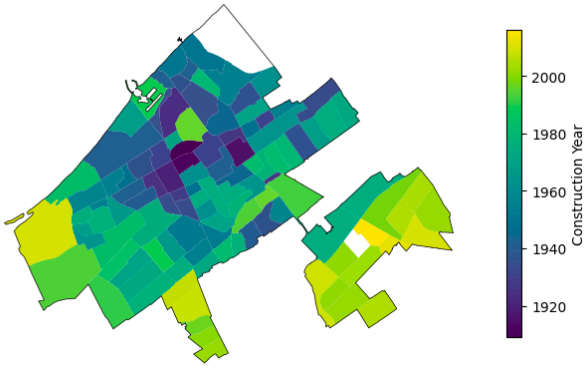

Figure 54: Average construction year of the RO building stock per neighborhood.

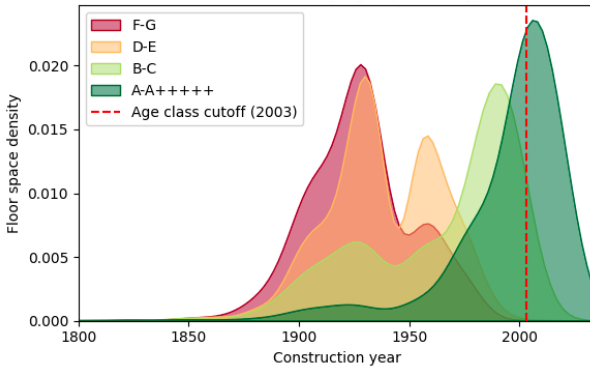

Figure 55: Statistical distribution of building age (expressed by construction year) across the different energy label classes.

4.1.1.4 Have Offices Fulfilled Minimum Energy Label Policy Requirements?

According to Dutch policy, energy label C must be attained by office buildings exceeding 100 m² by 2023 (Bouwbesluit, 2012; RVO, 2018). Figure 56 demonstrates that roughly 30% of The Hague offices do not adhere to these policy requirements, although these make up 9% of the total floor space. Hence, it is likely that these offices are medium-sized, or close to the 100 m² cutoff, while the largest offices generally adhere to the policy. Figure 57 shows the spatial distribution of the offices which adhere to the ruling.

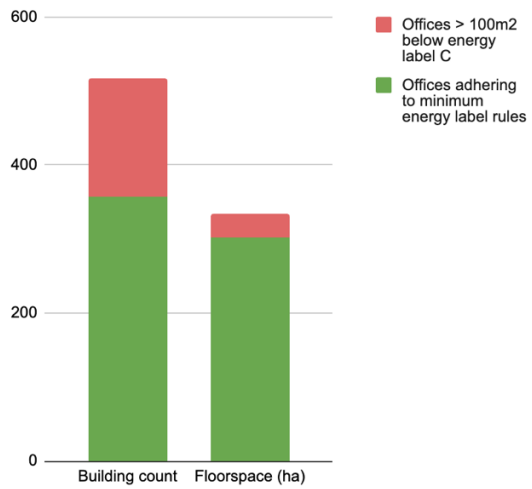

Figure 56: Share of offices adhering to minimum energy label requirements, by building count and floor space.

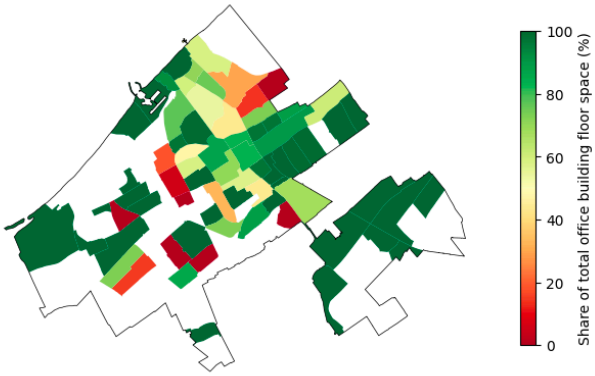

Figure 57: Share of office buildings adhering to minimum energy label requirements per neighborhood.

4.1.1.5 Economic Status and the UHI Effect

As mentioned in section 2.4.2.2, an example of climate injustice is the unequal distribution of the urban heat island (UHI) effect across socioeconomic groups. Figure 59 illustrates a spatial connection between household income, house value, and the UHI effect. Notably, severe UHI effects exceeding 2 °C are predominantly found in economically disadvantaged, densely populated neighborhoods at the heart of The Hague, including Schilderswijk, Spoorwijk, and Transvaalkwartier. A Spearman correlation test of UHI and household income confirms a statistically significant positive correlation (see Figure 58, Figure 60, and Table 40). Note that household income data per census block was only available in €10,000 bands, hence the discrete distribution of incomes in Figure 60b.

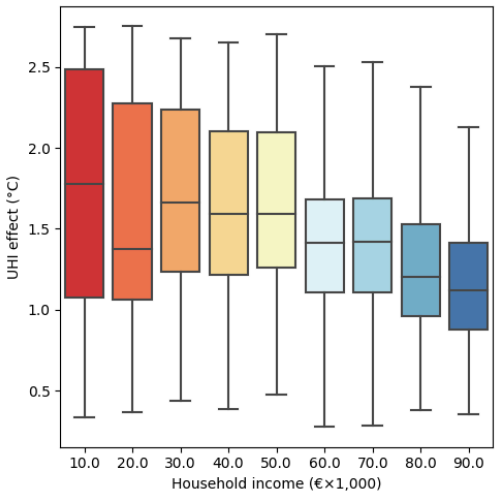

Figure 58: Distribution of the UHI effect across census blocks in The Hague, segmented by household income bands.

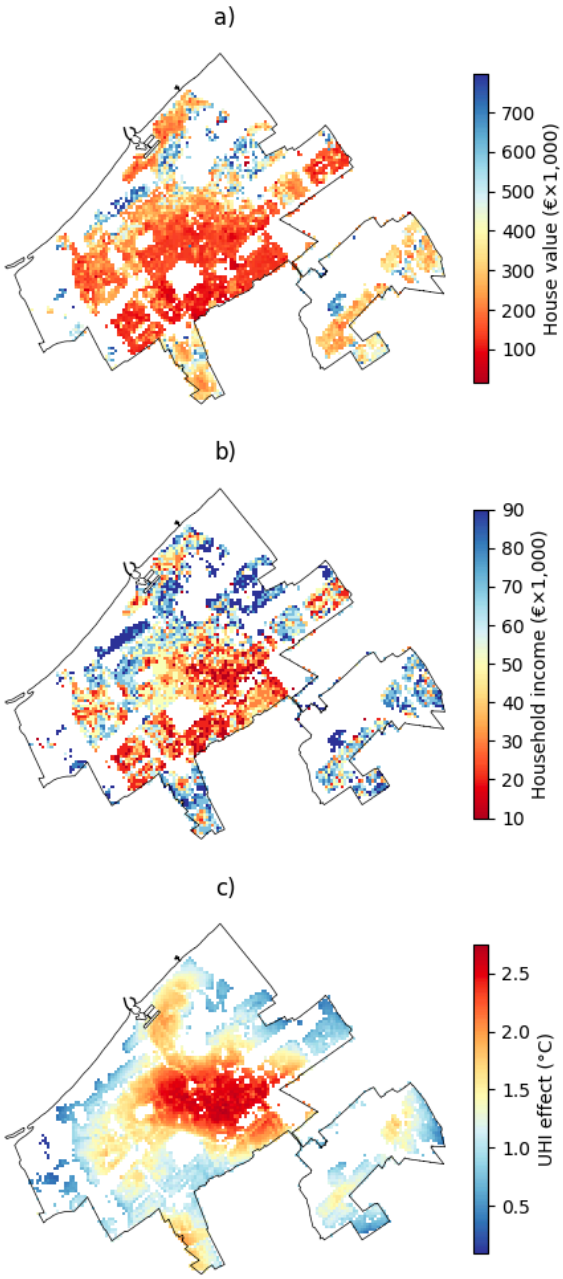

Figure 59: Geospatial distribution of mean house value (a), median household income (b), and UHI effect (c) per 100m×100m census block in The Hague. Based on data from the Atlas Natural Capital and CBS (Atlas Natuurlijk Kapitaal, 2017; PDOK, 2023d).

Table 40: Spearman correlation between house value and household income, and UHI effect in The Hague.

Variable pair	Spearman correlation	p-value
House value, UHI effect	-0.23	$2 \cdot 10^{-52}$
Household income, UHI effect	-0.27	$2 \cdot 10^{-73}$

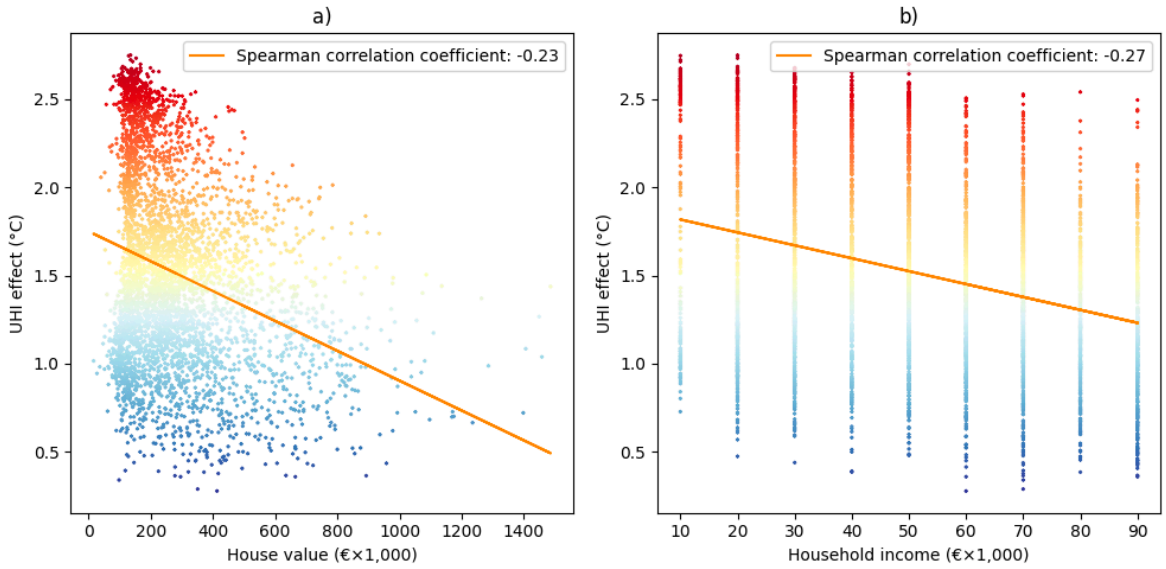

Figure 60: Scatter plots and regression lines of the mean house value and UHI effect (a), and the median household income and UHI effect (b). Based on data from the Atlas Natural Capital and CBS (Atlas Natuurlijk Kapitaal, 2017; PDOK, 2023d).

4.1.2 What is the Current Cooling Demand of the Residential and Office Building Stock?

Figure 61 shows the breakdown of cumulative thermal flows of all RO buildings in The Hague during a heat wave. This provides an indication of the relative contribution of various thermal flows (transmission, infiltration, etc.) towards the total cooling demand during a hot summer's day. Heat gains through transmission dominate other thermal flows, peaking at 600 MW. Internal heat gains, infiltration, and solar radiation all peak between 300–400 MW. Heat gains from ventilation, which was modeled as only present in newer offices and newer high rise residential buildings, is negligible compared to the other thermal flows. Together, these five thermal flows result in a peak cooling power demand of roughly 1500 MW for the RO building stock on a hot summer's day.

During nighttime, the cooling demand is modeled to decrease to (near) zero, mostly due to heat losses via transmission. It is important to note that his analysis does not consider the dynamic effects of thermal mass, which may result in an overestimation of transmission in nighttime passive cooling. In reality, buildings with thermal mass will continue to radiate heat within the interior space, emphasizing the importance of nighttime ventilation.

In terms of building type, offices have an overall higher cooling demand due to higher internal heat gains than in residential buildings (see Figure 63).[39] This likely results from greater population density (see Table 41) and the assumed appliance power density being higher in offices than in residential buildings.

Table 41: Total modeled population and floor area of residential and office buildings.

End use	Floor space (ha)	Population	Population density (people/ha)
Residential	2,144	475,353	222
Office	334	233,569	700

Thermal flows in office buildings vary by age. Older offices have significant cooling demand from infiltration, while in newer offices infiltration is minimal due to improved envelope sealing. Newer offices also see ventilation, alongside internal heat gains, as major heat sources in summer, whether controlled or uncontrolled. For residential buildings, newer buildings demand less cooling due to reduced transmission and infiltration heat flows, likely from better insulation and window factors. Specifically, old low-rise residential buildings (type 4) exhibit the highest peak cooling demand, around 70 MW, primarily from transmission heat flows.

The hourly thermal flows from 2018 through 2022 were aggregated to produce an average annual cooling demand profile for The Hague. The annual cooling energy demand is 1,146 GWh, or 1,118 GWh when capped at the 98th percentile of cooling power demand. The peak cooling power demand is 1,431 MW[40], while the 98th percentile is at 783 MW (see

[39] The thermal flow and cooling load graphics for specific building types were derived from a sample of 2,000 buildings, proportionately representing various building types and energy classes per the scenario. However, this means that for certain building types, the data is based on a limited number of buildings (fewer than 20), which may not precisely reflect the entire category. Therefore, while the exact values in the graphs might not be fully representative, they do offer an indication of the relative magnitude and proportions of thermal flows within those building types.

[40] The cooling demand profile is presented in megawatt-hours (MWh) for each hour over a year, which can also be read as the average cooling power demand in megawatts (MW), calculated by dividing the hourly energy demand by that one hour.

Figure 62).[41]

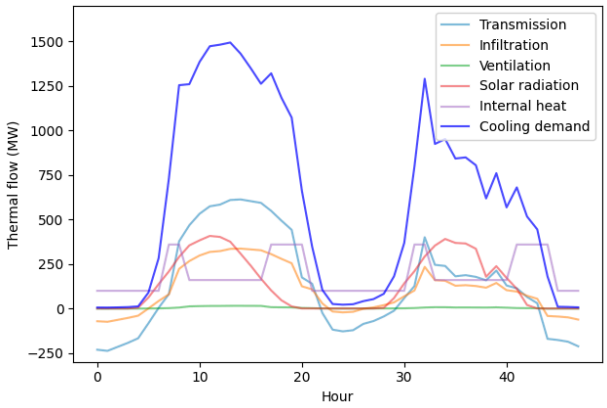

Figure 61: Thermal flows for all residential and office buildings during a heatwave (July 25th - 27th, 2019).

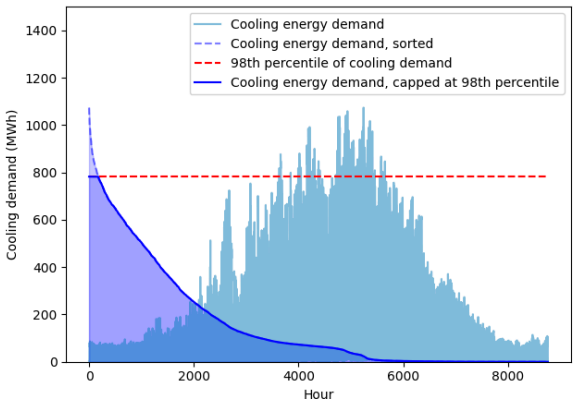

Figure 62: Annual cooling demand profile for all residential and office buildings in The Hague, averaged over 2018–2022.

Peak cooling demand varies by building type, as seen in Figure 64. Following the same trends as cooling demand thermal flows, offices having the highest cooling demand across the board, followed by old residential buildings. The distribution of cooling demand loads varies between offices and residential buildings, with residential buildings having a relatively even distribution of cooling loads between zero and peak values, while offices have a steep drop-off to zero. This is likely due to the modeling of ventilation and internal heat gains in discrete time steps (both are zero during the night), as people are assumed present in offices only during the day.

[41] The capped cooling power and capped energy demand refer to the 98th percentile of the annual cooling power demand and the cooling energy demand capped at that 98th percentile, respectively.

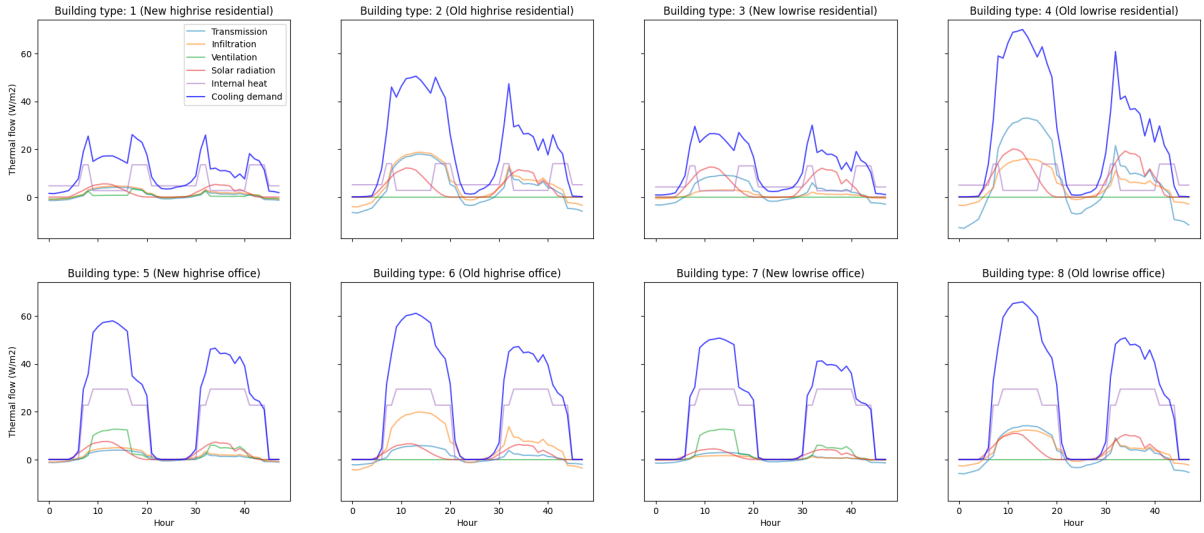

Figure 63: Thermal flows for varying building types during a heatwave in The Hague (July 25th-27th, 2019).

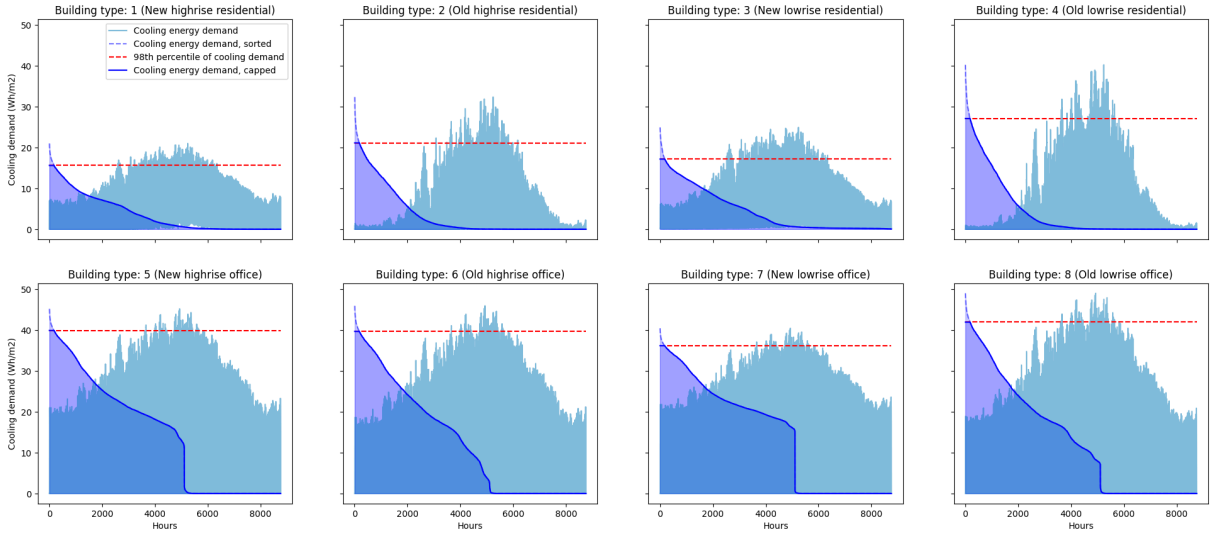

Figure 64: Annual cooling demand load for varying building types, averaged over 2018–2022.

Within the residential building types, new high rise residential buildings have the lowest power demand intensities, followed by new low rise residential. As shown in Figure 65, the largest building type by floor area, old low rise residential building, displays a wide-spread distribution of cooling power demand intensities, peaking at 13–25 W/m^2 with a tail at between 50 and 100 W/m^2. Offices have a slightly higher but narrower spread power demand intensity than residential buildings, peaking at 35–40 W/m^2. Further, it can be observed that within the cooling power demand intensity distribution of offices, low-rise offices have a slightly lower cooling power demand intensity than high-rise offices.

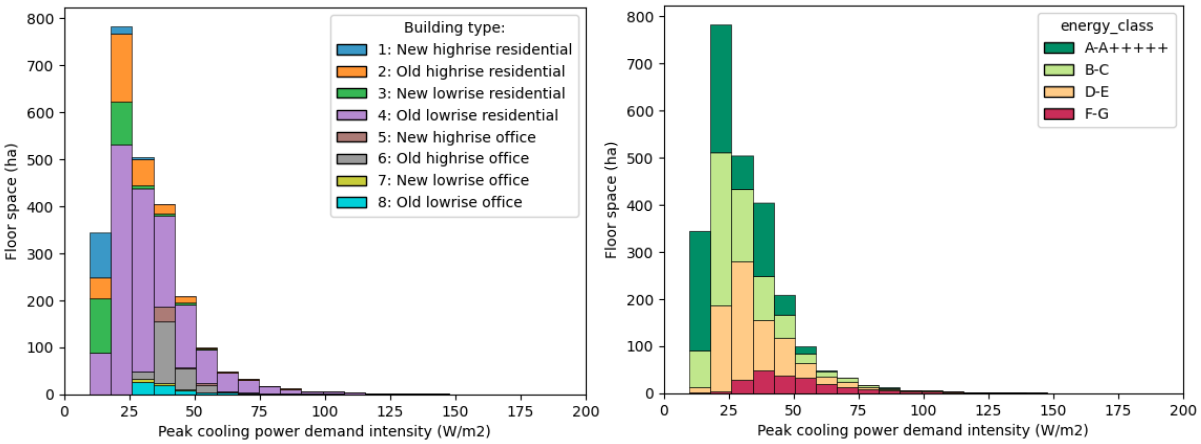

Figure 65: Distribution of the capped cooling power demand intensity by floor space, broken down by building type (left), and energy class (right).

As for energy classes, peak power demand intensity increases as energy labels worsen, with A–A+++++ and B–C peaking at 20–25 W/m², D–E peaking at 25–30 W/m², and F–G peaking at 35–40 W/m².

The cooling energy demand distribution, depicted in Figure 66, exhibits a more notable disparity, characterized by two distinct peaks. The first and more prominent peak, ranging between 13 and 33 kWh/m², is primarily attributed to the extensive residential building stock. The second, smaller peak, observed within the range of 100 to 133 kWh/m², primarily consists of office buildings. When examining the breakdown of cooling energy demand by energy label, a balanced distribution is evident for residential buildings (i.e., the left peak). Conversely, the right peak is predominantly composed of buildings with energy labels A to A+++++. It might initially suggest that buildings with these energy labels exhibit higher cooling energy demand. However, this observation is clarified by recognizing that these buildings are offices, which typically possess higher energy labels than residential counterparts. In essence, the presence of A to A+++++ energy labels within the second peak of cooling demand can be attributed to the inherent characteristics of office buildings, which result in higher cooling energy demand, rather than the energy label itself being the direct cause of increased cooling energy demand.

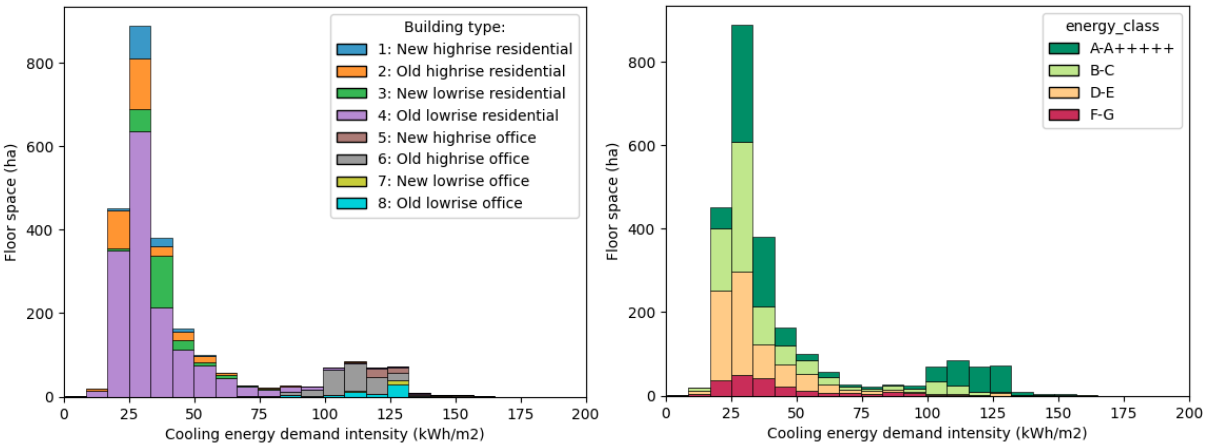

Figure 66: Distribution of capped cooling energy demand intensity by floor space, broken down by building type (left) and energy class (right).

The heightened cooling energy demand of offices can be further displayed by the spatial distribution of cooling energy demand, as seen in Figure 67. The highest cooling energy demands are concentrated in the business districts of The Hague. Regarding the spatial distribution of cooling power demand, higher power demands are concentrated in the city center and older neighborhoods, which aligns with offices and older residential buildings generally experiencing a higher peak cooling power demand intensity.

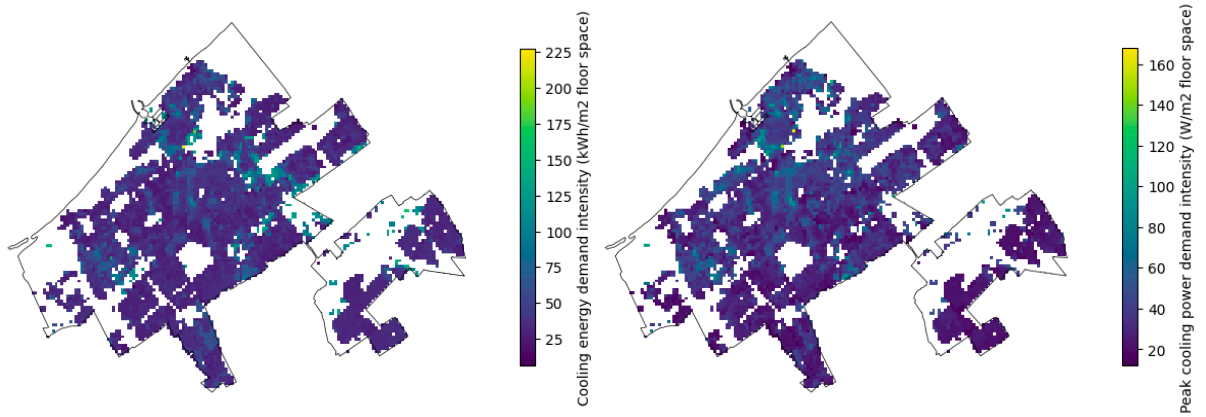

Figure 67: Spatial distribution of capped cooling energy demand intensity (left) and capped cooling power demand intensity (right) per grid cell in The Hague.

4.1.3 What are the Beyond Use-Phase Environmental Impacts of Cooling Technologies?

A simplified impact analysis based on life cycle assessments (LCAs) of ventilation systems with heat exchangers was performed to estimate the environmental impacts of active

cooling equipment beyond the use phase.[42] This analysis targeted climate change impacts during the production and end-of-life phases, along with the abiotic depletion potential (ADP) and crustal scarcity index (CSI) of the material footprint, with key results compiled in Table 42.

Table 42: Life-cycle assessment results per product mass, for chosen impact metrics.

Impact metric	Value	Standard deviation	Unit
GHG emissions (production phase)	4.15	0.13	kg CO_2-eq/kg
GHG emissions (end-of-life phase)	0.30	0.11	kg CO_2-eq/kg
Abiotic depletion potential	$2.64 \cdot 10^{-4}$	$5.57 \cdot 10^{-5}$	kg Sb-eq/kg
Crustal scarcity indicator	1,625	295	kg Si-eq/kg

The production-phase and end-of-life carbon intensities of the average ventilation system are **4.15 CO_2-eq/kg** and **0.30 CO_2-eq/kg**, respectively. This results in a total average carbon intensity of **4.45 kg CO_2-eq/kg**, excluding the use phase. These results were used to calculate the environmental performances of the cooling technologies included in the model, as shown in Appendix H.

The average abiotic depletion potential (ADP) for each kilogram of installed cooling technology is $2.64 \cdot 10^{-4}$ kg Sb-eq. The average ADP per kg of the material footprint, which is approximately seven times larger than the product's mass, is estimated to be $3.6 \cdot 10^{-5}$ kg Sb-eq/kg — on par with metals like tantalum and nickel (van Oers & Guinée, 2016).

Figure 68 illustrates the material footprint, with mining tailings – waste byproducts of mineral extraction – constituting around 60% and posing potential environmental risks. The remainder comprises fossil fuels: coking coal (a critical raw material, CRM), crude oil, and brown coal, accounting for 25% of the footprint. These are primarily used as energy sources during production, with some allocation to manufacturing components like plastic casings and steel.

[42] Ventilation systems with heat exchangers were determined to be the products that most closely resemble air conditioners and heat pumps within the ecoinvent database (Wernet et al., 2016). Hence, they were used as a proxy in the determination of the production- and end of life-phase environmental impacts of active cooling equipment in this research.

The crustal scarcity indicator for the material content in cooling equipment, excluding mining tailings, is 534 kg Si-eq/kg.[43] This is comparable to the scarcity of phosphorus, a notable CRM, as depicted in Figure 69.

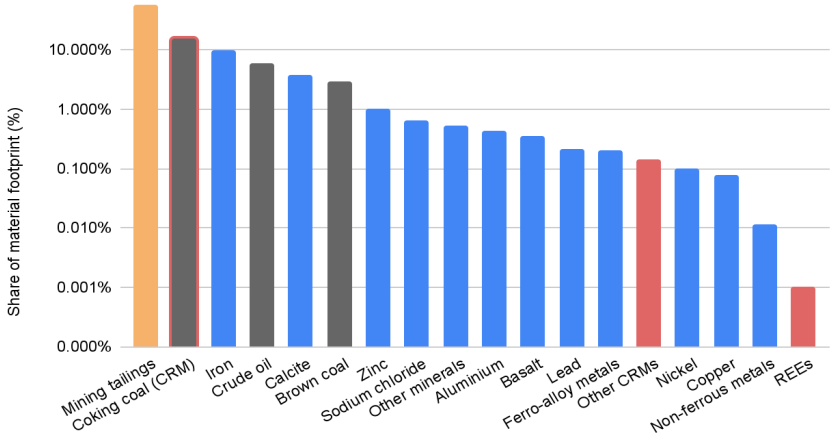

Figure 68: Prevalence of materials in the ventilation system supply chain. Mining tailings are marked in orange, fossil fuels in dark gray, and CRMs in red. Note: coking coal is considered both a fossil fuel and CRM, and platinum group metals are omitted as they make up <1 ppm of the material footprint.

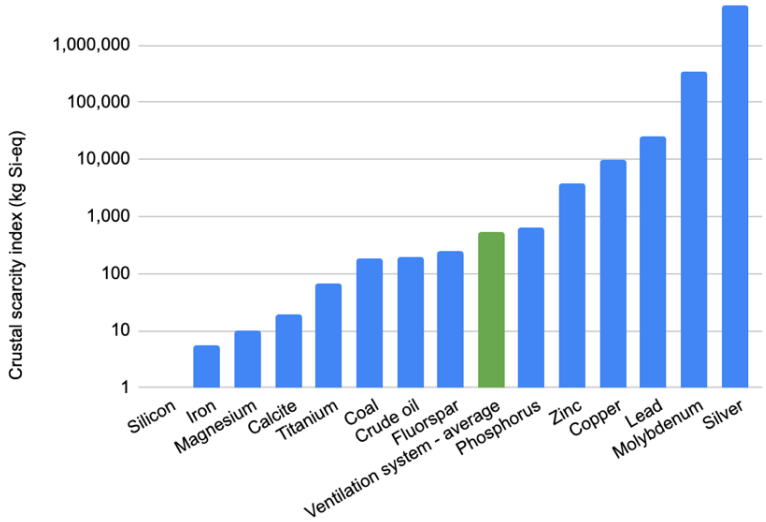

Figure 69: Average crustal scarcity indicator of the material footprint of ventilation systems (excluding mining tailings), compared to some common materials.

[43] Note that the crustal scarcity index per kilogram of the modeled ventilation equipment, as detailed in Table 42, is about three times higher than this, because the production supply chain's material footprint (excluding mining tailings) is roughly three times heavier than the end-product.

4.1.3.1 Critical Raw Material Presence in the Material Footprint of Cooling Equipment

The presence of CRMs in the material footprint of cooling equipment is noteworthy. Thirteen CRMs were found to have a presence of more than 1 part per million (ppm) in the material footprint of the ventilation systems. They are listed in

Figure 70 based on prevalence and crustal scarcity impact. These CRMs have been correlated with the EU list of critical raw materials in Figure 71 (Grohol & Veeh, 2023).

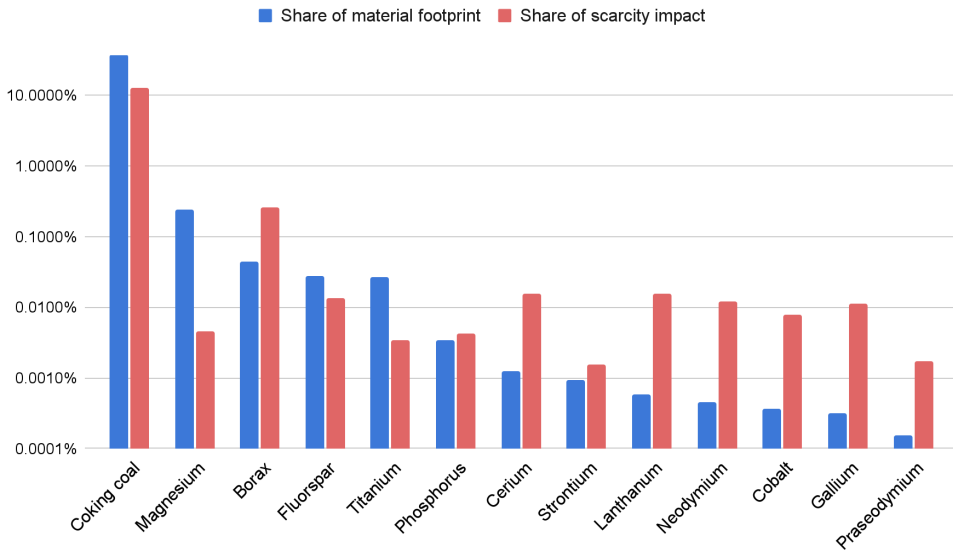

Figure 70: Share of material footprint and scarcity impact of CRMs > 1 ppm used in ventilation systems.

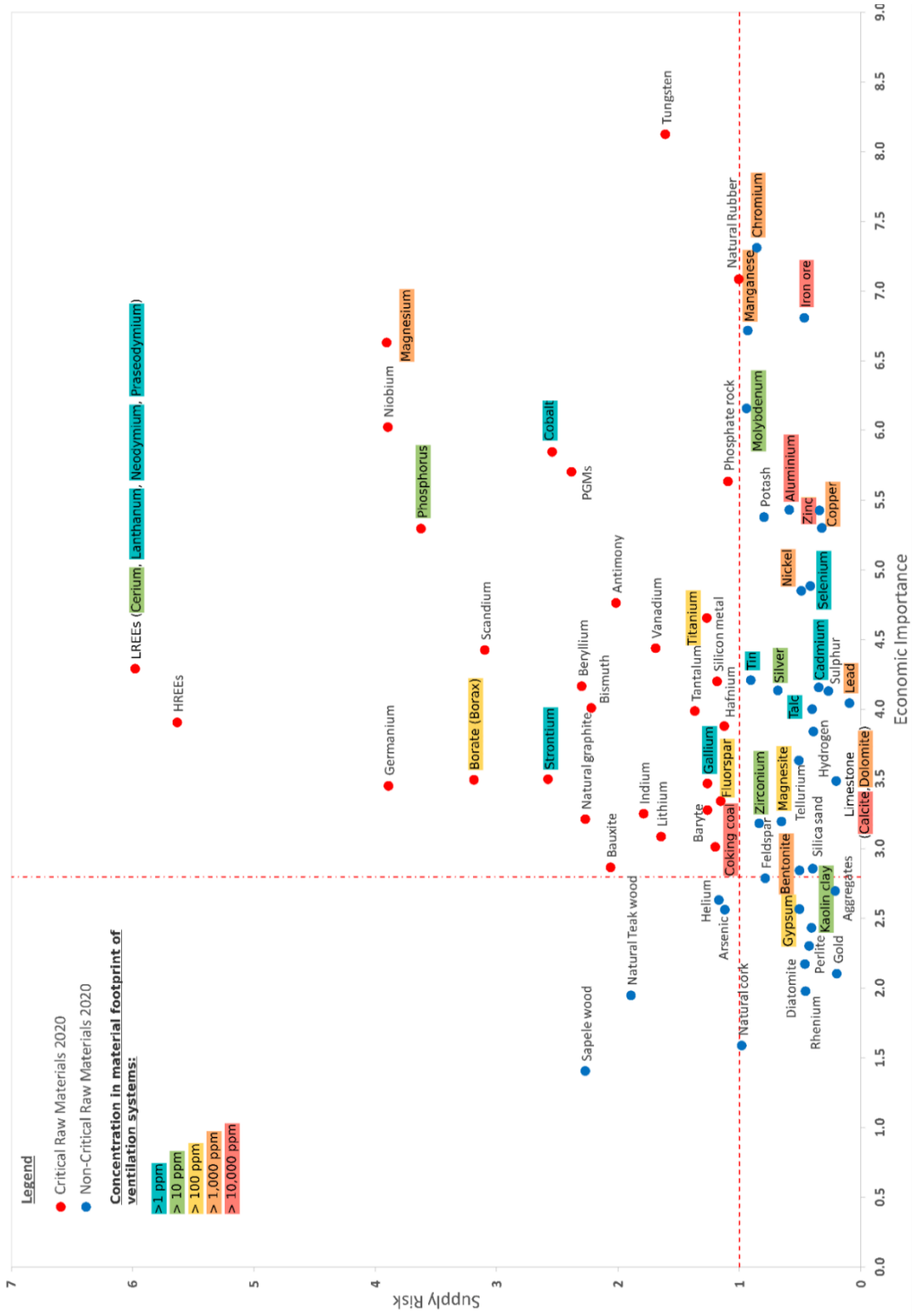

Figure 71: Mapping of materials with a presence of > 1 ppm in the material footprint of ventilation systems onto the European CRM framework. Adapted from (Grohol & Veeh, 2023).

4.1.4 What are the Environmental Impacts of Residential and Office Cooling in The Hague?

4.1.4.1 Electricity Use

While the capped cooling energy demand, as calculated in section 4.1.2, is 1,118 GWh per year, only a fraction of demand is fulfilled by cooling technologies. Approximately 23% of the cooling demand is fulfilled, meaning the remaining portion of cooling needs are left unmet in The Hague (see Figure 72). This is referred to as the 'cooling gap', which leaves 77%, or 860 GWh of the thermal discomfort unmanaged, even when accounting for a 2% tolerance window. Of the cooling demand fulfilled by equipment, the energy efficiency of the installed equipment and size of the cooling demand result in an annual 101 GWh of electricity use from cooling equipment.

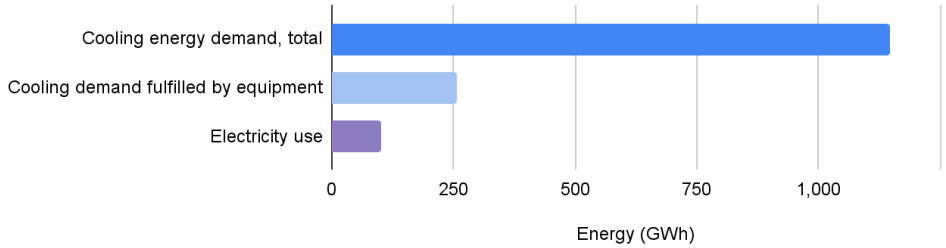

Figure 72: Total cooling energy demand, the share that is fulfilled by cooling equipment, and the resulting electricity use of the RO building stock in The Hague, in the Status Quo (2020) scenario.

The total electricity use derives from the energy intensities of the eight building types (see also Figure 131). The difference in cooling demand between residential and office buildings, as elucidated in section 4.1.1.5, is further magnified when considering their energy use. The average energy use intensity of offices is 21 kWh/m², which is 14 times higher than that of residential buildings at 1.5 kWh/m² (see Figure 73). This is a result of offices fulfilling a greater portion of the cooling demand due to the higher penetration rate of cooling equipment in offices. This also means that while offices only take up 13% of the floor space, they are responsible for 68% of space cooling energy use (see Figure 77).

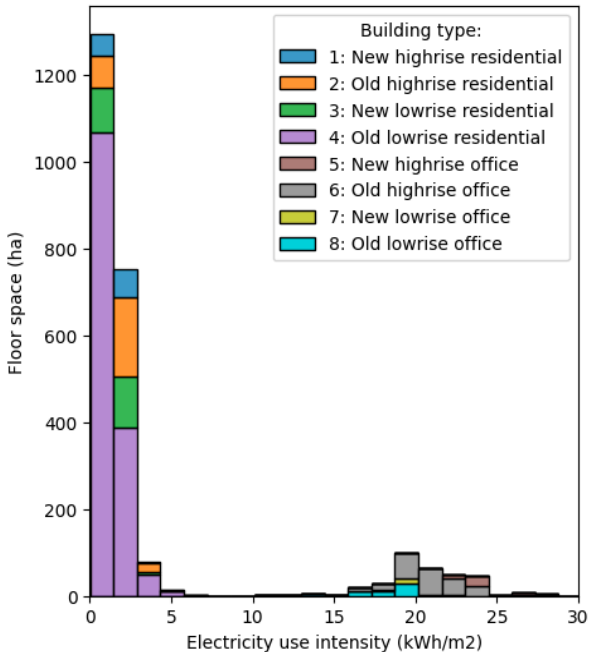

Figure 73: Distribution of electricity use intensities by building type in the Status Quo (2020) scenario.

4.1.4.2 Material Use

Based on the modeled cooling equipment installed in The Hague, the total mass of cooling equipment in the RO building stock is approximately 3,003 tonnes. This can be annualized to 232 tonnes per year, which represents the annual inflow of new cooling equipment needed to sustain the cooling equipment stock, as well as the resulting outflow of waste equipment. The extraction, use, and waste treatment of this material mass has environmental implications including non-renewable resource depletion and pressures on supply chains of scarce materials, which are measured through the ADP and the CSI (see Table 43).

Table 43: Material use and environmental impact metrics of cooling technologies in the Status Quo (2020) model of The Hague.

Value	Material use (tonne)	ADP (kg Sb-eq)	CSI (kt Si-eq)
Impact of total cooling equipment stock	3,003	755	4,720
Annualized impacts	232	58	365

The material use depends on the installation size of cooling equipment, which itself is based on the peak cooling power demand. As can be seen in Figure 74, the peak cooling power demand displays a smaller disparity than the cooling energy demand. Hence, the material use intensity also shows a smaller disparity between offices and residential

buildings compared to the electricity demand. Where residential buildings have an average of only 0.06 kg of cooling equipment installed per square meter, this rises nine-fold to 0.52 kg/m² for offices (see Figure 74). Variations in material use intensity across building types roughly follow modeled market penetration rates (MPRs) of prevalent cooling technologies (see Figure 33).

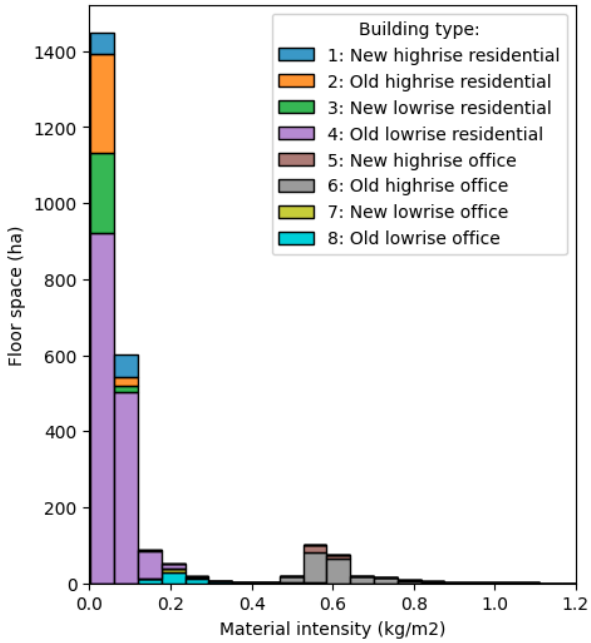

Figure 74: Distribution of material use intensities by building type in the Status Quo (2020) scenario.

4.1.4.3 Climate Change Impacts

The climate change impact of cooling in The Hague results from the combined electricity use, refrigerant leaks, and material requirements. Figure 75 presents their relative contribution to the total annual greenhouse gas (GHG) emissions of 48.83 kt CO_2-eq, which is driven by cooling energy demand and peak cooling power demand. Emissions from electricity use make up the vast majority (88%) of total emissions, followed by refrigerant leaks (10%), production (2%), and finally waste treatment (0.1%) of cooling equipment. In terms of life cycle phases, the use-phase of cooling equipment makes up 98% of total GHG emissions.

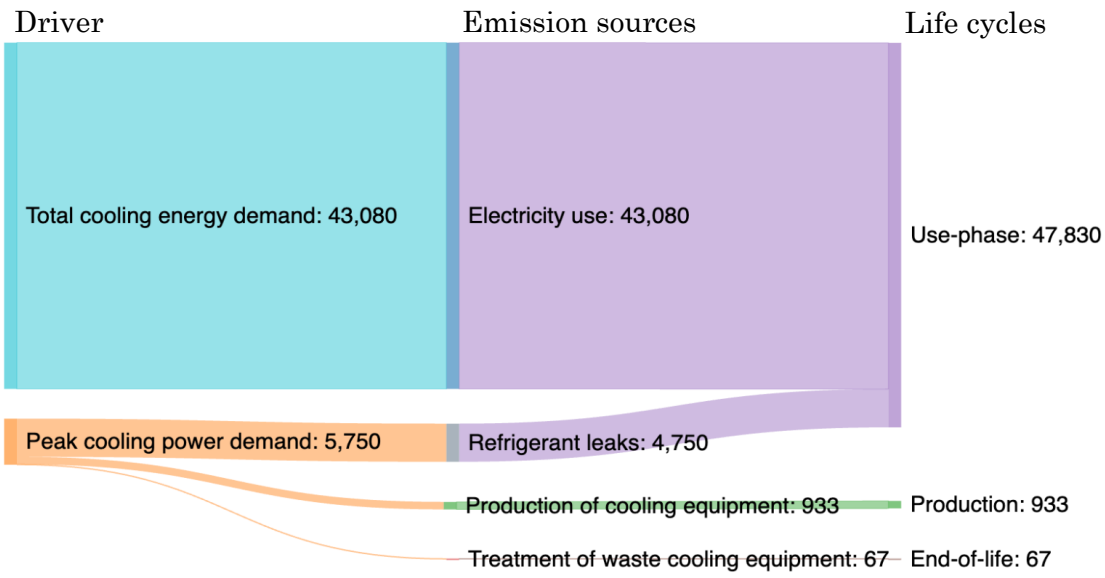

Figure 75: Breakdown of total greenhouse gas emissions (tonne CO_2-eq) per driver (left), source (middle), and life-cycle phase (right).

Like electricity use intensity, offices have a GHG intensity roughly 12 times higher than residential buildings (see Figure 133), with new high-rise offices surpassing other building types at a GHG intensity of 11 kg CO_2-eq/m². While residential buildings have 12 times lower GHG intensity, their predominance in the building stock results in a contribution of 27% of the total GHG emissions for The Hague (see Figure 76).

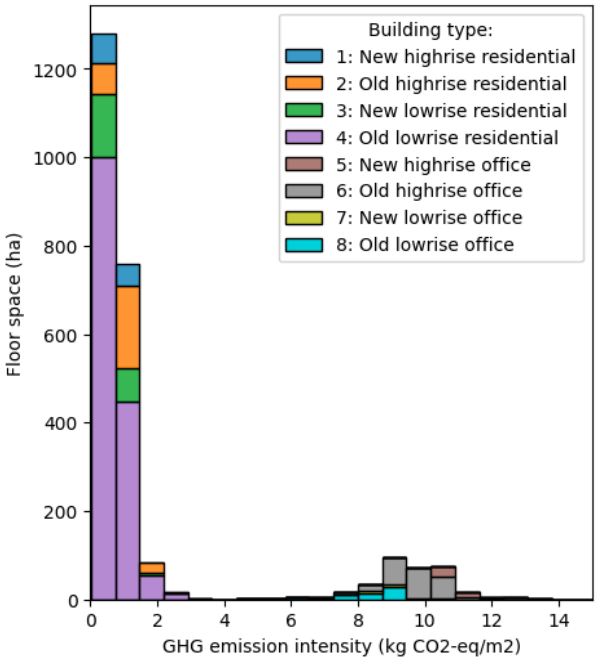

Figure 76: Distribution of GHG emission intensities by building type in the Status Quo (2020) scenario.

4.1.5 Contribution Analysis of Building Types Across Key Impact Metrics

Figure 77 provides an overview of the comparative contribution of residential and office buildings to the floor space, population, cooling demand, and ensuing environmental impacts. Most notable is the overrepresentation of offices across impact metrics in relation to their share of 13% of the floor area. This is a result of two notable characteristics of offices: (1) their relatively high cooling energy demand intensity, and (2) the relatively high MPR of cooling equipment in offices. The higher population density of offices compared to residences results in greater internal heat gains, and the presence of ventilation systems in high-rise offices contributes to the ventilation heat gains (as shown in section 4.1.1.5). This increases overall cooling demand in offices, rendering offices responsible for 34% of the total cooling energy demand — 2.5 times higher than their share of floor area.

In terms of environmental impacts, the MPR of cooling equipment is greater in offices than residential buildings, further increasing the disparity between offices and residential buildings when it comes to the electrical energy use. Essentially, offices fulfill a greater portion of cooling demand with cooling systems, increasing thermal comfort in offices compared to residences. Hence GHG emissions from offices comprise 65% of total emissions, nearly five times their share of floor area.

In contrast, offices are less overrepresented in peak cooling power demand. This is due to the more consistent cooling demand of offices throughout the year which is less volatile to the outside environment than in residences (see section 4.1.2). This results in peak cooling power demand for offices being slightly higher than that for residences, but with less of a disparity compared to cooling energy demand. Hence, material footprint, which largely depends on peak cooling power demand, is less skewed towards offices in comparison to the energy use and GHG emissions, which mainly depend on cooling energy demand.

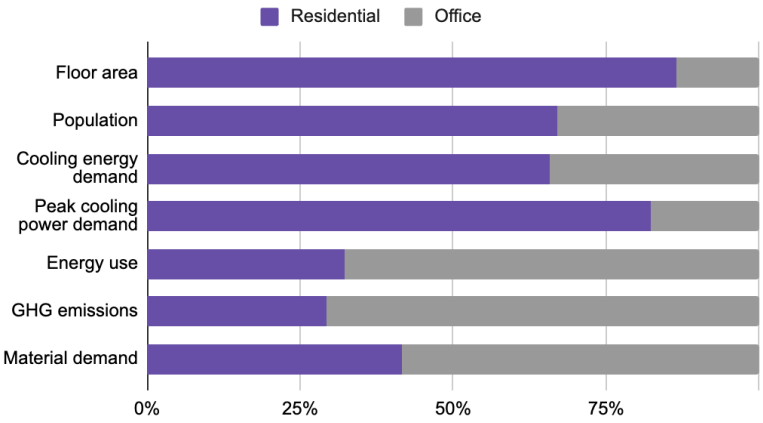

Figure 77: Relative share of residential and office buildings in building stock characteristics and key impact metrics, in the Status Quo (2020) scenario.[44]

When breaking down contribution by building type, as shown in Figure 78, it becomes evident that within the subset of residential buildings (types 1–4), the cooling demand and environmental impacts are distributed in a manner largely proportional to the floor space and population size. A similar distribution pattern is observed within the office buildings (types 5–8). Building type 4 (Old low rise residential) and building type 6 (Old low-rise office) emerge as the primary contributors to the environmental impacts of cooling due to their dominance in floor space within their respective end uses, accounting for 22%–33%, and 43%–44% of the environmental impacts, respectively.

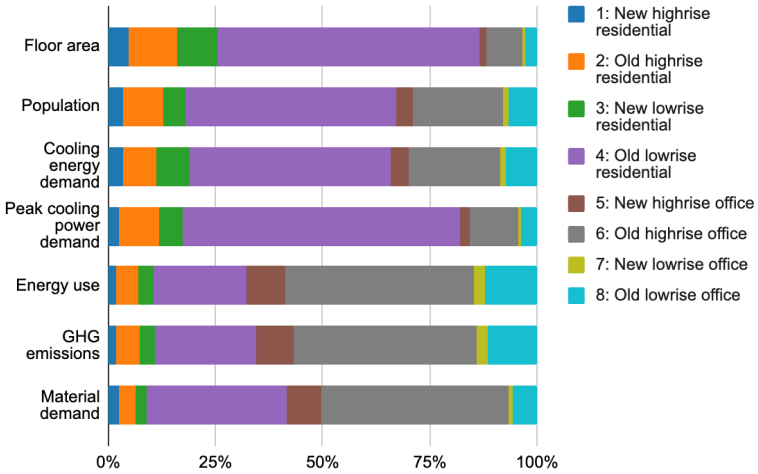

Figure 78: Relative share of building types in building stock characteristics and key impact metrics, in the Status Quo (2020) scenario.

[44] It's important to clarify that the *population* figures in this graphic are for modeling purposes only. In reality, there is considerable overlap between the office and residential populations, as many individuals who work in The Hague also reside there.

4.2 Exploring Future Cooling Scenarios

4.2.1 How Will the Cooling Demand for the Residential and Office Building Stock in The Hague Evolve in 2030 and 2050 Scenarios?

The cooling energy demand of The Hague's RO building stock increases by an average of 32% between 2020 and 2050 across scenarios, and peak cooling power demand increases by an average of 6% (see Figure 79) in the same period.[45] In the 2030 scenario, which extrapolates current trends and planned policies over the next decade, cooling energy demand increases slightly by 0.8% to 1,127 GWh, while peak cooling power demand drops by 3.8% from 783 MW to 753 MW. Figure 80 shows the contribution of thermal flows to cooling demand for each scenario on a hot summer's day. While most thermal flows remain relatively stable in magnitude, there is a slight dip in transmission heat gains compared to the Status Quo (SQ) scenario, likely attributed to modeled improvements in thermal insulation (i.e., enhancements in the average energy label). This accounts for the reduction in peak cooling power demand observed in Figure 81, as buildings with higher energy labels have better insulation, leading to fewer extreme heat peaks during hot days. On the other hand, higher temperatures and solar radiation throughout the year will result in a greater number of cooling degree days (CDDs) annually, increasing the overall cooling energy demand.

This decrease in peak cooling power demand and increase in cooling energy demand applies not only to 2030, but to the 2050-L and 2050-M scenarios as well. In the 2050-M scenario, which represents a middle-of-the-road scenario for both temperature increases and climate change mitigation, cooling energy demand increases by 19%, while the cooling power demand stays constant at 783 MW. As shown in Figure 79, this decrease in cooling power demand is likely due to the further decrease in transmission-based heat gains from increased thermal insulation, i.e., energy label improvements.

[45] In this section, it should be noted that the terms *peak cooling power demand* and *cooling energy demand* refer to the capped values; specifically, the 98th percentile of the annual cooling power demand and the cooling energy demand capped at that 98th percentile of power, respectively.

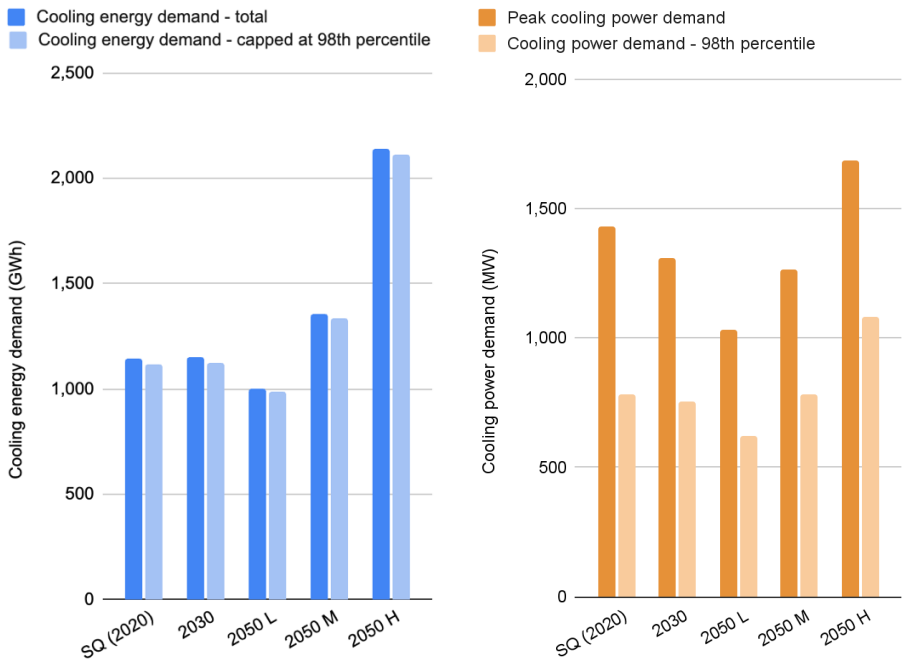

Figure 79: Overview of the total and capped cooling energy and power demand of residential and office buildings in The Hague, across scenario.

In the 2050-H scenario, where climate change impacts increase and minimal mitigation measures are taken, both cooling energy demand and peak cooling power demand increase compared to the status quo. The increase in cooling energy demand outpaces the growth in peak power demand, with the former almost doubling from 1,118 GWh to 2,111 GWh, while the latter experiences a more modest 38% increase to 1,079 MW. This discrepancy can likely be attributed to a substantial rise in CDDs across the year, as opposed to the likely marginal growth in maximum annual temperatures, which primarily determine peak cooling power demand. This is reflected in Figure 80 with an increase in all thermal flows (except the internal heat gains, which stay constant). Transmission heat gains increase due to a stagnation in energy label improvements from 2030 onwards, resulting in insulation ill-equipped to combat the increasing temperatures and solar radiation. Ventilation and infiltration heat gains also increase slightly.

2050-L is the only scenario where both cooling energy demand and cooling power demand decrease, by 12% and 21%, respectively (see Figure 82 and Figure 83). In 2050-L, stringent climate change mitigation adaptation policies have been enacted, combatting temperature and solar radiation increases, reducing the UHI effect, and greatly improving the energy performance of the RO building stock. Despite increases in outdoor temperatures, building insulation and lower solar factors for windows reduce the transmission and solar

radiation thermal flows significantly, offsetting a rise in outdoor temperatures, and hence reducing the peak cooling power and cooling energy demand.

It should be noted that the thermal flow and cooling load figures, as shown in Figure 80 and Figure 81, were generated using a sample of 2,000 buildings, with a representative proportion of building types and energy classes according to the scenario. However, this entails that the graphs for some of the building types are founded on simulations involving a small number of buildings (n < 5). Consequently, the exact magnitudes depicted in the graphs should not be assumed to represent the entire building type accurately. Nonetheless, these figures can provide insights into the order of magnitude and proportions among thermal flows within that building type.

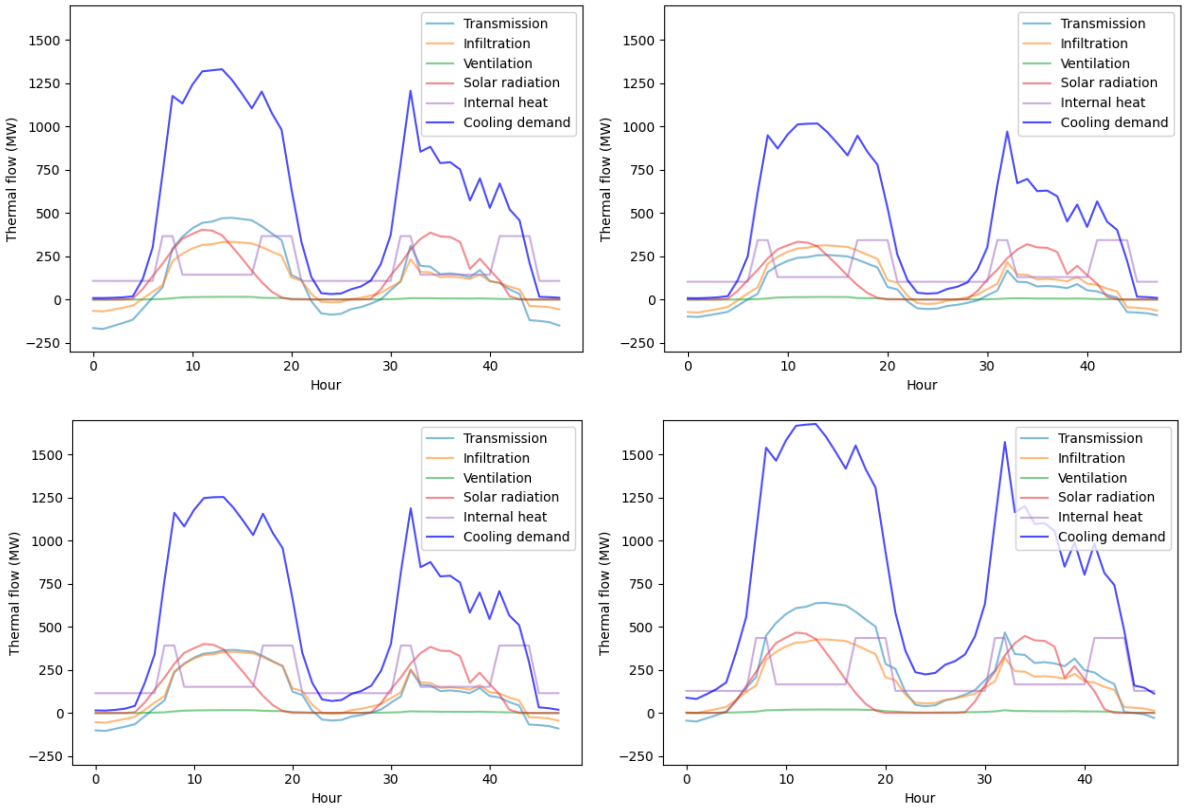

Figure 80: Thermal flows for all residential and office buildings during a future heatwave for four scenarios: (top-left) 2030; (top-right) 2050-L; (bottom-left) 2050-M; (bottom-right) 2050-H.

Analyzing the differences between residential buildings and offices, the evolution of cooling energy demand in The Hague is characterized by varying energy demand intensities and shifts in building stock. In terms of cooling energy demand intensities, offices consistently maintain higher levels compared to residential buildings. However, the growth rates differ significantly between the two. As can be seen in Figure 82, The

cooling energy demand intensity for offices shows a relatively modest increase of only 24% from the status quo to the 2050-H scenario. In contrast, residential buildings experience a substantial growth of 78%, rising from 24 to 68 kWh/m² during the same period. This results in a narrowing gap between cooling energy demand intensities of the two end uses. Notably, the intensities remain stable between the SQ and 2050-L scenarios for both residential and office buildings. For a detailed overview of the cooling energy and power demand intensities per building type, see Appendix Q.

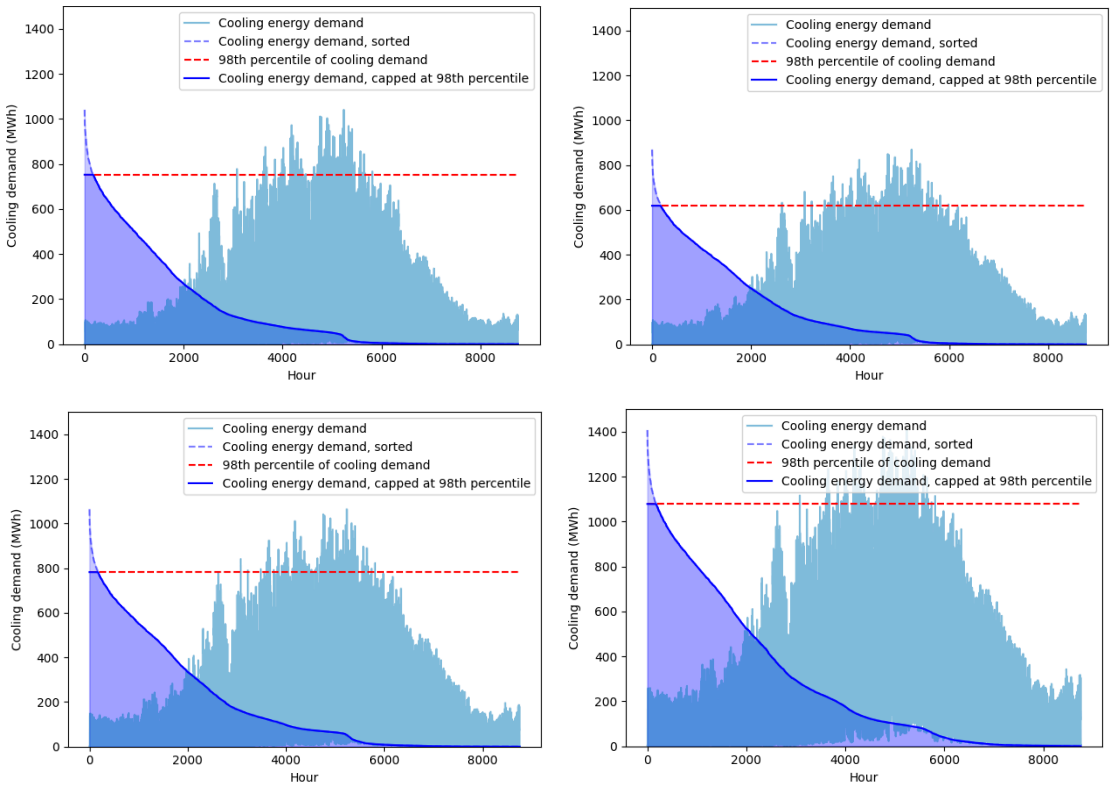

Figure 81: Annual cooling demand profile for all residential and office buildings in The Hague for four scenarios: (top-left) 2030; (top-right) 2050-L; (bottom-left) 2050-M; (bottom-right) 2050-H.

Examining the overall energy demand, the substantial increase in cooling energy demand intensity for residential buildings is further exacerbated by the projected growth in the residential building stock. This results in a more than doubling of residential cooling energy demand, increasing from 736 to 1,694 GWh between the SQ (2020) and the 2050-H scenario. In the most optimistic scenario for 2050 (2050-L), residential cooling energy demand experiences minimal growth, with only a 4 GWh increase to reach 740 GWh.

On the other hand, the office building stock is projected to shrink, which offsets the relatively modest increases in energy demand intensity. Consequently, the total cooling

energy demand from offices decreases significantly, declining by 36% from 334 to 213 GWh between the SQ and 2050-L scenarios. Notably, even between the SQ and the 2050-H scenario, offices only witness a 9% increase in cooling energy demand, rising from 382 to 417 GWh.

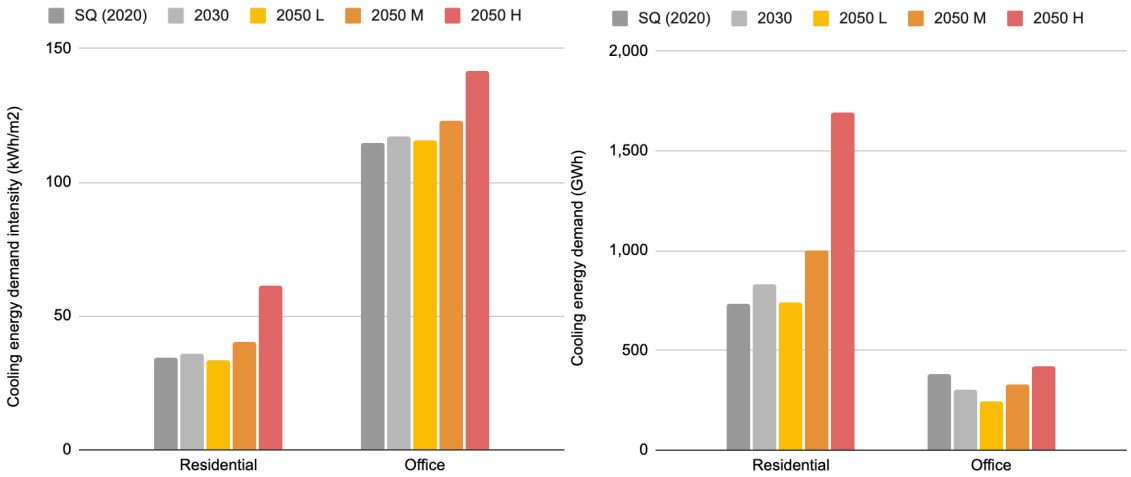

Figure 82: Evolution of the cooling energy demand intensity (left) and total cooling energy demand (right) for residential buildings and offices, across scenarios.

Changes in peak cooling power intensities are subtler than those in energy demand. Peak cooling power demand intensities exhibit a consistent decrease in all scenarios, except for the 2050-H scenario (see also Figure 83). For residential buildings, the reduction in peak cooling power demand intensities is more pronounced, experiencing a 20% decline from 30 to 24 W/m² between the Status Quo and 2050-L scenarios. In contrast, office buildings witness a milder decrease, shrinking by only 5% from 42 to 40 W/m² over the same period.

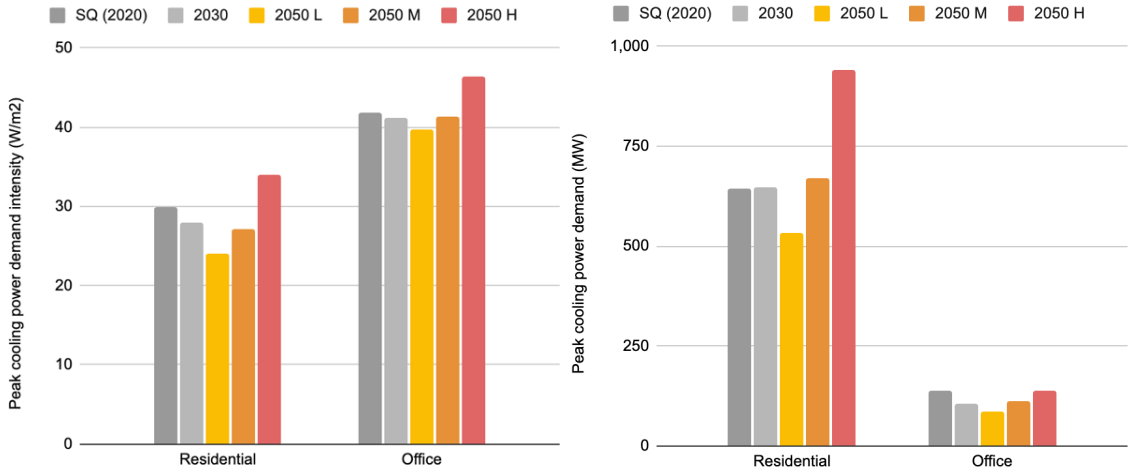

Figure 83: Evolution of the capped peak cooling power demand intensity (left) and total capped peak cooling power demand (right) for residences and offices, across scenarios.

In total peak cooling power demand, residential demand rises by 50% from 643 MW in the Status Quo to 943 MW by 2050-H. Meanwhile, office demand consistently drops, reaching a maximum of 137 MW in 2050-H, a 2% decline. Between the Status Quo and 2050-L, residential demand decreases by 17%, while office cooling power demand reduce by 40%.

4.2.2 How Will the Environmental Impacts of Residential and Office Cooling in The Hague Evolve across the 2030 and 2050 Scenarios?

4.2.2.1 Electricity Use

Besides the changes in cooling energy demand, the evolution of the electrical energy use depends on the share of buildings with an active cooling installation, and the energy efficiency of those installations. With MPRs of cooling equipment anticipated to grow rapidly in the coming decades, especially for residential buildings, the cooling gap is projected to narrow from 77% in the status quo (2020) to 17% in 2050-H (see

Figure 84). Even in the low-impact 2050-L scenario, the cooling gap is cut in half, resulting in only 38% of the cooling demand going unfulfilled.

Resulting from an increase in both determining factors, electricity use increases in all scenarios except 2050-L, in which it drops one third from the current 101 GWh to 67 GWh. By 2030, electricity usage from cooling equipment is expected to rise by 28%, with an additional 15% increase in the 2050-M scenario. In the most extreme scenario, 2050-H, electricity demand for cooling is estimated to quadruple compared to the status quo, reaching 419 GWh. The proportionally smaller increases in electricity use compared to the growth in the fulfilled cooling demand can be explained by modeled improvements in the energy efficiency of cooling technologies.

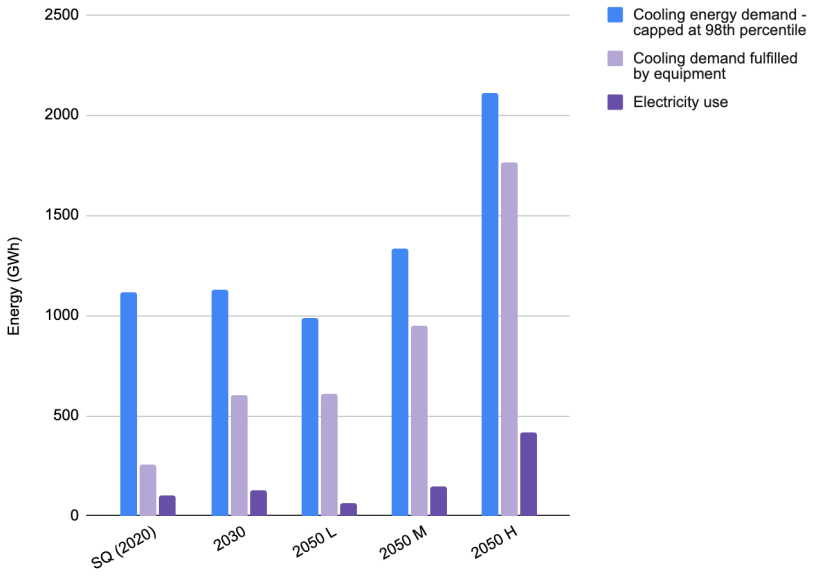

Figure 84: The evolution of the cooling energy demand, the share of the cooling demand fulfilled by cooling equipment, and the electricity needed to fulfill cooling demand across scenarios.

Differences between residential and office buildings are apparent when examining their electricity use intensities. In the Status Quo scenario, residential electricity use intensity is 14 times smaller than that of offices, at a ratio of 1.5 to 21 kWh/m^2. However, residential intensity undergoes a rapid growth trajectory in the future scenarios. Specifically, as can be seen in Figure 85, it doubles from 1.5 to 3.1 kWh/m^2 in 2030 and is projected to grow eightfold to 12.5 kWh/m^2 in the 2050-H scenario. These increases can likely be attributed to the anticipated surge in the MPR of cooling equipment in residential buildings, which rises from an average of 15% to 34% in 2030 and eventually to 78% in the 2050-H scenario. In the 2050-L scenario, residential electricity use intensity remains virtually the same as in the status quo scenario, at 1.6 kWh/m^2. This is likely due to the projected improvements in energy efficiency of cooling equipment offsetting the increased cooling demand and MPR of cooling equipment.

In contrast, changes in electricity use intensity for offices are more moderate, primarily due to the modest rise in cooling equipment MPR. The average MPR in offices is expected to increase from 73% to 100% by 2030, maintaining at 100% in all 2050 scenarios, leaving limited room for substantial increases in electricity use. Consequently, the electricity use intensity of offices is only projected to grow by 11%, increasing from 21 to 23 kWh/m^2 by 2030, and increasing by another 10% to 25 kWh/m^2 in the 2050-H scenario.

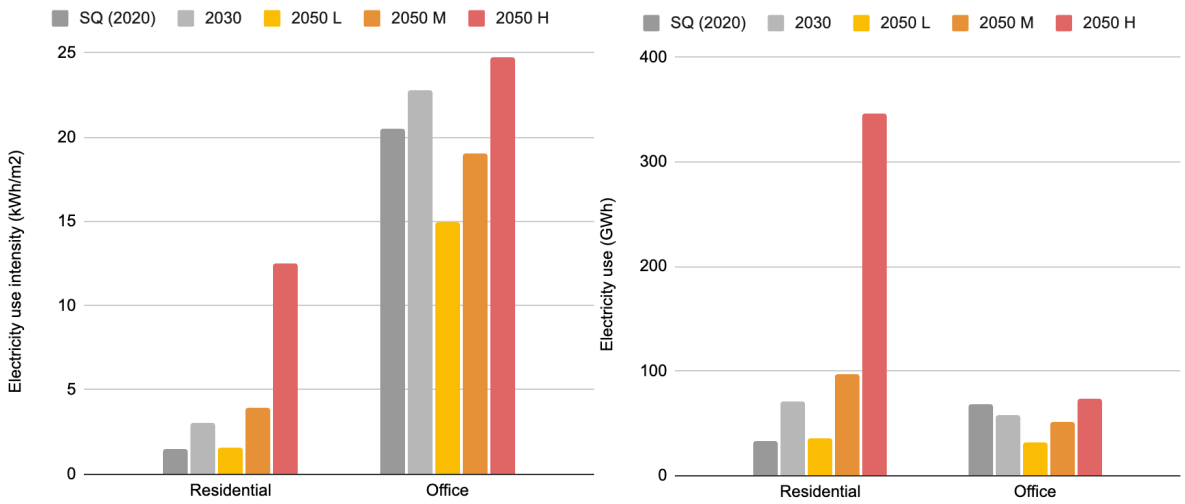

Figure 85: Evolution of the electricity use intensity (left) and total electricity use (right) for residential buildings and offices, across scenarios.

In contrast, the 2050-M and 2050-L scenarios indicate a 7% to 27% reduction to 19 and 15 kWh/m², respectively. These variations are likely attributed to modeled improvements in energy efficiencies and the slightly lower cooling demand intensities for offices. Figures displaying the evolution of the electricity use intensity per building type can be found in Appendix Q.

The disparities in the absolute electricity use are further exacerbated by projected changes in the building stock. While the residential building stock is expected to increase between 3% and 29% between 2020 and 2050, office floor space in The Hague is projected to shrink 14% to 47% in the same period. Consequently, electricity use from residential buildings grows significantly, while that of offices remains relatively stable.

In the residential sector, electricity use for space cooling experiences significant growth across all scenarios. Notably, it more than doubles by 2030, increasing from 32 to 71 GWh, and undergoes an eleven-fold surge in the 2050-H scenario, reaching 346 GWh. The only exception is the 2050-L scenario, in which the electricity use grows modestly with 8% to reach 35 GWh. Conversely, total electricity use in office buildings shrinks in all but one scenario, halving in the 2050-L scenario from 68 GWh to 32 GWh. Even in the worst-case 2050-H scenario, it grows only slightly with 6% to 73 GWh.

4.2.2.2 Material Demand

The projected increase in the market penetration of cooling equipment, combined with the expected rise in the cooling demand, has significant implications for material demand in future scenarios. The material demand of cooling equipment across the total building

stock increases in all scenarios, ranging from a 55% increase by 2030 to a more than three-fold increase in 2050-H, with relatively linear shifts between scenarios (see Table 44). Given that the ADP *intensity* and the CSI *intensity* remain unchanged across scenarios in the modeling,[46] the total resource depletion and crustal scarcity impacts are expected to grow at the same rate as the total material demand. This translates into increased risks of resource depletion from the increased cooling equipment stock, and higher associated environmental risks.

Table 44: Material demand and related environmental impact metrics of the modeled cooling equipment stock for all scenarios. Note that this is the impact of the installed cooling equipment stock; please see Appendix Q for the annualized impacts.

Scenario	Material demand (kt)	ADP (tonne Sb-eq)	CSI (Mt Si-eq)
SQ (2020)	3.00	0.76	4.72
2030	4.67	1.21	7.56
2050-L	7.99	2.08	13.0
2050-M	8.94	2.36	14.8
2050-H	10.7	2.82	17.6

Whereas the intensity of cooling equipment material demand for offices is much higher than that for residences in the Status Quo (0.52 kg/m^2 vs. 0.06 kg/m^2), the future scenarios project a narrowing in this gap, with residential material demand intensity rising at a faster rate than office intensity across scenarios. This is primarily due to increases in the MPR of cooling equipment in the residential sector from 15% in the Status Quo. In comparison, offices are assumed to have reached a 73% MPR in the Status Quo scenario, leaving less room for growth. It is noteworthy that material intensities are projected to increase for both offices and residential buildings in all future scenarios.

As seen in Figure 86, the material demand intensity of the residential sector is expected to roughly double from 0.06 kg/m^2 to around 0.14 kg/m^2 by 2030. This intensity is projected to double again by 2050, reaching 0.29—0.31 kg/m^2. In contrast, the office sector is projected to rise moderately by 12% to 0.59 kg/m^2 by 2030. By 2050, it is expected to increase between 17% and 37% to reach a maximum of 0.72 kg/m^2.

[46] In other words, the ADP and CSI impacts – in kg Sb-eq and kg Si-eq per kg of cooling equipment respectively – were assumed not to change in the future scenarios.

Notably, the best-case 2050-L scenario exhibits a higher material demand intensity for offices compared to the 2050-M and 2050-H scenarios. This deviation is likely attributed to the higher proportion of heat pumps in the cooling technology mix – as opposed to chillers, split-type, and portable air conditioners (ACs) – for offices in the 2050-L scenario. While heat pumps boast superior energy efficiency and lower climate change impact than traditional ACs, they are modeled to be more materially intensive. For a detailed overview of the material use intensities per building type, see Appendix Q.

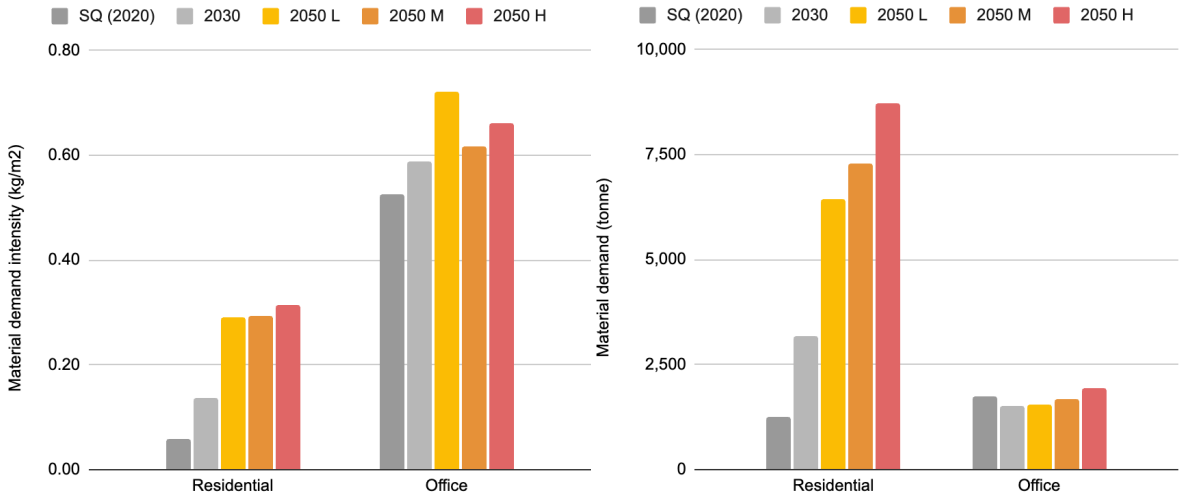

Figure 86: Evolution of the material demand intensity (left) and total material demand (right) for residential buildings and offices, across scenarios.

Regarding the total material demand, which is largely driven by offices in the Status Quo scenario, the rapid surge in material demand intensity within residential buildings, coupled with the projected growth of the residential building stock, results in a substantial increase in total material demand for cooling equipment in residential buildings. Specifically, residential material demand for cooling equipment is set to more than double by 2030, escalating from 1.3 kt to 3.2 kt by 2030. It is then projected to grow two- to threefold between 2030 and 2050, reaching a range of 6.5 to 8.7 kt by the end of that period.

Conversely, the material demand of cooling equipment in offices is anticipated to slightly decrease by 2030, declining from 1.8 to 1.5 kt. Comparable figures are projected for the 2050-L and 2050-M scenarios, with material demands of 1.5 and 1.6 kt, respectively. This decrease is largely attributed to the shrinking building stock for offices. However, material demand experiences marginal growth in the 2050-H scenario, increasing by 11% to 1.9 kt.

4.2.2.3 Climate Change Impacts

The climate change impacts resulting from electricity use, refrigerant leaks, and the production and end-of-life phases of cooling equipment decrease in all scenarios compared to the Status Quo, except for 2050-H, where impacts increase significantly (see Figure 87). In the 2030 scenario, GHG emissions are projected to drop from 48.8 to 25.1 kilotons (kt) CO_2-eq per year. This is likely caused by the decrease in electricity-related emissions. Despite an increase in cooling-related electricity use of 28% by 2030, the projected increase in the share of renewable energy technologies within the Dutch energy mix reduces the carbon intensity of the grid, decreasing net GHG emissions. Emissions from refrigerant leaks are also anticipated to decrease, due to reductions in the leakage rates of cooling technologies and choices for refrigerants with a lower global warming potential (GWP). On the other hand, emissions from production and end-of-life processes increase by 58% as the cooling equipment stock increases in The Hague.

In the 2050-L scenario, GHG emissions are projected to reduce by 90% from 48.8 to 4.7 kt CO_2-eq, which is the most severe reduction of all scenarios. This is largely due to the electricity-related emissions dropping by 95% to 1.9 kt CO_2-eq, due to dramatic decarbonization of the electricity grid, where fossil fuels only make up 0.5% of the electricity mix. In addition, GHG emissions from refrigerant leaks have been eliminated due to a modeled widespread adoption of zero-GWP refrigerants and best practices and policies for leakage rate reductions. Instead, production and end-of-life treatment of cooling equipment are responsible for the majority of GHG emissions at 2.6 and 0.19 kt CO_2-eq respectively, due to an increasing size of the cooling equipment stock.

2050-M follows a similar pattern to 2050-L, with total GHG emissions dropping by 81% to 9.3 kt CO_2-eq. In 2050-M, although significant decarbonization of the electricity grid takes place, the mix of renewable energy technologies results in slightly higher carbon intensity than in 2050-L, mostly due to the higher share of solar PV which has higher scope 3 impacts than e.g., wind energy. This results in annual electricity-based GHG emissions of 6.2 kt CO2-eq – still an 86% drop compared to the status quo. Refrigerant-related emissions are dramatically reduced from 4.8 kt CO2-eq in the status quo scenario to only 3 tonnes CO_2-eq per year. Greater market penetration of cooling technologies in 2050-M compared to 2050-L result in slightly larger emissions from production and end-of-life treatment of the equipment, at 2.9 and 0.21 kt CO_2-eq respectively.

In contrast, GHG emissions increase by 71% from 48.8 to 83.6 kt CO_2-eq in the 2050-H scenario. Emissions from all sources increase, and electricity remains the largest source of emissions, growing by 55% from 43.1 to 66.6 kt CO_2-eq. This is most likely a result of stagnation in the decarbonization of the electricity grid from 2030 onwards, combined with a large increase in cooling energy demand due to climate change, and high market penetration of cooling technologies in both residential and office buildings. Emissions from refrigerant leaks grow almost threefold from 4.8 to 13.3 kt CO_2-eq, due to a high growth in the demand for cooling equipment and only minimal improvements in leakage rates and refrigerant choices. This increase in the market penetration of cooling equipment also results in much higher GHG emissions in the required production and waste treatment process, increasing from 0.9 to 3.5 kt CO_2-eq and from 67 to 251 tonnes CO_2-eq, respectively.

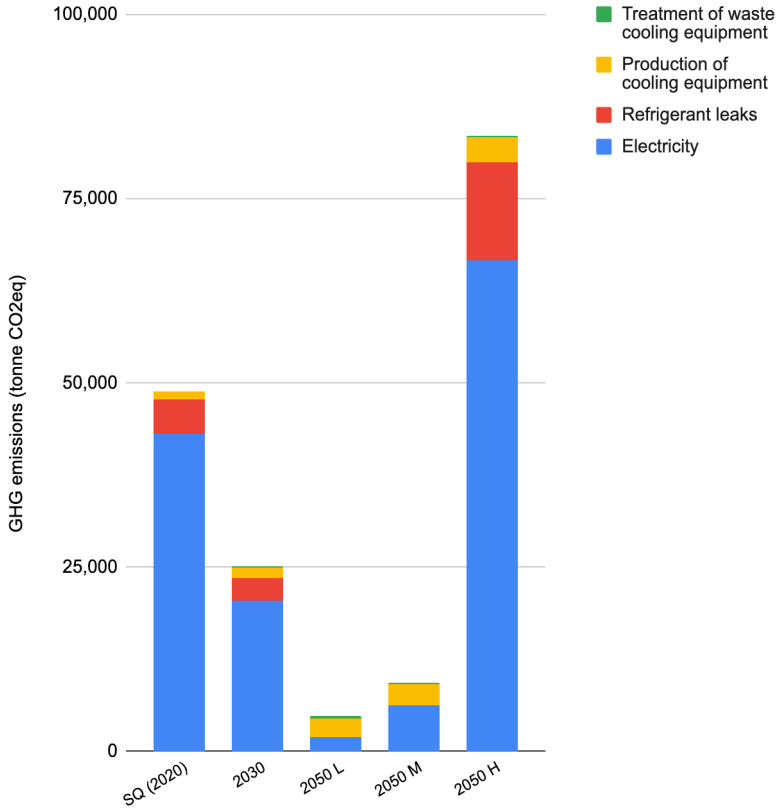

Figure 87: Breakdown of total GHG emissions by source, across scenarios.

Significant differences in carbon intensities can be observed between residential and office buildings. In the case of residential buildings, the carbon intensity of space cooling is projected to decrease in all scenarios except for 2050-H, as can be seen in Figure 88. By 2030, it is expected to reduce by one fifth, dropping from 0.79 to 0.64 kg CO_2-eq/m^2. It decreases further by 77% decrease in the 2050-L scenario, down to 0.15 kg CO_2-eq/m^2.

This remarkable decline is largely attributed to the steady decarbonization of the electricity grid, which is anticipated to be nearly carbon neutral in the 2050-L scenario. In stark contrast, the carbon intensity triples to 2.53 kg CO_2-eq/m^2 in the 2050-H scenario. Here, the decarbonization of the grid stagnates from 2030 onwards, proving insufficient to counteract the increasing market penetration of cooling equipment and the heightened cooling demand resulting from climate change.

The carbon intensity of offices experiences a decrease across all scenarios, primarily due to electricity grid decarbonization. It halves from 9.6 to 4.1 kg CO_2-eq/m^2 by 2030 and further drops by 83% to 0.67 kg CO_2-eq/m^2 in the 2050-L scenario. In the 2050-H scenario, the carbon intensity moderately increases from the 2030 level to 4.6 kg CO_2-eq/m^2, which still reflects a 52% reduction compared to the status quo. For a detailed overview of the carbon intensities per building type, see Appendix Q.

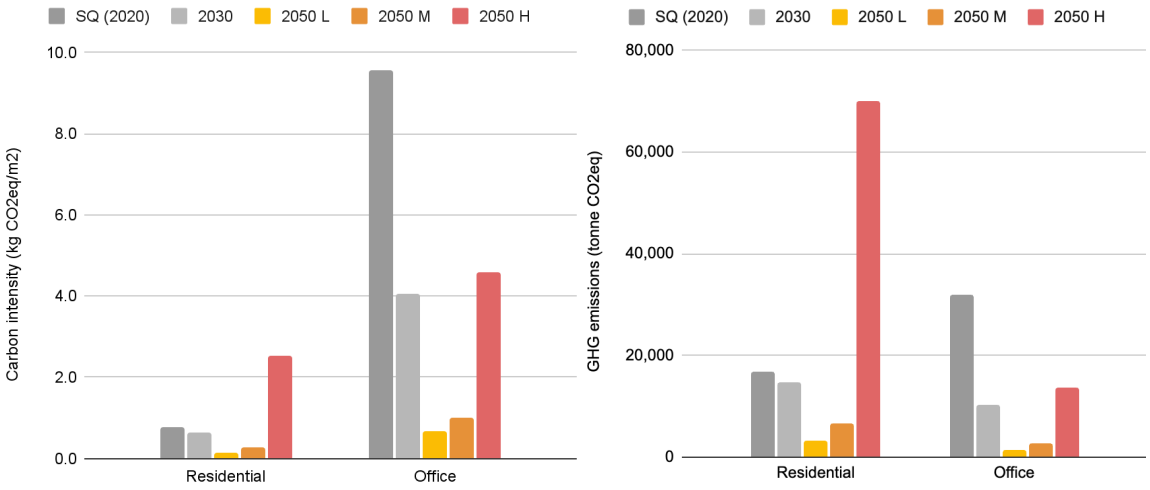

Figure 88: Evolution of the carbon intensity (left) and total GHG emissions (right) for residential buildings and offices, across scenarios.

The total GHG emissions closely mirror the trend observed in carbon intensities but are influenced by changing building stock dynamics. In the status quo scenario, office GHG emissions are approximately double those of residential buildings, at 32.0 vs. 16.9 kt CO_2-eq, respectively. However, in all future scenarios, residential emissions are expected to surpass those of office buildings, with the residential-to-office emission ratio reaching five to one in the 2050-H scenario.

Residential GHG emissions are projected to undergo a moderate reduction of 13%, declining to 14.8 kt CO2-eq by 2030, followed by a more substantial four-fifths reduction to 3.3 kt CO2-eq in the 2050-L scenario. In contrast, these emissions experience a

dramatic four-fold increase to 70.1 kt CO2-eq between the status quo and the 2050-H scenario. This significant rise can likely be attributed to a combination of increased electricity usage, grid decarbonization stagnation, and a substantial expected growth in the number of residential buildings.

Total GHG emissions from office buildings, on the other hand, are expected to decrease across all scenarios. After a two-thirds reduction from 32.0 to 10.3 kt CO2-eq by 2030, office emissions are projected to drop even further, decreasing by 86% to 1.4 kt CO2-eq in the 2050-L scenario. Even in the worst-case 2050-H scenario, emissions are 58% lower than in the status quo, totaling 13.5 kt CO2-eq.

4.2.3 Summary and Contribution Analysis

Table 45 presents an overview of the main impacts across scenarios. Section 4.1.5 highlights how in the status quo (2020) model, offices are overrepresented in cooling demand and the consequent environmental impacts in relation to their share of floor space in the building stock. Figure 89 presents the divide between offices and residential buildings in terms of their contribution towards future impacts. Due to the projected growth in the residential building stock of The Hague, while office space is expected to decrease, the share of offices in total floor space drops slightly from 14% in the status quo to 9–10% in future scenarios.

Table 45: Energy and environmental impacts across scenarios for the RO building stock of The Hague.

Scenario	Cooling energy demand (GWh)	Peak cooling power demand (MW)	Electricity use (GWh)	GHG emissions (kt CO_2-eq)	Cooling equipment stock (kt)
SQ (2020)	1,118	1,431	101	48.8	3.00
2030	1,127	1,307	129	25.1	4.67
2050-L	987	1,030	67	4.74	7.99
2050-M	1,334	1,266	148	9.32	8.94
2050-H	2,111	1,685	419	83.6	10.7

In terms of environmental impacts, the overrepresentation of offices in the status quo diminishes across scenarios, as residential buildings account for an increasingly larger share of impacts. For instance, in the 2050-H scenario, the share of residential buildings in electricity use increases by 259% from the status quo; 200% in material demand; and by 242% in terms of GHG emissions. This contrasts with the modest increase in residential buildings in floor area by 5% between the status quo and 2050-H. This increase

in the representation of residences in cooling impacts is mainly a result of the rapidly increasing MPR of cooling equipment in the residential sectors, whereas offices already had a relatively high MPR in the status quo, leaving less room for environmental impact growth in the future.

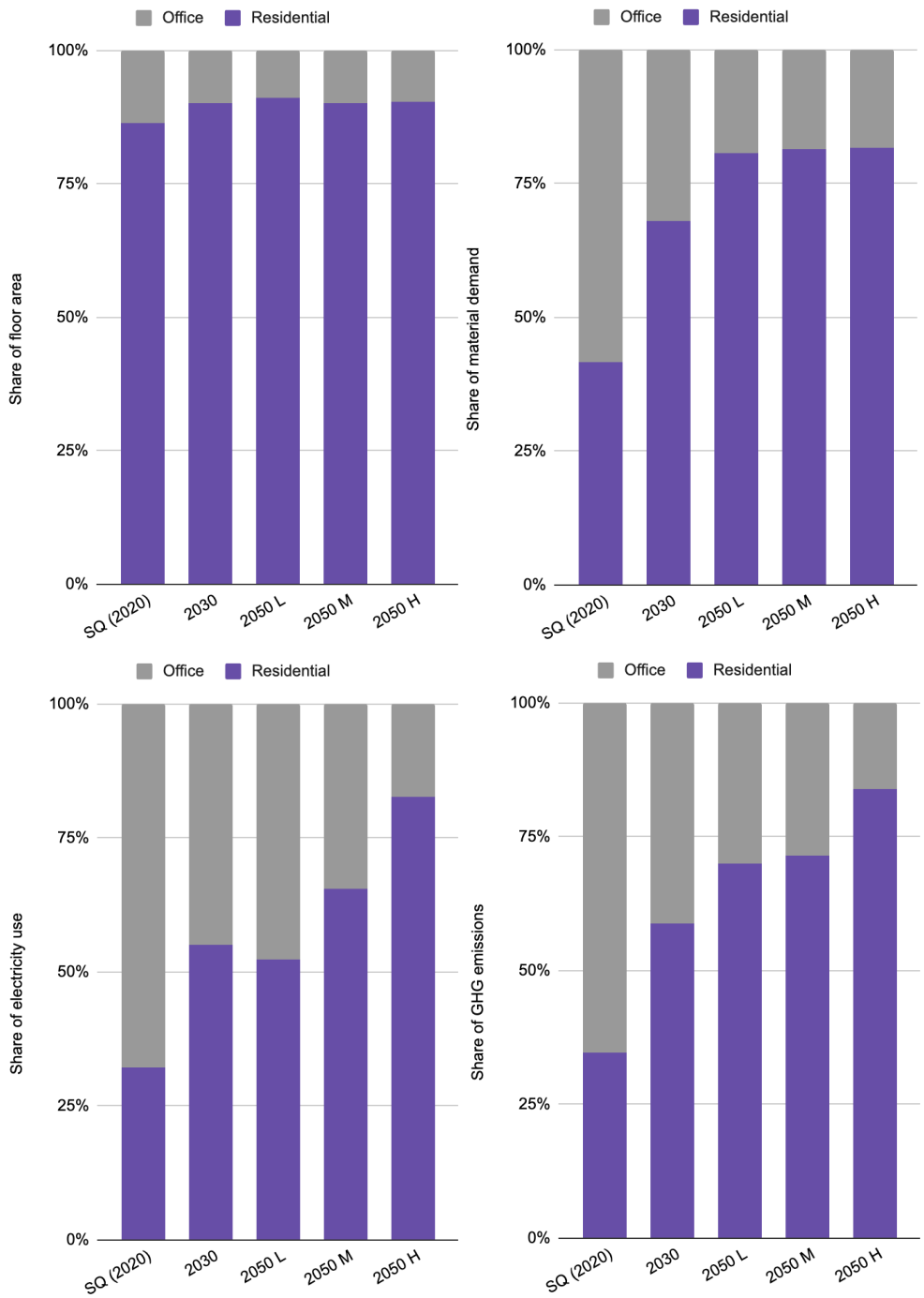

Figure 89: Evolution of the share of residential and office buildings in floor space (top-left), electricity use (top-right), material demand (bottom-left), and GHG emissions (bottom-right). Note: additional figures of impact shares by building type can be found in Appendix Q.

4.3 Supplementary Results

4.3.1 Sensitivity Analyses

Sensitivity analyses were performed to determine the responsiveness of environmental impacts to changes in input parameters. An overview of the resulting elasticities can be seen in Table 46. While most input parameters exert some degree of influence on the environmental impacts, seven parameters stand out as having the highest elasticity, which as discussed in detail below, apart from MPR. The total MPR of cooling equipment has a considerable influence on environmental impacts, with an exact one-to-one relationship between them. Nevertheless, these elasticities remain constant across the full input range of the MPR, underscoring its leverage power.

Table 46: The elasticities of the three primary impacts with regards to various input parameters.

Input parameter	Reference value	Unit	Elasticity		
			Electricity use	*GHG emissions*	*Material demand*
Cooling demand cap percentile	98%	%	1.56	3.05	10.5
Effective cooling temperature	25	°C	-3.41	-3.15	-1.82
Summertime temperature	18	°C	1.11	1.08	0.93
Total market penetration rate of cooling technologies	12	% of the market	1.00	1.00	1.00
Daytime UHI effect	8.3	°C	0.91	0.85	0.52
Energy efficiency of cooling technologies (SEER)	5.0	kWh cooling / kWh electricity	-1.0	-0.80	0.00
Carbon intensity of electricity grid	0.427	kg CO_2-eq/kWh	0.00	0.83	0.00
Summertime solar radiation	229	W/m²	0.26	0.28	0.36
Internal heat gains	6.0	W/m²	0.21	0.19	0.08
Density of people in offices	0.067	-	0.06	0.06	0.04
Average amount of people per household	2.01	-	0.06	0.05	0.02
Refrigerant leakage	9.0	% of charge per year	0.00	0.14	0.00
Global warming potential of refrigerant	1,603	kg CO_2-eq/kg	0.00	0.11	0.00
Nighttime UHI effect	2.1	°C	0.02	0.02	0.00

Note: Comprehensive data illustrating the influence of input parameters on absolute and normalize cooling demand and environmental impacts can be found in Appendix O. It should also be noted that these elasticities may not remain constant across the entire range of input parameters, and the values shown represent the elasticities at the reference value.

4.3.1.1 Cooling Demand Cap Percentile

The cooling demand cap percentile, i.e., the percentile at which the cooling demand is capped, serves as a proxy for thermal discomfort tolerance. Throughout the scenarios, a consistent value of 98% is used, reflecting the installation of cooling systems based on the 98th percentile of power and energy demand. These installations are designed to meet cooling needs for 98% of the year, leaving occupants in a state of thermal discomfort during 2% of the time.

Out of the examined input parameters, the cap percentile has the largest influence on environmental impacts. Notably, moving from a 98% cap percentile to 97% results in a 1.6% reduction in electricity use, a 3.1% decrease in GHG emissions, and a 10.5% decrease in material demand (see Table 46).[47] The large decrease in material demand can be attributed to the direct influence of the cooling demand cap percentile on the total cooling equipment installations. As illustrated in, the impact elasticities vary significantly with regards to the cooling demand cap percentile. While impact elasticities are stable for cooling demand cap percentiles up to 97% (serving as a proxy for thermal discomfort tolerances of 3% and up), they increase dramatically in the final stretch towards 100% coverage of cooling demand. For example, moving from 98% to 100%, corresponding to a zero-tolerance approach for thermal discomfort, would exponentially escalate environmental impact. Notably, material demand would increase by 70% compared to the status quo scenario, as shown in Figure 91.

[47] Such a transition can be seen as a proxy for increasing the thermal discomfort tolerance from 2% to 3% of the hottest hours in the year.

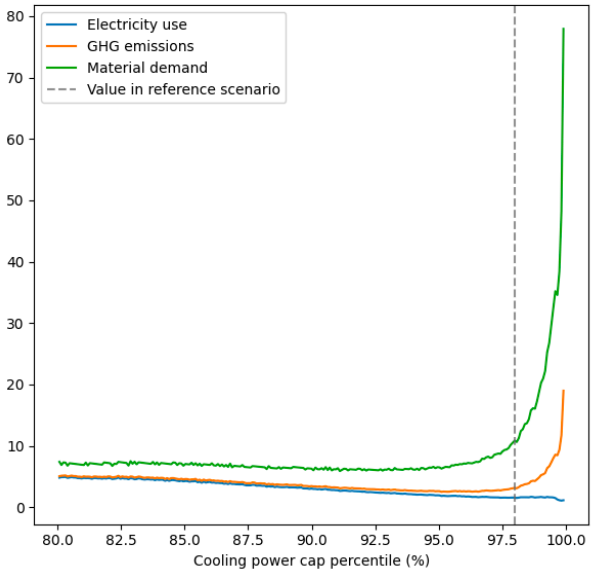

Figure 90: Variation of cooling-related environmental impact elasticities with respect to the peak cooling power percentile cap.

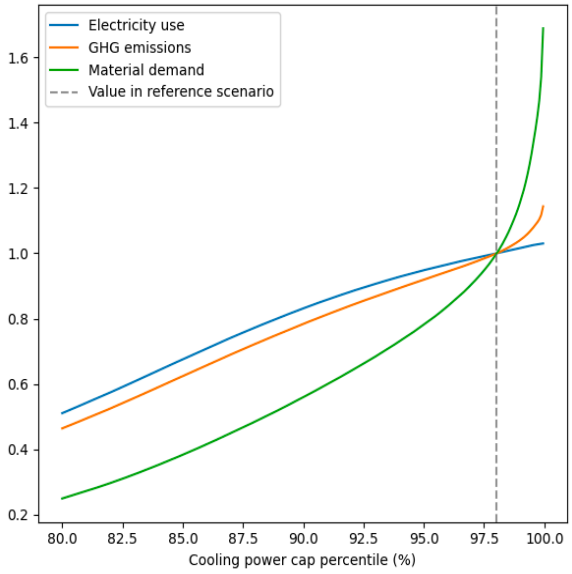

Figure 91: The influence of the cooling demand cap percentile, normalized to the reference value at 98%.

4.3.1.2 Effective Cooling Temperature

Furthermore, the effective cooling temperature, or the threshold above which cooling is deemed necessary, has considerable influence on the final cooling demand impacts within The Hague, with elasticities ranging from 1.8 for material demand to 3.4 for electricity usage. As shown in Figure 92, a reduction in the effective cooling temperature from 25 °C to 23 °C (as in the 2050-H scenario) results in a 15% increase in material demand and a 30% rise in electricity usage and GHG emissions, respectively. Conversely, a 1 °C increase in effective cooling temperature (as in the 2050-L scenario) leads to a 7% reduction in material demand, as well as a 14% decline in electricity usage and GHG emissions.

It is noteworthy that the impact elasticities exhibit an increase in magnitude as the effective cooling temperature rises, particularly at higher effective cooling temperatures nearing 30 °C, as illustrated in Figure 93. At these elevated temperatures, the elasticities increase from 1.5 for material demand and 3.0 for electricity usage and GHG emissions to 3.0 and 4.5, respectively. This implies that as the effective cooling temperature is raised, more-than-linear impact reductions can be achieved, especially in the case of electricity usage and GHG emissions.

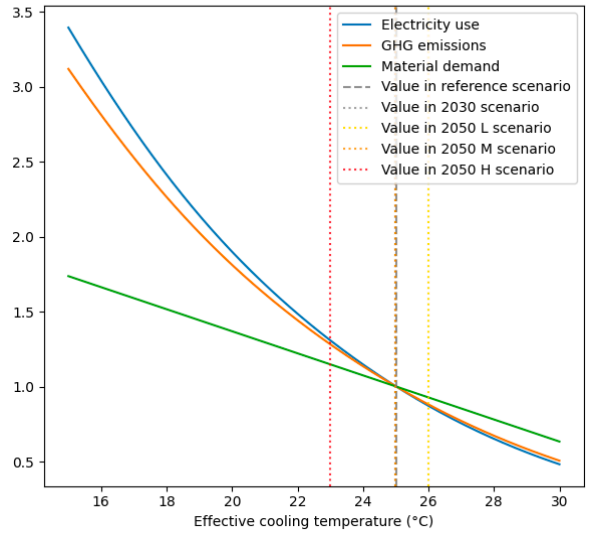

Figure 92: The influence of the effective cooling temperature on environmental impacts, normalized to the reference value at 25 °C.

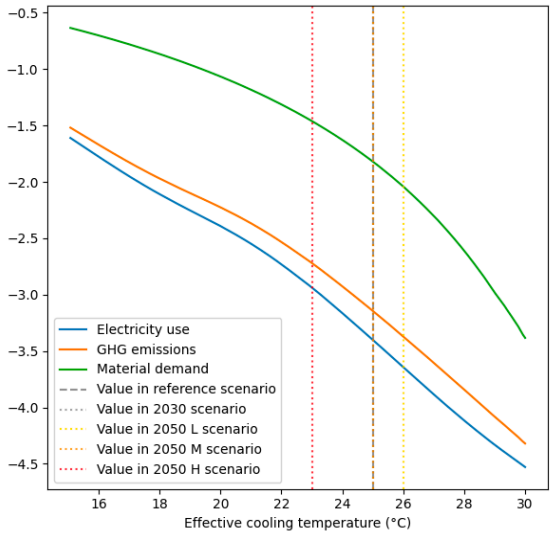

Figure 93: The variation of the cooling-related environmental impact elasticities with respect to the effective cooling temperature.

4.3.1.3 Summertime Temperature

The influence of the average summertime temperature on environmental impacts is significant, as environmental impacts increase by 6–7 % solely due to the temperature rise in the 2050-H scenario. At the reference value, elasticity is approximately one, signifying that a 1% increase in temperature corresponds to a similar increase in environmental impacts. This elasticity increases slightly as the summertime temperature increases. For example, the elasticity of electricity use and GHG emissions escalates to approximately 1.3 with a summertime warming of 4 °C (see Figure 94 and Figure 95).

However, it is important to note that The Hague municipality has a negligible influence over global temperature rise, and the policy recommendations of this research primarily target local actions within the municipality's jurisdiction. Hence, this sensitivity analysis of summertime temperature is not taken into further consideration.

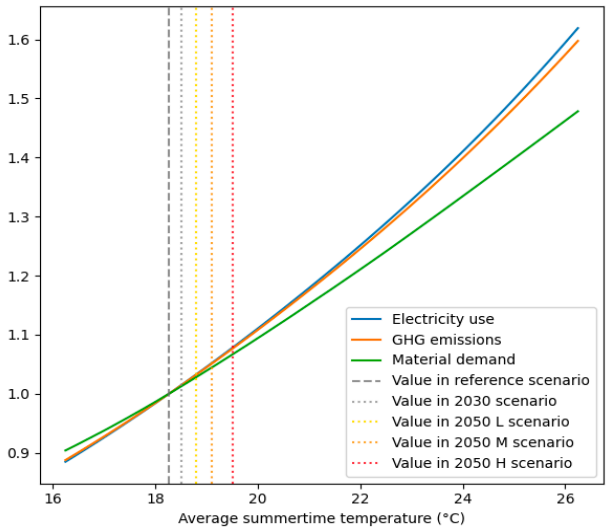

Figure 94: The influence of the average summertime temperature on environmental impacts, normalized to the reference value at 18.2 °C.

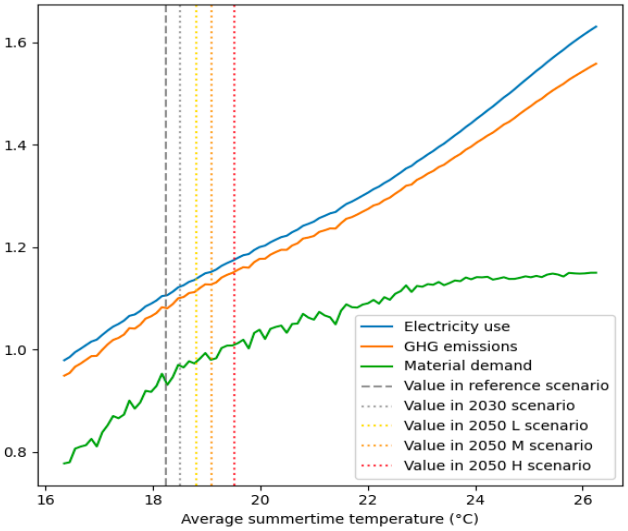

Figure 95: The variation of the cooling-related environmental impact elasticities with respect to the average summertime temperatures.

4.3.1.4 Daytime UHI Effect

The daytime UHI effect has the fifth largest impact on cooling demand environmental impacts, with considerable elasticities greater than 0.5 for all impact categories. As shown in Figure 96, these high elasticities cause in the expected 1.5 °C increase in the UHI effect within the 2050-H scenario to lead to an 18% rise in electricity usage and GHG emissions, accompanied by a 10% increase in material demand.

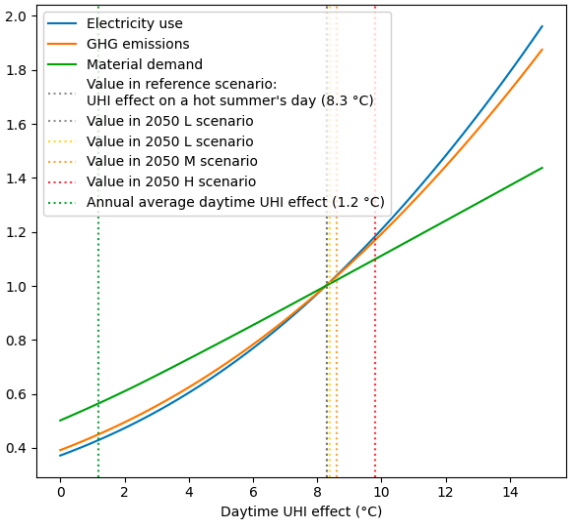

Figure 96: The influence of the daytime UHI effect on environmental impacts, normalized to the reference value at 8.3 °C.

As discussed in section 3.2.2.1, the UHI effect is not constant throughout the year or the city. However, due to the unavailability of comprehensive data on its temporal or spatial variation, a constant daytime UHI effect was assumed in the model. Given the primary focus of this research on space cooling, which predominantly occurs on hot summer days, a UHI value of 8.3 °C was used in the Status Quo scenario, aligning with the UHI effect experienced during such hot summer days. In order to assess the impact of this modeling decision, a comparison was made between the environmental impacts of the SQ scenario and those of an alternative model wherein the UHI effect was set at 1.2 °C, representing the annual average UHI effect in The Hague based on the available sources (van der Hoeven & Wandl, 2018a). This shift to the annual average UHI effect yielded a substantial decrease in environmental impacts, as shown in Table 47.

Table 47: Reduction in cooling demand and related environmental impacts by shifting from a daytime UHI effect of 8.3 °C to 1.2 °C.

Impact	Impact reduction
Cooling energy demand	46%
Peak cooling power demand	42%
Electricity use	41%
GHG emissions	40%
Material demand	33%

4.3.1.5 Energy Efficiency of Cooling Equipment

Lastly, the energy efficiency of cooling equipment significantly impacts electricity use and GHG emissions, with elasticities of -1 and -0.8, respectively. It is worth noting that the potential for environmental impact reduction through energy efficiency diminishes as the importance of electricity within the total GHG emissions decreases. For instance, enhancing the average energy efficiency by 80% from 5 to 9 units of cooling energy provided per unit of electrical energy used, as demonstrated in the 2050-L scenario, results in a 37% reduction in GHG emissions, as depicted in Figure 97.

4.3.1.6 Carbon Intensity of the Electricity Grid

The carbon intensity of the electricity grid exclusively impacts GHG emissions and does not affect the electricity or material use resulting from cooling demand. However, it plays a pivotal role in determining total GHG emissions, with an elasticity of 0.83. As depicted in Figure 98, transitioning from the status quo value of 0.427 kg CO_2-eq to 0.029 kg CO_2-eq in the 2050-L scenario results in a substantial 78% reduction in total GHG emissions

attributed solely to the decarbonization of the electricity grid. Conversely, if the Netherlands were to adopt the carbon intensity level of Poland, standing at 0.67 kg CO_2-eq (Ritchie et al., 2022), it would lead to a 47% increase in total cooling-related GHG emissions.

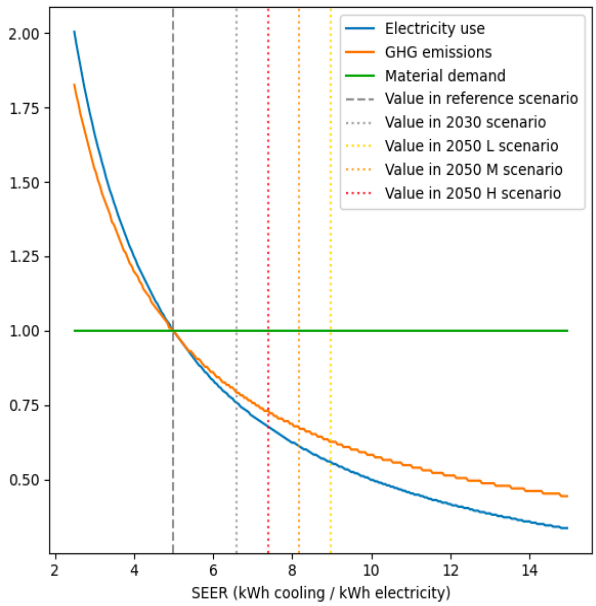

Figure 97: The impact of average energy efficiency (expressed as SEER) of cooling equipment on environmental impacts, normalized to the reference value (5).

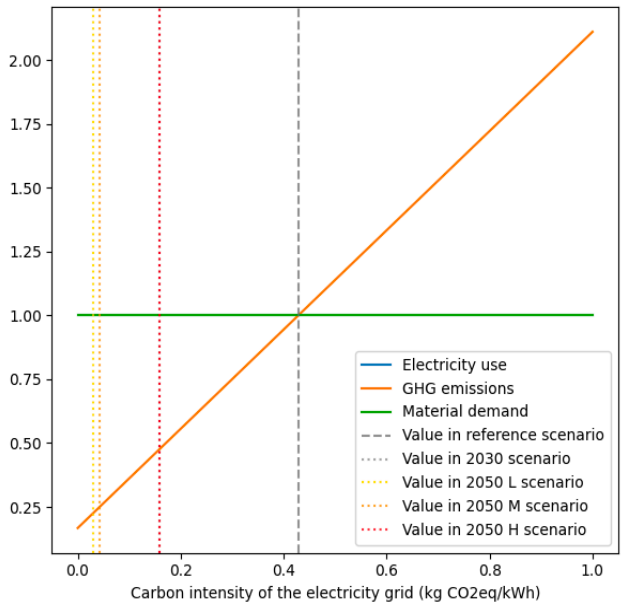

Figure 98: The influence of the carbon intensity of the electricity grid on environmental impacts, normalized to the reference value at 0.43 kg CO_2-eq.

4.3.1.7 Impact Elasticities of Cooling Technology Choices

A sensitivity analysis was performed on the transition from one cooling technology to another, and its influence on environmental impacts (see Table 48). Most evident is the reduction in environmental impacts when transitioning away from portable ACs, which reduce electricity use and GHG emissions. However, portable ACs have a comparatively low material demand, which results in higher material demand impacts when transitioning towards other active cooling technologies. A transition towards heat pumps in particular shows the greatest reductions in electricity use and GHG emissions compared to other technologies. However, heat pumps have a much higher material demand, which increases material footprint. In relation to chillers and large split ACs, both which are suitable for larger buildings, the transition from large split ACs to chillers is predicted to result in small reductions in electricity use and GHG emissions, with an even smaller increase in material demand. It should be noted that these figures are based

on proxy sample models for each technology, so the precise numerical percentage changes hold a high uncertainty. Instead, the overall relationships should be the focus of analysis.

Table 48: Overview of the percent change in environmental impacts when moving from a cooling technology mix of 100% one technology to 100% of another.

Moving from ...	**... to**	**Elasticity**		
		Electricity use	*GHG emissions*	*Material demand*
Portable AC	Large split AC	-34%	-34%	5%
Portable AC	Heat pump	-47%	-41%	27%
Portable AC	Chiller	-25%	-28%	2%
Heat pump	Large split AC	10%	5%	-29%
Chiller	Large split AC	-8%	-6%	3%
Chiller	Heat pump	-20%	-12%	26%
Heat pump	Chiller	17%	10%	-33%
Heat pump	Heat pump	-1%	-1%	-3%
Large split AC	Heat pump	-12%	-6%	23%
Large split AC	Chiller	7%	6%	-3%
Heat pump	Portable AC	36%	32%	-35%
Chiller	Portable AC	22%	24%	-2%

4.3.2 Extrapolation of impacts

The cooling demand and the corresponding environmental impact assessments are grounded in the subset of The Hague's RO building stock for which energy label data was accessible. Approximately 20% of the total floor space within the RO building stock lacked assigned energy labels as of 2023. Since thermal insulation characteristics could not be modeled for these unlabeled buildings, adjustments were made by scaling up the cooling demand and environmental impact results. This extrapolation was guided by the assumption that the energy label distribution for the unlabeled buildings mirrored that of the building stock with assigned energy labels.

Table 49 provides a summary of the extrapolated results, revealing that the environmental impacts for the extrapolated data are approximately 25% higher across all impact categories compared to those calculated for the base building stock, as presented in section 4.2.3. For further insights into the extrapolated cooling demand and environmental impact assessments, including data pertaining to the primary building

subset, extrapolated values for buildings lacking energy label data, and the total impacts for the entire residential and office building stock of The Hague, refer to Appendix R.

Table 49: Total impacts for the entire residential and office building stock of The Hague, including extrapolation on buildings lacking energy label data.

Scenario	Cooling energy demand (GWh)	Peak cooling power demand (MW)	Electricity use (GWh)	GHG emissions (kt CO_2-eq)	Cooling equipment stock (kt)
SQ (2020)	1,398	1,631	125	60.5	3.70
2030	1,408	1,497	161	31.3	5.82
2050-L	1,232	1,186	83	5.90	9.94
2050-M	1,665	1,462	184	11.6	11.1
2050-H	2,635	1,956	521	104	13.3

5 Analysis and Discussion

5.1 What is the Current Cooling Demand of Residential and Office Buildings in The Hague?

The analysis of cooling in residential and office buildings in The Hague reveals key insights about the city's building stock and opportunities for reducing environmental impact. Residential buildings are predominant, making up 99% of the total count, while office buildings, though fewer, account for 13% of the total floor space. Most buildings are between 10 and 15 meters tall, with high-rise buildings (over 17.5 meters) comprising just 2.1% of total buildings but holding 26% of floor space. Old low-rise residential buildings are the most common in terms of both count and floor space. Old high-rise offices are the most prevalent within the office building stock. Offices cluster in the city center and business district, featuring a mix of old and newer high-rise offices, while new low-rise residential buildings are mainly located on the outskirts, reflecting urbanization trends.

5.1.1 Energy Label Distribution

Furthermore, the distribution of energy labels reveals that there is room for improvement in terms of building energy performance. Energy label A is the single most prevalent label, but labels B through E together represent most of the floor space. Labels A+-A+++++ are uncommon, likely due to their association with newer constructions. Overall, offices perform better in energy label standards than residential buildings. Importantly, there is a strong correlation between building age and energy labels, indicating that older buildings tend to have lower energy performance. This remains the case despite extensive efforts to renovate the existing residential building stock as part of the transition to sustainable heating (“warmtetransitie” in Dutch) (DSO, 2022). This suggests that over the past years, either insufficient renovations have occurred, or they have been ineffective to significantly raise the energy labels of the older building stock to newer standards. This calls for the implementation of more stringent energy label regulations for renovation projects and efforts into formulating best practices and guidelines for renovations in the context of the energy transition.

In addition, a substantial portion of office buildings in The Hague do not meet the minimum energy label requirements of label C or above by 2023, as set by Dutch policy. Approximately 30% of office buildings fail to adhere to the policy, although they represent

only 9% of the total floor space. This suggests that medium-sized offices may be struggling to meet the energy efficiency standards. Considering that offices make up a large portion of the status quo cooling demand, it is essential for policymakers to address this issue by providing incentives and stricter regulations to stimulate these offices to improve their energy efficiency.

5.1.2 Economic Status and the Urban Heat Island Effect

The findings presented in this study shed light on a significant aspect of the environmental and social impacts of space cooling in The Hague—the unequal distribution of the urban heat island (UHI) effect among different socioeconomic groups. Results revealed a statistically significant correlation between increased UHI and lower income neighborhoods in The Hague. When combined with the fact that economically disadvantaged groups tend to have poorer access to cooling equipment, as shown in Figure 15, it becomes evident that they are less well-equipped to combat heat stress compared to counterparts in wealthier, cooler neighborhoods.

This situation presents a case of climate injustice in The Hague, underscoring the vulnerability of low-income communities to heat stress, especially among vulnerable populations like the elderly and children. These findings emphasize the urgency of targeted interventions and policy measures, such as enhancing green spaces, improving building insulation, and reducing heat island effects in these vulnerable areas. Moreover, it shows the need to prioritize social equity in urban climate adaptation and space cooling policies.

5.1.3 Cooling Demand

The Hague's building stock has a significant cooling demand, with a peak cooling power demand of approximately 1,431 MW.[48] This drops significantly to 783 MW when accounting for a 2% thermal discomfort tolerance. This demand is driven primarily by heat gains through transmission, but internal heat gains, infiltration, and solar radiation also contribute substantially.

[48] Note that this is the cooling power demand, not the electrical power demand needed to fulfill that cooling, which will be discussed in the following section.

Aggregating these flows throughout the year, the total cooling demand at a 2% thermal discomfort tolerance is 1,118 GWh.[49] Comparing this to similar research, the EU Horizon *Hotmaps* project estimates a total annual space cooling demand for The Hague of 400 GWh, three times lower than the findings of this research (The Hotmaps Team, 2021). However, the *Hotmaps* estimate does not take the UHI effect into account, which, as seen in the sensitivity analysis in section 4.3.1, is a large contributor to cooling demand, which may explain the difference in outcomes (A. Müller, 2015). Removing the UHI effect from the cooling demand model used in this research, the annual cooling demand is calculated to be 358 GWh, on par with the *Hotmaps* results. This highlights the importance of accounting for the UHI effect in cooling demand models and confirms the comparability of results with external research.

The distribution of cooling demand intensities varies between office and residential buildings, with offices' cooling energy demand on average three times higher due to factors such as a higher population density and appliance density. Thus, the theoretical cooling demand intensity for offices is 115 kWh/m^2, and 34 kWh/m^2 for residential buildings. Under current market penetration rates (MPRs) of cooling devices, the intensity of fulfilled cooling demand for office and residential buildings is 87 kWh/m^2 and 5.3 kWh/m^2, respectively. In comparison, research on the transition to sustainable heating in The Hague found that the average heating intensity of residential buildings in The Hague is 86 kWh/m^2 (de Boer et al., 2022). This indicates that in the Status Quo scenario, heating demand is a more pressing concern than cooling (at least for residential buildings), which is reflected in current policy efforts.

The residential cooling energy demand of 34 kWh/m^2, compared to a previous estimate of 16 kWh/m^2 for Dutch residences, shows a similar order of magnitude but still a notable difference (Werner, 2016). This difference is likely due to the earlier study not accounting for the UHI effect, emphasizing the need to consider UHI when assessing cooling energy demands.

As seen in the building stock characteristics, older low rise residential buildings make up most of the building stock, and they also have the worst average energy labels of all

[49] A 2% thermal discomfort tolerance corresponds with capping the cooling energy and power demand at the 98th percentile, as discussed in section 4.3.1.1.

building types. In result, they account of most of the cooling demand, both in terms of cooling energy and peak cooling power, likely due to their lower-than average thermal insulation. This suggests that efforts in mitigating future cooling needs should be focused on renovating or updating the large old low rise residential building stock to achieve higher energy efficiency performance, which would, in turn, reduce cooling demands.

5.2 What are the Environmental Impacts of the Current Cooling Demand in The Hague?

The environmental impacts of the current cooling demand were assessed by considering various key factors, including electricity use, material demand, and greenhouse gas (GHG) emissions. Impacts were analyzed in the context of different building types and their relative contributions.

5.2.1 Electricity Use

The total cooling energy demand in The Hague is substantial, reaching 1,118 GWh per year in the Status Quo scenario. However, only approximately 23% of demand is met by cooling equipment, leaving a significant portion unmanaged. The other 77% of the cooling energy demand (860 GWh), known as the 'cooling gap,' is not fulfilled, leading to thermal discomfort. This highlights the need for measures to close the cooling gap through eco-friendly cooling strategies to meet thermal comfort standards while avoiding a rise in environmental impacts as much as possible. The cooling equipment stock currently used for the 23% of cooling energy demand that is fulfilled consumes 101 GWh of electricity annually, of which 32 GWh occurs in residences and 68 GWh in offices. In other words, offices, making up just 13% of the floor area, drive 71% of The Hague's total current space cooling energy consumption. This underscores, in the short term, the need to prioritize cooling energy reduction efforts in offices rather than residential buildings.

The electrical power demand for space cooling of The Hague's residential and office (RO) building stock reaches a peak of 69 MW on hot summer days, which is roughly equivalent to 27 windmills or 53% of the total installed capacity of the nearby Luchterduinen offshore wind park (CBS, 2022d; Eneco, 2023).

The electricity demand for cooling varies significantly between building types, with offices having a much higher electricity use intensity of 21 kWh/m^2 compared to 1.5 kWh/m^2 for residential buildings. In comparison, the average total electricity intensity of residences

in The Hague is estimated to be 83.3 kWh/ m^2 for offices,[50] and 25 kWh/m^2 for residential buildings (CBS, 2019a, 2022a, 2023b). Thus, based on findings of this research, space cooling is responsible for 25% of the annual electricity consumption of offices, and 5.5% of residential electricity use. In sum, space cooling makes up an average of 8% of electricity consumption in the entire RO building stock of The Hague. While this figure is less than half of the global average, which stood at 18.5% of total global electricity use in buildings as of 2016, it is still a significant share of electricity demand (IEA, 2018a).

5.2.2 Material Demand

The combined mass of cooling equipment in The Hague's residences and offices totals approximately 3,003 tonnes, roughly equivalent to the weight of 1,500 cars. This results in an annual in- and outflow of 232 tonnes of cooling equipment, or 0.43 kg per person (The Hague Municipality, 2023). This figure closely aligns with the 0.34 kg/year estimate for waste space cooling equipment from Statistics Netherlands' *Waste Over Time* algorithm, as employed in the Horizon 2020 *ProSUM* project (Huisman et al., 2017; van Straalen et al., 2016).[51] The same algorithm estimates the total amount of waste electrical and electronic equipment (WEEE) generation to be 30.6 kg per person, putting waste space cooling equipment at a 1% share of this total. This points to the importance of R-strategies and lifetime extension programs for cooling equipment, to reduce the size and relative environmental impacts of the in- and outflows of cooling equipment needed to fulfill The Hague's RO cooling demand.

This material use has environmental implications, namely annual abiotic resource depletion of 58 kg Sb-eq, and a pressure on supply chains for scarce materials, with the crustal scarcity indicator of the material footprint at 365 kt Si-eq/year. Moreover, thirteen critical raw materials (CRMs) were identified with a presence of more than 1 part per million (ppm) in the material footprint of the cooling equipment used in The Hague, including coking coal, magnesium, and tantalum and nickel, and rare earth elements

[50] This is the value for offices between 5,000 and 10,000 m^2 in The Hague. The average floor space of offices in The Hague (6,003 m^2) falls within this range.

[51] This is the sum of categories "0111 - Air Conditioners (household installed and portable)" and "0112 - Other Cooling equipment".

(REEs). As with most WEEE, this also highlights the potential for urban mining in discarded cooling equipment.

It is worth noting that material usage varies across different building types, with offices having nine times higher material intensity than residential buildings, making it imperative to focus on environmental impact reduction in office spaces, especially in the short term.

5.2.3 Climate Change Impacts

The climate change impact of cooling in The Hague is the result of a combination of factors, including electricity use, refrigerant leaks, and the above-mentioned material requirements. The total annual GHG emissions from cooling amount to 48.8 kt CO_2-eq, or 89.4 kg CO_2-eq per resident (The Hague Municipality, 2023). Considering that the average Dutch person has a carbon footprint of approximately 13.6 tonnes CO_2-eq, the current greenhouse gas (GHG) emissions of space cooling make up 0.7% of that annual footprint (Koops et al., 2022). The majority of GHG emissions (88%) stem from electricity use, with refrigerant leaks (10%), and production (2%) and waste treatment (0.1%) of cooling equipment contributing to a lesser extent. The use-phase of cooling equipment accounts for 98% of total GHG emissions. This isolates electricity use as the prime area for environmental impact reduction, particularly in reference to offices, which have a GHG intensity twelve times higher than that of residential buildings.

Overall, old low rise residential and office buildings emerge as primary contributors to the environmental impacts. These building types arise as starting points for environmental impact reduction and should be the focus of policies on space cooling.

5.3 How will the Cooling Demand and Environmental Impacts of cooling in The Hague Evolve Until 2050?

In examining the environmental impacts of residential and office cooling in The Hague across the 2030 and 2050 scenarios, several noteworthy findings and trends emerge. These findings provide valuable insights into the evolution of environmental impacts and underscore the need for targeted policies and strategies for sustainable cooling solutions.

5.3.1 Cooling Demand

A consistent increase in cooling energy demand can be found across scenarios, indicating that cooling will play a growing role in the city's energy consumption. In the 2030 scenario, aligned with current trends and planned policies, cooling energy demand sees only a marginal 0.8% rise, which can be attributed to the ongoing improvements in building insulation and the adoption of higher energy efficiency standards. Looking ahead to 2050, a more substantial increase in cooling energy demand is observed, ranging from 18% in the 2050-M scenario to a striking 88% surge in the 2050-H scenario. In stark contrast, the 2050-L scenario stands out with a noteworthy reduction in both cooling energy demand and peak cooling power demand when compared to the status quo. This is achieved through stringent climate change mitigation and adaptation policies and the absence of buildings with energy labels below C. This scenario highlights the substantial impact that lies between laissez-faire and stringent policies, offering a pathway from a potential doubling of cooling energy demand to a 12% reduction.

Surprisingly, peak cooling power demand tends to decrease, primarily due to factors such as improved thermal insulation upgrades in renovated buildings, reducing extreme peak demands on hot days. Furthermore, significant differences can be observed between residential and office buildings. Offices maintain relatively stable cooling energy demand intensities, while residential buildings experience substantial growth, especially in the 2050-H scenario. Due to the expected increase in residential buildings, cooling energy demand from homes increases by an average of 13% by 2030 and 56% between 2020 to 2050.

Interestingly, these figures align closely with projections from the Netherlands Organization for Applied Scientific Research (TNO), which anticipate a 13.5% increase of residential cooling demand by 2030 and a 36.5% increase by 2050 (Rovers et al., 2021). It is worth noting, however, that the TNO projections pertain to two specific building types and may not represent the entire building stock. Conversely, the office building stock is likely to shrink, resulting in an average 13% reduction in total cooling energy demand during the same period. These findings emphasize the need for future policies to prioritize the up-and-coming residential cooling demand.

5.3.2 Electricity Use

Electricity use results suggest that the growth in market penetration rates of cooling equipment, especially in residential buildings, will play a pivotal role in narrowing the cooling gap. This gap is projected to decrease substantially, from 77% in the status quo (2020) to as low as 17% in the 2050-H scenario.

It is essential to highlight that electricity consumption is expected to rise in most scenarios, reflecting the increased demand for cooling. By 2030, electricity usage from cooling equipment is projected to increase by 28%, and this trend intensifies in the 2050-H scenario, representing a business-as-usual scenario with minimal policy intervention, where it grows four-fold to 419 GWh compared to the current 101 GWh.

In contrast, the 2050-L scenario stands out with a remarkable 34% reduction in electricity consumption. Notably, this reduction occurs even as the cooling demand fulfillment rate jumps from 23% to 62%, owing to significant enhancements in the average energy efficiency of cooling equipment and a slight decrease in cooling energy demand. This underlines the potential advantages of implementing stringent policies aimed at reducing cooling demand and enhancing the energy efficiency of cooling equipment.

The disparity between residential and office buildings in electricity consumption intensity is striking. Currently, residential buildings consume just a fraction of the electricity used by offices, with a range of 1.5 to 21 kWh/m^2. However, residential electricity consumption intensity is projected to significantly increase in all scenarios, reaching up to 12.5 kWh/m^2 by 2050, driven by a surge in cooling equipment usage. In contrast, office buildings maintain a relatively stable intensity, ranging from 15 to 25 kWh/m^2 by 2050, due to their already high cooling equipment MPR.

Projected building stock changes indicate a significant increase in residential cooling electricity use across all scenarios. By 2030, it is expected to double to 71 GWh and surge eleven-fold to 346 GWh in the 2050-H scenario. In stark contrast, the best-case scenario, 2050-L, shows only a slight increase in residential cooling electricity use, reaching 35 GWh. This figure is 90% lower than the business-as-usual case in 2050-H, underscoring the profound impact of stringent policies. Meanwhile, total office electricity use declines in all scenarios except 2050-H, never reaching more than 73 GWh. These projections underscore the importance of policies over the next 25 years that prevent extreme growth in electricity use for residential cooling and reduce the current cooling electricity consumption in offices.

Table 50: Residential cooling electricity use, and the share of total residential electricity use and total residential energy use, across scenarios, using the same energy transition models as in section 3.3.3.2 (Hammingh et al., 2021; Ouden et al., 2020; Zaccagnini et al., 2023).

Scenario	Cooling electricity use (GWh)	Share of total electricity use	Share of total energy use
SQ (2020)	32	6%	1%
2030	71	14%	3%
2050-L	35	5%	2%
2050-M	97	15%	6%
2050-H	346	66%	14%

Currently, residential cooling uses about 5.5% of total electricity demand and 1% of overall energy demand in The Hague residences (RVO, 2020). However, Table 50 shows that by 2030, these figures could rise to 14% and 3% respectively. By 2050, the highest scenario (2050-H) anticipates cooling to consume 66% of residential electricity and 14% of total residential energy. These figures, derived from section 3.3.3.2's energy models, underscore the escalating role of space cooling in The Hague, stressing the need for proactive energy and environmental strategies.

5.3.3 Material Use

Rising cooling demand and market penetration significantly impact material needs. All scenarios predict an increase in material demand for cooling equipment, with the 2050-H scenario tripling from current levels. This trend brings environmental concerns, especially around resource depletion.

The residential sector is set to see a significant rise in material demand intensity, especially when compared to the office sector. This surge is largely attributed to the expected increase in the MPR of cooling equipment in homes. By 2030, the yearly per capita WEEE generation from cooling devices is projected to rise from 0.43 kg to 0.6 kg, reaching 1.1–1.2 kg by 2050. This means that by 2050, cooling equipment could account for 4% of total WEEE generation, up from 1% today, assuming WEEE generation remains stable (Huisman et al., 2017; van Straalen et al., 2016). Additionally, the potential for urban mining of CRMs is likely to increase due to a larger cooling equipment stock and a possible rise in CRM concentration in cooling equipment, stemming from a more intricate supply chain and end-product.

5.3.4 Climate Change Impacts

The study examines climate change impacts resulting from various factors, including electricity use, refrigerant leaks, and the production and end-of-life phases of cooling equipment. The findings suggest a general reduction in climate change impacts in most cases. The optimistic 2050-L scenario projects a 90% emission reduction, driven by grid decarbonization and improved refrigerant practices. In contrast, the 2050-H scenario predicts a 71% increase, attributed to stalled green initiatives and an exponential rise in cooling demands.

Notably, the GHG emissions of space cooling vary between residential and office buildings. While the total GHG emissions from offices are expected to drop with 58%–96% by 2050, residential buildings are projected to experience lower reductions, and even a four-fold increase in the 2050-H scenario. This trend underscores the importance of targeted interventions for residential buildings. The overarching narrative suggests that while advancements in renewable energy and cooling technologies can significantly mitigate GHG emissions, any stagnation in these areas can lead to detrimental outcomes, emphasizing the critical role of policy and technological innovation in shaping future climate impacts.

In assessing GHG emission contributors, electricity consistently stands out as the primary source, except for the 2050-L scenario. Its central role highlights the potential of grid decarbonization as a strategy to offset the anticipated increase in cooling equipment MPRs. In the Status Quo scenario, electricity accounts for 88% of emissions. This share reduces in subsequent scenarios due to advancements in grid efficiency and an expanding cooling equipment inventory. By 2050-L, emissions from equipment production and end-of-life phases become dominant, holding a 59% share. This shift emphasizes the importance of policies addressing the life-cycle impacts of cooling equipment. Nonetheless, electricity's role remains significant, contributing 41% to 80% of emissions in 2050 scenarios.

Table 51 shows the projected GHG emissions from RO cooling compared to the 2020 estimate of The Hague's total carbon footprint, and the targeted 49% and 95% reductions from 1990 levels as described in the Klimaatakkoord (Klimaatakkoord, 2019; The Hague Municipality, 2021b).

Table 51: Projected GHG emissions from RO cooling compared to the total aspired carbon footprint of The Hague, across scenarios.

Scenario	GHG emissions from RO cooling (kt CO_2-eq)	The Hague's targeted carbon footprint (kt CO_2-eq)	% of RO cooling in targeted footprint
SQ (2020)	48.8	1,590	3.1%
2030	25.1	1,274	2.0%
2050 L	4.7	125	3.8%
2050 M	9.3	125	7.5%
2050 H	83.6	125	67%

In 2020, RO cooling emissions in The Hague accounted for 48.8 kt CO_2eq, or 3.1% of the city's total carbon footprint of 1,590 kt CO2-eq (The Hague Municipality, 2021b). By 2030, projections show a promising 49% reduction to 25.1 kt CO_2eq, aligning with the Paris Agreement and Klimaatakkoord's goals. The 2050-L scenario further reduces emissions to 4.7 kt CO_2eq, again aligning well with the net zero by 2050 goals. However, the 2050-H scenario predicts a concerning rise to 83.6 kt CO_2eq, or 67% of The Hague's permissible carbon footprint under the Klimaatakkoord. These figures highlight the challenges posed by space cooling and the need for strategic interventions to ensure The Hague's sustainable future.

5.4 Policy Recommendations

The following recommendations can be given to minimize the projected environmental impacts of the future cooling demand of residential and office buildings in The Hague.

5.4.1 Reduce Cooling Demand Through Building-Level Measures

Incentivize effective renovations in two ways. Incentivize **building owners to renovate and retrofit** residential buildings through **financial subsidies and tax breaks**, with a focus on older low-rise residential buildings which currently have the highest cooling demand. Introduce more **stringent energy regulation for renovations**. Currently, new buildings are required to adhere to stringent energy performance rules. However, most of the activity in the building sector takes place in the form of renovations, which do not have a minimum energy performance standard. This is especially pertinent for older (low-rise) residential buildings, which have the lowest energy labels.

Support, monitor, and enforce **energy label standards** for buildings. A 30% of offices currently fail to adhere to the energy label requirement of C or above, the majority of

which are mid-sized office. Providing support through renovation guidelines (as mentioned above) and financial incentives may improve compliance. In addition, **monitoring of energy label standard adherence** and subsequent enforcement through penalties may be needed to ensure improvements in building energy efficiencies to lower cooling demand. This will be particularly important for rented residential buildings, which must exceed energy label E by 2030 (NOS, 2022).

5.4.2 Reduce Cooling Demand Through Changes in the Urban Environment

The cooling demand can further be reduced by changes in the urban environment, specifically addressing the UHI effect, which is a major contributor to current and future cooling demand in The Hague (refer to section 4.3.1.4).

Cooling demand can further be reduced by **intensifying the use of urban design strategies** to mitigate the UHI effect, a major contributor to The Hague's cooling demand (see section 4.3.1.4). These design strategies include urban greening (green roofs, parks, gardens, tree-lined streets), water features, low-albedo building materials, building orientation, and shading optimization (details in section 2.2.2). The UHI effect is particularly severe in poor, densely populated neighborhoods in The Hague (see section 4.1.1.5), necessitating focused mitigation efforts in these areas. Policies must consider **financial accessibility for cooling equipment and thermal mitigation strategies**. For instance, The Hague municipality offers subsidies of up to 50% for green roofs (The Hague Municipality, 2023). However, these subsidies may not reach the neighborhoods that need them most. Implementing a sliding scale approach or similar measures can promote environmental justice and alleviate heat stress across all areas.

Furthermore, while research on the UHI effect in the Netherlands exists, it relies on Europe-wide assumptions rather than empirical microclimate measurements (RIVM, Atlas Natuurlijk Kapitaal, 2017). To better understand the UHI effect and monitor policy effectiveness, **further (empirical) research on the spatial and temporal variations of the UHI effect in The Hague** is essential.

5.4.3 Reduce Cooling Demand Through Thermal Comfort Standards

Adjusting thermal comfort expectations is more challenging in terms of lowering them (i.e., broadening and shifting the comfort ranges upward in summer) than raising them (de Dear et al., 2020). However, there is a reciprocal relationship between policy and the

societal acceptance of thermal comfort ranges. Shifting policy to endorse higher recommended temperature ranges can lead to gradual adaptation within certain limits, resulting in their eventual societal acceptance. It is recommended to **incorporate a higher effective cooling temperature** (the upper limit of indoor thermal comfort) in office policies and residential recommendations. For instance, adopting the Spanish government's requirement of 27 °C instead of the earlier 25 °C (Jones, 2022), could reduce material impacts by 15% and cut electricity and GHG emissions by 25%, as by section 4.3.1.2. Conversely, Figure 92 illustrates that the absence of policies on recommended effective cooling temperatures, exemplified by a shift from 25 °C to a self-reported average preference of 20 °C from the TNO study, leads to a doubling in electricity demand and GHG emissions (Rovers et al., 2021).

Furthermore, it is recommended **to implement adaptive temperature strategies** in offices and promote them in residential buildings. This approach can lead to substantial energy savings, up to 50%, compared to fixed cooling temperature settings (Albatayneh et al., 2019; Yang et al., 2014). Furthermore, studies on machine learning-based adaptive thermal comfort systems show that energy reduction can coexist with improved thermal comfort (Gao et al., 2020).

In addition to advocating for adaptive cooling temperature strategies, it is important to **promote thermal adaptation behavior** more broadly to minimize the reliance on active cooling equipment. Thermal adaptation can be achieved through various means (Liu et al., 2014). These include:

- **Personalized regulation devices**, like fans, represent an effective solution, especially in offices (Rupp et al., 2015).
- **Clothing adjustment** can be an effective means of thermal adaptation.
- **Consuming cold beverages** can help individuals manage their thermal comfort.
- **Adjusting activity levels** to match environmental conditions can contribute to thermal adaptation.
- The **use of shading devices** such as curtains or blinds can help control indoor temperatures.

It is worth noting that some of these adaptation strategies have already been integrated into The Hague's heat plan (The Hague Municipality, 2021a).

The sensitivity analysis on the cooling demand cap percentile in section 4.3.1.1. provides insights into thermal discomfort tolerance, a factor that can be improved through alternative cooling strategies and the promotion of thermal adaptation behavior. It is vital to allow for some thermal discomfort to reduce environmental impacts. A shift from covering 100% to 99% of the cooling demand hours decreases material demand by at least 10%. Secondly, the optimal cooling demand cap percentile for minimal environmental impact is around 97%, avoiding full-blast cooling during the hottest 3% of the year while maintaining reasonable thermal comfort for most of the year. Policy should **emphasize some expected thermal discomfort**, encourage active cooling equipment for baseline comfort, and promote alternative strategies on the hottest days.

Please note that the choice of the cooling demand cap percentile minimally affects cooling energy demand but significantly reduces peak power demand and required installation size, as seen in Figure 91. In the Status Quo scenario, electricity use dominates climate impact (88% of total GHG emissions), making the choice of cooling demand cap percentile less critical. However, in future scenarios with a lower carbon-intensive grid, the proportion of GHG emissions linked to cooling equipment size increases, heightening the importance of the cooling demand cap percentile, i.e. the thermal discomfort tolerance.

5.4.4 Cooling Gap Reduction

In The Hague, 77% of cooling demand goes unmet, leading to heat stress and discomfort for residents. Low-income neighborhoods in the city center, shown in Figure 59, face heightened UHI effects and heat stress, but financial constraints prevent their residents from acquiring adequate cooling equipment. As, discussed in section 2.4.2.2, even when they invest in cooling equipment, it is often less efficient, contributing to greater environmental impact. To combat cooling inequality and enhance thermal comfort, particularly for vulnerable households, two policy measures are proposed:

Implementing a **carbon or circular economy tax** at the national or international level that factors in the externalities associated with low-efficiency and cheaper cooling equipment. While some forms of carbon taxes exist at the EU level (EU ETS and more

recently CBAM),[52] they do not comprehensively account for environmental impacts related to complex goods like cooling equipment. A well-designed tax should fully price in these externalities, making high-impact cooling technologies more expensive and generating revenue for public funds, which can be used for the next recommended policy.

Introduce **sliding-scale subsidies for low-impact cooling solutions**. Currently, there are no subsidies for cooling equipment,[53] and existing green subsidies predominantly benefit wealthy households due to eligibility criteria demanding substantial initial capital and property ownership. Sliding-scale subsidies would help lower-income households overcome the initial cost barrier, encouraging the adoption of energy-efficient cooling equipment. This approach promotes environmental responsibility more equitably than existing subsidies and would make low-impact cooling solutions more accessible in areas with the highest cooling demand, ultimately reducing the cooling gap and addressing climate injustice.

[52] The Emissions Trading System (ETS) is a market-based approach designed to reduce greenhouse gas emissions by setting a cap on total emissions and allowing companies to trade emission allowances, encouraging more efficient emission reductions (Dechezleprêtre et al., 2023). However, most cooling equipment is manufactured outside the EU, which means emissions produced during production are not subject to ETS pricing. The European Union has recently introduced the Carbon Border Adjustment Mechanism (CBAM), a policy that imposes carbon tariffs on select carbon-intensive imports (Establishing a Carbon Border Adjustment Mechanism, 2023). CBAM aims to curb the relocation of companies to countries with less stringent carbon regulations, known as carbon leakage. CBAM, an important part of the European Green Deal, will come into effect in 2026, with reporting starting in 2023. While CBAM currently targets six sectors, including aluminum, cement, iron and steel, electricity, hydrogen, and fertilizers, it does not yet cover many products, including complex goods like air conditioners, with uncertainty about their future inclusion in the CBAM framework. Moreover, use-phase emissions resulting from poor energy efficiency are not addressed by either EU ETS or CBAM and require separate policy measures.

[53] While there are subsidies in place for heat pumps and building insulation, these are focused on reducing-heating-related environmental impacts. There are no subsidies specifically focused on reducing the impacts of space cooling.

5.4.5 Reduce Cooling-related Energy Use in Buildings

The sensitivity analysis in section 4.3.1.5 emphasizes the importance of energy efficiency in reducing cooling-related energy consumption and GHG emissions. Energy efficiency improvements alone cause a 37% drop in GHG emissions from RO cooling in the 2050-L scenario. This highlights the need for policies **promoting energy-efficient cooling systems**, which offer both energy savings and a lower climate change impact.

Strengthening minimum energy performance standards (MEPSs) is a highly effective strategy for improving energy efficiency of cooling equipment (UNEP & IEA, 2020). By enforcing stricter MEPS, manufacturers are compelled to improve baseline energy efficiency and innovate to achieve higher efficiency ceilings. Financial incentives for high-efficiency cooling equipment, such as rebates and tax deductions, can further encourage the adoption of technologies with high seasonal energy efficiency ratios (SEERs). As shown in Figure 9, Europe's cooling equipment efficiency is half of the top-tier standards. By elevating the average SEER from 5 to the current best of 11, energy consumption could be reduced by 53% and GHG emissions by 44%.

Promoting reversible heat pumps over portable and split-type ACs is recommended. Section 4.3.1.7 indicates that heat pumps surpass these ACs in energy efficiency. While they come with higher material demand, subsidies for heat pumps are still advisable, especially given their dual functionality for both cooling and heating. Given the higher costs of heat pumps compared to traditional ACs, a sliding scale subsidy for heat pumps is recommended to ensure equitable access.

Lastly, it is essential to highlight the advantages of passive cooling. It not only delays the need for active systems but also, when active cooling is necessary, reduces their energy consumption. Therefore, **promoting passive cooling technologies** serves both environmental and economic interests.

5.4.6 Minimize the Material Impacts of Cooling Equipment

To reduce the material impacts of residential and office cooling, it is recommended that a **circular economy approach in cooling equipment production, use, and disposal** is promoted.

Minimizing the material footprint in the production phase can be achieved by enhancing the material-to-power ratio, defined as kg of product per kW of power, through the

establishment of robust **material efficiency standards**. It is also recommended to **limit the use of critical raw materials** (CRMs) and other materials that are scarce or have significant environmental implications, where technologically possible. The **integration of R-strategies in the production phase**, such as incorporating recycled materials and refurbished components, can further lower the material footprint. These strategies often align with reduced GHG emissions compared to traditional production methods. Additionally, adopting **low-carbon production techniques**, like utilizing low-carbon steel and renewable energy sources, can further minimize the climate change impact of cooling equipment.

The focus in the use phase should be on **extending the equipment's lifespan**. Support for reuse, repair, and refurbishment initiatives is essential, for example through community-led activities like repair cafes. Refurbishment, and remanufacturing programs by original equipment manufacturers (OEMs) are also important. Finally, sharing of information on DIY maintenance and repair can further enhance equipment longevity.

In the disposal phase, the focus is on waste impact reduction. Proper **waste electrical and electronic equipment (WEEE) management** is essential to prevent avoidable refrigerant leaks and address e-waste challenges. This ensures cooling devices and their CRMs maintain value in the circular economy. These strategies might also help in reducing greenhouse gas emissions during disposal.

5.4.7 Reduce Greenhouse Gas Emissions from Cooling

Beyond the GHG emission reductions achieved through more circular production and end-of-life practices, there are additional avenues to further lower the carbon footprint of residential and office cooling:

Decarbonizing the electricity grid can drastically cut GHG emissions from space cooling. Section 4.3.1.6 shows a potential 80% reduction with a move to carbon neutral electricity. While The Hague lacks direct control over carbon efficiency, it can advocate for low-carbon electricity in homes and offices, aiding in citywide emission reductions.

Promotion of low global warming potential (GWP) refrigerants, such as CO_2, propane, water, and R-1234yf can further curtail GHG emissions from space cooling. However, it is important to consider their broader environmental impacts, such as ozone depletion potential and ecotoxicity, and how they might affect energy efficiency.

Strengthening regulations to limit refrigerant leakages, aiming for a maximum leakage rate of 1% of the charge annually, is essential. Regular maintenance to prevent such leaks should also be emphasized.

5.4.8 Increase Public Awareness of the Environmental Impacts of Cooling

To ensure residents and office occupants in The Hague actively engage in the recommended improvements–like buying energy-efficient cooling systems, setting optimal cooling temperatures, and adopting renewable energy–it is necessary to cultivate a culture of pro-environmental behavior regarding space cooling. This can be done in multiple ways.

Social norm interventions leverage societal expectations and peer behaviors to influence individual actions, and have been shown to be effective in promoting pro-environmental behavior. (Farrow et al., 2017; Spandagos et al., 2021). Furthermore, promoting **environmental education**, i.e. teaching people about the environmental consequences of their actions, can guide them towards greener choices (Nguyen et al., 2017; Varela-Candamio et al., 2018). Finally, creating **greener built environments** can boost environmental awareness and encourage sustainable behavior (Xie et al., 2020). This strategy aligns well with the policy recommendations on mitigating the UHI effect presented in section 5.4.2.

However, while environmental awareness is important, factors like cost and ease of use often take precedence for most individuals (Gadenne et al., 2011; Osunmuyiwa et al., 2020). Therefore, a **holistic approach that combines environmental education, community-driven social norm interventions, and economic incentives** is the most likely effectively steer people towards eco-friendly cooling equipment choices and practices.

5.4.9 Address Future Space Cooling Demand in Planning and Policymaking

The increasing need for space cooling and its potential environmental impacts highlights a policy gap, as current emphasis in local and national policy is on space heating. To build climate-resilient cities, it is vital to **incorporate space cooling and its environmental impacts in climate and energy policy**. Policymakers should act now, integrating the

suggested recommendations before market trends set cooling preferences, avoiding further environmental issues.

A cohesive strategy should merge space cooling with sustainable heating measures. Reversible heat pumps, which efficiently cater to both heating and cooling needs, are a prime example. As shown in Table 34, current heating plans for The Hague suggest that 8% of homes should rely on heat pumps, 49% on heat districts, with the remaining 43% yet to be decided. This research recommends reversible heat pumps for the 8% and urges **consideration of the dual benefits of reversible heat pumps** for the remaining 43%. Homes on heat districts will need separate cooling solutions.

5.5 Limitations of the Research and Recommendations for Further Research

This section presents a discussion of the methodological limitations of the research scope, the data collection, and modeling choices, as well as recommendations for further research.

5.5.1 Research Scope

5.5.1.1 Temporal Scope

The temporal scope of the research involves a relatively short and recent reference period spanning five years (2018–2022) in the status quo scenario. This choice was made to manage algorithmic computing complexity and model runtime. However, aligning the reference period with the KNMI weather projections, covering the years 1981 to 2010, is recommended to enhance the robustness of the status quo assessment and facilitate integration with KNMI climate scenarios (Attema et al., 2014).

For future scenarios, the current analysis is limited to two years, specifically 2030 and 2050, due to data availability constraints for other years. To provide more specific insights into the environmental impacts of cooling, it is advisable to extend the analysis to include additional years, such as 2040, and expand the scenarios until 2085 to align with the KNMI climate projections and gain more insights in the long-term evolution of space cooling and its environmental impacts.

5.5.1.2 Spatial Scope

The spatial scope of the research is centered on The Hague as a case study, limiting insights into variations between urbanization levels and potential cooling demand hot spots in the Netherlands. To overcome the current computational limitations, which would mean a model runtime of several hours for an analysis on the scale of the Netherlands, optimization and expansion of the model are required. This would enable its application to any region in the Netherlands, based on any subset of the BAG database.

5.5.1.3 Technological Scope

Concerning the technological scope related to buildings, the current analysis includes the estimation of cooling demand and environmental impacts for residential and office buildings, given their majority share in the building stock floor space. Nevertheless, significant cooling demands may exist for other building types, such as utility buildings like supermarkets and industrial sites. Therefore, it is suggested that the research be expanded to encompass impacts from commercial, public, and industrial buildings. This expansion will provide a more comprehensive understanding of their cooling demand and their comparison to residential and office buildings.

Additionally, cooling demand and environmental impacts are currently calculated at the building level, neglecting variations within buildings. It is likely that higher floors have higher cooling demands than average, due to the fact thot hot air rises to the top of buildings through convection. Even if overall building conditions do not necessitate active cooling, there could be demand from the top floors. Therefore, it is advisable to enhance the model's granularity by extending it to a floor-level analysis to gain a better understanding of cooling demand and its environmental impacts.

As for cooling technologies, only the most prevalent active cooling technologies were included (heat pumps, chillers, split ACs and portable ACs) in the current model due to data limitations, excluding technologies like radiant cooling or district cooling. Further research is recommended to gain insights into the trade-offs between traditional active cooling methods and emerging alternatives.

Passive cooling technologies, such as phase-change materials and night ventilation, were also omitted from the analysis due to the necessity for dynamic modeling, which involves accounting for the time-lag effects of thermal mass as it absorbs and releases heat over several hours. These dynamic effects are not accommodated by the static hourly energy

balance-based thermodynamic model employed in this research. The omission of these dynamic aspects might also result in an overestimation of cooling demand, particularly in heavy buildings (van Bueren et al., 2012). To address this overestimation and enable the inclusion of passive cooling technologies, which could yield valuable insights into the environmental trade-offs between active and passive cooling methods, it is recommended that dynamic modeling of heat flows, including heat retention within the building, be undertaken. Dynamic modeling can be accomplished using software such as *EnergyPlus* (National Renewable Energy Laboratory, 2023).

Finally, several niche-level alternative cooling technologies exist, including adsorption and absorption cooling, magnetic cooling, and transcritical CO_2 cooling (Braungardt et al., 2018; Brown & Domanski, 2014). While these technologies were not explored in this study due to their limited use in residential and office cooling and the scarcity of data on their application and environmental impacts, a future investigation into their potential applications and environmental implications could be of significant value.

5.5.1.4 Impact Scope

The analysis in this research solely quantifies GHG emissions, electricity consumption, and material demand stemming from space cooling needs, with the exclusion of factors such as ozone depletion potential (ODP) and ecotoxicity. This omission is attributed to the limited availability of LCA data pertaining to cooling technologies. To enhance the comprehensiveness of the assessment and gain a more detailed understanding of the evolving environmental consequences of space cooling, as well as to identify precise trade-offs among cooling technologies and mitigation approaches, it is recommended that the assessment be extended with additional environmental impact categories. This could be realized by conducting an LCA on the predominant and most likely future cooling technologies, including passive cooling solutions like phase-change materials. This can also address two other limitations in this research:

The current model uses life cycle inventories (LCIs) of "ventilation system" processes from ecoinvent as a proxy for the production and end-of-life impacts for all cooling equipment due to the scarcity of specific data for these devices. This neglects material differences between different cooling technologies and hinders the ability to gain insights in the differences in their environmental performance and potential trade-offs between technologies. Additionally, the LCI data used in the model is outdated, dating back to 2003, and conducting an LCA would provide a more up-to-date assessment of modern

cooling technologies, which are suspected to have a different material make up (e.g., they may contain more CRMs due to a higher concentration of integrated circuits). This may involve collaboration with manufacturers or industry associations, teardown analyses of cooling devices, or the utilization of machine learning techniques to predict bill of materials from publicly available data and product specifications.

Additionally, the current model assumes constant production and end-of-life impacts for cooling technologies across scenarios. However, it is likely that these impacts will change, such as the anticipated decarbonization of energy sources in the production phase resulting in lower GHG emissions. To address this limitation, conducting ex-ante LCAs on existing and emerging cooling technologies is suggested. Exploring methodologies such as technology forecasting and scenario analysis could prove beneficial in developing dynamic and flexible models of cooling device evolution.

5.5.2 Data Collection

The climate projections for future scenarios are reliant upon the latest available climate projections provided by KNMI, last updated in 2014, thus rendering them somewhat outdated. To enhance the accuracy of projected cooling demand and its associated environmental impacts, it is suggested that the model be updated using the forthcoming Climate scenarios from KNMI, slated for release in October 2023, offering more up-to-date climate projections.

Secondly, the currently used energy label data is limited in complexity, using a ranking system between G and A+++++. Moreover, a significant portion of buildings lack this data, hindering the estimation of their thermal insulation properties. However, the 2023 introduction of the Dutch technical agreement (NTA) 8800 standard has improved energy label calculations, including heat and cooling demand profiles (NEN, 2023). With stricter regulations, it is expected that more buildings will have energy labels in the future. Integrating this updated data into the model can enhance the understanding of cooling impacts and expand its applicability beyond The Hague.

Another potential source of uncertainty within the model stems from certain cooling technology parameters, including mass per unit, refrigerant charge, and cooling installation power, which are currently based on singular proxy products for each cooling technology category. This singular representation may introduce significant variability in the related results, such as material demand and associated environmental impacts (ADP

and CSI), as well as refrigerant related GHG emissions. Consequently, it is strongly recommended to establish a comprehensive library of cooling equipment, ideally encompassing a minimum of five models per category. This approach will enable a more accurate representation of the diverse equipment available in the market, thereby enhancing the reliability of the model's outputs.

The determination of the MPR for cooling technologies, along with the breakdown of MPR among different cooling technologies, known as the cooling technology mix, relied solely on a singular source: the 2021 TNO survey source (Rovers et al., 2021). This singular data source presents a substantial source of uncertainty within the model, as the total MPR and specific cooling technology mix ultimately determines the environmental impacts of the cooling demand. It is therefore recommended to conduct in-depth market and econometric research specific to cooling equipment within the Netherlands. Optionally, surveys could be employed to gather relevant data. Additionally, it is recommended to incorporate neighborhood-specific projections for future heating solutions published by The Hague municipality (de Boer et al., 2022). considering that buildings equipped with heat pumps will likely employ heat pumps for cooling as well, while those in regions with heat districts may require the installation of separate cooling technologies.

Several input parameters, assumed to remain constant throughout this research, might exhibit significant variability over time. Notables are the makeup of the building stock and the carbon intensity of the grid. Given that the building stock forms the bedrock of the entire model, and the overall GHG emissions are significantly dependent on grid carbon intensity, this modeling choice can have a substantial influence on the calculated environmental impacts. This influence becomes more pronounced when extending the timespan of the reference scenario – which currently spans 5 years – to 10 or even 30 years, aligning with the KNMI climate reference periods. To enhance the model's precision in this regard, it is recommended to integrate annual building stock data from the BAG and yearly carbon intensity data sourced from Statistics Netherlands (CBS) (CBS, 2023d).

Furthermore, upstream (scope 3) emissions associated with electricity production have been assumed to remain static across future scenarios. These emissions are expected to decrease as the global electricity production supply chain decarbonizes. Addressing this complexity requires the implementation of more intricate system modeling techniques. This can be achieved through the use of prospective LCA models in combination with integrated assessment model (IAM) frameworks such as IMAGE (Stehfest et al., 2014).

Tools like Premise or ECOPT can potentially be used to streamline this process (Hung et al., 2022; Sacchi et al., 2022).

5.5.3 Modeling Choices

The weather series used in future scenarios of the current model are generated via the addition of static temperature and solar radiation enhancements to the reference (2018–2022) weather series. Seasonal temperature and solar radiation increases are considered, but changes in weather patterns, such as increased heatwaves, are not accounted for. Despite the alignment between the projected Cooling Degree Days (CDD) increase by KNMI and the temperature series derived from the seasonal temperature adjustments in the current model, further investigation is required to explore the possibility of modeling more realistic future weather series that incorporate changes attributed to climate change.

Within the model, the daytime UHI effect – equivalent to that of a hot summer's day at 8.3 °C – is assumed to be constant throughout the year. As mentioned in section 4.3.1.4, this assumption holds substantial influence on the model's outcomes, as it may overstate cooling demand on moderately warm days. To enhance accuracy, it is recommended to employ more variable data, both spatially and temporally.

Spatially, available data, such as the UHI map from the National Institute for Public Health and Environment (Atlas Natuurlijk Kapitaal, 2017), can be used for a more granular consideration of the UHI effect. Temporally, the adoption of a more advanced UHI model, assessing UHI effects on a seasonal or even hourly basis, is advisable. Two potentially useful models for this purpose include the *UrbClim* model (de Ridder et al., 2015), also employed in the current RIVM UHI maps, and the highly granular Physical Equivalent Temperature (PET) urban heat model, designed with future scenario development in mind (Koopmans et al., 2020). Implementing these models may increase the robustness of future UHI effect projections. Finally, the current model does not include the UHI effect on subsurface temperatures due to the unavailability of local data. Future research could explore the inclusion of this factor, as an advanced GIS-based model for the Subsurface UHI effect has recently been established (Schweighofer et al., 2021).

Another critical input parameter is the effective cooling temperature. The current model assumes a constant value throughout the year across all building types. A more accurate representation might involve specifying adjustments of the effective cooling temperature

based on building types (e.g., offices might necessitate lower indoor temperatures than residential buildings). Moreover, it could be beneficial to model the effective cooling temperature dynamically by incorporating adaptive thermal comfort ranges into the model, for example using the *thermofeel* Python library (Brimicombe et al., 2022). This approach, founded on research into weather-dependent comfort ratings, can enhance model realism.

Furthermore, each building is modeled as an isolated entity in the current research, not accounting for the fact that most buildings in The Hague are interconnected or closely situated. This oversight impacts a building's thermal balance through the omission of transmission heat flows between buildings and shading effects from neighboring structures. It is recommended that the magnitude of such effects be investigated, especially when incorporating the dynamic time-lag effects of thermal mass are to be included in the model.

Moreover, in this analysis, the energy efficiency of cooling equipment was assumed to be constant throughout the year. However, it should be noted that in real-world conditions, the efficiency of cooling equipment often diminishes at higher temperatures. This factor was not considered in the model, potentially leading to an underestimation of the total electricity demand and related environmental impacts.

Additionally, a single refrigerant is currently assumed for the entire cooling equipment stock. However, it may be advantageous to incorporate refrigerant mixes for each device type, for example the ones projected by (Mota-Babiloni & Makhnatch, 2021). Additionally, the model does not consider how refrigerant choice might affect the energy efficiency of cooling equipment. This becomes particularly important when assessing natural refrigerants, which could potentially counteract their positive environmental attributes (e.g., low GWP and ODP) with adverse impacts on energy efficiency. Exploring these aspects is recommended for further research.

Lastly, it is important to acknowledge the absence of a formal uncertainty analysis in this complex model. The intricacies of the model and extensive amount of input data, including weather data and other time series (each containing 43,800 hourly values across 5 years) and over 150 other parameters, make quantifying the uncertainty in the cooling demand and environmental results challenging. However, the sensitivity analyses and four future scenarios provide insights into the potential variability of results across varying

conditions. Conducting a comprehensive uncertainty analysis in future research is recommended to enhance model reliability.

5.5.4 Additional Recommendations for Further Research

Expanding the current model and conducting a similar analysis (evaluating the cooling energy demand and its environmental impacts) of combined heating and cooling solutions, such as reversible heat pumps, aquifer thermal energy storage (ATES), and the integration of data centers, supermarkets, and industrial facilities into local heating and cooling grids, should be considered. The objective would be to identify optimal climate control solutions that balance heating and cooling demands while minimizing environmental impacts. This endeavor could integrate neighborhood-specific projections for future heating solutions, as published by The Hague municipality (de Boer et al., 2022). Furthermore, it may be beneficial to expand this research with cost-benefit and stakeholder analyses to assess the relative impacts of combined heating and cooling strategies compared to separate measures for meeting cooling and heating needs.

Furthermore, the current model treats the local environment as an infinite heat source and lacks the capability to predict the local thermodynamic impacts resulting from projected rise of cooling equipment usage. To address this, it is recommended that a thermodynamic model that accounts for the interactions between buildings and the local external environment is developed. Such a model can shed light on the local feedback loop between heat stress and cooling demand, elucidated in Figure 3. This feedback loop entails that a hot external environment prompts the activation of cooling equipment, which subsequently transfers excess heat into the local environment, further elevating local outdoor temperatures and increasing the demand for cooling. Properly modeling the local environment and its interactions with buildings would enable the incorporation of this feedback loop and quantitative measurement of its strength and impacts.

For scenario modeling, the potential for double counting effects exists because the interactions between drivers have not been fully mapped. Significant rebound effects or other secondary feedback loops could impact the final environmental outcomes of cooling drivers. Therefore, it is recommended to conduct a more comprehensive exploration of the system dynamics involved in space cooling development.

Finally, to enhance replicability and communicability, it is recommended to manage model input data and results more effectively using for example SEED, an open-source

software designed for managing data on the energy performance of large groups of buildings (Long et al., 2023). This approach can also potentially allow the transformation of the model into a web application for wider accessibility and usability.

6 Conclusions

Despite its historically temperate climate, The Hague is subject to rising temperatures and increasingly frequent heatwaves, escalating the demand for space cooling. The demand is expected to grow significantly in the coming decades, yet there is a noticeable gap in research and preparations to address this demand in an environmentally and socially sustainable way. While studies have been conducted on the environmental impacts of residential heating in the Netherlands, similar studies for cooling are lacking. Furthermore, while The Hague municipality has implemented policy measures towards a sustainable heating transition, sustainable cooling policies are absent.

This study addressed these gaps by projecting cooling demand and the resulting energy use, material demand, and greenhouse gas emissions in The Hague using a bottom-up building-level approach. Using BAG geospatial data along with recent weather data and future climate scenarios from KNMI, the study calculated indoor cooling demand profiles for each residential and office building through a static thermodynamic model developed in Python. These profiles, combined with the estimated cooling technology mix in each building, were used to determine the related energy consumption, material demand, and GHG emissions. It is important to note, that the study focused on six active cooling technologies, excluding passive cooling methods due to the complexities involved in dynamic modeling. This omission limits the ability to evaluate the benefits of passive cooling solutions compared to conventional AC systems. This limitation could also lead to an overestimation of cooling needs, especially in thermally massive buildings, as the model does not account of the dynamic time-lag effects of heat retention in such buildings.

Projections were modeled for the status quo (2020), 2030, and three scenarios in 2050 representing low, medium, and high environmental impacts, based on the level of interventions taken. These projections, combined with the literature review in Chapter 2, informed the answers to the following research questions:

RQ 1: What is the current cooling demand in residential and office buildings in The Hague?

In The Hague, the current cooling demand in residential and office buildings peaks at about 1,431 MW, reducing to 783 MW with a 2% thermal discomfort tolerance. Annually, the city's cooling energy demand is 1,118 GWh, significantly exceeding the EU Horizon Hotmaps estimate of 400 GWh, largely due to the consideration of UHI effect in this study.

Office buildings have a cooling demand of 115 kWh/m², triple that of residential buildings at 34 kWh/m². While heating, at an average of 86 kWh/m², is a more pressing issue in residential buildings, the cooling energy demand is still over double the earlier estimate of 16 kWh/m² for Dutch residences. This again highlights the importance of considering the UHI effect into cooling demand assessments.

RQ 2: What are the environmental impacts of the current cooling demand in The Hague?

The environmental impacts of The Hague's cooling demand are considerable. While the city's annual cooling energy demand is 1,118 GWh, only 23% is met by existing equipment, creating a 'cooling gap' and thermal discomfort, particularly in poorer areas which suffer from stronger UHI effects. Offices are major energy consumers, using 71% of cooling electricity while occupying only 13% of the floor space. Overall, space cooling takes up 8% of total electricity usage in residential and office buildings, below the global average of 18.5% but still a major part of the city's electricity use.

The cooling equipment in The Hague's buildings totals around 3,003 tonnes, with an annual turnover of 232 tonnes. This equates to 0.43 kg of cooling equipment per person per year, aligning with previous estimates for waste cooling equipment and contributing to 1% of total electronic waste (WEEE). This brings considerable environmental impacts with it, including resource depletion and pressure on scarce materials, highlighted by thirteen critical raw materials in the equipment. With material intensity in offices being nine times that of residential buildings, there is a pressing need to focus on reducing the material demand of cooling equipment in office settings.

Climate change impacts from cooling in The Hague's residential and office spaces amount to 48.8 kt CO_2-eq in annual GHG emissions, equivalent to 89.4 kg CO_2-eq per resident or 0.7% of the Dutch per capita carbon footprint. With 88% of these emissions stemming from electricity use, reducing electricity consumption emerges as a critical area for environmental impact mitigation, particularly in office buildings where GHG intensity is twelve times that of residential buildings.

RQ 3: How will the cooling demand in The Hague and its environmental impacts evolve until 2050?

By 2050, The Hague's cooling demand is expected to significantly increase, with a potential rise up to 88% in the absence of active policies, and a notable decrease under

strict climate policies. Residential buildings will see an average 56% increase in cooling demand across scenarios, contrasting with a 13% reduction in office buildings. This shift emphasizes the need to focus on residential cooling in future policies.

The 'cooling gap' is projected to reduce substantially by 2050, mainly due to increased cooling equipment in homes. Electricity consumption from cooling is expected to rise by 28% by 2030 and could quadruple by 2050 in the absence of stringent policies. In contrast, the engaged policy-making in the 2050-L scenario shows a 34% reduction in electricity use while improving cooling fulfillment. The disparity in electricity use between residential and office buildings is also projected to increase. Residential cooling electricity use is estimated to double by 2030 and increase eleven-fold in the 2050-H scenario, while that of offices shrinks or stagnates in all scenarios.

Overall, residential cooling's share of total energy demand is set to increase substantially. By 2030, it could rise to 14% of total electricity and 3% of total energy use in residences, with the 2050-H scenario predicting as much as 66% and 14%, respectively. These projections emphasize the growing importance of cooling in The Hague's energy landscape and the need for proactive energy and environmental policies.

The material demand of cooling equipment in The Hague is expected to triple by 2050, raising environmental concerns like resource depletion and increased WEEE generation. Per capita generation of waste cooling devices will increase to up to 4% of total WEEE by 2050, compared to the current 1%. The surge in cooling equipment stocks, along with the anticipated complexity of supply chains, also suggests greater opportunities for urban mining of critical raw materials.

Climate change impacts from space cooling in The Hague show varied projections. The 2050-L scenario predicts a significant 90% reduction in emissions due to grid decarbonization and improved refrigerant practices, while the 2050-H scenario forecasts a 71% increase, primarily due to rising cooling demands and a lack of green initiatives. GHG emissions are expected to decrease substantially in office buildings, by 58%–96% by 2050, but residential buildings could see less reduction or even a four-fold increase under the 2050-H scenario, highlighting the necessity of focused interventions in residences.

Electricity usage is the main contributor to GHG emissions in most scenarios, except 2050-L where equipment production-phase and end-of-life emissions become more prominent, emphasizing the need for policies targeting equipment life-cycles.

In 2020, space cooling-related GHG emissions in The Hague made up 3.1% of the city's carbon footprint. The 2050-L scenario's projected 90% reduction aligns with climate goals, whereas the 2050-H scenario suggests a potential increase to two thirds of the city's total allowable carbon footprint. These projections underline the importance of cooling in The Hague's environmental strategy and the urgent need for sustainable interventions.

In conclusion, the study's projections highlight the importance of cooling in The Hague's energy landscape and the need for proactive energy and environmental policies. It underscores the need for The Hague to focus on sustainable cooling policies to avoid business-as-usual outcomes and align with the Netherlands' net-zero goals by 2050.

RQ 4: What recommendations can be given to minimize the projected environmental impacts of space cooling in The Hague?

The abovementioned results were combined with literature research to inform technology and policy recommendations for The Hague to minimize environmental impacts:

- **Building-Level Measures**: Encourage renovations in older residential buildings through financial incentives and stricter energy regulations, particularly focusing on the low-rise residential buildings, which have the highest cooling demand. Enhance compliance with energy label standards through support, monitoring, and enforcement, especially in rented residential buildings.
- **Urban Environment Changes**: Address the UHI effect through urban design strategies like green roofs, water features, and low-albedo materials. Prioritize these efforts in densely populated, low-income neighborhoods.
- **Thermal Comfort Standards**: Implement policy to endorse higher indoor temperature ranges in summer to reduce cooling demands. Implement adaptive temperature strategies in offices and promote them in residential buildings for energy savings.
- **Cooling Gap Reduction**: Tackle the 77% unmet cooling demand in The Hague, focusing on low-income areas. Implement a carbon tax on low-efficiency cooling equipment and introduce sliding-scale subsidies for energy-efficient cooling solutions.
- **Energy Use Reduction**: Promote energy-efficient cooling systems, including strengthening minimum energy performance standards and promoting reversible heat pumps over traditional ACs. Communicate the benefits of passive cooling.

- **Material Impact Minimization**: Adopt a circular economy approach in cooling equipment production, use, and disposal. Focus on extending equipment lifespan, minimizing the material footprint, and proper waste management.
- **GHG Emissions Reduction**: Decarbonize the electricity grid and promote low global warming potential refrigerants. Emphasize regular maintenance to prevent refrigerant leaks.
- **Public Awareness:** Increase environmental awareness about cooling impacts through education, community-driven social norms, and economic incentives.
- **Policy Integration**: Address future cooling demand in climate and energy policy, integrating space cooling with sustainable heating measures, including emphasis on the double function of reversible heat pumps.

Overall, the findings of this study show the need for greater addressment of space cooling needs both in The Hague and in the Netherlands as a whole. If actions are not taken, environmental impacts will exacerbate the adverse impacts of climate change, feeding into a vicious cycle. It is imperative to focus on using cooling technologies with lower energy demands such as heat pumps and passive cooling technologies, using synergies between sustainable heating and cooling solutions, and considering environmental justice in policy measures. The challenge is clear: adapt or overheat. To prevent the latter, the Hague must choose the path of sustainable cooling.

7 Reference List

2015 Paris Agreement, UN Doc. FCCC/CP/2015/10/Add.1 Decision 1/CP.21 (2015). https://unfccc.int/sites/default/files/english_paris_agreement.pdf

Albà, C. G., Alkhatib, I. I. I., Llovell, F., & Vega, L. F. (2021). Assessment of Low Global Warming Potential Refrigerants for Drop-In Replacement by Connecting their Molecular Features to Their Performance. *ACS Sustainable Chemistry & Engineering*, *9*(50), 17034–17048. https://doi.org/10.1021/acssuschemeng.1c05985

Albatayneh, A., Alterman, D., Page, A., & Moghtaderi, B. (2019). The Significance of the Adaptive Thermal Comfort Limits on the Air-Conditioning Loads in a Temperate Climate. *Sustainability*, *11*(2), Article 2. https://doi.org/10.3390/su11020328

Alsouda, F., Bennett, N. S., Saha, S. C., Salehi, F., & Islam, M. S. (2023). Vapor Compression Cycle: A State-of-the-Art Review on Cycle Improvements, Water and Other Natural Refrigerants. *Clean Technologies*, *5*(2), Article 2. https://doi.org/10.3390/cleantechnol5020030

A new Circular Economy Action Plan For a cleaner and more competitive Europe, (2020). https://eur-lex.europa.eu/legal-content/EN/TXT/?qid=1583933814386&uri=COM:2020:98:FIN

Archer, D., & Rahmstorf, S. (2010). *The Climate Crisis: An Introductory Guide to Climate Change*. Cambridge University Press.

Arrhenius, P. S. (1896). On the influence of carbonic acid in the air upon the temperature of the ground. *The London, Edinburgh, and Dublin Philosophical Magazine and Journal of Science*. https://doi.org/10.1080/14786449608620846

Arvidsson, R., Söderman, M. L., Sandén, B. A., Nordelöf, A., André, H., & Tillman, A.-M. (2020). A crustal scarcity indicator for long-term global elemental resource assessment in LCA. *The International Journal of Life Cycle Assessment*, *25*(9), 1805–1817. https://doi.org/10.1007/s11367-020-01781-1

Ashmawy, R. E., & Azmy, N. Y. (2018). Buildings Orientation and its Impact on the Energy Consumption. *The Academic Research Community Publication*, *2*, 35. https://doi.org/10.21625/archive.v2i3.344

ASHRAE. (2010). *Energy Standard for Buildings Except Low-Rise Residential Buildings*. https://www.ashrae.org/File%20Library/Technical%20Resources/Standards%20and%20Guidelines/Standards%20Addenda/90-1-2007/90_1_2007_bu.pdf

ASHRAE. (2019). *Addendum f to ANSI/ASHRAE Standard 34*. https://www.ashrae.org/file%20library/technical%20resources/standards%20and%20guidelines/standards%20addenda/34_2019_f_20191213.pdf

ASHRAE. (2020). *Thermal Environmental Conditions for Human Occupancy* (55). https://www.ashrae.org/technical-resources/bookstore/standard-55-thermal-environmental-conditions-for-human-occupancy

ASHRAE. (2021). *2021 ASHRAE Handbook: Fundamentals*. ASHRAE.

Atlas Natuurlijk Kapitaal. (2017). *Stedelijk hitte-eiland effect (UHI) in Nederland* [dataset]. https://www.nationaalgeoregister.nl/geonetwork/srv/api/records/c9aa9109-3f32-4f65-84e5-bb1c9ebdfbec

Attema, J., Bakker, A., Beersma, J., Bessembinder, J., Boers, R., Brandsma, T., van den Brink, H., Drijfhout, S., Eskes, H., Haarsma, R., Hazeleger, W., Jilderda, R., Katsman, C., Lenderink, G., Loriaux, J., van Meijgaard, E., van Noije, T., van Oldenborgh, G. J., Selten, F., … van Zadelhoff, G.-J. (2014). *KNMI'14: Climate Change scenarios for the 21st Century – A Netherlands perspective* (WR2014-01; p. 115). KNMI. https://cdn.knmi.nl/knmi/pdf/bibliotheek/knmipubWR/WR2014-01.pdf

Bahadori, M. N. (1978). Passive Cooling Systems in Iranian Architecture. *Scientific American*, *238*(2), 144–155. JSTOR. https://doi.org/10.1038/scientificamerican0278-144

Baranzelli, C., Blagoeva, D., Blengini, G. A., Ciupagea, C., Dewulf, J., Dias, P., Kayam, Y., Latunussa, C. E. L., Mancini, L., Manfredi, S., Marmier, A., Mathieux, F., Nita, V., Nuss, P., Pavel, C., Pennington, D., Talens Peirò, L., Torres De Matos, C., Tzimas, E., … European Commission. (2017). *Methodology for establishing the EU list of critical raw materials: Guidelines.* European Commission. http://dx.publications.europa.eu/10.2873/769526

Barker, R. (2020). *Haagse Daken Kleuren Groen* (p. 26). Partij voor de Dieren Den Haag. https://denhaag.raadsinformatie.nl/document/8919103/3/RIS305633+Gewijzigd+Initiatiefvoorstel+Haagse+Daken+Kleuren+Groen

Barrett, S. (2013). Local level climate justice? Adaptation finance and vulnerability reduction. *Global Environmental Change*, *23*(6), 1819–1829. https://doi.org/10.1016/j.gloenvcha.2013.07.015

Bashir, D. F., Inam, B., Ali Basit, H. M., Iqbal, M. W., Javeed, S., & Mehmood, A. (2011). *Demand Estimation, Elasticity, and Forecasting of LG Air Conditioners: A Case Study of MASHALLAH Electronics* (SSRN Scholarly Paper 1855594). https://doi.org/10.2139/ssrn.1855594

Basner, M., Babisch, W., Davis, A., Brink, M., Clark, C., Janssen, S., & Stansfeld, S. (2014). Auditory and non-auditory effects of noise on health. *The Lancet*, *383*(9925), 1325–1332. https://doi.org/10.1016/S0140-6736(13)61613-X

Beek, M., Kurvers, S., van der Linden, A., Cauberg, J., Eijdems, H. H. E. W., & Mimpen, J. M. J. M. (2007). Praktijkonderzoek thermisch comfort, vergelijking van de Adaptieve Temperatuur-Grenswaarden (ATG) Methode met de Gewogen Temperatuur-Overschijdingen (GTO) Methode in de praktijk. *Bouwfysica Blad*, *18 2007*(1), 22–27.

Beer, J. de, Gaag, N. vander, Duin, C. van, & Ekamper, P. (2020). *Bevolking 2050 in beeld: Drukker, diverser en dubbelgrijs*. CBS. https://open.overheid.nl/documenten/ronl-06ecccd9-84ab-4aeb-b034-670065a37a14/pdf

Berardi, U., & Jafarpur, P. (2020). Assessing the impact of climate change on building heating and cooling energy demand in Canada. *Renewable and Sustainable Energy Reviews*, *121*, 109681. https://doi.org/10.1016/j.rser.2019.109681

Bicer, Y., & Khalid, F. (2020). Life cycle environmental impact comparison of solid oxide fuel cells fueled by natural gas, hydrogen, ammonia and methanol for combined heat and power generation. *International Journal of Hydrogen Energy*, *45*(5), 3670–3685. https://doi.org/10.1016/j.ijhydene.2018.11.122

Blok, M., & Roemers, G. (2017). *PROSPECTING THE URBAN MINES OF AMSTERDAM: Refining the PUMA method based on findings from practice.*

Metabolic. http://code.waag.org/puma/data/Prospecting_the_urban_mines_of_Amsterdam_v03_CB-lg.pdf

Boerstra, A. C., & Leijten, J. L. (2003). Binnenmilieu en productiviteit: Eindelijk harde cijfers. *Verwarming & Ventilatie*. https://www.sunatec.nl/brochures/binnenmilieu_en_productiviteit.pdf

Bouwbesluit, Pub. L. No. Bouwbesluit 2012 (2012). https://rijksoverheid.bouwbesluit.com/Inhoud/docs/wet/bb2012/hfd5/afd5-3

BP p.l.c. (2022). *Bp Statistical Review of World Energy 2022*. BP p.l.c. https://www.bp.com/content/dam/bp/business-sites/en/global/corporate/pdfs/energy-economics/statistical-review/bp-stats-review-2022-full-report.pdf

Braungardt, S., Bürger, V., Zieger, J., & Kenkmann, T. (2018). *Contribution of Renewable Cooling to the Renewable Energy Target of the EU*. RVO. https://www.rvo.nl/sites/default/files/2018/07/Contribution%20of%20Renewable%20Cooling%20to%20the%20Renewable%20Energy%20Target%20of%20the%20EU.pdf

Brimicombe, C., Napoli, C. D., Quintino, T., Pappenberger, F., Cornforth, R., & Cloke, H. L. (2022). Thermofeel: A python thermal comfort indices library. *SoftwareX*, *18*. https://doi.org/10.1016/j.softx.2022.101005

Brough, D., & Jouhara, H. (2020). The aluminium industry: A review on state-of-the-art technologies, environmental impacts and possibilities for waste heat recovery. *International Journal of Thermofluids*, *1–2*, 100007. https://doi.org/10.1016/j.ijft.2019.100007

Brown, J. S., & Domanski, P. A. (2014). Review of alternative cooling technologies. *Applied Thermal Engineering*, *64*(1), 252–262. https://doi.org/10.1016/j.applthermaleng.2013.12.014

Buitelaar, E., Berge, M. van den, Dongen, F. van, Weterings, A., & Maarseveen, R. van. (2017). *De toekomst van kantoren: Een scenariostudie naar de ruimtebehoefte*. PBL. https://www.cpb.nl/sites/default/files/omnidownload/PBL-CPB-Notitie-2mrt2017-De-toekomst-van-kantoren.pdf

Busby, J. (2015). UK shallow ground temperatures for ground coupled heat exchangers. *Quarterly Journal of Engineering Geology and Hydrogeology*, *48*(3–4), 248–260. https://doi.org/10.1144/qjegh2015-077

Calm, J. M. (2002). Emissions and environmental impacts from air-conditioning and refrigeration systems. *International Journal of Refrigeration*, *25*(3), 293–305. https://doi.org/10.1016/S0140-7007(01)00067-6

Calm, J. M. (2008). The next generation of refrigerants – Historical review, considerations, and outlook. *International Journal of Refrigeration*, *31*(7), 1123–1133. https://doi.org/10.1016/j.ijrefrig.2008.01.013

Calvin, K., Dasgupta, D., Krinner, G., Mukherji, A., Thorne, P. W., Trisos, C., Romero, J., Aldunce, P., Barrett, K., Blanco, G., Cheung, W. W. L., Connors, S., Denton, F., Diongue-Niang, A., Dodman, D., Garschagen, M., Geden, O., Hayward, B., Jones, C., … Péan, C. (2023). *Climate Change 2023: Synthesis Report. Contribution of Working Groups I, II and III to the Sixth Assessment Report of the Intergovernmental Panel on Climate Change* (First). IPCC. https://doi.org/10.59327/IPCC/AR6-9789291691647

Canal Marques, A., Cabrera, J.-M., & de Fraga Malfatti, C. (2013). Printed circuit boards: A review on the perspective of sustainability. *Journal of Environmental Management*, *131*, 298–306. https://doi.org/10.1016/j.jenvman.2013.10.003

Carlucci, S., Pagliano, L., O'Brien, W., & Kapsis, K. (2015). *Comfort considerations in Net ZEBs: Theory and design* (A. Athienitis & W. O'Brien, Eds.; pp. 75–106). Wilhelm Ernst & Sohn. https://doi.org/10.1002/9783433604625.ch03

CBS. (2019a). *Energy intensities of buildings in the services sector; floor area* [dataset]. https://opendata.cbs.nl/statline/#/CBS/en/dataset/83374ENG/table

CBS. (2021). *StatLine—Regionale prognose 2020-2050; huishoudens, intervallen, regio-indeling 2018* [dataset]. https://opendata.cbs.nl/#/CBS/nl/dataset/84526NED/table?ts=1623854205977

CBS. (2022a). *Energy consumption private dwellings; type of dwelling and regions* [dataset]. https://opendata.cbs.nl/#/CBS/en/dataset/81528ENG/table

CBS. (2022b). *StatLine—Voorraad woningen en niet-woningen; mutaties, gebruiksfunctie, regio* [dataset]. https://opendata.cbs.nl/statline/#/CBS/nl/dataset/81955NED/table?fromstatweb

CBS. (2022c). *StatLine—Warmtepompen; aantallen, thermisch vermogen en energiestromen* [dataset]. https://opendata.cbs.nl/statline/#/CBS/nl/dataset/82380NED/table

CBS. (2023a). *StatLine—Elektriciteitsbalans; aanbod en verbruik* [dataset]. https://opendata.cbs.nl/statline/#/CBS/nl/dataset/84575NED/table?dl=92781

CBS. (2023b). *Voorraad woningen; gemiddeld oppervlak; woningtype, bouwjaarklasse, regio* [dataset]. https://opendata.cbs.nl/#/CBS/nl/dataset/82550NED/table

CBS. (2015, January 22). Rendementen en CO2-emissie van elektriciteitsproductie in Nederland, update 2013. *Centraal Bureau voor de Statistiek*. https://www.cbs.nl/nl-nl/achtergrond/2015/04/rendementen-en-co2-emissie-van-elektriciteitsproductie-in-nederland-update-2013

CBS. (2019b, August 8). Hogere sterfte tijdens recente hittegolf. *Centraal Bureau voor de Statistiek*. https://www.cbs.nl/nl-nl/nieuws/2019/32/hogere-sterfte-tijdens-recente-hittegolf

CBS. (2022d). *Hoeveel windmolens staan er in Nederland? - Nederland in cijfers 2022 | CBS*. Centraal Bureau voor de Statistiek. https://longreads.cbs.nl/nederland-in-cijfers-2022/hoeveel-windmolens-staan-er-in-nederland

CBS. (2023c). *Windenergie op land; productie en capaciteit per provincie*. StatLine. https://opendata.cbs.nl/#/CBS/nl/dataset/70960ned/table?dl=6E74E

CBS. (2023d, June 15). *Elektriciteit en warmte; productie en inzet naar energiedrager*. Centraal Bureau voor de Statistiek. https://www.cbs.nl/nl-nl/cijfers/detail/80030ned

Chapman, S., Watson, J. E. M., Salazar, A., Thatcher, M., & McAlpine, C. A. (2017). The impact of urbanization and climate change on urban temperatures: A systematic review. *Landscape Ecology*, *32*(10), 1921–1935. https://doi.org/10.1007/s10980-017-0561-4

Claudia, T., Nedeff, F., Mirela, P., & Irimia, O. (2017). Solutions to reduce the noise generated by an air conditioning system. *Journal of Engineering Studies and Research*, *19*. https://doi.org/10.29081/jesr.v19i4.106

Creswell, J. W. (2014). *A Concise Introduction to Mixed Methods Research*. SAGE Publications.

Dale, V., Kline, K., Wiens, J., & Fargione, J. (2010). *Biofuels: Implications for Land Use and Biodiversity Biofuels: Implications for Land Use and Biodiversity*.

Dandsena, J., Mohapatra, K., Satapathy, A. K., & Jena, D. P. (2021). Noise control of outdoor unit of split type air-conditioner using periodic scatterers made with array of Helmholtz resonators. *Applied Acoustics*, *179*, 108054. https://doi.org/10.1016/j.apacoust.2021.108054

Davis, L., Gertler, P., Jarvis, S., & Wolfram, C. (2021). Air conditioning and global inequality. *Global Environmental Change*, *69*, 102299. https://doi.org/10.1016/j.gloenvcha.2021.102299

Davis, L. W., & Gertler, P. J. (2015). Contribution of air conditioning adoption to future energy use under global warming. *Proceedings of the National Academy of Sciences*, *112*(19), 5962–5967. https://doi.org/10.1073/pnas.1423558112

De Blois, J., Kjellstrom, T., Agewall, S., Ezekowitz, J. A., Armstrong, P. W., & Atar, D. (2015). The Effects of Climate Change on Cardiac Health. *Cardiology*, *131*(4), 209–217. https://doi.org/10.1159/000398787

de Boer, S., Geldhof, R., & Matser, J. (2022). *Transitievisie warmte: Achtergrondrapport*. Overmorgen. https://denhaag.raadsinformatie.nl/document/10850782/1/RIS310739_Bijlage

de Dear, R., Akimoto, T., Arens, E. A., Brager, G., Candido, C., Cheong, K. W. D., Li, B., Nishihara, N., Sekhar, S. C., Tanabe, S., Toftum, J., Zhang, H., & Zhu, Y. (2013). Progress in thermal comfort research over the last twenty years. *Indoor Air*, *23*(6), 442–461. https://doi.org/10.1111/ina.12046

de Dear, R., & Brager, G. S. (1998). *Developing an adaptive model of thermal comfort and preference*. https://escholarship.org/uc/item/4qq2p9c6

de Dear, R., Xiong, J., Kim, J., & Cao, B. (2020). A review of adaptive thermal comfort research since 1998. *Energy and Buildings*, *214*, 109893. https://doi.org/10.1016/j.enbuild.2020.109893

de Ridder, K., Lauwaet, D., & Maiheu, B. (2015). UrbClim – A fast urban boundary layer climate model. *Urban Climate*, *12*, 21–48. https://doi.org/10.1016/j.uclim.2015.01.001

de Ruiter, A., Lössbroek, T., Burgmans, J. W., de Boer, R., & Bastmeijer, K. (2019). *De Stad Natuurlijk—Natuurinclusief Bouwen in Den Haag* (p. 34). The Hague Municipality. https://denhaag.raadsinformatie.nl/document/7525647/1/RIS302383_bijlage_Magazine_%27De_stad_natuurlijk_-_natuurinclusief_bouwen_in_Den_Haag%27

Dechezleprêtre, A., Nachtigall, D., & Venmans, F. (2023). The joint impact of the European Union emissions trading system on carbon emissions and economic performance. *Journal of Environmental Economics and Management*, *118*, 102758. https://doi.org/10.1016/j.jeem.2022.102758

Demirbas, A. (2009). Political, economic and environmental impacts of biofuels: A review. *Applied Energy*, *86*, S108–S117. https://doi.org/10.1016/j.apenergy.2009.04.036

Deng, J.-Y., Wong, N. H., & Zheng, X. (2021). Effects of street geometries on building cooling demand in Nanjing, China. *Renewable and Sustainable Energy Reviews*, *142*, 110862. https://doi.org/10.1016/j.rser.2021.110862

DeWit A. (2020). *Heavy Metal: Critical Raw Materials and the Energy Transition*. *74*(2), 1–108.

Dittmann, F., Rivière, P., & Stabat, P. (2016). *Heat Roadmap Europe: Space Cooling Technology in Europe: Technology Data and Demand Modelling* (p. 54). Centre for Energy efficient Systems (CES). https://heatroadmap.eu/wp-content/uploads/2018/11/HRE4_D3.2.pdf#page=51

Dreyfus, G., Borgford-Parnell, N., Peters, T., Christensen, J., Fahey, D. W., Motherway, B., Picolotti, R., Shah, N., & Xu, Y. (2020). *Assessment of climate and development benefits of efficient and climate-friendly cooling*. nstitute for Governance & Sustainable Development and Centro Mario Molina.

https://www.ccacoalition.org/sites/default/files/resources//2020_Assessment-benefits-efficient-cooling_3_30_20.pdf

DSO. (2022). *Transitievisie Warmte* (p. 45). DSO. https://denhaag.raadsinformatie.nl/document/11234823/1#search=%22RIS311707%22

Ecodesign requirements for household refrigerating appliances, 191, 23.7.2009 OJ L (2009). http://data.europa.eu/eli/reg/2009/643/oj/eng

Ecodesign requirements for air conditioners and comfort fans, 206/2012 (2012).

Ecodesign requirements for air heating products, cooling products, high temperature process chillers and fan coil units, 346 OJ L (2016). http://data.europa.eu/eli/reg/2016/2281/oj/eng

Ecorys. (2022). *Onderzoek Nederlandse inkomens en CO2 voetafdruk*. Ecorys. https://milieudefensie.nl/actueel/rapport-klimaatkloof

EEA. (2023). *Greenhouse gas emission intensity of electricity generation in Europe*. https://www.eea.europa.eu/ims/greenhouse-gas-emission-intensity-of-1

Elshkaki, A., Graedel, T. E., Ciacci, L., & Reck, B. K. (2016). Copper demand, supply, and associated energy use to 2050. *Global Environmental Change*, *39*, 305–315. https://doi.org/10.1016/j.gloenvcha.2016.06.006

Ema, M., Naya, M., Yoshida, K., & Nagaosa, R. (2010). Reproductive and developmental toxicity of hydrofluorocarbons used as refrigerants. *Reproductive Toxicology*, *29*(2), 125–131. https://doi.org/10.1016/j.reprotox.2009.11.005

Eneco. (2023). *Windpark Eneco Luchterduinen*. https://www.eneco.nl/over-ons/wat-we-doen/duurzame-bronnen/windpark-eneco-luchterduinen/

Esen, H., Inalli, M., & Esen. (2007). A techno-economic comparison of ground-coupled and air-coupled heat pump system for space cooling. *Building and Environment*, *42*(5), 1955–1965. https://doi.org/10.1016/j.buildenv.2006.04.007

Esfandiari, M., Zaid, S. M., Ismail, M. A., Hafezi, M. R., Asadi, I., & Mohammadi, S. (2021). A Field Study on Thermal Comfort and Cooling Load Demand

Optimization in a Tropical Climate. *Sustainability*, *13*(22), Article 22. https://doi.org/10.3390/su132212425

Essent. (2020). Stroomverbruik stijgt tijdens hittegolf door airco | Essent. *Stroomverbruik stijgt tijdens hittegolf door airco | Essent*. https://www.essent.nl/over-essent/nieuws/extreme-stijging-stroomverbruik-tijdens-hittegolf-door-aircos/

European Commission. (2020). *The availability of refrigerants for new split air conditioning systems that can replace fluorinated greenhouse gases or result in a lower climate impact*. European Commission. https://climate.ec.europa.eu/system/files/2020-09/c_2020_6637_en.pdf

European Commission. (2021). *Special Eurobarometer: Climate Change* (513; Eurobarometer). European Commission. https://data.europa.eu/doi/10.2834/437

Establishing a Carbon Border Adjustment Mechanism, 130 OJ L (2023). http://data.europa.eu/eli/reg/2023/956/oj/eng

Regulation on fluorinated greenhouse gases, 150 OJ L (2014). http://data.europa.eu/eli/reg/2014/517/oj/eng

Eurostat. (2020). *Energy statistics—Cooling and heating degree days* [dataset]. https://ec.europa.eu/eurostat/cache/metadata/en/nrg_chdd_esms.htm

Eurostat. (2023). *Statistics on the production of manufactured goods* [dataset]. https://ec.europa.eu/eurostat/cache/metadata/en/prom_esms.htm

Eurovent Certification. (2022). *Technical Certification Rules of the Eurovent Certified Performance Mark*. Eurovent Certification. https://www.eurovent-certification.com/media/images/6a2/304/6a23048992033af69a27ed20a8ddd9189ebe3c9e.pdf

Evans, O., & Stevens, J. (1805). *The abortion of the young steam engineer's guide, invented by the author, a description of four other patented inventions* [Electronic resource]. Fry and Kammerer.

Eveloy, V., & Ayou, D. S. (2019). Sustainable District Cooling Systems: Status, Challenges, and Future Opportunities, with Emphasis on Cooling-Dominated Regions. *Energies*, *12*(2), Article 2. https://doi.org/10.3390/en12020235

Farid, M. M., Khudhair, A. M., Razack, S. A. K., & Al-Hallaj, S. (2004). A review on phase change energy storage: Materials and applications. *Energy Conversion and Management*, *45*(9), 1597–1615. https://doi.org/10.1016/j.enconman.2003.09.015

Farrow, K., Grolleau, G., & Ibanez, L. (2017). Social Norms and Pro-environmental Behavior: A Review of the Evidence. *Ecological Economics*, *140*, 1–13. https://doi.org/10.1016/j.ecolecon.2017.04.017

Fazeli, R., Ruth, M., & Davidsdottir, B. (2016). Temperature response functions for residential energy demand – A review of models. *Urban Climate*, *15*, 45–59. https://doi.org/10.1016/j.uclim.2016.01.001

Fedele, L., Lombardo, G., Greselin, I., Menegazzo, D., & Bobbo, S. (2023). Thermophysical Properties of Low GWP Refrigerants: An Update. *International Journal of Thermophysics*, *44*(5), 80. https://doi.org/10.1007/s10765-023-03191-5

Ferro, P., & Bonollo, F. (2019). Materials selection in a critical raw materials perspective. *Materials & Design*, *177*, 107848. https://doi.org/10.1016/j.matdes.2019.107848

Forti, V., Balde, C. P., Kuehr, R., & Bel, G. (2020). *The Global E-waste Monitor 2020: Quantities, flows and the circular economy potential*. United Nations University/United Nations Institute for Training and Research, International Telecommunication Union, and International Solid Waste Association. https://collections.unu.edu/view/UNU:7737#viewAttachments

Gadenne, D., Sharma, B., Kerr, D., & Smith, T. (2011). The influence of consumers' environmental beliefs and attitudes on energy saving behaviours. *Energy Policy*, *39*(12), 7684–7694. https://doi.org/10.1016/j.enpol.2011.09.002

Gao, G., Li, J., & Wen, Y. (2020). DeepComfort: Energy-Efficient Thermal Comfort Control in Buildings Via Reinforcement Learning. *IEEE Internet of Things Journal*, *7*(9), 8472–8484. https://doi.org/10.1109/JIOT.2020.2992117

Gasunie. (2023, April 20). *Green gas*. Gasunie. https://www.gasunie.nl/en/expertise/green-gas

Geels, F. W. (2002). Technological transitions as evolutionary reconfiguration processes: A multi-level perspective and a case-study. *Research Policy*, *31*(8–9), 1257–1274. https://doi.org/10.1016/S0048-7333(02)00062-8

Geels, F. W. (2004). From sectoral systems of innovation to socio-technical systems: Insights about dynamics and change from sociology and institutional theory. *Research Policy*, *33*(6), 897–920. https://doi.org/10.1016/j.respol.2004.01.015

Geravandi, S., Takdastan, A., Zallaghi, E., Niri, M. V., Mohammadi, M. J., Saki, H., & Naiemabadi, A. (2015). Noise Pollution and Health Effects. *Jundishapur Journal of Health Sciences*, *7*(1), Article 1. https://doi.org/10.5812/jjhs.25357

Geyer, R., Jambeck, J. R., & Law, K. L. (2017). Production, use, and fate of all plastics ever made. *Science Advances*, *3*(7), e1700782. https://doi.org/10.1126/sciadv.1700782

Godwin, D. S., & Ferenchiak, R. (2020). The implications of residential air conditioning refrigerant choice on future hydrofluorocarbon consumption in the United States. *Journal of Integrative Environmental Sciences*, *17*(3), 29–44. https://doi.org/10.1080/1943815X.2020.1768551

Grohol, M., & Veeh, C. (2023). *Study on the critical raw materials for the EU 2023: Final report*. European Commission. https://data.europa.eu/doi/10.2873/725585

Gubernot, D. M., Anderson, G. B., & Hunting, K. L. (2015). Characterizing Occupational Heat-Related Mortality in the United States, 2000–2010: An Analysis Using the Census of Fatal Occupational Injuries Database. *American Journal of Industrial Medicine*, *58*(2), 203–211. https://doi.org/10.1002/ajim.22381

Guinée, J. B., Huppes, G., de Koning, A., van Oers, L., Sleeswijk, A. W., & Suh, S. (2002). *Handbook on Life Cycle Assessment* (Vol. 7). https://doi.org/10.1007/0-306-48055-7

Gupta, S. K., Arora, B. B., & Arora, A. (2021). Economics-Based Payback and Life Cycle Cost Savings Assessment of Inverter Type Air Conditioners. *IOP Conference Series: Materials Science and Engineering*, *1206*(1), 012023. https://doi.org/10.1088/1757-899X/1206/1/012023

Haagse Hoogbouw. (2023). Toekomstige projecten Haagse Hoogbouw. *Haagse Hoogbouw*. https://haagsehoogbouw.nl/projecten-toekomst/

Hajat, S., O'Connor, M., & Kosatsky, T. (2010). Health effects of hot weather: From awareness of risk factors to effective health protection. *Lancet (London, England)*, *375*(9717), 856–863. https://doi.org/10.1016/S0140-6736(09)61711-6

Hammingh, P., Abels-van Overveld, M., van Beijnum, B., Blomjous, D., Boom, H., & van den Born, G. J. (2022). *Klimaat- en Energieverkenning 2022* (p. 249). PBL. https://www.pbl.nl/sites/default/files/downloads/pbl-2022-klimaat-en-energieverkenning-4838.pdf

Hammingh, P., Daniels, B., Koutstaal, P., & Menkveld, M. (2021). *Klimaat- en Energieverkenning 2021*. PBL. https://www.pbl.nl/sites/default/files/downloads/pbl-2021-klimaat-en-energieverkenning-2021-4681.pdf

Hansen, J., Sato, M., & Ruedy, R. (2012). Perception of climate change. *Proceedings of the National Academy of Sciences*, *109*(37), E2415–E2423. https://doi.org/10.1073/pnas.1205276109

Harlan, S. L., Brazel, A. J., Darrel, J. G., Jones, N. S., Larsen, L., Prashad, L., & Stefanov, W. L. (2007). In the shade of affluence: The inequitable distribution of the urban heat island. In R. C. Wilkinson & W. R. Freudenburg (Eds.), *Equity and the Environment* (Vol. 15, pp. 173–202). Emerald Group Publishing Limited. https://doi.org/10.1016/S0196-1152(07)15005-5

Harmelink, M., Bosselaar, L., Gerdes, J., Boonekamp, P., Segers, R., Pouwelse, H., & Verdonk, M. (2012). *Berekening van de CO2-emissies, het primair fossiel energiegebruik en het rendement van elektriciteit in Nederland*. Agentschap NL. https://www.rvo.nl/sites/default/files/Notitie%20Energie-CO2%20effecten%20elektriciteit%20Sept%202012.pdf

Hashimoto, K. (2006, October 17). Technology and Market Development of CO2 Heat Pump Water Heaters in Japan. *HPT - Heat Pumping Technologies*. https://heatpumpingtechnologies.org/publications/technology-and-market-development-ofco2-heat-pump-water-heaterseco-cute-in-japan/

Hauck, M., van Schot, M., & Koornneef, J. (2020). *North Sea Energy: Carbon footprint of grey, blue and green Hydrogen*. TNO. https://north-sea-energy.eu/static/1a8004c68fb16f7ed588ef2d10ea51bf/9.-FINAL-NSE3_D4.1-Report-on-life-cycle-comparison-of-environmental-performance-of-grey-blue-green-hydrogen-pathways.pdf

Heikkilä, K. (2004). Environmental impact assessment using a weighting method for alternative air-conditioning systems. *Building and Environment*, *39*(10), 1133–1140. https://doi.org/10.1016/j.buildenv.2004.02.009

Heikkilä, K. (2008). Environmental evaluation of an air-conditioning system supplied by cooling energy from a bore-hole based heat pump system. *Building and Environment*, *43*(1), 51–61. https://doi.org/10.1016/j.buildenv.2006.11.027

Hensen Centnerová, L., van Duijnhoven, J., Groot Zwaaftink, M., Hennep, R., Höngens, T., Jacobs, P., Loomans, M., Middendorf, G., van der Putten, R., Vugts, J., Rooijakkers, E., van Veen, M., Verbaan, G., & Zeguers, J. (2021). *Programma van Eisen Gezonde Kantoren 2021*. Binnenklimaat techniek. https://www.binnenklimaattechniek.nl/wp-content/uploads/2022/01/Digitaal_Publicatie-PVE-Gezonde-kantoren_BinnenklimaatTechniek16.pdf

Hickel, J. (2020a). Quantifying national responsibility for climate breakdown: An equality-based attribution approach for carbon dioxide emissions in excess of the planetary boundary. *The Lancet Planetary Health*, *4*(9), e399–e404. https://doi.org/10.1016/S2542-5196(20)30196-0

Hickel, J. (2020b, September 10). *And yet, according to the Climate Vulnerability Monitor, the South suffers more than 90% of the costs of climate breakdown, and 98% of the deaths associated with climate breakdown.* [Tweet]. Twitter. https://twitter.com/jasonhickel/status/1303959215250210817

Hodnebrog, Ø., Aamaas, B., Fuglestvedt, J. S., Marston, G., Myhre, G., Nielsen, C. J., Sandstad, M., Shine, K. P., & Wallington, T. J. (2020). Updated Global Warming Potentials and Radiative Efficiencies of Halocarbons and Other Weak Atmospheric Absorbers. *Reviews of Geophysics*, *58*(3), e2019RG000691. https://doi.org/10.1029/2019RG000691

Hoffmann, P., & Schlünzen, K. H. (2013). Weather Pattern Classification to Represent the Urban Heat Island in Present and Future Climate. *Journal of Applied Meteorology and Climatology*, *52*(12), 2699–2714. https://doi.org/10.1175/JAMC-D-12-065.1

Howarth, R. W., & Jacobson, M. Z. (2021). How green is blue hydrogen? *Energy Science & Engineering*, *9*(10), 1676–1687. https://doi.org/10.1002/ese3.956

Huijbregts, M. A. J., Steinmann, Z. J. N., Elshout, P. M. F., Stam, G., Verones, F., Vieira, M., Zijp, M., Hollander, A., & Van Zelm, R. (2017). ReCiPe2016: A harmonised life cycle impact assessment method at midpoint and endpoint level. *The International Journal of Life Cycle Assessment*, *22*(2), 138–147. https://doi.org/10.1007/s11367-016-1246-y

Huisman, J., Leroy, P., Tertre, F., Ljunggren, M., Chancerel, P., Cassard, D., Løvik, A., Wäger, P., Kushnir, D., Rotter, V., Mählitz, P., Herreras, L., Emmerich, J., Hallberg, A., Habib, H., Wagner, M., & Downes, S. (2017). *Prospecting Secondary Raw Materials in the Urban Mine and mining wastes (ProSUM)—Final Report*. https://doi.org/10.13140/RG.2.2.10451.89125

Hung, C. R., Kishimoto, P., Krey, V., Strømman, A. H., & Majeau-Bettez, G. (2022). ECOPT2: An adaptable life cycle assessment model for the environmentally constrained optimization of prospective technology transitions. *Journal of Industrial Ecology*, *26*(5), 1616–1630. https://doi.org/10.1111/jiec.13331

Hurwitz, M. M., Fleming, E. L., Newman, P. A., Li, F., Mlawer, E., Cady-Pereira, K., & Bailey, R. (2015). Ozone depletion by hydrofluorocarbons. *Geophysical Research Letters*, *42*(20), 8686–8692. https://doi.org/10.1002/2015GL065856

Hussein, I., A. Rahman, M. H., & Maria, T. (2009). Field studies on thermal comfort of air-conditioned and non air-conditioned buildings in Malaysia. *2009 3rd International Conference on Energy and Environment (ICEE)*, 360–368. https://doi.org/10.1109/ICEENVIRON.2009.5398622

HVAC Investigators. (2020). The Basics of Chillers. *HVAC Investigators*. https://www.hvacinvestigators.com/webinars/the-basics-of-chillers-how-they-work-where-theyre-used-and-common-problems/

IEA. (2018a). *The Future of Cooling: Opportunities for energy-efficient air conditioning* (p. 92). IEA. https://iea.blob.core.windows.net/assets/0bb45525-277f-4c9c-8d0c-9c0cb5e7d525/The_Future_of_Cooling.pdf

IEA. (2021a). *Renewables 2021—Analysis and forecast to 2026*. IEA. https://iea.blob.core.windows.net/assets/5ae32253-7409-4f9a-a91d-1493ffb9777a/Renewables2021-Analysisandforecastto2026.pdf

IEA. (2021b). *World Energy Outlook 2021*. IEA. https://iea.blob.core.windows.net/assets/4ed140c1-c3f3-4fd9-acae-789a4e14a23c/WorldEnergyOutlook2021.pdf

IEA. (2018b). *Global air conditioner stock, 1990-2050*. IEA - Charts – Data & Statistics. https://www.iea.org/data-and-statistics/charts/global-air-conditioner-stock-1990-2050

Inayat, A., & Raza, M. (2019). District cooling system via renewable energy sources: A review. *Renewable and Sustainable Energy Reviews*, *107*, 360–373. https://doi.org/10.1016/j.rser.2019.03.023

Ioannou, A. (2018). Thermal comfort and energy related occupancy behavior in Dutch residential dwellings. *A+BE | Architecture and the Built Environment*, *27*, Article 27. https://doi.org/10.7480/abe.2018.27.2773

ISO. (2005). *ISO 7730:2005 Ergonomics of the thermal environment—Analytical determination and interpretation of thermal comfort using calculation of the PMV and PPD indices and local thermal comfort criteria*. ISO. https://www.iso.org/standard/39155.html

ISSO. (2014). *ISSO-publicatie 74 Thermische behaaglijkheid*. ISSO. https://open.isso.nl/publicatie/isso-publicatie-51-warmteverliesberekening-voor-woningen-en-woongebouwen/2023

Itard, L. (2015). *Energy balance model* [Excel file].

Jariwala, H., Syed, H., Pandya, M., & Gajera, Y. (2017, March 17). *Noise Pollution & Human Health: A Review*. Noise and Air Pollution: Challenges and Opportunities.

https://www.researchgate.net/publication/319329633_Noise_Pollution_Human_Health_A_Review

Jones, S. (2022, August 2). Spain puts limits on air conditioning and heating to save energy. *The Guardian*. https://www.theguardian.com/world/2022/aug/02/spain-puts-limits-on-air-conditioning-and-heating-to-save-energy

Jordahl, K., van den Bossche, J., Fleischmann, M., Wasserman, J., McBride, J., Gerard, J., & Leblanc, F. (2020). *GeoPandas* (v0.8.1) [Computer software]. GeoPandas. http://doi.org/10.5281/zenodo.3946761

Karonen, I. (2017). File:Heatpump.svg. In *Wikipedia*. https://en.wikipedia.org/wiki/File:Heatpump.svg

Kawakubo, S., Sugiuchi, M., & Arata, S. (2023). Office thermal environment that maximizes workers' thermal comfort and productivity. *Building and Environment*, *233*, 110092. https://doi.org/10.1016/j.buildenv.2023.110092

Kemp, L., Xu, C., Depledge, J., Ebi, K. L., Gibbins, G., Kohler, T. A., Rockström, J., Scheffer, M., Schellnhuber, H. J., Steffen, W., & Lenton, T. M. (2022). Climate Endgame: Exploring catastrophic climate change scenarios. *Proceedings of the National Academy of Sciences*, *119*(34), e2108146119. https://doi.org/10.1073/pnas.2108146119

Kennard, H., Oreszczyn, T., Mistry, M., & Hamilton, I. (2022). Population-weighted degree-days: The global shift between heating and cooling. *Energy and Buildings*, *271*, 112315. https://doi.org/10.1016/j.enbuild.2022.112315

Kenny, G. P., Yardley, J., Brown, C., Sigal, R. J., & Jay, O. (2010). Heat stress in older individuals and patients with common chronic diseases. *CMAJ*, *182*(10), 1053–1060. https://doi.org/10.1503/cmaj.081050

Kigali Amendment to the Montreal Protocol, C.N.872.2016 (2016). https://treaties.un.org/Pages/ViewDetails.aspx?src=IND&mtdsg_no=XXVII-2-f&chapter=27&clang=_en

Kjellstrom, T., Briggs, D., Freyberg, C., Lemke, B., Otto, M., & Hyatt, O. (2016). Heat, Human Performance, and Occupational Health: A Key Issue for the Assessment

of Global Climate Change Impacts. *Annual Review of Public Health*, *37*, 97–112. https://doi.org/10.1146/annurev-publhealth-032315-021740

Kleerekoper, L., van Esch, M., & Salcedo, T. B. (2012). How to make a city climate-proof, addressing the urban heat island effect. *Resources, Conservation and Recycling*, *64*, 30–38. https://doi.org/10.1016/j.resconrec.2011.06.004

Klimaatakkoord, (2019). https://www.klimaatakkoord.nl/documenten/publicaties/2019/06/28/klimaatakkoord

Klok, E. J., Schaminée, S., Duyzer, J., & Steeneveld, G. J. (2012). *De stedelijke hitte-eilanden van Nederland in kaart gebracht met satellietbeelden*. https://repository.tno.nl/islandora/object/uuid%3A0f567784-9384-4663-998b-72bcc0fa021c

Klok, E. J., Shaminee, S., Duyzer, J., & Steeneveld, G. J. (2012). *De stedelijke hitte-eilanden van Nederland in kaart gebracht met satellietbeelden*. Stichting Kennis voor Klimaat.

KNMI. (2021). *KNMI Klimaatsignaal '21—Hoe het klimaat in Nederland snel verandert* (p. 72). KNMI. https://cdn.knmi.nl/knmi/asc/klimaatsignaal21/KNMI_Klimaatsignaal21.pdf

KNMI. (2022a). *KNMI - Bodemtemperaturen*. https://www.knmi.nl/nederland-nu/klimatologie/bodemtemperaturen

KNMI. (2022b). *KNMI - Daggegevens van het weer in Nederland*. https://www.knmi.nl/nederland-nu/klimatologie/daggegevens

KNMI. (2023a). *Klimaatviewer*. KNMI. https://www.knmi.nl/klimaat-viewer/kaarten/temperatuur/gemiddelde-temperatuur/januari/Periode_1991-2020

KNMI. (2023b). *KNMI - Uurgegevens van het weer in Nederland*. https://www.knmi.nl/nederland-nu/klimatologie/uurgegevens

Kondo, K., Mabon, L., Bi, Y., Chen, Y., & Hayabuchi, Y. (2021). Balancing conflicting mitigation and adaptation behaviours of urban residents under climate change and the urban heat island effect. *Sustainable Cities and Society*, *65*, 102585. https://doi.org/10.1016/j.scs.2020.102585

Koomen, E., & Diogo, V. (2017). Assessing potential future urban heat island patterns following climate scenarios, socio-economic developments and spatial planning strategies. *Mitigation and Adaptation Strategies for Global Change*, *22*(2), 287–306. https://doi.org/10.1007/s11027-015-9646-z

Koopmans, S., Heusinkveld, B. G., & Steeneveld, G. J. (2020). A standardized Physical Equivalent Temperature urban heat map at 1-m spatial resolution to facilitate climate stress tests in the Netherlands. *Building and Environment*, *181*, 106984. https://doi.org/10.1016/j.buildenv.2020.106984

Koops, O., Melief, H., Schoenaker, N., Schenau, S., & van Rossum, M. (2022). *Broeikasgassen in de Nederlandse economie*. CBS. https://www.cbs.nl/nl-nl/longread/de-nederlandse-economie/2022/broeikasgassen-in-de-nederlandse-economie?onepage=true

Kragh, J., Rose, J., & Svendsen, S. (2005). Mechanical ventilation with heat recovery in cold climates. *Proceedings of the Seventh Nordic Symposium on Building Physics in Nordic Countries*.

Krayenhoff, E. S., Broadbent, A. M., Zhao, L., Georgescu, M., Middel, A., Voogt, J. A., Martilli, A., Sailor, D. J., & Erell, E. (2021). Cooling hot cities: A systematic and critical review of the numerical modelling literature. *Environmental Research Letters*, *16*(5), 053007. https://doi.org/10.1088/1748-9326/abdcf1

Kurvers, S., van der Linden, K., & Cauberg, H. (2012). *Literatuurstudie thermisch comfort*. RVO. https://www.rvo.nl/sites/default/files/Literatuurstudie%20thermisch%20comfort.pdf

Leitão, A. F. J. C. (2017). *Building Performance Evaluation: A Dutch Perspective in Thermal Comfort and Energy Consumption* [Lisbon University]. https://repositorio.ul.pt/bitstream/10451/30364/1/ulfc122074_tm_Andr%C3%A9_Leit%C3%A3o.pdf

Levin, K., Cashore, B., Bernstein, S., & Auld, G. (2012). Overcoming the tragedy of super wicked problems: Constraining our future selves to ameliorate global climate change. *Policy Sciences*, *45*(2), 123–152. https://doi.org/10.1007/s11077-012-9151-0

Li, G. (2015). Investigations of life cycle climate performance and material life cycle assessment of packaged air conditioners for residential application. *Sustainable Energy Technologies and Assessments*, *11*, 114–125. https://doi.org/10.1016/j.seta.2015.07.002

Liu, J., Yao, R., & McCloy, R. (2014). An investigation of thermal comfort adaptation behaviour in office buildings in the UK. *Indoor and Built Environment*, *23*(5), 675–691. https://doi.org/10.1177/1420326X13481048

Long, N., Summer, T., Swindler, A., & Addy, N. (2023). *SEED-platform/seed* [Python]. National Renewable Energy Laboratory (NREL). https://github.com/SEED-platform/seed

Lundgren, K., & Kjellstrom, T. (2013). Sustainability Challenges from Climate Change and Air Conditioning Use in Urban Areas. *SUSTAINABILITY*, *5*(7), 3116–3128. https://doi.org/10.3390/su5073116

Manders, T., & Kool, C. (2015). *Nederland in 2030 en 2050: Twee referentiescenario's*. PBL. https://www.cpb.nl/sites/default/files/publicaties/download/cpb-pbl-boek-19-wlo-2015-nederland-2030-en-2050.pdf

Matthews, H. D., Tokarska, K. B., Nicholls, Z. R. J., Rogelj, J., Canadell, J. G., Friedlingstein, P., Frölicher, T. L., Forster, P. M., Gillett, N. P., Ilyina, T., Jackson, R. B., Jones, C. D., Koven, C., Knutti, R., MacDougall, A. H., Meinshausen, M., Mengis, N., Séférian, R., & Zickfeld, K. (2020). Opportunities and challenges in using remaining carbon budgets to guide climate policy. *Nature Geoscience*, *13*(12), Article 12. https://doi.org/10.1038/s41561-020-00663-3

McCulloch, A., & Lindley, A. A. (2003). From mine to refrigeration: A life cycle inventory analysis of the production of HFC-134a. *International Journal of Refrigeration*, *26*(8), 865–872. https://doi.org/10.1016/S0140-7007(03)00095-1

McKinnon, M., Lissner, T., Romanello, M., Ahmed, S., Rosas, A., Baarsch, F., & Schaeffer, M. (2022). *Climate Vulnerability Monitor Third Edition: A Planet on Fire*. Climate Vulnerable Forum & V20. https://knowledge4policy.ec.europa.eu/publication/climate-vulnerability-monitor-third-edition-planet-fire_en

Memon, S. A. (2014). Phase change materials integrated in building walls: A state of the art review. *Renewable and Sustainable Energy Reviews*, *31*, 870–906. https://doi.org/10.1016/j.rser.2013.12.042

Ministerie van Algemene Zaken. (2020, April 1). *Klimaatplan 2021-2030*. Ministerie van Algemene Zaken. https://www.rijksoverheid.nl/documenten/beleidsnotas/2020/04/24/klimaatplan-2021-2030

Ministerie van Economische Zaken en Klimaat. (2019). *Integrated National Energy and Climate Plan 2021-2030: The Netherlands*. Ministerie van Economische Zaken en Klimaat. https://energy.ec.europa.eu/system/files/2020-03/nl_final_necp_main_en_0.pdf

Montreal Protocol on Substances that Deplete the Ozone Layer, C.N.285.1988. (1987). https://treaties.un.org/doc/publication/unts/volume%201522/volume-1522-i-26369-english.pdf

Moser, S. C. (2010). Communicating climate change: History, challenges, process and future directions. *WIREs Climate Change*, *1*(1), 31–53. https://doi.org/10.1002/wcc.11

Mota-Babiloni, A., & Makhnatch, P. (2021). Predictions of European refrigerants place on the market following F-gas regulation restrictions. *International Journal of Refrigeration*, *127*, 101–110. https://doi.org/10.1016/j.ijrefrig.2021.03.005

Motie "Vertaling Klimaatakkoord Parijs naar Haagse doelstellingen," RIS295447, Gemeenteraad van Den Haag (2016). https://denhaag.raadsinformatie.nl/document/4501953/2/M_26

Müller, A. (2015). *Energy Demand Assessment for Space Conditioning and Domestic Hot Water: A Case Study for the Austrian Building Stock* [Vienna University of Technology]. https://www.invert.at/Dateien/Dissertation_AndreasM.pdf

Müller, N., Kuttler, W., & Barlag, A.-B. (2014). Analysis of the subsurface urban heat island in Oberhausen, Germany. *Climate Research*, *58*(3), 247–256. https://doi.org/10.3354/cr01195

Munroe, R. (2023). *Heat Pump* [Digital graphic]. https://xkcd.com/2790/

National Renewable Energy Laboratory. (2023). *EnergyPlus* [C++]. National Renewable Energy Laboratory. https://github.com/NREL/EnergyPlus

Nawaz, K., & Ally, M. R. (2019). Options for low-global-warming-potential and natural refrigerants Part 2: Performance of refrigerants and systemic irreversibilities. *International Journal of Refrigeration*, *106*, 213–224. https://doi.org/10.1016/j.ijrefrig.2019.05.030

NEN. (2007). *Indoor environmental input parameters for design and assessment of energy performance of buildings addressing indoor air quality, thermal environment, lighting and acoustics* (EN 15251; Version 2007). Nederlands Normalisatie Instituut (NEN). https://www.nen.nl/en/nen-en-15251-2007-en-114091

NEN. (2023). *NTA 8800:2023 nl: Energieprestatie van gebouwen—Bepalingsmethode* (NTA 8800; Version 2023). NEN. https://www.nen.nl/nta-8800-2023-nl-304951

Nguyen, T. N., Lobo, A., & Greenland, S. (2017). Energy efficient household appliances in emerging markets: The influence of consumers' values and knowledge on their attitudes and purchase behaviour. *International Journal of Consumer Studies*, *41*(2), 167–177. https://doi.org/10.1111/ijcs.12323

Nicol, F., & Wilson, M. (2011). A critique of European Standard EN 15251: Strengths, weaknesses and lessons for future standards. *Building Research & Information*, *39*, 183–193. https://doi.org/10.1080/09613218.2011.556824

Nižetić, S., Djilali, N., Papadopoulos, A., & Rodrigues, J. J. P. C. (2019). Smart technologies for promotion of energy efficiency, utilization of sustainable resources and waste management. *Journal of Cleaner Production*, *231*, 565–591. https://doi.org/10.1016/j.jclepro.2019.04.397

NOS. (2021, January 31). Grote werkgevers gaan na corona kantoorruimte schrappen. *NOS*. https://nos.nl/nieuwsuur/artikel/2366749-grote-werkgevers-gaan-na-corona-kantoorruimte-schrappen

NOS. (2022, June 1). De Jonge: Vanaf 2030 geen woningen meer verhuren met slecht energielabel. *NOS*. https://nos.nl/artikel/2431054-de-jonge-vanaf-2030-geen-woningen-meer-verhuren-met-slecht-energielabel

NOS. (2023a, January 12). *Netbeheerder waarschuwt voor stroomtekort in 2030*. https://nos.nl/artikel/2459559-netbeheerder-waarschuwt-voor-stroomtekort-in-2030

NOS. (2023b, July 7). Steeds meer mensen een airco, maar experts zien liever zonwering. *NOS*. https://nos.nl/artikel/2481925-steeds-meer-mensen-een-airco-maar-experts-zien-liever-zonwering

Nouvel, R., Zirak, M., Coors, V., & Eicker, U. (2017). The influence of data quality on urban heating demand modeling using 3D city models. *Computers, Environment and Urban Systems*, *64*, 68–80. https://doi.org/10.1016/j.compenvurbsys.2016.12.005

Olmez, G. M., Dilek, F. B., Karanfil, T., & Yetis, U. (2016). The environmental impacts of iron and steel industry: A life cycle assessment study. *Journal of Cleaner Production*, *130*, 195–201. https://doi.org/10.1016/j.jclepro.2015.09.139

Osunmuyiwa, O. O., Payne, S. R., Vigneswara Ilavarasan, P., Peacock, A. D., & Jenkins, D. P. (2020). I cannot live without air conditioning! The role of identity, values and situational factors on cooling consumption patterns in India. *Energy Research & Social Science*, *69*, 101634. https://doi.org/10.1016/j.erss.2020.101634

Ouden, B. den, Terwel, R., Tiihonen, T., Warnaars, J., Kerkhoven, J., Koot, A., Coenen, M., & Verboon, T. (2020). *Klimaatneutrale energiescenario's 2050*. Berenschot. https://www.berenschot.nl/media/hl4dygfq/rapport_klimaatneutrale_energiescenario_s_2050_2.pdf

OzonAction. (2016). *The Kigali Amendment to the Montreal Protocol: HFC Phase-down*. OzonAction. https://wedocs.unep.org/bitstream/handle/20.500.11822/26589/HFC_Phasedown_EN.pdf?sequence=1&isAllowed=y

PDOK. (2023a). *Basisregistratie Adressen en Gebouwen (BAG)* [dataset]. https://www.pdok.nl/atom-downloadservices/-/article/basisregistratie-adressen-en-gebouwen-ba-1

PDOK. (2023b). *Bestuurlijke Gebieden* [dataset]. https://www.pdok.nl/introductie/-/article/bestuurlijke-gebieden

PDOK. (2023c). *CBS Postcode4* [dataset]. https://www.pdok.nl/introductie/-/article/cbs-postcode4

PDOK. (2023d). *CBS Vierkantstatistieken 100m* [dataset]. https://www.pdok.nl/introductie/-/article/cbs-vierkantstatistieken-100m

PDOK. (2023e). *CBS Wijken en Buurten* [dataset]. https://www.pdok.nl/introductie/-/article/cbs-wijken-en-buurten

Pehl, M., Arvesen, A., Humpenöder, F., Popp, A., Hertwich, E. G., & Luderer, G. (2017). Understanding future emissions from low-carbon power systems by integration of life-cycle assessment and integrated energy modelling. *Nature Energy*, *2*(12), Article 12. https://doi.org/10.1038/s41560-017-0032-9

Penman, J., Kruger, D., Galbally, I., Hiraishi, T., Nyenzi, B., Emmanul, S., Buendia, L., Hoppaus, R., Martinsen, T., Meijer, J., & Miwa, K. (2000). *Good Practice Guidance and Uncertainty Management in National Greenhouse Gas Inventories—Methodology Report*. IPCC. https://www.ipcc.ch/publication/good-practice-guidance-and-uncertainty-management-in-national-greenhouse-gas-inventories/

Peters, R., Dukai, B., Vitalis, S., van Liempt, J., & Stoter, J. (2022). Automated 3D Reconstruction of LoD2 and LoD1 Models for All 10 Million Buildings of the Netherlands. *Photogrammetric Engineering & Remote Sensing*, *88*(3), 165–170. https://doi.org/10.14358/PERS.21-00032R2

Peters, T. (2018). *A Cool World: Defining the Energy Conundrum of Cooling for All* (p. 19). Birmingham Energy Institute – University of Birmingham. https://www.birmingham.ac.uk/Documents/college-eps/energy/Publications/2018-clean-cold-report.pdf

Petrecca, G. (1993). *Industrial Energy Management: Principles and Applications: Principles and Applications*. Springer US. https://doi.org/10.1007/978-1-4615-3160-9

Philipps, D. S., & Warmuth, W. (2023). *Photovoltaics Report*. Fraunhofer ISE. https://www.ise.fraunhofer.de/content/dam/ise/de/documents/publications/studies/Photovoltaics-Report.pdf

Pollack, H. N., Huang, S., & Shen, P.-Y. (1998). Climate Change Record in Subsurface Temperatures: A Global Perspective. *Science*. https://doi.org/10.1126/science.282.5387.279

Pörtner, H. O., Roberts, D. C., Adams, H., Adler, C., Aldunce, P., Ali, E., Begum, R. A., Betts, R., Kerr, R. B., Biesbroek, R., Birkmann, J., Bowen, K., Castellanos, E., Cissé, G., Constable, A., Cramer, W., Dodman, D., Eriksen, S. H., Fischlin, A., … Ibrahim, Z. Z. (2022). *Climate change 2022: Impacts, adaptation and vulnerability*. IPCC. https://research.wur.nl/en/publications/climate-change-2022-impacts-adaptation-and-vulnerability

Pörtner, H. O., Roberts, D. C., Poloczanska, E. S., Mitenbeck, K., Tignor, M., Alegria, M., Langsdorf, S., Löscke, S., Möller, V., & Okem, A. (2022). *IPCC, 2022: Summary for Policymakers*. IPCC. https://www.ipcc.ch/report/ar6/wg2/downloads/report/IPCC_AR6_WGII_SummaryForPolicymakers.pdf

Pothitou, M., Hanna, R. F., & Chalvatzis, K. J. (2016). Environmental knowledge, pro-environmental behaviour and energy savings in households: An empirical study. *Applied Energy*, *184*, 1217–1229. https://doi.org/10.1016/j.apenergy.2016.06.017

Purohit, P., Höglund-Isaksson, L., Dulac, J., Shah, N., Wei, M., Rafaj, P., & Schöpp, W. (2020). Electricity savings and greenhouse gas emission reductions from global phase-down of hydrofluorocarbons. *Atmospheric Chemistry and Physics*, *20*(19), 11305–11327. https://doi.org/10.5194/acp-20-11305-2020

QGIS.org. (2023). *QGIS Geographic Information System. Open Source Geospatial Foundation Project* (3.28) [Computer software]. QGIS Association. http://www.qgis.org

Rapson, D. (2014). Durable goods and long-run electricity demand: Evidence from air conditioner purchase behavior. *Journal of Environmental Economics and Management*, *68*(1), 141–160. https://doi.org/10.1016/j.jeem.2014.04.003

Richter, M. (2016). Urban climate change-related effects on extreme heat events in Rostock, Germany. *Urban Ecosystems*, *19*(2), 849–866. https://doi.org/10.1007/s11252-015-0508-y

Rijksoverheid. (2019). *Uitvoeringsprogramma Circulaire Economie 2019—2023*. https://open.overheid.nl/documenten/ronl-13a37442-cbd9-45e5-8e97-8fa81d657cff/pdf

Rijksoverheid. (2023). *Openbare data energielabels* [dataset]. https://www.ep-online.nl/PublicData

Rinawati, D. I., Keeley, A. R., Takeda, S., & Managi, S. (2022). Life-cycle assessment of hydrogen utilization in power generation: A systematic review of technological and methodological choices. *Frontiers in Sustainability*, *3*. https://www.frontiersin.org/articles/10.3389/frsus.2022.920876

Ritchie, H., Rodés-Guirao, L., & Roser, M. (2023). Ozone Layer. *Our World in Data*. https://ourworldindata.org/ozone-layer

Ritchie, H., Roser, M., & Rosado, P. (2022, October 27). *Energy*. Our World in Data. https://ourworldindata.org/electricity-mix

RIVM. (2020). *Hitte en gezondheid: Herken de klachten en weet wat je moet doen | RIVM*. RIVM. https://www.rivm.nl/hitte/documenten/hitte-herken-klachten

Rizwan, A. M., Dennis, L. Y. C., & Liu, C. (2008). A review on the generation, determination and mitigation of Urban Heat Island. *Journal of Environmental Sciences*, *20*(1), 120–128. https://doi.org/10.1016/S1001-0742(08)60019-4

Robinson, B. H. (2009). E-waste: An assessment of global production and environmental impacts. *Science of The Total Environment*, *408*(2), 183–191. https://doi.org/10.1016/j.scitotenv.2009.09.044

Rouault, E., Warmerdam, F., Schwehr, K., Kiselev, A., Butler, H., Łoskot, M., Szekeres, T., Tourigny, E., Landa, M., Miara, I., Elliston, B., Chaitanya, K., Plesea, L., Morissette, D., Jolma, A., & Dawson, N. (2023). *GDAL* (v3.7.2) [Computer software]. Open Source Geospatial Foundation. https://doi.org/10.5281/ZENODO.5884351

Rovers, V., Bosch, P., Albers, R., Hove, B., Blocken, B., Dobbelsteen, A., Spit, T. J. M., Dikmans, M., Boonstra, B., Brolsma, R. J., Daanen, H., Echevarria, L., Groot, A., Hartogensis, O., Hensen, J., Heusinkveld, B., Hofman, J., Hutjes, R., Jacobs, C., & Zevenbergen, C. (2015). *Climate Proof Cities—Final Report*.

Rovers, V., Niessink, R., Wal, A. van der, Loonen, P., & Matthijssen, E. (2021). *Energievraag van ruimtekoeling in woningen* (P12657). TNO. https://publications.tno.nl/publication/34639092/k8jFX5/TNO-2021-R12657.pdf

Rupp, R. F., Vásquez, N. G., & Lamberts, R. (2015). A review of human thermal comfort in the built environment. *Energy and Buildings*, *105*, 178–205. https://doi.org/10.1016/j.enbuild.2015.07.047

RVO. (2018). *Energielabel C kantoren*. RVO.nl. https://www.rvo.nl/onderwerpen/wetten-en-regels-gebouwen/energielabel-c-kantoren

RVO. (2019). *EP-Online | Rijksdienst voor Ondernemend Nederland*. https://www.rvo.nl/onderwerpen/duurzaam-ondernemen/gebouwen/hulpmiddelen-tools-en-inspiratie-gebouwen/ep-online

RVO. (2020). *Klimaatmonitor—Energieverbruik Woningen*. https://klimaatmonitor.databank.nl/Jive/

RVO. (2023). *Investeringssubsidie duurzame energie en energiebesparing voor woningeigenaren (ISDE)*. RVO.nl. https://www.rvo.nl/subsidies-financiering/isde/woningeigenaren

Sacchi, R., Terlouw, T., Siala, K., Dirnaichner, A., Bauer, C., Cox, B., Mutel, C., Daioglou, V., & Luderer, G. (2022). PRospective EnvironMental Impact asSEment (premise): A streamlined approach to producing databases for prospective life cycle assessment using integrated assessment models. *Renewable and Sustainable Energy Reviews*, *160*, 112311. https://doi.org/10.1016/j.rser.2022.112311

Sachindra, D. A., Ng, A. W. M., Muthukumaran, S., & Perera, B. J. C. (2016). Impact of climate change on urban heat island effect and extreme temperatures: A case-study. *Quarterly Journal of the Royal Meteorological Society*, *142*(694), 172–186. https://doi.org/10.1002/qj.2642

Saheb, Y., Becirspahic, S., & Simon, J. (2006, April). *Effect of the Certification on Chillers Energy Efficiency*. IEECB, Frankfurt. https://inspectapedia.com/aircond/Saheb_ESEER_Chiller_Efficiency.pdf

Salamanca, F., Georgescu, M., Mahalov, A., Moustaoui, M., & Wang, M. (2014). Anthropogenic heating of the urban environment due to air conditioning. *Journal of Geophysical Research: Atmospheres*, *119*(10), 5949–5965. https://doi.org/10.1002/2013JD021225

Salman, Ö. (2018). Use of Land Surface Temperature (LST) Data in the Determination of High Areas of Forest FIre Risk in Erdemli District. *Journal of International Social Research*, *11*(57), 227–232. https://doi.org/10.17719/jisr.2018.2440

Sanchez, L., & Reames, T. G. (2019). Cooling Detroit: A socio-spatial analysis of equity in green roofs as an urban heat island mitigation strategy. *Urban Forestry & Urban Greening*, *44*, 126331. https://doi.org/10.1016/j.ufug.2019.04.014

Santamouris, M., & Vasilakopoulou, K. (2021). Present and future energy consumption of buildings: Challenges and opportunities towards decarbonisation. *E-Prime - Advances in Electrical Engineering, Electronics and Energy*, *1*, 100002. https://doi.org/10.1016/j.prime.2021.100002

Scarlat, N., Prussi, M., & Padella, M. (2022). Quantification of the carbon intensity of electricity produced and used in Europe. *Applied Energy*, *305*, 117901. https://doi.org/10.1016/j.apenergy.2021.117901

Schellen, L., Loomans, M. G. L. C., Wit, M. H. de, & Lichtenbelt, W. D. van M. (2013). Optimaal Thermisch Comfort. *TVVL Magazine*. https://tvvl.nl/wp-content/uploads/2023/05/2192_Optimaal-thermisch-comfort-TM06-2013.pdf

Schlosberg, D. (2013). Theorising environmental justice: The expanding sphere of a discourse. *Environmental Politics*, *22*(1), 37–55. https://doi.org/10.1080/09644016.2013.755387

Schwarz, W., & Harnisch, J. (2003). *Establishing the Leakage Rates of Mobile Air Conditioners* (p. 61). European Commission. https://ec.europa.eu/clima/system/files/2016-11/leakage_rates_final_report_en.pdf

Schweighofer, J. A. V., Wehrl, M., Baumgärtel, S., & Rohn, J. (2021). Calculating Energy and Its Spatial Distribution for a Subsurface Urban Heat Island Using a GIS-Approach. *Geosciences*, *11*(1), Article 1. https://doi.org/10.3390/geosciences11010024

Seltenrich, N. (2015). Between Extremes: Health Effects of Heat and Cold. *Environmental Health Perspectives*, *123*(11), A275–A279. https://doi.org/10.1289/ehp.123-A275

Seppänen, O. A., & Fisk, W. (2006). Some Quantitative Relations between Indoor Environmental Quality and Work Performance or Health. *HVAC&R Research*, *12*(4), 957–973. https://doi.org/10.1080/10789669.2006.10391446

Sepulveda, N. A., Jenkins, J. D., Edington, A., Mallapragada, D. S., & Lester, R. K. (2021). The design space for long-duration energy storage in decarbonized power systems. *Nature Energy*, *6*(5), Article 5. https://doi.org/10.1038/s41560-021-00796-8

SER. (2022). *Advies Hybride werken*. SER. https://www.ser.nl/-/media/ser/downloads/adviezen/2022/hybride-werken.pdf

Shah, V. P., Debella, D. C., & Ries, R. J. (2008). Life cycle assessment of residential heating and cooling systems in four regions in the United States. *Energy and Buildings*, *40*(4), 503–513. https://doi.org/10.1016/j.enbuild.2007.04.004

Shindell, D., Zhang, Y., Scott, M., Ru, M., Stark, K., & Ebi, K. L. (2020). The Effects of Heat Exposure on Human Mortality Throughout the United States. *GeoHealth*, *4*(4), e2019GH000234. https://doi.org/10.1029/2019GH000234

Singh, P., & Jitendra, Dr. (2022). A Review Paper on Natural and Synthetic Refrigerants. *IJIREM*. https://www.ijirem.org/view_abstract.php?title=-A-Review-Paper-on-Natural-and-Synthetic-Refrigerants&year=2022&vol=9&primary=QVJULTU5OQ==

Soeta, Y., & Shimokura, R. (2017). Sound quality evaluation of air-conditioner noise based on factors of the autocorrelation function. *Applied Acoustics*, *124*, 11–19. https://doi.org/10.1016/j.apacoust.2017.03.015

Solgi, E., Hamedani, Z., Fernando, R., Skates, H., & Orji, N. E. (2018). A literature review of night ventilation strategies in buildings. *Energy and Buildings*, *173*, 337–352. https://doi.org/10.1016/j.enbuild.2018.05.052

Spandagos, C., Baark, E., Ng, T. L., & Yarime, M. (2021). Social influence and economic intervention policies to save energy at home: Critical questions for the new

decade and evidence from air-condition use. *Renewable and Sustainable Energy Reviews*, *143*, 110915. https://doi.org/10.1016/j.rser.2021.110915

Srocka, M., Ciroth, A., Di Noi, C., & Lohse, T. (2023). *OpenLCA* (2.0.1) [Computer software]. GreenDelta. https://www.openlca.org/

Stehfest, E., Bouwman, L., Biemans, H., Elzen, M. den, Minnen, J. van, Prins, A. G., Vuuren, D. van, Kram, T., Alkemade, R., Bakkenes, M., Bouwman, A., Janse, J., Lucas, P., & Müller, C. (2014). *Integrated Assessment of Global Environmental Change with Model description and policy applications IMAGE 3.0*. PBL. https://www.pbl.nl/sites/default/files/downloads/pbl-2014-integrated_assessment_of_global_environmental_change_with_image30_735.pdf

Tang, R., & Etzion, Y. (2004). On thermal performance of an improved roof pond for cooling buildings. *Building and Environment*, *39*(2), 201–209. https://doi.org/10.1016/j.buildenv.2003.09.005

Tawalbeh, M., Al-Othman, A., Kafiah, F., Abdelsalam, E., Almomani, F., & Alkasrawi, M. (2021). Environmental impacts of solar photovoltaic systems: A critical review of recent progress and future outlook. *Science of The Total Environment*, *759*, 143528. https://doi.org/10.1016/j.scitotenv.2020.143528

te Riele, S., Huisman, C., Stoeldraijer, L., de Jong, A., van Duin, C., & Husby, T. (2019). *Regionale bevolkings- en huishoudensprognose 2019–2050*. CBS. https://www.pbl.nl/sites/default/files/downloads/pbl2019-pbl-cbs-regionale-bev-en-hhprognose-2019-2050-belangrijkste-uitkomsten-3812.pdf

Tendero, M. (2021). The time has come! The development of the European environmental conscience: Evidence from the Eurobarometer surveys from 1974 to 2020. In *The European Environmental Conscience in EU Politics*. Routledge.

TenneT TSO B.V. (2022). *Monitoring Leveringszekerheid 2022*. TenneT TSO B.V. https://tennet-drupal.s3.eu-central-1.amazonaws.com/default/2023-01/Monitoring%20Leveringszekerheid%202022_12JAN2023.pdf

The Engineering Toolbox. (2004a). *Air—Density, Specific Weight and Thermal Expansion Coefficient vs. Temperature and Pressure*. The Engineering Toolbox. https://www.engineeringtoolbox.com/air-density-specific-weight-d_600.html

The Engineering Toolbox. (2004b). *Air—Specific Heat vs. Temperature at Constant Pressure*. The Engineering Toolbox. https://www.engineeringtoolbox.com/air-specific-heat-capacity-d_705.html

The Hague Municipal Council. (2017). *Woonvisie Den Haag 2017-2030* (Raadsvoorstel 296833; p. 54). https://denhaag.raadsinformatie.nl/document/5234618/1/RIS296833_bijlage_Woonvisie_Den_Haag_2017-2030_

The Hague Municipality. (2019). *The Hague Resilience Strategy* (p. 58). The Hague Municipality. https://resilientthehague.nl/site/assets/files/1141/resilience_strategy_the_hague.pdf

The Hague Municipality. (2020). *Schone Energie voor Den Haag—Ontwerp Stedelijk Energieplan,* (p. 64). The Hague Municipality. https://denhaag.raadsinformatie.nl/document/9651577/1/RIS306869_Bijlage_3

The Hague Municipality. (2021a). *Haags Hitteplan* (p. 19). The Hague Municipality. https://denhaag.raadsinformatie.nl/document/11237059/1/RIS311683_Bijlage

The Hague Municipality. (2021b). *Voortgangsbrief Duurzaamheid 2021*. https://denhaag.raadsinformatie.nl/document/11475253/1/RIS311965_bijlage#:~:text=De%20CO2%2Duitstoot%20in%20Den,39%25%20ten%20opzichte%20van%201990.

The Hague Municipality. (2023, September). *Maandmonitor bevolking Den Haag*. Den Haag in Cijfers. https://denhaag.incijfers.nl/dashboard/en-us/bevolking-en-wonen/maandmonitor-bevolking

The Hotmaps Team. (2021). *Hotmaps* [dataset]. https://www.hotmaps.eu/map

The Kyoto Protocol to the UNFCCC, (1997). https://treaties.un.org/Pages/ViewDetails.aspx?src=IND&mtdsg_no=XXVII-7-a&chapter=27&clang=_en

tudelft3d & 3DGI. (2023). *3D BAG Viewer* (v2023.08.09) [dataset]. https://3dbag.nl/en/download

UNEP. (2017). *GEO-6: Global Environment Outlook: Regional assessment for the Pan-European Region*. UNEP. http://www.unep.org/resources/report/geo-6-global-environment-outlook-regional-assessment-pan-european-region

UNEP. (2022). *Refrigeration, Air Conditioning and Heat Pumps Technical Options Committee: 2022 Assessment Report*. UNEP. https://ozone.unep.org/system/files/documents/RTOC-assessment%20-report-2022.pdf

UNEP & IEA. (2020). *Cooling Emissions and Policy Synthesis Report: Benefits of cooling efficiency and the Kigali Amendment*. https://iea.blob.core.windows.net/assets/71c8db7e-1137-41ef-99c3-8f2c8d3a5d86/Cooling_Emissions_and_Policy_Synthesis_Report.pdf

Urchuegia, Z. M., Zacarés, M., Corberán, J. M., Montero, Á., Martos, J., & Witte, H. (2008). Comparison between the energy performance of a ground coupled water to water heat pump system and an air to water heat pump system for heating and cooling in typical conditions of the European Mediterranean coast. *Energy Conversion and Management*, *49*(10), 2917–2923. https://doi.org/10.1016/j.enconman.2008.03.001

U.S. Energy Information Administration. (2023). *International Electricity Consumption* [dataset]. https://www.eia.gov/international/data/world/electricity/electricity-consumption?pd=2&p=0000002&u=1&f=A&v=mapbubble&a=-&i=none&vo=value&t=I&g=none&l=2--2&l=163-00000000000000000000000000000000002000000000000002&l=48--48&l=140--140&l=9-01000002&l=73--73&l=72--72&l=71--71&s=1514764800000&e=1609459200000&&ev=false

USGBC. (2023). *LEED rating system | U.S. Green Building Council*. U.S. Green Building Council. https://www.usgbc.org/leed

Vabi. (2015). *Comforteisen toetsen met gebouwsimulatie* (p. 3). Vabi Software B.V. juli 2015 3. https://www.vabi.nl/wp-content/uploads/2016/02/Open-hier-Comforteisen-toetsen-met-gebouwsimulatie.pdf

Valancius, R., Singh, R. M., Jurelionis, A., & Vaiciunas, J. (2019). A Review of Heat Pump Systems and Applications in Cold Climates: Evidence from Lithuania. *Energies*, *12*(22), Article 22. https://doi.org/10.3390/en12224331

van Bueren, E., van Bohemen, H., Itard, L., & Visscher, H. (Eds.). (2012). *Sustainable Urban Environments*. Springer Netherlands. https://doi.org/10.1007/978-94-007-1294-2

van den Wijngaart, R., Folkert, R., & van Middelkoop, M. (2014). *Op weg naar een klimaatneutrale woningvoorraad in 2050: Achtergronden en uitgebreide resultaten*. PBL. https://www.pbl.nl/sites/default/files/downloads/pbl-2014-op-weg-naar-een-klimaatneutrale-woningvoorraad-in-2050-achtergrond_1333_1.pdf

van der Hoeven, F., & Wandl, A. (2018a). Haagse Hitte. In *BK BOOKS*. https://doi.org/10.7480/isbn.9789463660037

van der Hoeven, F., & Wandl, A. (2018b). Hotterdam: Mapping the social, morphological, and land-use dimensions of the Rotterdam urban heat island. *Urbani Izziv*, *29*(1), 58–72. https://doi.org/10.5379/urbani-izziv-en-2018-29-01-001

van der Niet, S., & Bruinsma, M. (2022). *Ketenemissies elektriciteit*. CE Delft. https://ce.nl/wp-content/uploads/2022/01/CE_Delft_210436_Ketenemissies_elektriciteit_Def.pdf

van Hove, L. W. A., Steeneveld, G. J., Jacobs, C. M. J., Heusinkveld, B. G., Elbers, J. A., Moors, E. J., & Holtslag, A. a. M. (2011). *Exploring the urban heat island intensity of Dutch cities: Assessment based on a literature review, recent meteorological observation and datasets provide by hobby meteorologists* (2170; p.). Alterra. https://library.wur.nl/WebQuery/wurpubs/406819

van Kempen, P. P. (2000). *Marktanalyse en prognose van airconditioningsystemen. - Rapportage van een markt-onderzoek naar causale factoren en trends*. https://docplayer.nl/8600513-Marktanalyse-en-prognose-van-airconditioningsystemen-rapportage-van-een-markt-onderzoek-naar-causale-factoren-en-trends.html

van Oers, L., & Guinée, J. (2016). The Abiotic Depletion Potential: Background, Updates, and Future. *Resources*, *5*(1), Article 1. https://doi.org/10.3390/resources5010016

van Oers, L., Koning, A., Guinée, J. B., & Huppes, G. (2002). *Abiotic resource depletion in LCA*. Rijkswaterstaat. https://web.universiteitleiden.nl/cml/ssp/projects/lca2/report_abiotic_depletion_web.pdf

van Straalen, V. M., Roskam, A. J., & Baldé, C. P. (2016). *Waste over Time* [R]. Statistics-Netherlands. https://github.com/Statistics-Netherlands/ewaste

Varela-Candamio, L., Novo-Corti, I., & García-Álvarez, M. T. (2018). The importance of environmental education in the determinants of green behavior: A meta-analysis approach. *Journal of Cleaner Production*, *170*, 1565–1578. https://doi.org/10.1016/j.jclepro.2017.09.214

Varrasi, J. (2022). Global Cooling: The History of Air Conditioning. *The American Society of Mechanical Engineers*. https://www.asme.org/topics-resources/content/Global-Cooling-The-History-of-Air-Conditioning

Vergeer, R. (2017). *Wie profiteert van het klimaatbeleid?* CE Delft. https://ce.nl/wp-content/uploads/2021/03/CE_Delft_7L42_Wie_profiteert_van_het_klimaatbeleid_def.pdf

Vicedo-Cabrera, A. M., Scovronick, N., Sera, F., Royé, D., Schneider, R., Tobias, A., Astrom, C., Guo, Y., Honda, Y., Hondula, D. M., Abrutzky, R., Tong, S., Coelho, M. de S. Z. S., Saldiva, P. H. N., Lavigne, E., Correa, P. M., Ortega, N. V., Kan, H., Osorio, S., … Gasparrini, A. (2021). The burden of heat-related mortality attributable to recent human-induced climate change. *Nature Climate Change*, *11*(6), Article 6. https://doi.org/10.1038/s41558-021-01058-x

Vienna Convention for the Protection of the Ozone Layer, (1985).

Wang, H., Zhao, L., Cao, R., & Zeng, W. (2021). Refrigerant alternative and optimization under the constraint of the greenhouse gas emissions reduction target. *Journal of Cleaner Production*, *296*, 126580. https://doi.org/10.1016/j.jclepro.2021.126580

Wang, S., & Wang, S. (2015). Impacts of wind energy on environment: A review. *Renewable and Sustainable Energy Reviews*, *49*, 437–443. https://doi.org/10.1016/j.rser.2015.04.137

Wang, Z., Dear, R. de, Luo, M., Lin, B., He, Y., Ghahramani, A., & Zhu, Y. (2018). Individual difference in thermal comfort: A literature review. *Building and Environment*, *138*, 181–193. https://doi.org/10.1016/j.buildenv.2018.04.040

Werner, S. (2016). European space cooling demands. *Energy*, *110*, 148–156. https://doi.org/10.1016/j.energy.2015.11.028

Wernet, G., Bauer, C., Steubing, B., Reinhard, J., Moreno-Ruiz, E., & Weidema, B. (2016). The ecoinvent database version 3 (part I): Overview and methodology. *The International Journal of Life Cycle Assessment*, *21*(9), 1218–1230. https://doi.org/10.1007/s11367-016-1087-8

WHO. (2008). *Heat-health action plans: Guidance*. WHO. https://www.who.int/publications-detail-redirect/9789289071918

Wi, A., & Chang, C.-H. (2019). Promoting pro-environmental behaviour in a community in Singapore – from raising awareness to behavioural change. *Environmental Education Research*, *25*(7), 1019–1037. https://doi.org/10.1080/13504622.2018.1528496

Wijsmuller, J. (2015a). *Actieprogramma Klimaatbestendige stad 2015/2016*. https://denhaag.raadsinformatie.nl/document/3323148/1/RIS283893_bijlage%202%20Programma%20Klimaatbestendig%20Den%20Haag

Wijsmuller, J. (2015b, July 10). *Programma Klimaatbestendig Den Haag*. https://denhaag.raadsinformatie.nl/document/3323148/1/RIS283893_bijlage%202%20Programma%20Klimaatbestendig%20Den%20Haag

Wijzigingswet Elektriciteitswet 1998, enz. (Voortgang energietransitie), (2021). https://wetten.overheid.nl/BWBR0040852/2021-01-01

WMO. (2023, January 11). Past eight years confirmed to be the eight warmest on record. *Press Releases*. https://public.wmo.int/en/media/press-release/past-eight-years-confirmed-be-eight-warmest-record

Xie, X., Qin, S., Gou, Z., & Yi, M. (2020). Can Green Building Promote Pro-Environmental Behaviours? The Psychological Model and Design Strategy. *Sustainability*, *12*(18), Article 18. https://doi.org/10.3390/su12187714

Yanagitani, K., & Kawahara, K. (2000). LCA study of air conditioners with an alternative refrigerant. *The International Journal of Life Cycle Assessment*, *5*(5), 287–290. https://doi.org/10.1007/BF02977581

Yang, L., Yan, H., & Lam, J. C. (2014). Thermal comfort and building energy consumption implications – A review. *Applied Energy*, *115*, 164–173. https://doi.org/10.1016/j.apenergy.2013.10.062

Yuan, F., Yao, R., Sadrizadeh, S., Li, B., Cao, G., Zhang, S., Zhou, S., Liu, H., Bogdan, A., Croitoru, C., Melikov, A., Short, C. A., & Li, B. (2022). Thermal comfort in hospital buildings – A literature review. *Journal of Building Engineering*, *45*, 103463. https://doi.org/10.1016/j.jobe.2021.103463

Yusliza, M. Y., Amirudin, A., Rahadi, R. A., Nik Sarah Athirah, N. A., Ramayah, T., Muhammad, Z., Dal Mas, F., Massaro, M., Saputra, J., & Mokhlis, S. (2020). An Investigation of Pro-Environmental Behaviour and Sustainable Development in Malaysia. *Sustainability*, *12*(17), Article 17. https://doi.org/10.3390/su12177083

Zaccagnini, P., Williams, A., Bijkerk, M. A., & Lubben, M. W. B. (2023). *Energy Transition Model* [Ruby]. Quintel. https://energytransitionmodel.com/

Zhan, W., Ju, W., Hai, S., Ferguson, G., Quan, J., Tang, C., Guo, Z., & Kong, F. (2014). Satellite-Derived Subsurface Urban Heat Island. *Environmental Science & Technology*, *48*(20), 12134–12140. https://doi.org/10.1021/es5021185

Zhou, X., & Chen, H. (2018). Impact of urbanization-related land use land cover changes and urban morphology changes on the urban heat island phenomenon. *Science of The Total Environment*, *635*, 1467–1476. https://doi.org/10.1016/j.scitotenv.2018.04.091

Zhuang, L., Huang, J., Li, F., & Zhong, K. (2022). Psychological adaptation to thermal environments and its effects on thermal sensation. *Physiology & Behavior*, *247*, 113724. https://doi.org/10.1016/j.physbeh.2022.113724

Zmeureanu, R., & Yu Wu, X. (2007). Energy and exergy performance of residential heating systems with separate mechanical ventilation. *Energy*, *32*(3), 187–195. https://doi.org/10.1016/j.energy.2006.04.007

8 Appendices

Appendix A GIS Data Files and Background Research Used in the Cooling Demand Model

The GIS data files used as input for the cooling demand model, as well as the geodata files containing the spatial results, are of a size that exceeds GitHub's storage capacity. Hence, these are hosted on Zenodo. Furthermore, background research was conducted to ascertain the projections of input parameters for future scenarios. The primary data and calculations conducted during this background research are contained within an Excel file, which is also accessible on Zenodo.

Both the GIS geodata files and the background research spreadsheet are available at the following URL: https://zenodo.org/doi/10.5281/zenodo.8344580.

Appendix B GIS Methodology Flow

This appendix contains a detailed overview of the steps performed to extract and pre-process the building data necessary to calculate the cooling demand and resulting environmental impacts in the cooling demand model. This extraction and processing was done using Geographic Information Systems (GIS) modeling, specifically using QGIS and the GeoPandas library in Python (Jordahl et al., 2020; QGIS.org, 2023). The portion of the processing that was performed in Python is further documented in Appendix C. Multiple data sources were used, mainly:

- Statistical regions: several shapefiles containing statistical regions were used to organize and clip the spatial data and the resulting cooling demand and environmental impact data.
- *Basisregistratie Adressen en Gebouwen* (BAG; Registry of Addresses and Buildings): contains spatial information of all registered buildings, residences and addresses in the Netherlands (PDOK, 2023a). It also contains administrative information such as the construction year, end use, use status, etc.
- 3D BAG: a separate data source containing height profiles for each building in the BAG (tudelft3d & 3DGI, 2023). It does not contain any administrative information.
- *EP-online* (Energy label registry): The registry contains energy label data which can be linked to BAG residences (RVO, 2019).

Statistical regions

- The outline of The Hague municipality through the Municipal boundaries (*Gemeenten*) layer, sourced from the Administrative boundaries (*Bestuurlijke Gebieden*) dataset on the PDOK WFS service (PDOK, 2023b)
- District (*Wijken*) and Neighborhood (*Buurten*) layers were downloaded from the PDOK WFS service (from the *CBS Wijken en Buurten 2022* data package) and clipped to the outline of The Hague (PDOK, 2023e)
- The 4-digit postcodes layer was downloaded from PDOK WFS service (*CBS Postcode4 statistieken 2020*) and clipped to The Hague's outline (PDOK, 2023c)
- The census block layer was downloaded from the PDOK WFS service (from the *CBS Vierkantstatistieken 100m 2021* data package) and also clipped to the outline of The Hague (PDOK, 2023d).

BAG

- BAG data was acquired through the download of a BAG GeoPackage from the BAG ATOM download page (PDOK, 2023a).
- In the resulting GeoPackage, the Residences (*Verblijfsobject*) and Building (*Pand*) layers were used in further analysis.
- These layers were subsequently clipped to match The Hague's outline.
- The ground floor area for buildings was determined by the GeoPandas *area* function on the geometry of the *Building* layer.

3D BAG

- Due to limitations imposed by the PDOK WFS service, which restricts the number of downloadable buildings to 10,000, it was necessary to acquire 145 individual GeoPackages for tiles covering The Hague from the 3D BAG website (tudelft3d & 3DGI, 2023).
- These GeoPackages were merged using the *ogr2ogr append* function from the GDAL library in bash (Rouault et al., 2023).
- Roof elevation data was extracted from the *LoD 1.2 2D* layer from the resulting GeoPackage.
- Ground elevation data was obtained from the *Pand* layer.
- Both layers were clipped to match The Hague's outline.
- Roof and ground elevation data from the *LoD 1.2 2D* and *Pand* layers were joined to the *Pand* layer in the BAG dataset using the BAG ID of each building.
- Building height was calculated as the difference between the 70th percentile of roof elevation (accounting for spires and slanted roofs) and the elevation of the ground floor below the building (*building_height = b3_h_70p - b3_h_maaiveld*).
- Building volume was determined by multiplying the ground-floor area (derived from the vector shape) with the calculated height. This method was chosen over BAG 3D's volume metrics due to the simpler calculation process and minimal differences in results. The volume data of the latter also contained a significant number of outliers and negative values, which would further complicate the data processing.

Energy labels

- Energy labels were downloaded from the Energy label registry (EP-online) as a 1 GB CSV file (RVO, 2019).
- Postcodes within The Hague were extracted from the postcodes layer, and the CSV file was filtered accordingly.
- To integrate energy labels into the analysis, they were joined to the Residence layer using the BAG residence ID.
- Energy label data was available for 55% of the total floor area across all end uses, while it was available for 61% and 68% of the residential and office floor space, respectively.

Further processing

A spatial join was performed to join residence-level data to BAG buildings, using the GeoPandas *within* predicate. Join rules were defined as follows:

- Residence floor area: Sum and save as the total floor area of the building.
- Residence count: Sum and save as the number of residences in the building.
- Residence end use: The main end use within the building was determined by grouping the constituent residences by their end use, and then selecting the end use with the largest floors area. Buildings without a residential or office end-use were excluded from the cooling demand model.[54]
- Residence energy label: The mean energy label was calculated by translating energy labels to integers (A+++++: 1, A++++: 2, ..., G: 12), taking the average numerical energy label, weighing it by the floor area of the residences, rounding it to the nearest integer, and then translating it back into an energy label.

[54] Some buildings have a mixed end use (e.g., residential and office, or office and industrial). These mixed end-use buildings make up roughly 2% of the total floor area in The Hague. It is not determinable which of these is the dominant end use within the building, as these mixed end uses are registered on the residence level. Hence, these buildings are not considered in the cooling demand model.

Appendix C Python Implementation of the Cooling Demand Model

The main cooling demand model, the extraction and pre-processing of GIS data, the sensitivity analyses, and the generation of figures for the interpretation of results were all implemented in Python. The repository containing the python code can be found on this URL: https://github.com/simonvanlierde/msc-thesis-ie.

This repository contains all the python code and input parameter files used in the analysis. However, due to file size limitations, it does not include the GIS data files used as input for the CDM or the GIS data files containing the CDM results. For these, please refer to Appendix A.

Appendix D Global Input Parameters for the Cooling Demand Model

This appendix contains the global input parameters for each scenario, i.e., the parameters that are assumed to be equal for each building.

Table 52: Global input parameters which are varied throughout the scenarios.

	Scenario							
Parameter	*SQ (2020)*	*2030*	*2050-L*	*2050-M*	*2050-H*	**Unit**	**Description**	**Source**
Daytime UHI effect	8.3	8.3	8.4	8.6	9.8	°C	The UHI effect by day	Assumption
Nighttime UHI effect	2.1	2.1	2.2	2.4	3.6	°C	The UHI effect by day	Assumption
Winter-time temperature boost	0.0	0.4	0.6	1.0	1.5	°C	The climate change-induced temperature rise during winter months (Dec - Feb)	Based on (Attema et al., 2014)
Spring-time temperature boost	0.0	0.2	0.5	0.8	1.2	°C	The climate change-induced temperature rise during spring months (Mar - May)	Based on (Attema et al., 2014)
Summer-time temperature boost	0.0	0.3	0.6	0.9	1.3	°C	The climate change-induced temperature rise during summer months (Jun - Aug)	Based on (Attema et al., 2014)
Autumn-time temperature boost	0.0	0.3	0.6	1.0	1.3	°C	The climate change-induced temperature rise during autumn months (Sep - Nov)	Based on (Attema et al., 2014)
Annual-average temperature boost	0.0	0.3	0.6	0.9	1.3	°C	The climate change-induced temperature rise, average throughout the year (for adding to the subsurface temperature)	Based on (Attema et al., 2014)
Solar radiation increase - summer	0	0.5%	1.6%	2.2%	4.8%	-	The relative increase in solar radiation, in summer	Based on (Attema et al., 2014)
Solar radiation increase - rest of year	0	0.1%	0.5%	0.3%	0.9%	-	The relative increase in solar radiation, outside of summer	Based on (Attema et al., 2014)
Effective cooling temperature	25	25	26	25	23	°C	The upper limit of the desired indoor temperature range, i.e., the temperature at which cooling is activated	Assumption
Subsurface temperature	11.8	12.1	12.4	12.7	13.1	°C	The average subsurface temperature in reference period	
Carbon intensity of electric grid	0.43	0.16	0.03	0.04	0.16	kg CO_2-eq / kWh	The carbon intensity of the Dutch electricity grid	Based on (Hammingh et al., 2021; Ouden et al., 2020; van der Niet & Bruinsma, 2022)
Global warming potential of refrigerant	1,603	809	0	1	809	kg CO_2-eq / kg	The global warming potential of the refrigerant within active cooling equipment	(Hodnebrog et al., 2020)
New residential building stock growth	0%	50%	21%	97%	182%	-	The growth of the post-2003 fraction of the residential building stock	(te Riele et al., 2019)
Old office building stock growth	0%	-28%	-43%	-23%	-14%	-	The shrinkage of the pre-2003 office building stock	(Manders & Kool, 2015)

Table 53: Global input parameters which are constant throughout the scenarios.

Parameter	Value	Unit	Description	Source
The end year of the reference weather data series	2018	year	The start of the reference period for the status quo scenario in the cooling demand model. The same reference period is used for the scenarios and climate change is modeled on top of the raw weather data	Assumption
The end year of the reference weather data series	2022	year	The end of the reference period for the status quo scenario in the cooling demand model	Assumption
The weather station for which to the fetch weather data	330	-	The KNMI number for the Hoek van Holland weather station	Assumption
The average household size	2.01	-	Average number of people per household in The Hague	(The Hague Municipality, 2023)
Office dweller density	0.067	-	The average amount of people per area in offices, assumed from 15 m^2 per person	Assumption
Heat capacity of air	1,006	$Jkg^{-1}K^{-1}$	The heat capacity of dry air in typical room conditions	(The Engineering Toolbox, 2004b)
Density of air	1.2	kgm^{-3}	The mass density of dry air in typical room conditions	(The Engineering Toolbox, 2004a)
Building type age division year	2003	year	The cutoff year between old and new building types	Assumption
Building type height division	17.5	m	The cutoff height between low- and high-rise buildings	Assumption
Cooling demand cap percentile	98	-	The percentile of the cooling demand power that the cooling load profiles should be capped at, which is a proxy for the thermal discomfort tolerance	Assumption
Indoor heat transfer coefficient	7.5	$Wm^{-2}K^{-1}$	Indoor combined heat transfer coefficients for convection and radiation	(van Bueren et al., 2012)
Outdoor heat transfer coefficient	27.5	$Wm^{-2}K^{-1}$	Outdoor combined heat transfer coefficients for convection and radiation	(van Bueren et al., 2012)
Heat generation per person	120	W	The heat produced per person	(van Bueren et al., 2012)
Lighting heat generation density	6	Wm^{-2}	The average heat produced by lighting per floor area	(van Bueren et al., 2012)
Abiotic resource depletion intensity	$2.6 \cdot 10^{-5}$	kg Sb-eq/kg	The relative abiotic resource depletion of cooling equipment	Based on ecoinvent processes
Crustal scarcity intensity	1,625	kg Si-eq/kg	The relative crustal scarcity of cooling equipment	Based on ecoinvent processes
Carbon intensity of production	4.2	kg CO_2-eq/kg	The relative climate change impact of cooling equipment production	Based on ecoinvent processes
Carbon intensity of EoL phase	0.3	kg CO_2-eq/kg	The relative climate change impact of treatment of waste cooling equipment	Based on ecoinvent processes

Appendix E Building Type Dependent Input Parameters for the Cooling Demand Model

This appendix presents the input parameters used in the cooling demand model which are dependent on the building type. Note that building population, presence load factors, and cooling technology mixes also depend on the building type, but these are presented in Appendix D, Appendix G, and Appendix I respectively.

Table 54: Descriptions of the building type-dependent input parameters used in the cooling demand model.

Parameter	Unit	Description	Source
Glazing fraction	-	The fraction of each facade covered by windows. It is assumed to be 15% for residential buildings and 25% for office buildings.	Assumption
Ventilation rate per person	m^3h^{-1}	The mechanical ventilation rate per person. It is assumed to be 25 m^3h^{-1} for newer offices and new residential high rises, and zero for all other buildings.	Based on (van Bueren et al., 2012)
Infiltration rate	h^{-1}	The air change rate by infiltration (in terms of building volume per hour). It is assumed to be 0.1 h^{-1} for newer buildings and 0.5 h^{-1} for older buildings.	Based on (van Bueren et al., 2012)
Appliance heat generation density	Wm^{-2}	The average heat produced by other electrical appliances per floor area, in residences. Assumed to be 5 Wm^{-2} for residential buildings and 15 Wm^{-2} for offices.	Based on (van Bueren et al., 2012)

Table 55: The values of the building type-dependent input parameters used in the cooling demand model. These values are not altered throughout the scenarios.

Building type	Glazed fraction of facade	Ventilation rate per person (m^3h^{-1})	Infiltration (ACH)	Internal heat gain from appliances (Wm^{-2})
1: New high-rise residential	0.15	25	0.10	5
2: Old high-rise residential	0.15	0	0.50	5
3: New low-rise residential	0.15	0	0.10	5
4: Old low-rise residential	0.15	0	0.50	5
5: New high-rise office	0.25	25	0.10	15
6: Old high-rise office	0.25	0	0.50	15
7: New low-rise office	0.25	25	0.10	15
8: Old low-rise office	0.25	0	0.50	15

Appendix F Energy Class Dependent Input Parameters for the Cooling Demand Model

This appendix presents the input parameters used in the cooling demand model which are dependent on the energy class (which is a collection of energy labels) of a building.

Table 56: Descriptions of the energy class-dependent input parameters used in the cooling demand model.

Parameter	Unit	Description	Source
Heat resistance of outer walls	m^2KW^{-1}	The thermal resistance of the outer walls.	Based on (van Bueren et al., 2012)
Heat resistance of the roof	m^2KW^{-1}	The thermal resistance of the roof.	Based on (van Bueren et al., 2012)
Heat resistance of the ground floor	m^2KW^{-1}	The thermal resistance of the ground floor with respect to the soil.	Based on (van Bueren et al., 2012)
Heat transmittance of windows	$Wm^{-2}K^{-1}$	Heat transmittance of windows. Transmittance is simply the inverse of resistance, but insulation values for windows are typically presented in terms of the heat transmittance.	Based on (van Bueren et al., 2012)
Solar factor of windows	-	The fraction of solar radiation let through by the window glass, also known as the *g value*.	Based on (van Bueren et al., 2012)

Table 57: The values of the energy class-dependent input parameters used in the cooling demand model. These values are not altered throughout the scenarios.

Energy class	Heat resistance of outer walls (m^2KW^{-1})	Heat resistance of roof (m^2KW^{-1})	Heat resistance of ground floor (m^2KW^{-1})	Heat transmittance of windows ($Wm^{-2}K^{-1}$)	Solar factor of windows
A–A+++++	8	10	6	1	0.4
B–C	3	4	2	2	0.6
D–E	1	1.5	0.75	3	0.7
F–G	0.35	0.5	0.25	6	0.8

Note that while the energy class dependent parameters are not varied throughout the scenarios, the allocation of energy labels to energy classes is shifted as a proxy for shifting thermal insulation values over time. See section 3.3.2.5 for more details.

Appendix G Presence Load Factors Used in the Cooling Demand Model

This appendix contains the presence or activation load factors used in the cooling demand model. The presence load is expressed in the fraction of the full amount of people, or the fraction of the full activation of lights or appliances throughout the day. For example, a people presence load factor of 0.2 implies that 20% of the full population of the building is present in that hour. A lighting presence load factor of 0.5 implies that 50% of the lighting in the building is activated.

Table 58: Presence and activation load factors of people, lights, and appliances.

	Presence of people		**Activation of lighting**		**Activation of appliances**	
Hour of the day	*Residential*	*Office*	*Residential*	*Office*	*Residential*	*Office*
1	1	0.2	0.2	0	0	0
2	1	0.2	0.2	0	0	0
3	1	0.2	0.2	0	0	0
4	1	0.2	0.2	0	0	0
5	1	0.2	0.2	0	0	0
6	1	0.2	0.2	0	0	0
7	1	0.2	0.2	0	0	0
8	1	1	1	0.2	1	1
9	1	1	1	0.2	1	1
10	0.2	0.2	0.2	1	1	1
11	0.2	0.2	0.2	1	1	1
12	0.2	0.2	0.2	1	1	1
13	0.2	0.2	0.2	1	1	1
14	0.2	0.2	0.2	1	1	1
15	0.2	0.2	0.2	1	1	1
16	0.2	0.2	0.2	1	1	1
17	0.2	0.2	0.2	1	1	1
18	1	1	1	0.2	1	1
19	1	1	1	0.2	1	1
20	1	1	1	0.2	1	1
21	1	1	1	0.2	1	1
22	1	0.2	0.2	0	0	0
23	1	0.2	0.2	0	0	0
24	1	0.2	0.2	0	0	0

Appendix H Production- and End-of-Life Phase Environmental Impacts for each Cooling Technology

This appendix presents the integration of the LCA results presented in section 4.1.3 for each of the cooling technologies used in the model. The resulting properties and environmental impacts were used to determine the environmental impacts of the residential and office cooling demand.

Table 59: Proxy products, production- and end-of-life phase environmental impacts for each cooling equipment type.

Cooling equipment type	Proxy product	Mass per unit (kg)	Average lifetime (year)	Cooling power capacity (kW)	Production- phase GHG emissions (kg CO_2-eq/(kW·yr))	EoL- phase GHG emissions (kg CO_2-eq/(kW·yr))	Resource depletion (kg Sb-eq/(kW·year))	Resource scarcity (kg Si-eq/(kW·year))
Air-Source Heat pump (ASHP)	Daikin Altherma 3 R F lucht-waterpomp	198	13	6.0	11	0.78	$7.0 \cdot 10^{-5}$	4,278
Ground-source heat pump (GSHP)	Kensa Shoebox ground source heat pump	100	13	6.0	5.5	0.39	$3.5 \cdot 10^{-5}$	2,166
Water-Source Heat pump (WSHP)	W/W Warmtepomp 5G - 6,5 kW	92	13	6.5	4.7	0.34	$3.0 \cdot 10^{-5}$	1,847
Chiller	AQVL Air Cooled Chiller	1,111	20	105	2.2	0.16	$1.4 \cdot 10^{-5}$	860
Split AC	Panasonic split airco 3.5kW	40	13	3.5	3.8	0.27	$2.4 \cdot 10^{-5}$	1,485
Portable AC	Just Cooling Mobile SMart AC 9000 BTU	27	12	2.6	3.5	0.25	$2.3 \cdot 10^{-5}$	1,386

Appendix I Cooling Technology Mix Choices for Scenarios

This appendix presents a collection of tables and charts showcasing the cooling technology mixes assumed for each building types in the various scenarios. These visuals offer insights into the changing landscape of cooling solutions per building type, reflecting the influence of technological progress, market trends, and policy dynamics on the distribution of cooling equipment. The methodology used to determine these figures is described as described in section 3.2.3.1 and section 3.3.3.6. Note that for building type 2 (old high-rise residences), the same total market penetration rate (MPR) of heat pumps is assumed as for building types 3 and 4 (low-rise residences). Note that in the following tables and figures, WSHP, ASHP, and GSHP stand for water-, air-, and ground-source heat pump, respectively.

Table 60: Estimated cooling equipment mix per building type used in the Status Quo (2020) scenario, based on (Rovers et al., 2021).

Building type	Total MPR	ASHP	GSHP	WSHP	Chiller	Split AC	Portable AC	No active cooling equipment
1	18%	3%	1%	1%	14%	-	-	82%
2	15%	-	-	-	-	-	15%	86%
3	14%	1%	1%	1%	-	6%	6%	86%
4	14%	1%	1%	1%	-	6%	6%	86%
5	69%	10%	4%	2%	54%	-	-	31%
6	69%	10%	4%	2%	54%	-	-	31%
7	51%	1%	2%	1%	-	22%	25%	49%
8	51%	1%	2%	1%	-	22%	25%	49%

Table 61: Cooling technology mix choices for the 2030 scenario.

Building type	Total MPR	ASHP	GSHP	WSHP	Chiller	Split AC	Portable AC	No active cooling equipment
1	46%	6%	2%	3%	36%	0%	0%	54%
2	37%	4%	2%	2%	0%	0%	29%	63%
3	36%	4%	2%	2%	0%	13%	15%	64%
4	36%	4%	2%	2%	0%	13%	15%	64%
5	100%	8%	3%	1%	88%	0%	0%	0%
6	100%	8%	3%	1%	88%	0%	0%	0%
7	100%	3%	6%	3%	0%	41%	47%	0%
8	100%	3%	6%	3%	0%	41%	47%	0%

Table 62: Cooling technology mix choices for the 2050-L scenario.

Building type	Total MPR	ASHP	GSHP	WSHP	Chiller	Split AC	Portable AC	No active cooling equipment
1	61%	34%	12%	16%	0%	0%	0%	39%
2	48%	26%	9%	12%	0%	0%	0%	52%
3	48%	26%	9%	12%	0%	0%	0%	52%
4	48%	26%	9%	12%	0%	0%	0%	52%
5	100%	33%	12%	6%	49%	0%	0%	0%
6	100%	33%	12%	6%	49%	0%	0%	0%
7	100%	13%	26%	13%	0%	23%	26%	0%
8	100%	13%	26%	13%	0%	23%	26%	0%

Table 63: Cooling technology mix choices for the 2050-M scenario.

Building type	Total MPR	ASHP	GSHP	WSHP	Chiller	Split AC	Portable AC	No active cooling equipment
1	76%	21%	7%	10%	39%	0%	0%	24%
2	61%	16%	6%	8%	0%	0%	31%	39%
3	60%	16%	6%	8%	0%	14%	16%	40%
4	60%	16%	6%	8%	0%	14%	16%	40%
5	100%	19%	7%	4%	70%	0%	0%	0%
6	100%	19%	7%	4%	70%	0%	0%	0%
7	100%	7%	15%	7%	0%	33%	37%	0%
8	100%	7%	15%	7%	0%	33%	37%	0%

Table 64: Cooling technology mix choices for the 2050-H scenario.

Building type	Total MPR	ASHP	GSHP	WSHP	Chiller	Split AC	Portable AC	No active cooling equipment
1	100%	5%	2%	3%	36%	0%	54%	0%
2	80%	4%	2%	2%	0%	0%	72%	20%
3	79%	4%	2%	2%	0%	13%	58%	21%
4	79%	4%	2%	2%	0%	13%	58%	21%
5	100%	8%	3%	1%	88%	0%	0%	0%
6	100%	8%	3%	1%	88%	0%	0%	0%
7	100%	3%	6%	3%	0%	41%	47%	0%
8	100%	3%	6%	3%	0%	41%	47%	0%

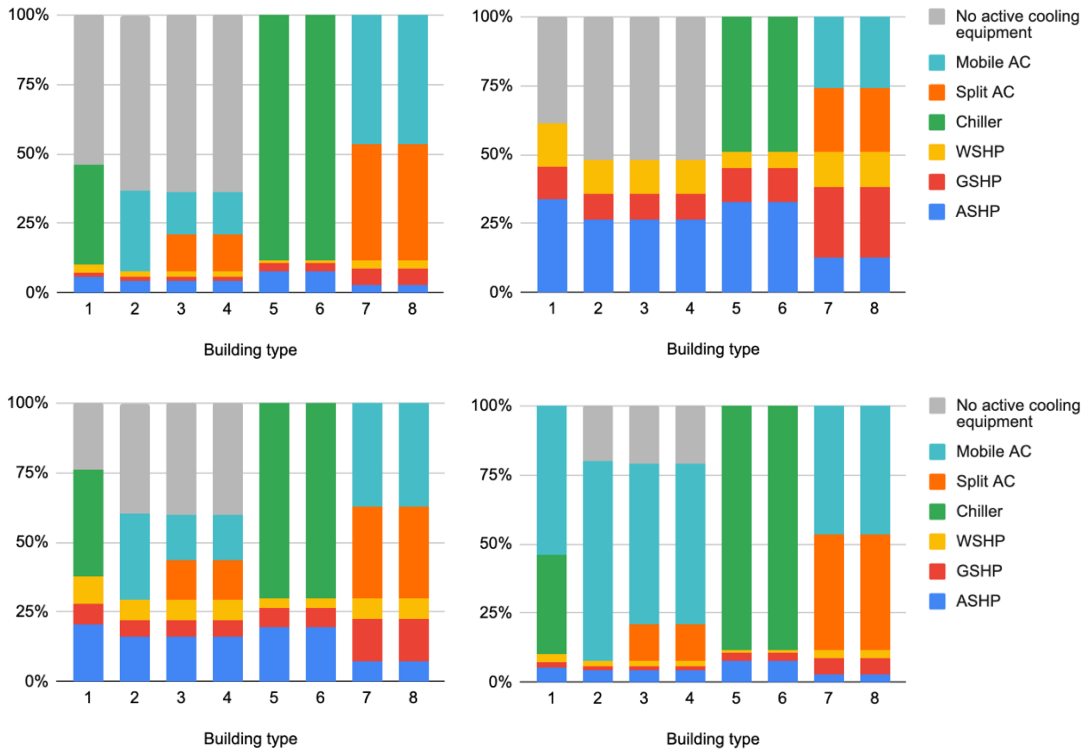

Figure 99: Cooling technology mix choices for the 2030 (top-left), 2050-L (top-right), 2050-M (bottom-left), and 2050-H (bottom-right) scenarios.

Appendix J Cooling Technology Dependent Input Parameters for the Cooling Demand Model

This appendix presents the input parameters used in the cooling demand model which are dependent on the energy class (which is a collection of energy labels) of a building.

Table 65: Descriptions of the cooling technology-dependent input parameters used in the cooling demand model.

Parameter	Unit	Description	Source
Average lifetime	year	The average operational lifetime of the cooling technology. Used to annualize life-cycle impacts.	Based on (Penman et al., 2000)
Material density	kg/kW	The mass of cooling equipment (in kg) per installed power capacity (in kW)	Based on market research
Refrigerant density	kg/kW	The mass of the refrigerant charge within the cooling equipment (in kg) per installed power capacity (in kW)	Based on market research
Effective refrigerant leakage rate	%/year	The percentage of the refrigerant charge that escapes into the environment each year, including leaks during installation and equipment disposal, averaged over the equipment's typical lifespan.	Based on (Penman et al., 2000)
Energy efficiency (SEER)	-	The SEER rating represents the ratio of cooling output over the course of a standard cooling season to the overall electrical energy consumption during that same timeframe.	Based on (Dittmann et al., 2016)

Table 66: The values of static cooling technology-dependent input parameters used in the cooling demand model. These values are not altered throughout the scenarios.

Cooling technology	Average lifetime (year)	Refrigerant density (kg/kW)	Material density (kg/kW)
Air-source heat pump (ASHP)	12.5	0.3	32.9
Ground-source heat pump (GSHP)	12.5	0.3	16.7
Water-source heat pump (WSHP)	12.5	0.2	14.2
Chiller	20.0	0.1	10.6
Large split AC	12.5	0.2	11.4
Portable AC	12.0	0.1	10.2

Table 67: The values of energy efficiencies (SEERs) used for each cooling technology as input for the cooling demand model.

Cooling technology	Scenario				
	SQ (2020)	*2030*	*2050-L*	*2050-M*	*2050-H*
Air-source heat pump (ASHP)	4.8	6.5	8.9	8.1	7.31
Ground-source heat pump (GSHP)	6.2	8.5	11.5	10.5	9.50

Water-source heat pump (WSHP)	7.5	10.2	13.9	12.7	11.5
Chiller	4.1	5.0	6.5	6.0	5.49
Large split AC	4.8	6.5	8.9	8.1	7.31
Portable AC	2.5	2.9	4.1	3.7	3.30

Table 68: The effective annual refrigerant leakage rates (as a percentage of the total refrigerant charge) used for each cooling technology as input for the cooling demand model.

Cooling technology	**Scenario**				
	SQ (2020)	*2030*	*2050-L*	*2050-M*	*2050-H*
Air-source heat pump (ASHP)	5%	4%	1%	2%	5%
Ground-source heat pump (GSHP)	5%	4%	1%	2%	5%
Water-source heat pump (WSHP)	5%	4%	1%	2%	5%
Chiller	10%	4%	2%	2%	10%
Large split AC	5%	4%	1%	2%	5%
Portable AC	23%	18%	6%	9%	23%

Appendix K The Urban Heat Island Effect and Sub-Surface Temperatures

In addition to air temperatures, the UHI effect also tends to increase urban subsurface temperatures relative to the surrounding countryside. While a lot of research has been performed on the UHI effects of air- and surface temperatures, not much quantitative research has been performed on subsurface (i.e., soil) UHI effects.[55]

While the available research shows that there is a significant subsurface UHI (SubUHI) effect, it is highly dependent on the geographic location, measurement depth, and definitions of urban vs. rural areas (see Table 69). The De Bilt weather station is in a semi-urban area, making it even more complex to estimate the relative SubUHI effect between De Bilt and The Hague. Therefore, the SubUHI effect is not considered in this analysis; instead, subsurface temperatures at De Bilt weather station and The Hague were assumed to be the same.

Table 69: Several records of the Subsurface Urban Heat Island effect.

Location	Annual average SubUHI effect (°C)	Depth (m)	Source
Oberhausen, Germany	2.8	0.7	(N. Müller et al., 2014)
United Kingdom	0.6	1	(Busby, 2015)
Beijing, China	4.3	1.5	(Zhan et al., 2014)

[55] Confusingly, in the literature both the surface and the subsurface UHI effect are sometimes abbreviated to SUHI. To avoid ambiguity, SubUHI is used to indicate the subsurface UHI effect.

Appendix L Background Data Used in the Determination of Scenario Parameters

This appendix contains tables and figures describing the background data used to determine future weather- and electricity grid-related parameters.

Season [A]	Variable	Indicator	Climate [B] 1951–1980	Climate [B] 1981–2010 = reference period	Scenario change values for the climate around 2050 [C] (2036–2065)				Scenario change values for the climate around 2085 [C] (2071–2100)				Natural variations averaged over 30 years [D]
					G_L	G_H	W_L	W_H	G_L	G_H	W_L	W_H	
	Global temperature rise:				+1 °C	+1 °C	+2 °C	+2 °C	+1.5 °C	+1.5 °C	+3.5 °C	+3.5 °C	
	Change in air circulation pattern:				Low value	High value	Low value	High value	Low value	High value	Low value	High value	
Year	Sea level at North Sea coast	absolute level [E]	4 cm below NAP	3 cm above NAP	+15 to +30 cm	+15 to +30 cm	+20 to +40 cm	+20 to +40 cm	+25 to +60 cm	+25 to +60 cm	+45 to +80 cm	+45 to +80 cm	± 1.4 cm
		rate of change	1.2 mm/year	2.0 mm/year	+1 to +5.5 mm/year	+1 to +5.5 mm/year	+3.5 to +7.5 mm/year	+3.5 to +7.5 mm/year	+1 to +7.5 mm/year	+1 to +7.5 mm/year	+4 to +10.5 mm/year	+4 to +10.5 mm/year	± 1.4 mm/year
	Temperature	mean	9.2 °C	10.1 °C	+1.0 °C	+1.4 °C	+2.0 °C	+2.3 °C	+1.3 °C	+1.7 °C	+3.3 °C	+3.7 °C	± 0.16 °C
	Precipitation	mean amount	774 mm	851 mm	+4%	+2.5%	+5.5%	+5%	+5%	+5%	+7%	+7%	± 4.2%
	Solar radiation	solar radiation	346 kJ/cm² [F]	354 kJ/cm² [F]	+0.6%	+1.6%	-0.8%	+1.2%	-0.5%	+1.1%	-0.9%	+1.4%	± 1.6%
	Evaporation	potential evaporation (Makkink)	534 mm [F]	559 mm	+3%	+5%	+4%	+7%	+2.5%	+5.5%	+6%	+10%	± 1.9%
	Fog	number of hours with visibility < 1 km	412 hours	300 hours [G]	-110 hours	-110 hours	-110 hours	-110 hours	-120 hours	-120 hours	-120 hours	-120 hours	± 39 hours
Winter	Temperature	mean	2.4 °C	3.4 °C	+1.1 °C	+1.6 °C	+2.1 °C	+2.7 °C	+1.3 °C	+2.0 °C	+3.2 °C	+4.1 °C	± 0.48 °C
		year-to-year variation [H]	-	± 2.6 °C	-8%	-16%	-13%	-20%	-10%	-17%	-15%	-24%	-
		daily maximum	5.1 °C	6.1 °C	+1.0 °C	+1.6 °C	+2.0 °C	+2.5 °C	+1.2 °C	+2.0 °C	+3.1 °C	+3.8 °C	± 0.46 °C
		daily minimum	-0.3 °C	0.5 °C	+1.1 °C	+1.7 °C	+2.2 °C	+2.8 °C	+1.4 °C	+2.1 °C	+3.5 °C	+4.4 °C	± 0.51 °C
		coldest winter day per year	-7.5 °C	-5.9 °C	+2.0 °C	+3.6 °C	+3.9 °C	+5.1 °C	+2.7 °C	+4.1 °C	+5.6 °C	+7.3 °C	± 0.91 °C
		mildest winter day per year	10.3 °C	11.1 °C	+0.6 °C	+0.9 °C	+1.7 °C	+1.7 °C	+1.0 °C	+1.2 °C	+2.8 °C	+3.1 °C	± 0.42 °C
		number of frost days (min temp < 0°C)	42 days	38 days	-30%	-45%	-50%	-60%	-35%	-50%	-70%	-80%	± 9.5%
		number of ice days (max temp < 0°C)	11 days	7.2 days	-50%	-70%	-70%	-90%	-60%	-80%	-90%	< -90%	± 31%
	Precipitation	mean amount	188 mm	211 mm	+3%	+8%	+8%	+17%	+4.5%	+12%	+13%	+30%	± 8.3%
		10-day amount exceeded once in 10 years [I]	-	± 96 mm	+4.5%	+9%	+10%	+17%	+6.5%	+12%	+16%	+30%	-
		number of wet days (≥ 0.1 mm)	80 mm	89 mm	+6%	+10%	+12%	+17%	+8%	+12%	+18%	+25%	± 11%
		number of days ≥ 10 mm	56 days	55 days	-0.3%	+1.4%	-0.4%	+2.4%	+0.3%	+1.0%	-1.1%	+3%	± 4.7%
		mean wind speed	4.1 days	5.3 days	+9.5%	+19%	+20%	+35%	+14%	+24%	+30%	+60%	± 14%
	Wind	highest daily mean wind speed per year	-	6.9 m/s	-1.1%	+0.5%	-2.5%	+0.9%	-2.0%	+0.5%	-2.5%	+2.2%	± 3.6%
		number of days between south and west	44 days	15 m/s	-3%	-1.4%	-3%	0.0%	-2.0%	-0.9%	-1.8%	+2.0%	± 3.9%
Spring	Temperature	mean	8.3 °C	9.5 °C	+0.9 °C	+1.1 °C	+1.8 °C	+2.1 °C	+1.2 °C	+1.5 °C	+2.8 °C	+3.1 °C	± 0.24 °C
	Precipitation	mean amount	148 mm	173 mm	+4.5%	+2.3%	+11%	+9%	+8%	+7.5%	+15%	+12%	± 8.0%
Summer	Temperature	mean	16.1 °C	17.0 °C	+1.0 °C	+1.4 °C	+1.7 °C	+2.3 °C	+1.2 °C	+1.7 °C	+3.2 °C	+3.7 °C	± 0.25 °C
		year-to-year variation [H]	-	± 1.4 °C	+3.5%	+7.5%	+4%	+9.5%	+5%	+9%	+7.5%	+14%	-
		daily maximum	20.7 °C	21.9 °C	+0.9 °C	+1.4 °C	+1.5 °C	+2.3 °C	+1.0 °C	+1.7 °C	+3.0 °C	+3.8 °C	± 0.35 °C
		daily minimum	11.2 °C	11.9 °C	+1.1 °C	+1.3 °C	+1.9 °C	+2.2 °C	+1.4 °C	+1.7 °C	+3.4 °C	+3.7 °C	± 0.18 °C
		coolest summer day per year	10.3 °C	11.1 °C	+0.9 °C	+1.1 °C	+1.6 °C	+2.0°C	+1.0 °C	+1.4 °C	+2.7 °C	+3.1°C	± 0.43 °C
		warmest summer day per year	23.2 °C	24.7 °C	+1.4 °C	+1.9 °C	+2.3 °C	+3.3 °C	+2.0 °C	+2.6 °C	+4.2 °C	+4.9 °C	± 0.52 °C
		number of summer days (max temp ≥ 25°C)	13 days	21 days	+22%	+35%	+40%	+70%	+30%	+50%	+100%	+130%	± 13%
		number of tropical nights (min temp ≥ 20°C)	< 0.1 days	0.1 days	+0.5%	+0.6%	+1.4%	+2.2%	+0.9%	+1.2%	+6.5%	+7.5%	-
	Precipitation	mean amount	224 mm	224 mm	+1.2%	-8%	+1.4%	-13%	+1.0%	-8%	-5%	-23%	± 9.2%
		year-to-year variation [H]	-	± 113 mm	+2.1 to +5%	-2.5 to +1.0%	+1.4 to +7%	-4 to +2.2%	+1.2 to +5.5%	-2.5 to +1.9%	-0.9 to +10%	-8.5 to +2.3%	-
		daily amount exceeded once in 10 years [I]	44 mm	44 mm	+1.7 to +10%	+2.0 to +13%	+3 to +21%	+2.5 to +22%	+2.5 to +15%	+2.5 to +17%	+5.5 to +40%	+5 to +40%	± 15%
		maximum hourly intensity per year	14.9 mm/hour	15.1 mm/hour	+5.5 to +11%	+7 to +14%	+12 to +23%	+13 to +25%	+8 to +16%	+9 to +19%	+22 to +45%	+22 to +45%	± 14%
		number of wet days (≥ 0.1mm)	45 days	43 days	+0.5%	-5.5%	+0.7%	-10%	+2.1%	-5.5%	-5%	-16%	± 6.4%
		number of days ≥ 20 mm	1.6 days	1.7 days	+4.5 to +18%	-4.5 to +10%	+6 to +30%	-8.5 to +14%	+5 to +23%	-3.5 to +14%	+3 to +40%	-15 to +14%	± 24%
	Solar radiation	solar radiation	149 kJ/cm² [F]	153 kJ/cm² [F]	+2.1%	+5%	+1.0%	+6.5%	+0.9%	+5.5%	+3.5%	+9.5%	± 2.4%
	Humidity	relative humidity	78%	77%	-0.6%	-2.0%	+0.1%	-2.5%	0.0%	-2.0%	-0.6%	-3%	± 0.86%
	Evaporation	potential evaporation (Makkink)	253 mm [F]	266 mm	+4%	+7%	+4%	+11%	+3.5%	+8.5%	+9%	+15%	± 2.8%
	Drought	mean highest precipitation deficit during growing season [J]	140 mm	144 mm	+4.5%	+20%	+0.7%	+30%	+1.0%	+19%	+14%	+50%	±13%
		highest precipitation deficit exceeded once in 10 years [J]	-	230 mm	+5%	+17%	+4.5%	+25%	+3.5%	+17%	+15%	+40%	-
Autumn	Temperature	mean	10.0 °C	10.6 °C	+1.1 °C	+1.3 °C	+2.2 °C	+2.3 °C	+1.6 °C	+1.6 °C	+3.8 °C	+3.8 °C	± 0.27 °C
	Precipitation	mean amount	214 mm	245 mm	+7%	+8%	+3%	+7.5%	+7.5%	+9%	+6.5%	+12%	± 9.0%

Figure 100: Weather changes between the 1981–2010 reference period and 2050, for each of the four KNMI '14 climate scenarios, from Based on (Attema et al., 2014).

Season [A]	Variable	Indicator	Climate [B] 1981-2010 = reference period	Central estimate of change value for 2030 [C] (2016-2045)	Natural variations averaged over 30 years [D]
Year	Sea level at North Sea coast	absolute level [E]	3 cm above NAP	+10 tot +25 cm	±1.4 cm
		rate of change	2.0 mm/year	+1 to +6 mm/year	±1.4 mm/ year
	Temperature	mean	10.1 °C	+1.0 °C	± 0.16 °C
	Precipitation	mean amount	851 mm	+5%	± 4.2%
	Solar radiation	solar radiation	354 kJ/cm²	+0.2%	± 1.6%
	Evaporation	potential evaporation (Makkink)	559 mm	+2.5%	± 1.9%
	Fog	number of hours with visibility < 1 km	300 hour [G]	-100 hour	± 39 hour
Winter	Temperature	mean	3.4 °C	+1.2 °C	± 0.48 °C
	Precipitation	mean amount	211 mm	+8.5%	± 8.3%
		10-day amount exceeded once in 10 years [I]	89 mm	+9%	± 11%
		number of wet days (≥ 0.1 mm)	55 days	+1.5%	± 4.7%
	Wind	mean wind speed	6.9 m/s	+0.5%	± 3.6%
		highest daily mean wind speed per year	15 m/s	-1.0%	± 3.9%
		number of days between south and west	49 days	+2.5%	± 6.4%
Spring	Temperature	mean	9.5 °C	+0.8 °C	± 0.24 °C
	Precipitation	mean amount	173 mm	+5.5%	± 8.0%
Summer	Temperature	mean	17.0 °C	+0.9 °C	± 0.25 °C
	Precipitation	mean amount	224 mm	+0.2%	± 9.2%
		daily amount exceeded once in 10 years [I]	44 mm	+1.7 tot +10%	± 15%
		maximum hourly intensity per year	15.1 mm/hour	+5.5 tot +11%	± 14%
		number of wet days (≥ 0.1mm)	43 days	+0.5%	± 6.4%
	Solar radiation	solar radiation	153 kJ/cm²	+1.9%	± 2.4%
	Humidity	relative humidity	77%	-0.6%	± 0.86%
	Evaporation	potential evaporation (Makkink)	266 mm	+3.5%	± 2.8%
	Drought	mean highest precipitation deficit during growing season [J]	144 mm	+4%	± 13%
Autumn	Temperature	mean	10.6 °C	+1.0 °C	± 0.27 °C
	Precipitation	mean amount	245 mm	+5.5%	± 9.0%

Figure 101: Weather changes between the 1981–2010 reference period and 2030, based on the KNMI '14 climate scenarios from (Attema et al., 2014).

Table 70 contains the projected electricity mixes of the Dutch grid used to determine the carbon intensities of the electric grid for future scenarios. Values are expressed in the total annual production in petajoules (PJ). Solar PV and Wind energy are further subdivided based on assumptions (see also Appendix N) to align better with available ecoinvent processes. The 2030 mix is derived from the Dutch Climate and Energy exploration (Hammingh et al., 2021), the 2050 mixes from an exploration of net zero energy mix scenarios (Ouden et al., 2020). Both were accessed through the online Energy transition model (Zaccagnini et al., 2023).

Table 70: Projected electricity production mix of the Dutch grid (PJ). Based on (Hammingh et al., 2021; Ouden et al., 2020; Zaccagnini et al., 2023).

Electricity source	**Scenario in source literature**				
	2030	*2050 Regional*	*2050 National*	*2050 European*	*2050 International*
Biogas	9	2	0	63	7
Coal gas	0	0	6	12	6
Hydroelectric	0	0	0	0	0
Hydrogen	0	78	59	0	61
Imported electricity	107	90	135	327	339
Natural gas	134	0	0	0	0
Nuclear	12	0	0	0	0
Residual waste	19	0	2	6	6
Solid biomass	1	0	0	0	0
Solar PV	84	376	320	174	156
Solar PV (open ground)	57	200	172	102	104
Solar PV (roof-panel)	27	176	148	72	52
Wind	262	718	1,050	594	554
Wind (offshore)	199	503	216	486	446
Wind (onshore)	63	215	834	108	108
Total	629	1,264	1,573	1,176	1,129

Appendix M Correlation between Subsurface and Air Temperatures

In the modeling of the 2030 and 2050 scenarios, a lack of direct subsurface temperature projections in the existing literature or from the KNMI (Royal Netherlands Meteorological Institute) was encountered. To address this limitation, the possibility of using projected air temperature changes as a proxy for subsurface temperature changes was explored. To establish this relationship, an analysis of daily air and subsurface temperature data at a depth of 1 meter covering the period from 1981 to 2021 was conducted, with the data being obtained from the KNMI website (KNMI, 2022a, 2022b). The results of this analysis can be found in the following figures.

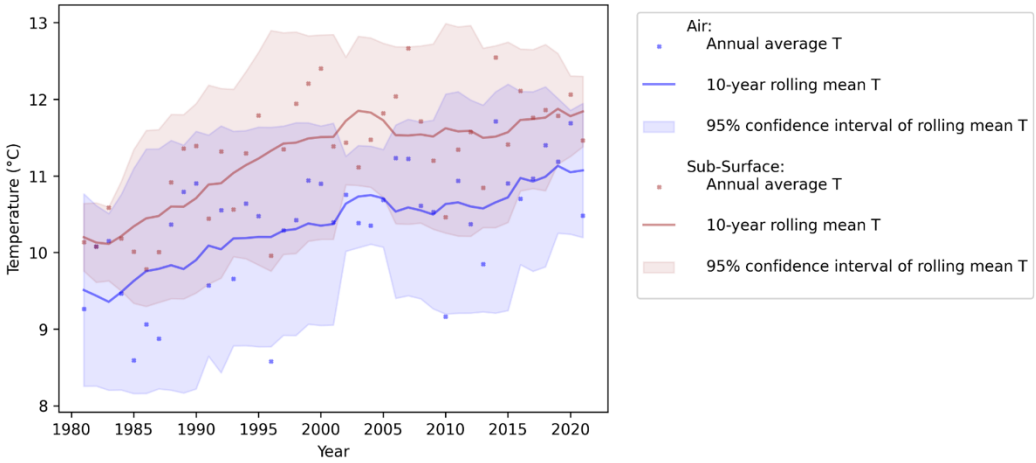

Figure 102: Annual air and subsurface (1m depth) temperatures in De Bilt, 1981–2021.

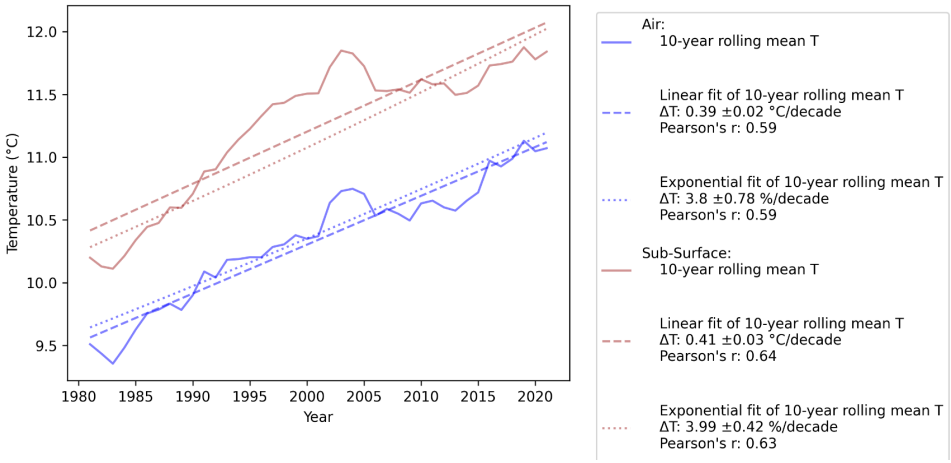

Figure 103: Linear and exponential fits to 10-year rolling mean air and subsurface (1m depth) temperatures in De Bilt, 1981–2021.

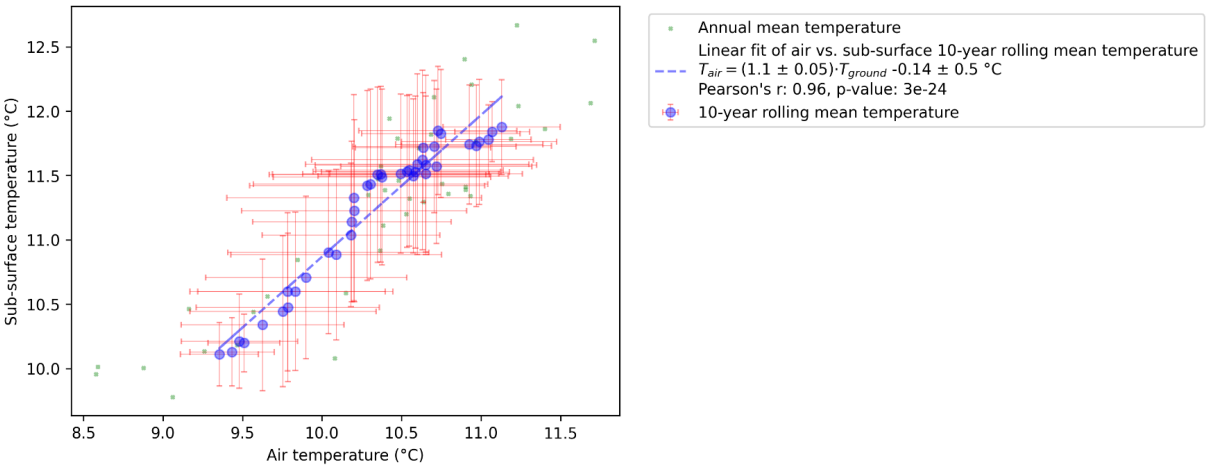

Figure 104: Air vs. subsurface (1m depth) temperatures in De Bilt, 1981–2021. A linear fit has been performed on the relationship between 10-year rolling mean air and subsurface temperatures.

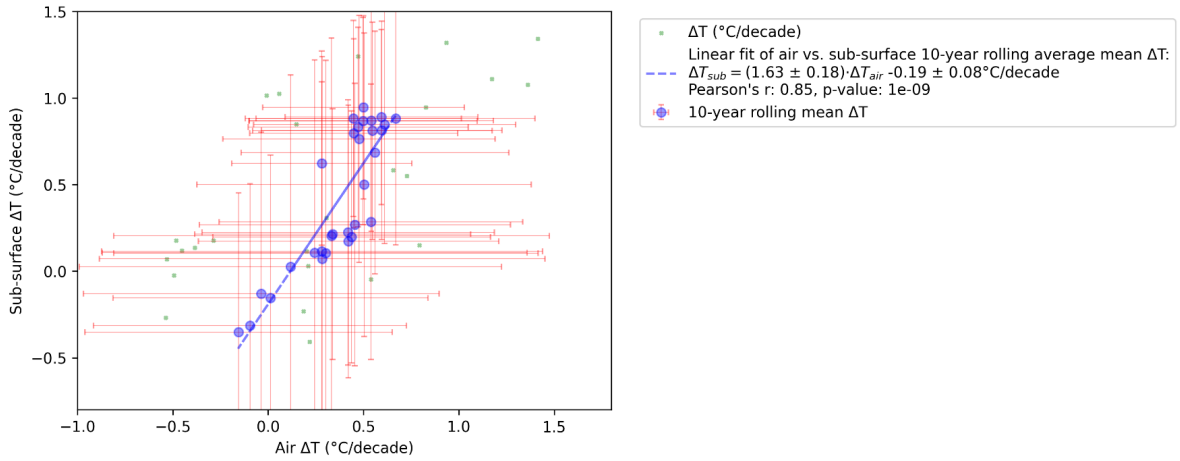

Figure 105: Air vs. subsurface (1m depth) temperature changes in De Bilt, 1981–2021. A linear fit has been performed on the relationship between 10-year rolling mean air and subsurface temperature increases.

From the above figures it can be concluded that the air and subsurface temperature levels exhibit a remarkable similarity, with the 10-year rolling mean temperatures demonstrating statistical indistinguishability for the most part (see Figure 102 and Figure 104).

The next inquiry revolves around the comparability of the decadal changes within the annual average air and subsurface temperature. To address this, both linear and exponential fits were generated for both subsurface and air temperatures. The results indicate that the linear fit reveals statistically indistinguishable air and subsurface

temperature growth, both falling within the range of 0.40 ± 0.04 °C per decade (see Figure 103).

It is noteworthy that this aligns with the findings presented by the KNMI in their 2021 Climate signal report (KNMI, 2021). Likewise, the exponential fit yields statistically indistinguishable growth rates for both variables, at 4% per decade.[56]

For greater precision, a depiction of the 10-year temperature increments for both air and subsurface temperatures is included to ascertain the quantitative relationship between the growth of air and subsurface temperatures, as presented in Figure 105.

While a robust linear correlation between the two is evident, it is important to note that this does not necessarily imply a linear cause-and-effect relationship. Additionally, the data exhibits noise, as reflected in the error bars.

To comprehensively understand the nature of the relationship between air and subsurface temperature increases in the context of climate change, further research is warranted. In the scope of this study, subsurface temperature growth is assumed to mirror air temperature growth. This assumption is based on the strong linear correlation between the two variables and the historical trend where both temperatures have converged to a common growth rate of 0.40 ± 0.04 °C per decade over the past 30 years.

[56] Note that this exponential growth rate is based on temperatures measured in °C, and not in Kelvin (K). The heat energy stored in the environment is linearly related to the temperature measured in K. Hence, it is not the heat energy stored in the environment that grows by 4% every decade, but merely the temperature denoted in degrees Celsius. The growth rate of temperature measured in K, and thus that of heat energy, will be lower than the growth rate of temperature measured in °C.

Appendix N Scenario parameters: Assumptions for the Carbon Intensity of the Grid

This appendix contains a detailed overview of the assumptions made in the estimation of the future Dutch electricity grid source mix, which impacts the evolution of the carbon intensity of the electricity grid. It is about five electricity sources that were problematic and required more research to determine its future impacts.

This appendix provides a detailed examination of the assumptions underpinning the projection of the future Dutch electricity grid source mix, which is used to determine the evolution of the carbon intensity of the electricity grid. Specifically, it delves into five electricity sources that posed challenges, necessitating more in-depth research to determine their future impacts.

Furthermore, Table 72 contains the life-cycle carbon intensities of electricity from different sources used in this assessment, based on ecoinvent processes and the "Climate change (GWP100)" impact indicator from the "ReCiPe Midpoint (H) V1.13" assessment method (Huijbregts et al., 2017; Wernet et al., 2016).

Solar Photovoltaic Power

In the global solar photovoltaic (PV) market, Mono-Si (also known as Single-Si) solar panels are dominant, constituting over 80% of global sales in 2020 (Philipps & Warmuth, 2023). This market share has been on the rise since 2015. For the sake of simplicity, it is assumed that all roof-installed solar panels will be of the Mono-Si variety in 2050.

Wind Energy

From Figure 45, it can be observed that most of the wind power is projected to be generated by offshore wind farms (as opposed to on-land windmills), accounting for 70% to 80% of the total wind power production. An average of 75% is assumed across all scenarios. The average capacity of on-land wind turbines in the Netherlands is 2.2 MW (CBS, 2023c). In consideration of this, it is assumed that all on-land wind turbines fall within the 1–3 MW category.

Hydrogen

Greenhouse gas (GHG) emissions from hydrogen production emissions depend upon the electricity source in the case of electrolysis and the presence of carbon capture and storage

in the case of natural gas derivation. Three distinct types of hydrogen exist, each associated with varying life-cycle carbon footprints (refer to Figure 106).

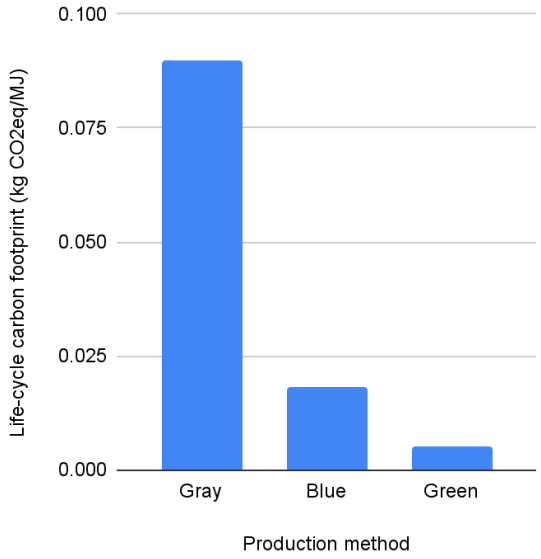

Figure 106: Life-cycle carbon footprint of hydrogen, per production method (Hauck et al., 2020).

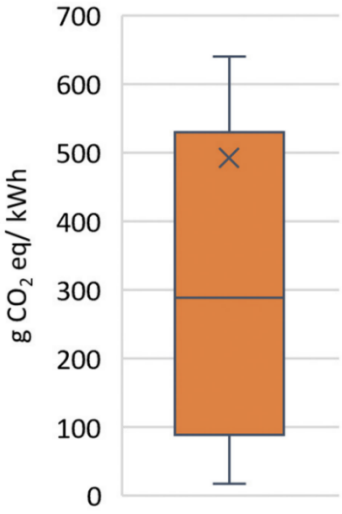

Figure 107: The range of GHG emission intensities of hydrogen-based electricity (Rinawati et al., 2022).

Gray hydrogen originates from fossil fuels, primarily steam methane reforming (SMR), and currently constitutes 96% of global hydrogen production (Howarth & Jacobson, 2021). Blue hydrogen denotes hydrogen production akin to the gray method but incorporating carbon capture and storage. Green hydrogen is derived through the electrolysis of water using renewable electricity. Given the typically low life-cycle carbon footprint of renewable electricity, green hydrogen serves as a low-carbon alternative to gray and blue hydrogen. Nevertheless, green hydrogen experiences significant conversion losses, with a round-trip conversion efficiency (electricity → hydrogen → electricity) ranging from 18% to 46% (Sepulveda et al., 2021). Additionally, it is presently not cost-competitive with gray or blue hydrogen (Howarth & Jacobson, 2021).

The current mixture of hydrogen types is inherently intricate, with a substantial portion of hydrogen being imported and the production source occasionally remaining obfuscated. This complexity, coupled with variations in the carbon footprint of electricity mixes employed in green hydrogen production, leads to a broad spectrum of emission factors for hydrogen-based electricity generation (see Figure 107) (Rinawati et al., 2022).

To estimate the impacts of hydrogen on electricity generation in this research, the following distribution of hydrogen types was assumed for each scenario year. Carbon

intensities for gray and green hydrogen were grounded in research on hydrogen-based solid-oxide fuel cells (SOFCs) in the European region (Bicer & Khalid, 2020).

Table 71: Assumptions on the hydrogen-based electricity production mix and the resulting life-cycle carbon footprint for future scenarios. Based on (Bicer & Khalid, 2020)

Scenario year	Production mix	Life-cycle carbon footprint (kg CO_2-eq/kWh)
2020	100% gray	0.64
2030	50% gray, 50% green	0.35
2050	100% green	0.05

Gas

Within the scenarios, a distinction is drawn between biogas and green gas. Although these terms are closely related, green gas can be regarded as a subset of biogas, specifically biogas that has been refined to a degree enabling it to replace natural gas (Gasunie, 2023).[57] It is important to note that this distinction has yet to be explored in LCA studies. Consequently, this study assumes that the carbon intensity of electricity derived from both biogas and green gas is equivalent.

Imported Electricity

Due to the absence of available data on the anticipated import mix, it is assumed that the carbon intensity of imported electricity aligns with the average carbon intensity of the Dutch grid.

[57] In other words, green gas can be transported in existing natural gas infrastructure and its quality is of such a degree that it can be used in applications for which natural gas is currently used.

Table 72: The ecoinvent products assigned to each electricity source and the resulting life-cycle carbon intensities.

Electricity source	ecoinvent product	Carbon intensity (kg CO_2-eq/kWh)	Notes
Biogas	Electricity, high voltage, from heat and power co-generation, biogas, gas engine (NL)	0.209	
Coal gas	Electricity, high voltage, from treatment of coal gas, in power plant (NL)	0.830	
Hydroelectric	Electricity, high voltage, from electricity production, hydro, run-of-river (NL)	0.004	
Hydrogen	Green (wind-powered EU), from Green (wind-powered EU) (EU28)	0.050	Hydrogen-based electricity is only used in the 2050 mixes; hence an all-green production method is assumed.
Natural gas	Electricity, high voltage, from electricity production, natural gas, conventional power plant (NL)	0.638	
Nuclear	Electricity, high voltage, from electricity production, nuclear, pressure water reactor (NL)	0.006	
Residual waste	Electricity, medium voltage, from electricity, from municipal waste incineration to generic market for electricity, medium voltage (NL)	0.000	
Solar PV (roof-panel)	Electricity, low voltage, from electricity production, photovoltaic, 3kWp slanted-roof installation, single-Si, panel, mounted (NL)	0.105	
Solar PV (open ground)	Electricity, low voltage, from electricity production, photovoltaic, 570kWp open ground installation, multi-Si (NL)	0.094	All roof-installed solar panels are assumed to be Mono-Si.
Solid biomass	Electricity, high voltage, from heat and power co-generation, biogas, gas engine (NL)	0.209	No emission factors for biomass are available, biogas is taken as proxy.
Wind (onshore)	Electricity, high voltage, from electricity production, wind, 1–3MW turbine, onshore (NL)	0.014	All on-land wind-turbines are assumed to be in the 1–3 MW category.
Wind (offshore)	Electricity, high voltage, from electricity production, wind, 1–3MW turbine, offshore (NL)	0.016	
Imported electricity	-	-	The average emission factor of the Dutch grid is used as a proxy. This varies by scenario.

Appendix O Additional Results of Sensitivity Analyses

This appendix presents comprehensive results from sensitivity analyses conducted on the input parameters of the cooling demand model. These analyses were carried out based on the Status Quo (2020) scenario parameter configuration, which is referred to as the *reference scenario* in the figures. The Cooling Demand Model (CDM) was executed 100 times using a sample dataset consisting of 314 buildings, selected to be representative of the larger building stock comprising 59,381 buildings that the primary results are based on. During these runs, the independent input parameters were systematically varied within predefined ranges. For detailed information on the input ranges and a comprehensive elasticity table, please refer to Table 73.

Table 73: Configuration and outcomes of sensitivity analyses conducted on a subset of input parameters. The elasticities of cooling demand and environmental impact metrics with respect to the input parameters are detailed on the right side of the table.

					Elasticities				
Input parameter	**Reference value**	**Unit**	**Analyzed range**	**Range description**	*Cooling energy demand*	*Cooling power demand*	*Electricity use*	*Material demand*	*GHG emissions*
Cooling demand cap percentile	98%	%	80–100	Between 870 and 0 hours of thermal discomfort	2	11.2	1.56	10.2	3
Effective cooling temperature	25	°C	15–30	The outer limits of thermal comfort ranges found in the literature	-4	-2	-3.41	-1.82	-3.15
Summer temperature	18	°C	16.2–26.2	A -2 °C and a +6 °C degree scenario	1	1.02	1.11	0.93	1.08
Total market penetration rate of cooling equipment	12	%	0–100		0	0	1	1	1
Daytime UHI effect	8.3	°C	0–15	Between zero and an extreme UHI effect as seen in cities like Phoenix	1	0.57	0.91	0.52	0.85
Energy efficiency of cooling equipment (SEER)	5.0	-	2.5–15	Amount of cooling provided per electricity use over the year	0	0	-0.96	0	-0.8
Summertime solar radiation	229	W / m²	227–252	A -1% to 10% increase	0	0.4	0.26	0.36	0.28
Carbon intensity of electricity grid	0.427	kg CO_2-eq / kWh	0–0.5	Between carbon-neutral and 100% hard coal-based electricity	0	0	0	0	0.83
Internal heat gains	6.0	W / m²	0.5–15	Between efficient LED and old-fashioned Incandescent light bulbs	0	0.08	0.21	0.08	0.19
Density of people in offices	0.067	-	0.04–0.2	Between 25 m² (large private offices) and 5 m² per person (slightly under the minimum requirement set by the NEN norm)	0	0.01	0.06	0.04	0.06
Average amount of people per household	2.01	-	1–6	Between single households and large families	0	0.03	0.06	0.02	0.05
Refrigerant leakage	9.0%	% of charge	0.5–18		0	0	0	0	0.14
Global warming potential of refrigerant	1,603	kg CO_2-eq / kg	0–20,000	Between water/propane as a refrigerant and R-13	0	0	0	0	0.11
Nighttime UHI effect	2.1	°C	0–15	Between zero and an extreme UHI effect as seen in cities like Phoenix	0	0	0.02	0	0.02

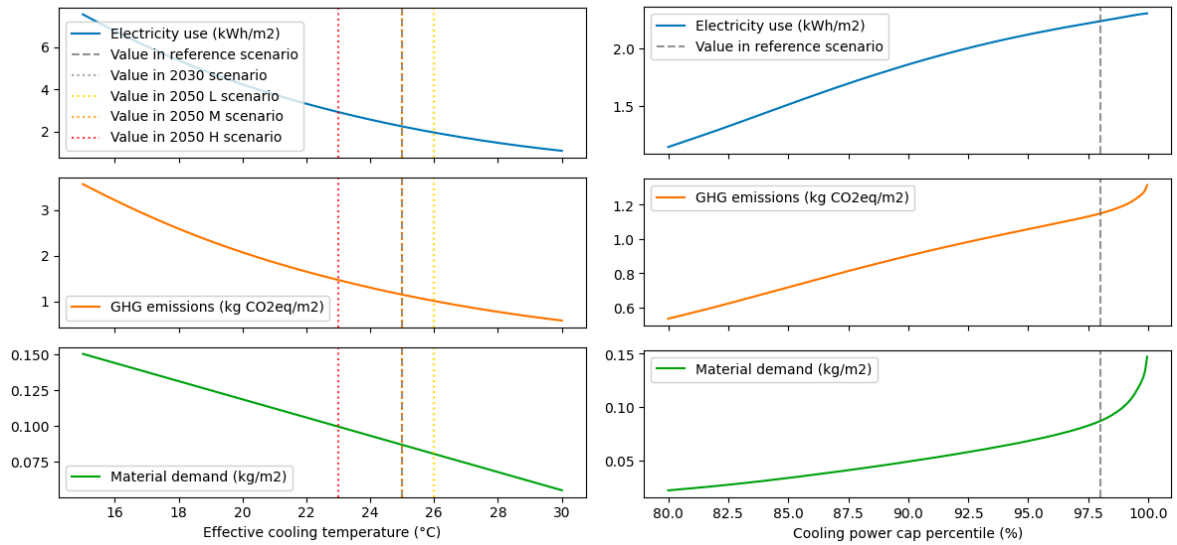

Figure 108: The influence of the effective or threshold cooling temperature (left) and the percentile at which the peak power is capped (right) on absolute impacts.

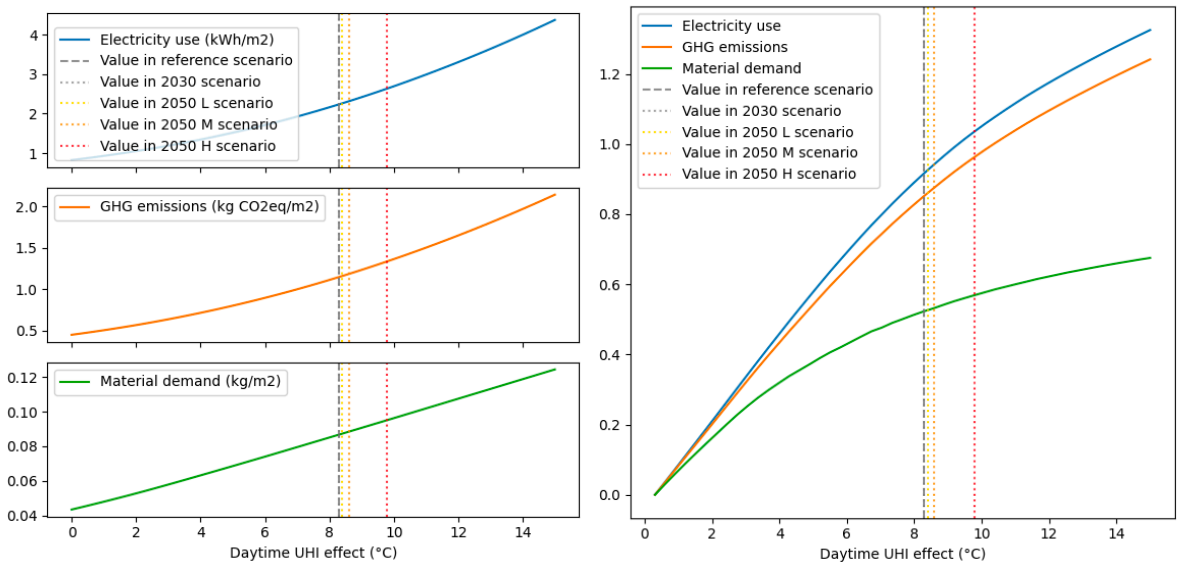

Figure 109: The influence of the daytime UHI effect on absolute impacts (left) and the variation of the impact elasticity across the input parameter range (right).

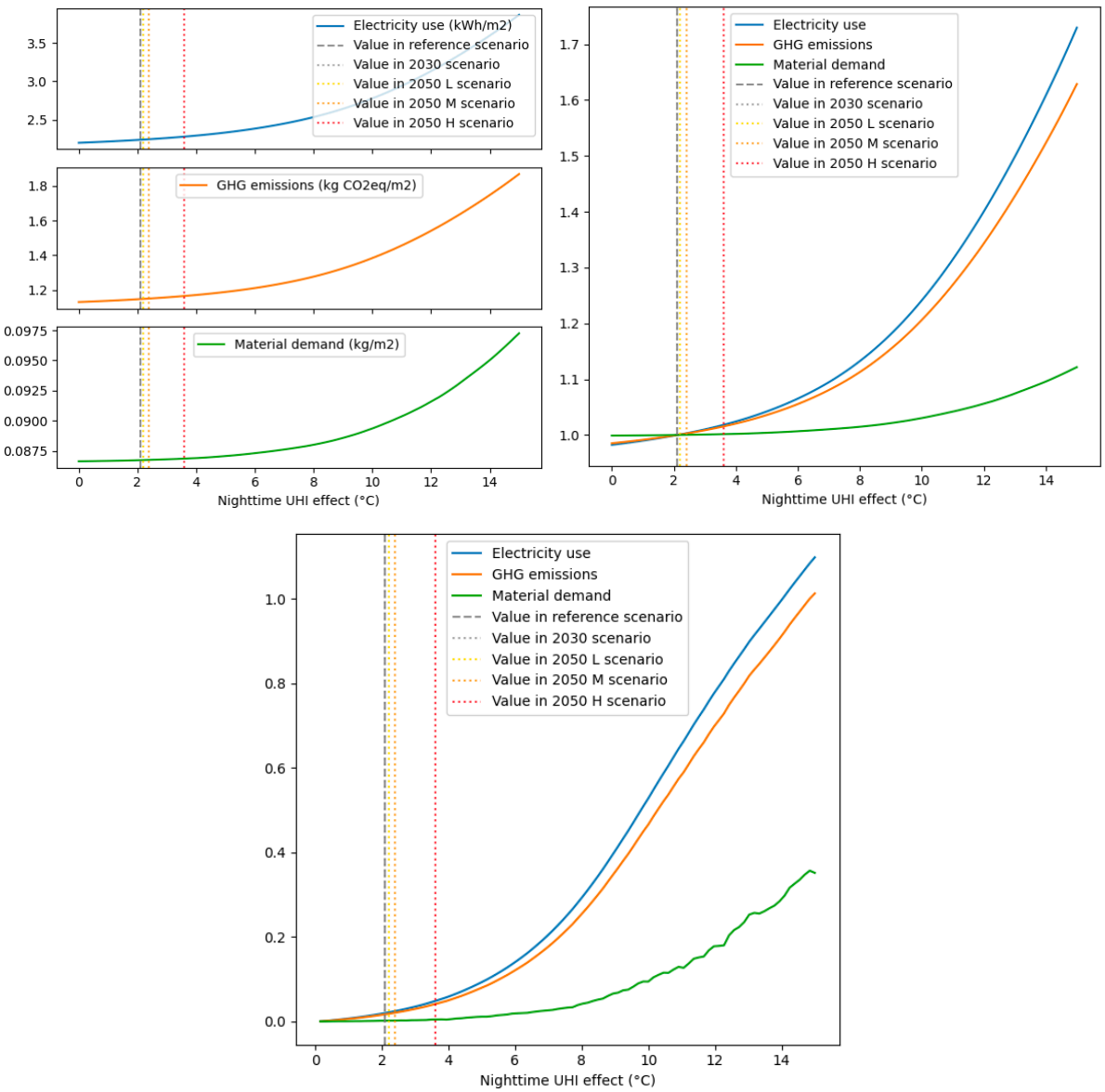

Figure 110: The influence of the nighttime UHI effect on impacts–absolute (top-left) and normalized (top-right)–and the variation of the impact elasticity across the input parameter range (bottom).

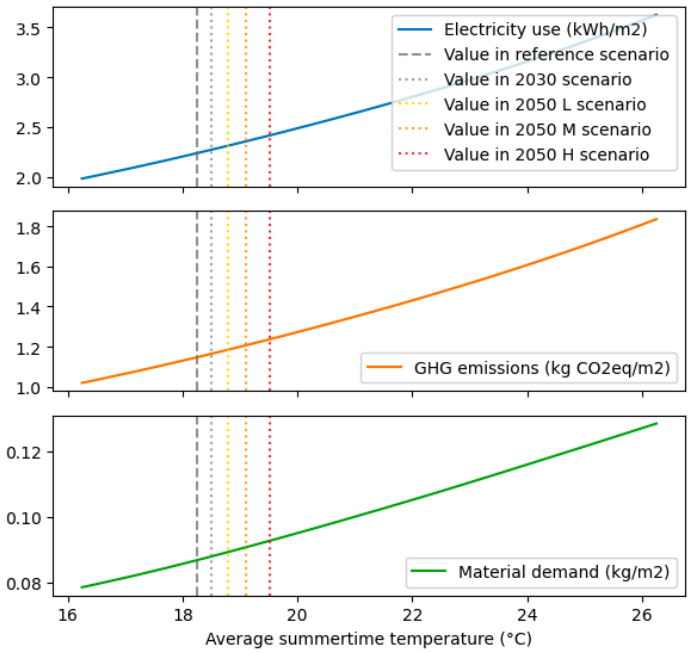

Figure 111: The influence of the summertime air temperature on absolute environmental impacts.

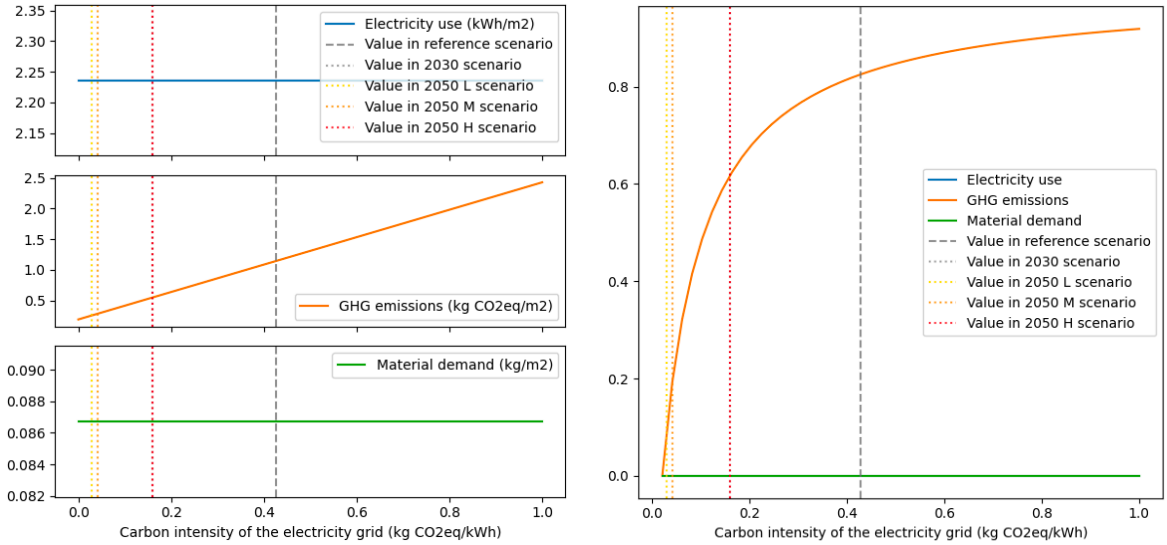

Figure 112: The influence of the carbon intensity of the electricity grid on absolute impacts (left), and the variation of the impact elasticity across the input parameter range (right).

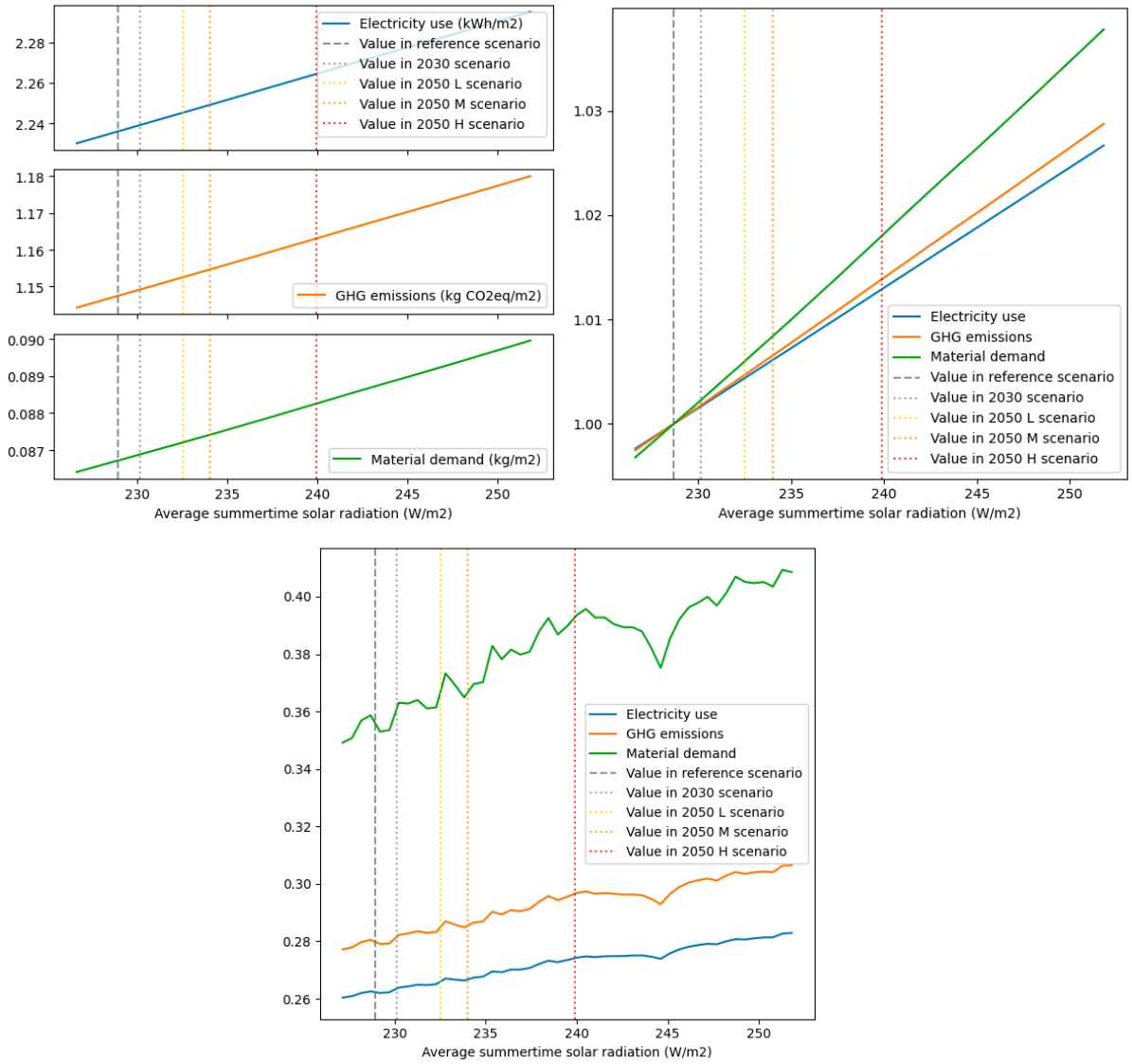

Figure 113: The influence of summertime solar radiation on absolute impacts (top-left) and normalized impacts (top-right), and the variation of the impact elasticity across the input parameter range (bottom).

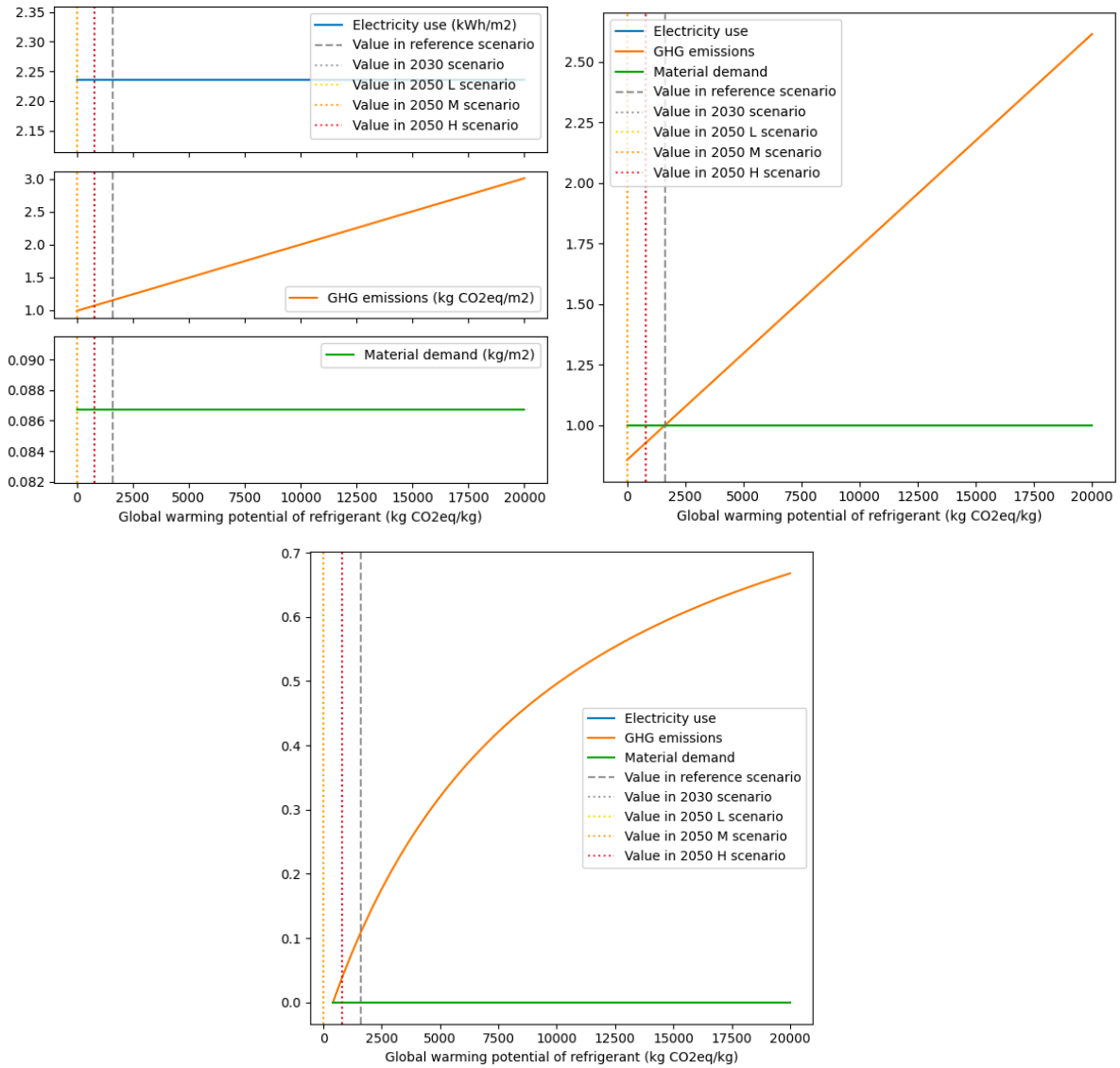

Figure 114: The influence of global warming potential of the refrigerants used in cooling equipment on absolute impacts (top-left) and normalized impacts (top-right), and the variation of the impact elasticity across the input parameter range (bottom).

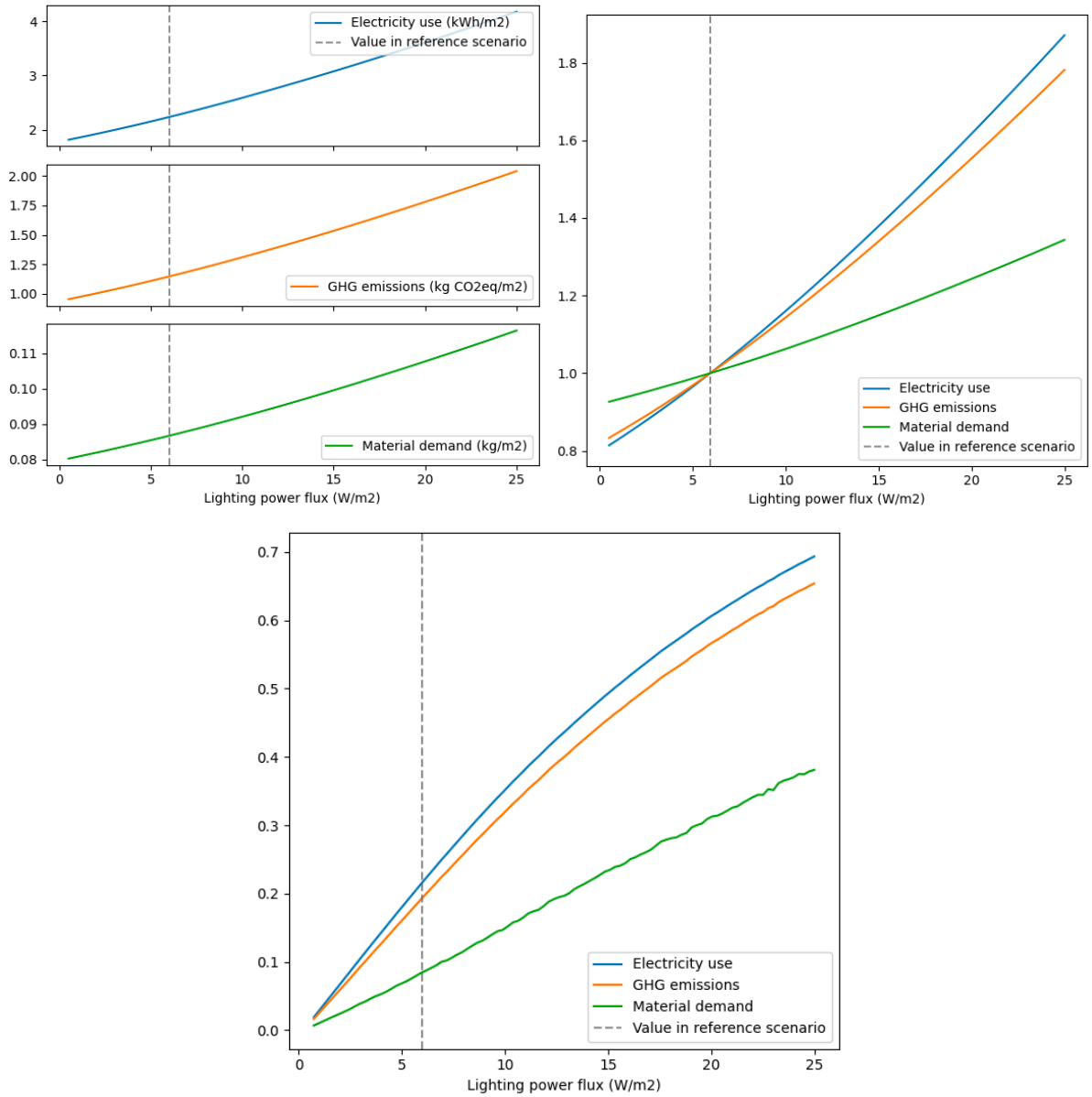

Figure 115: The influence of the indoor lighting intensity on absolute impacts (top-left) and normalized impacts (top-right), and the variation of the impact elasticity across the input parameter range (bottom).

It is worth noting that insights gained from the sensitivity analysis on indoor heat gains from lighting can also be applied to the heat gain from appliances, which typically ranges between 5 to 15 W/m² in the scenarios, and heat gain from occupants, which averages between 2.4 (for residential) and 8.4 (for office buildings) W/m². These values fall within a similar order of magnitude, making the insights relevant and transferable.

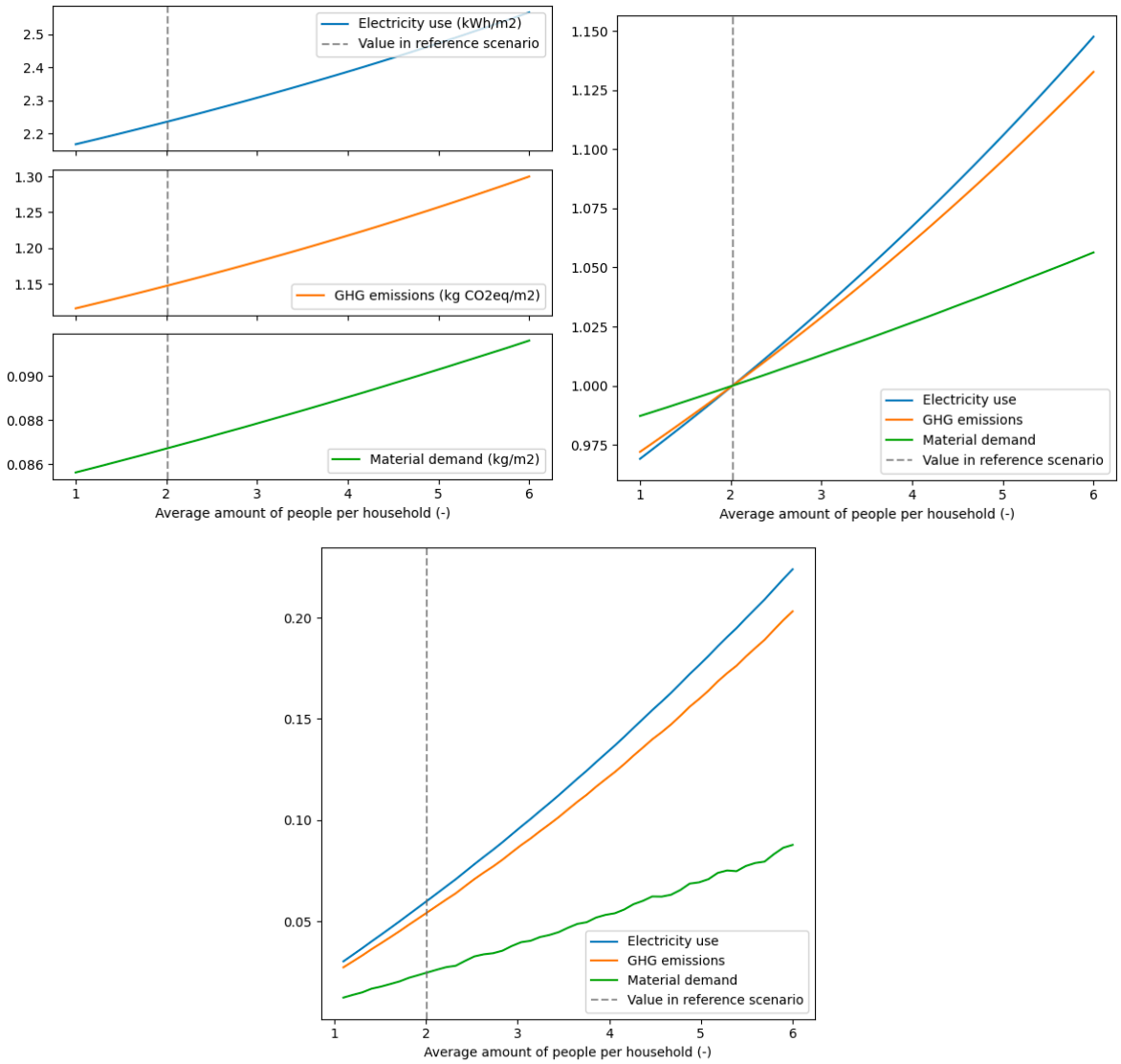

Figure 116: The influence of the average household size on absolute impacts (top-left) and normalized impacts (top-right), and the variation of the impact elasticity across the input parameter range (bottom).

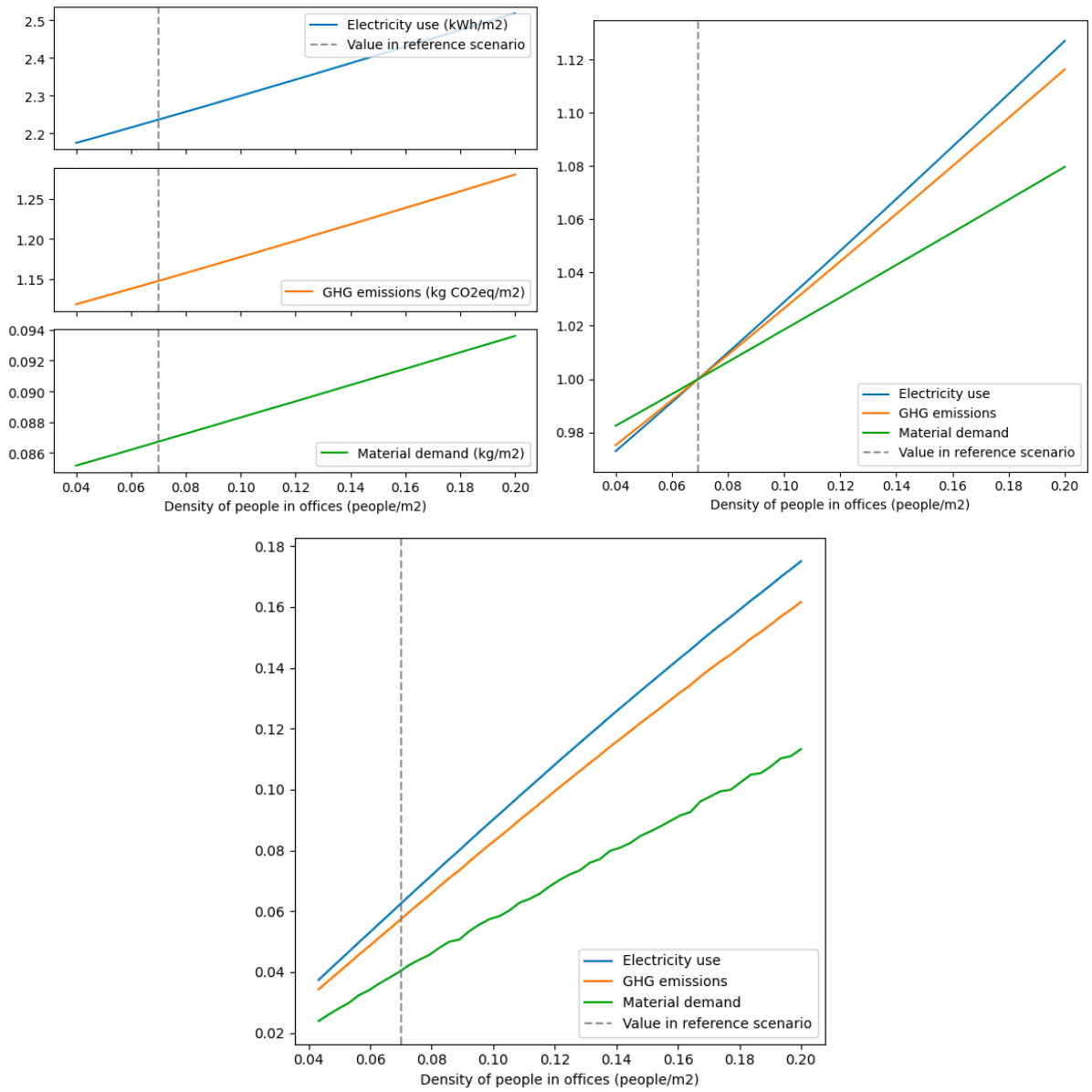

Figure 117: The influence of office occupancy density on absolute impacts (top-left) and normalized impacts (top-right), and the variation of the impact elasticity across the input parameter range (bottom).

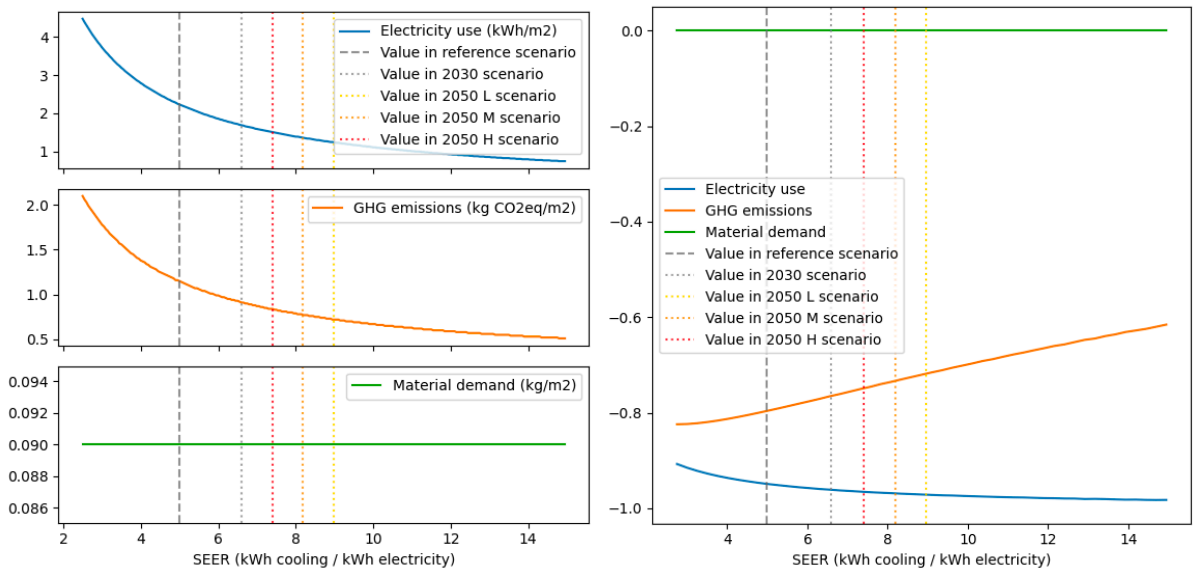

Figure 118: The influence of the average seasonally adjusted energy efficiency (SEER) on absolute impacts (left) and the variation of the impact elasticity across the input parameter range (right).

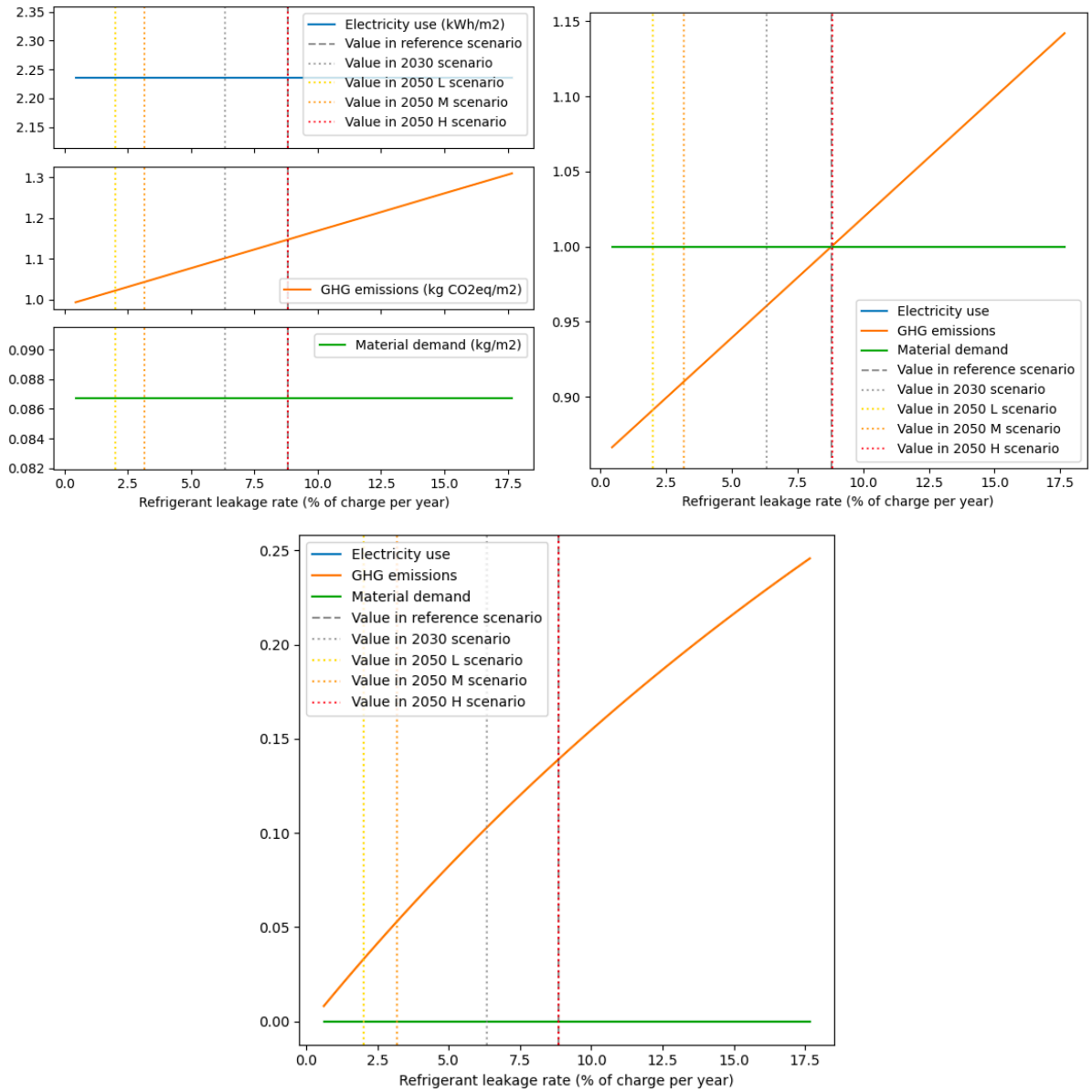

Figure 119: The influence of the refrigerant leakage rate (measured as % of the installed charge per year) on absolute impacts (top-left) and normalized impacts (top-right), and the variation of the impact elasticity across the input parameter range (bottom).

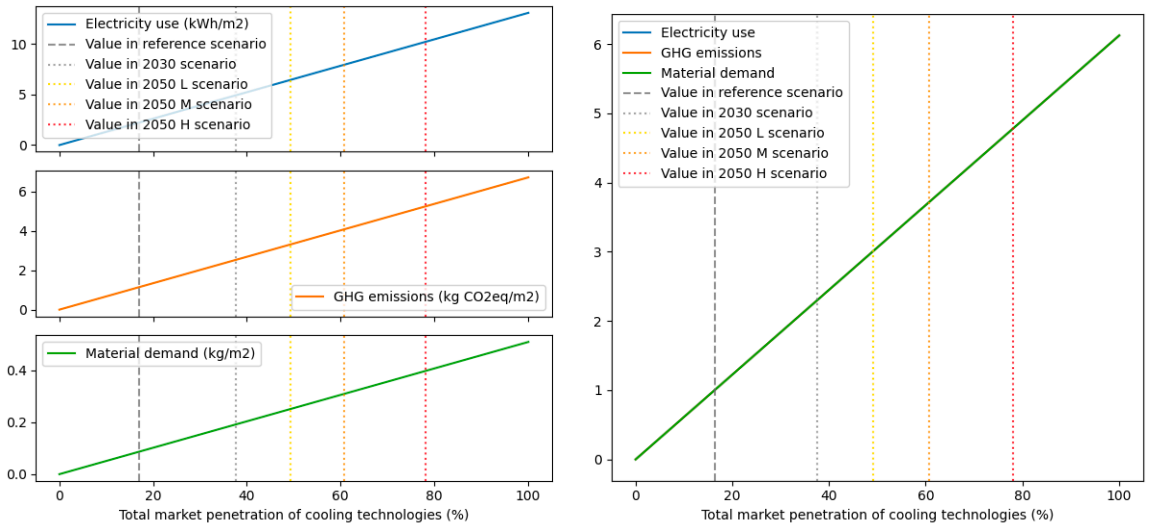

Figure 120: The influence of the total market penetration rate of cooling equipment (across the building stock) on absolute impacts (left) and normalized impacts (right). Note that the elasticities for each of the impact categories are equal to one across the input parameter range.

Appendix P Availability of Energy Label Data per Building Type

This appendix contains a table and visual representation of the distribution of floor space with and without registered energy data, per building type. This distribution data was used to extrapolate the impacts – which were calculated on the building stock subset with energy label data – to the total residential and office building stock of The Hague.

Table 74: Floor space distribution between the building stock with registered energy labels vs. the building stock without energy label data, per building type.

Building type	Floor area of buildings with energy labels (ha)	Floor area of buildings without energy labels (ha)
1: New high-rise residential	116	3
2: Old high-rise residential	284	8
3: New low-rise residential	226	76
4: Old low-rise residential	1,518	442
5: New high-rise office	39	8
6: Old high-rise office	213	38
7: New low-rise office	14	0
8: Old low-rise office	68	36
Total	2,478	611

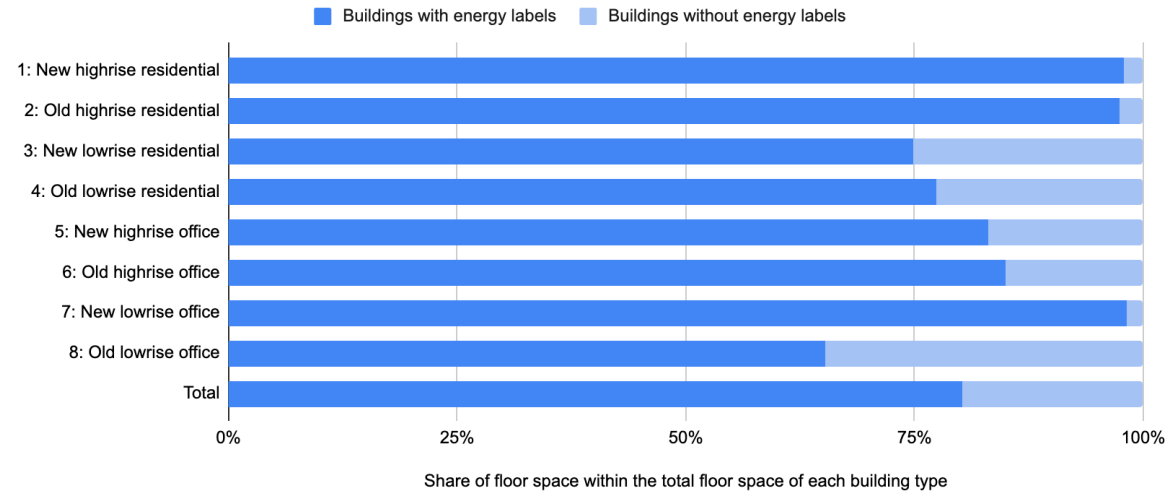

Figure 121: Floor space distribution between the building stock with registered energy labels vs. the building stock without energy label data, per building type.

Appendix Q Additional Cooling Demand and Environmental Impact Model Results

This appendix presents supplementary figures that depict results from the status quo and future scenarios. It is worth noting that these figures are constructed based on data from the residential and office building stock with registered energy labels, excluding buildings lacking such labels.

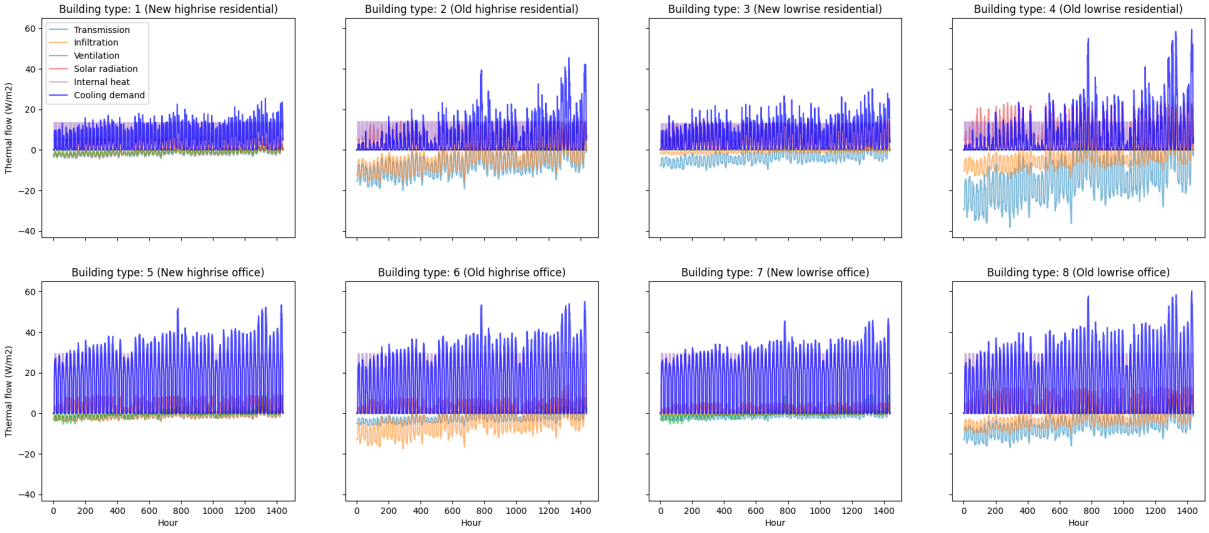

Figure 122: Thermal flows and the resulting cooling demand for each of the eight building types in the residential and office building stock, May - June 2019.

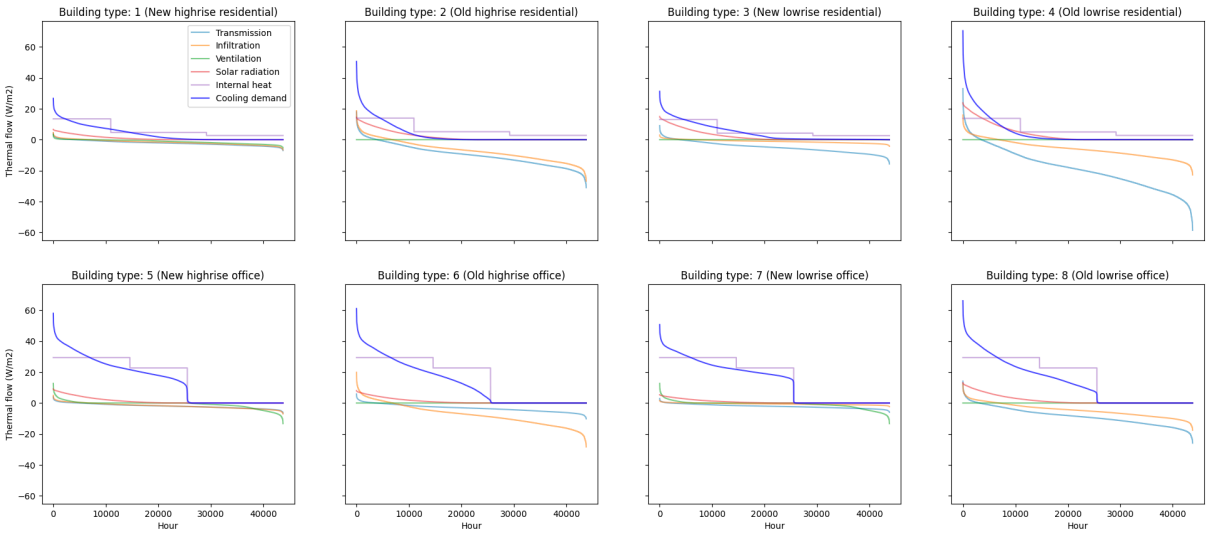

Figure 123: Thermal flows and the resulting cooling demand for each of the eight building types, sorted by size across the 2018–2022 reference period.

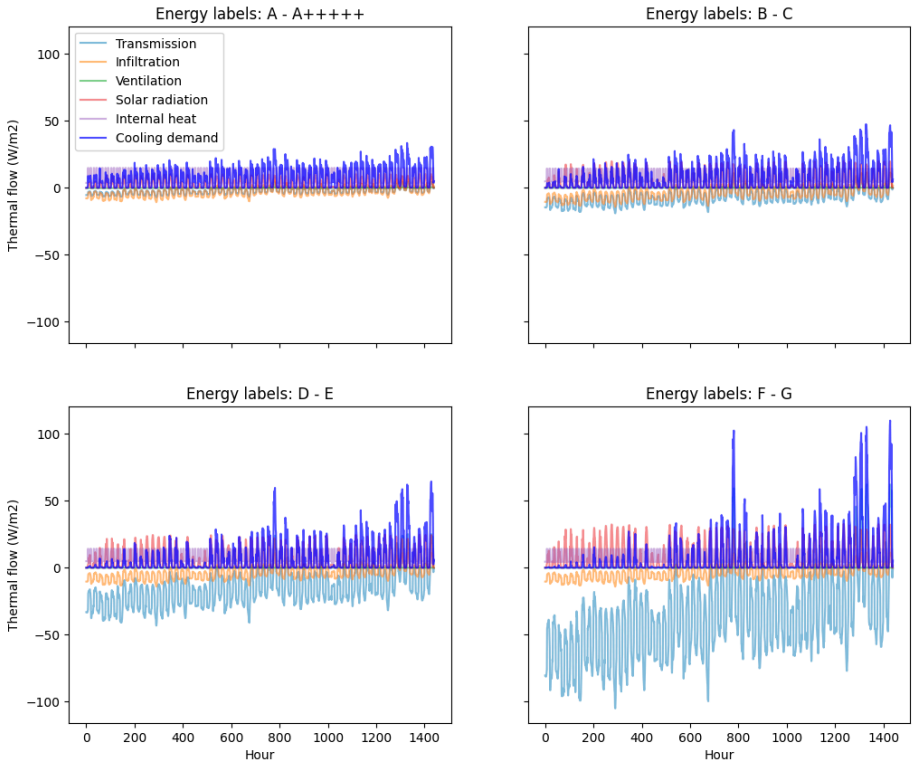

Figure 124: Thermal flows and the resulting cooling demand for buildings in each of the four energy classes in the residential and office building stock, May - June 2019.

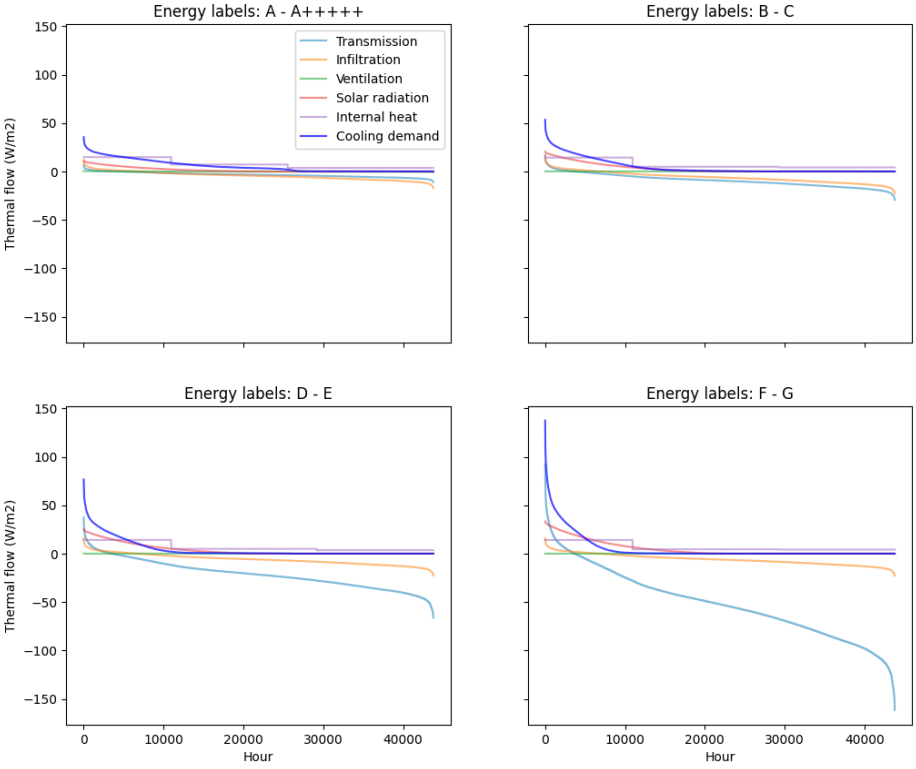

Figure 125: Thermal flows and the resulting cooling demand for buildings in each of the four energy classes, sorted by size across the 2018–2022 reference period.

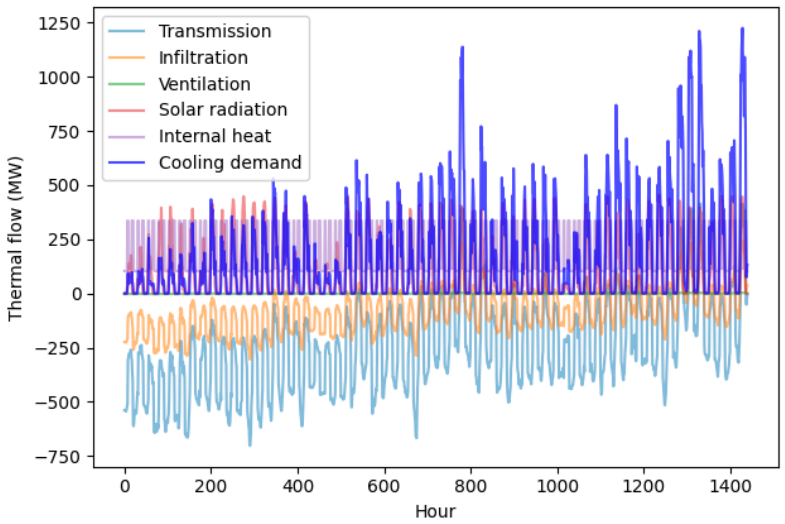

Figure 126: Thermal flows and the resulting cooling demand for the total residential and office building stock in The Hague, May - June 2019.

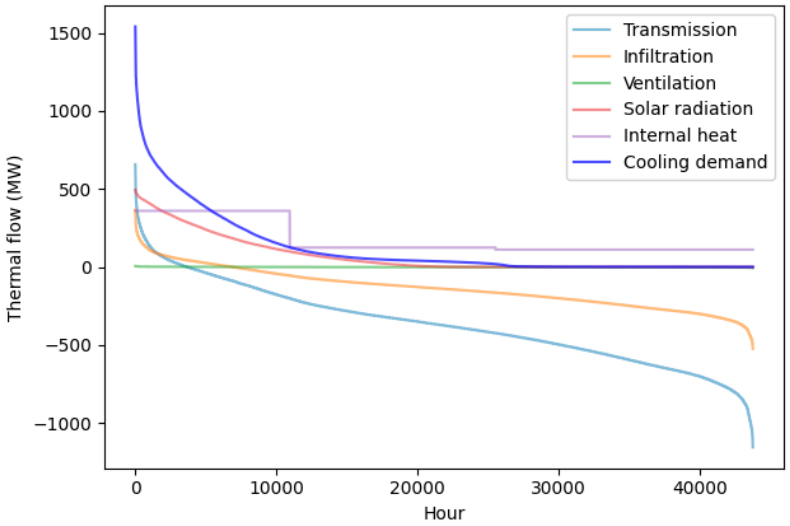

Figure 127: Thermal flows and the resulting cooling demand for the total residential and office building stock in The Hague, sorted by size across the 2018–2022 reference period.

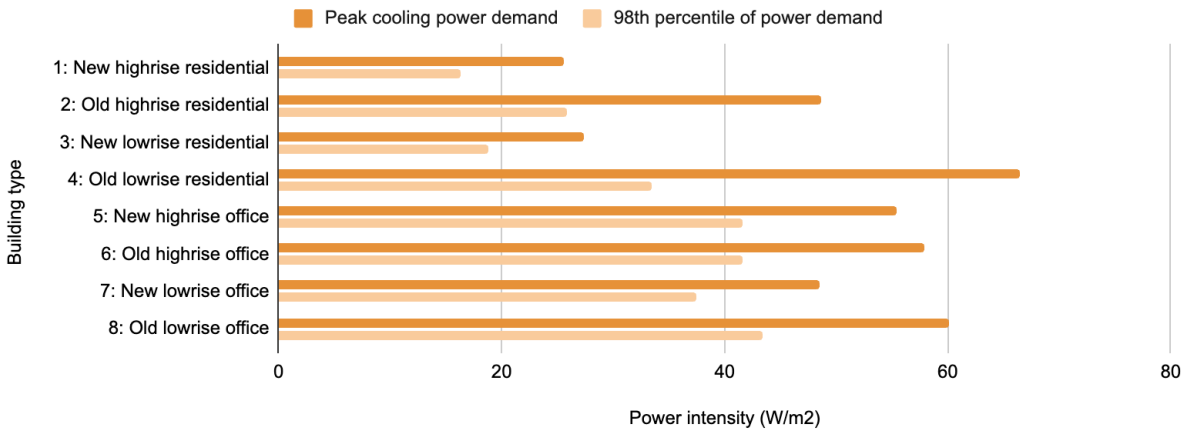

Figure 128: Peak cooling power demand intensity and 98th percentile of cooling power demand intensity for each building type, in the Status Quo (2020) scenario.

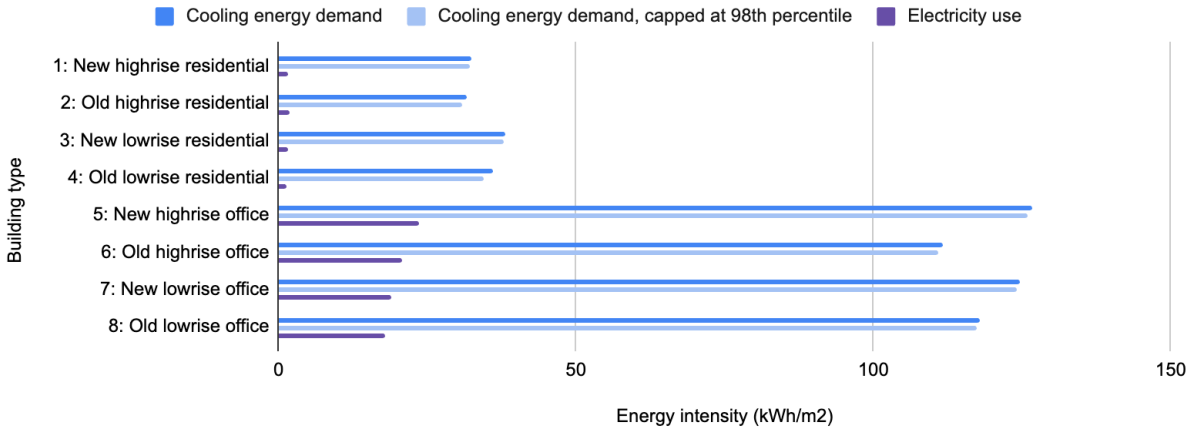

Figure 129: Total and capped cooling energy demand intensity and realized electricity use intensity for each building type, in the Status Quo (2020) scenario.

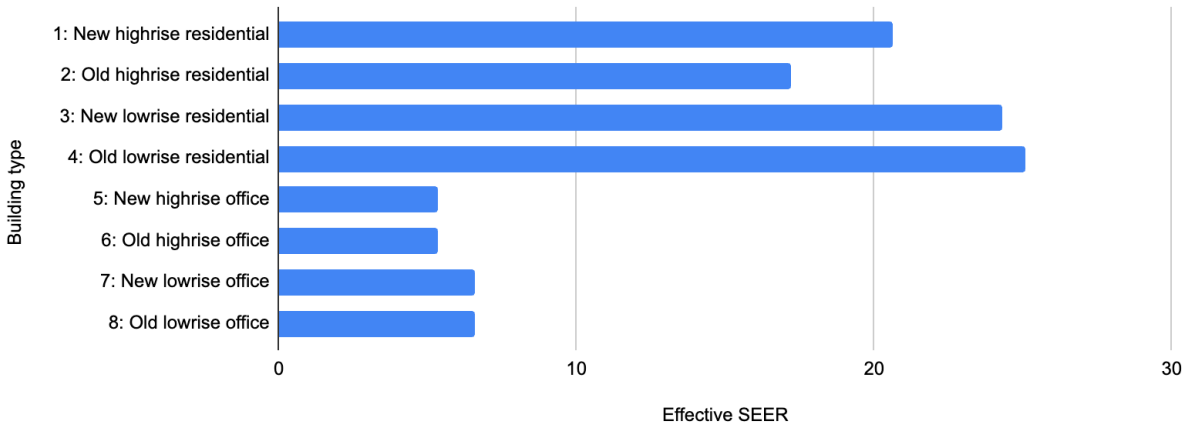

Figure 130: Effective SEER (electricity use per cooling energy demand) for each building type, in the Status Quo (2020) scenario.

Table 75: Life cycle analysis results on ventilation system with heat exchangers.

Product	Product mass (kg)	Production-phase carbon intensity (kg CO_2-eq/kg)	EoL-phase carbon intensity (kg CO_2-eq/kg)	ADP (kg Sb-eq/kg)	CSI (kg Si-eq/kg)
1: central ventilation system, polyethylene ducts	1,410	3.97	0.38	$2.08 \cdot 10^{-4}$	1,352
2: central ventilation system, steel ducts	2,300	4.12	0.19	$3.12 \cdot 10^{-4}$	1,891
3: decentralized ventilation system, polyethylene ducts	1,632	4.23	0.39	$2.25 \cdot 10^{-4}$	1,388
4: decentralized ventilation system, steel ducts	2,522	4.27	0.21	$3.13 \cdot 10^{-4}$	1,868
Average	1,966	4.15	0.30	$2.64 \cdot 10^{-4}$	1,625
Standard deviation	530	0.13	0.11	$5.57 \cdot 10^{-5}$	295

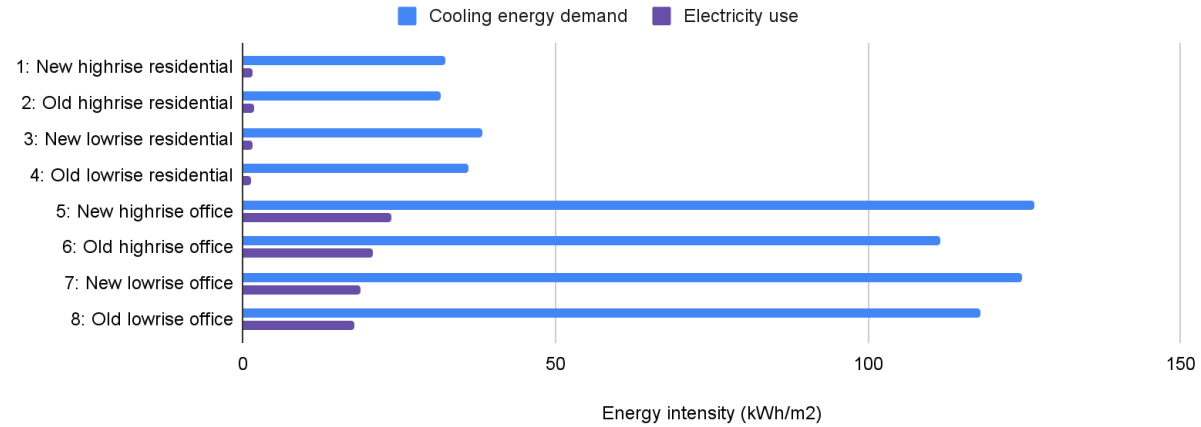

Figure 131: Total cooling energy demand and the resulting electricity use by building type in the Status Quo (2020) scenario.

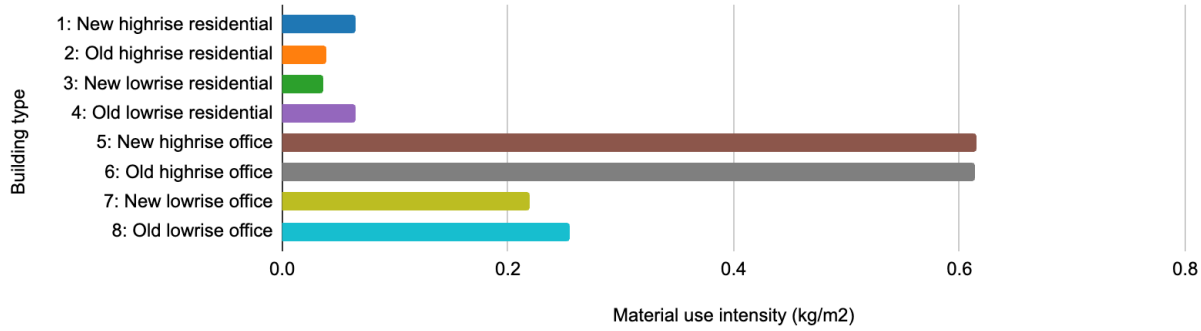

Figure 132: Material use intensity of installed cooling equipment stock by building type in the status quo (2020) model for The Hague.

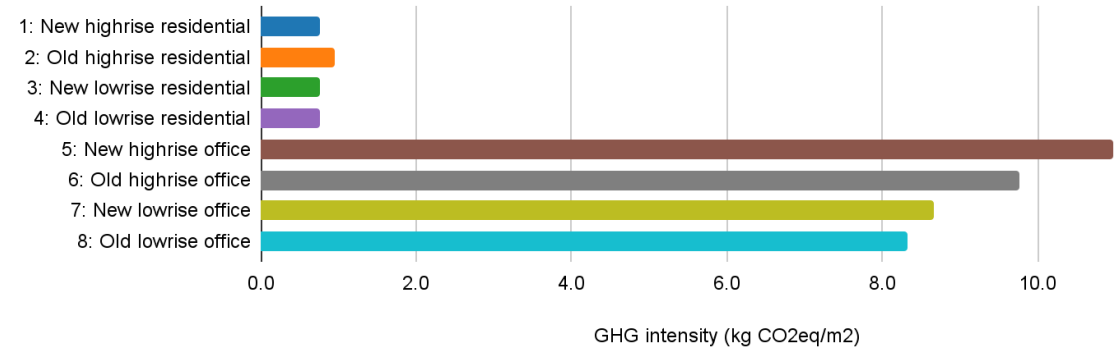

Figure 133: GHG emission intensity per building type in the Status Quo (2020) model.

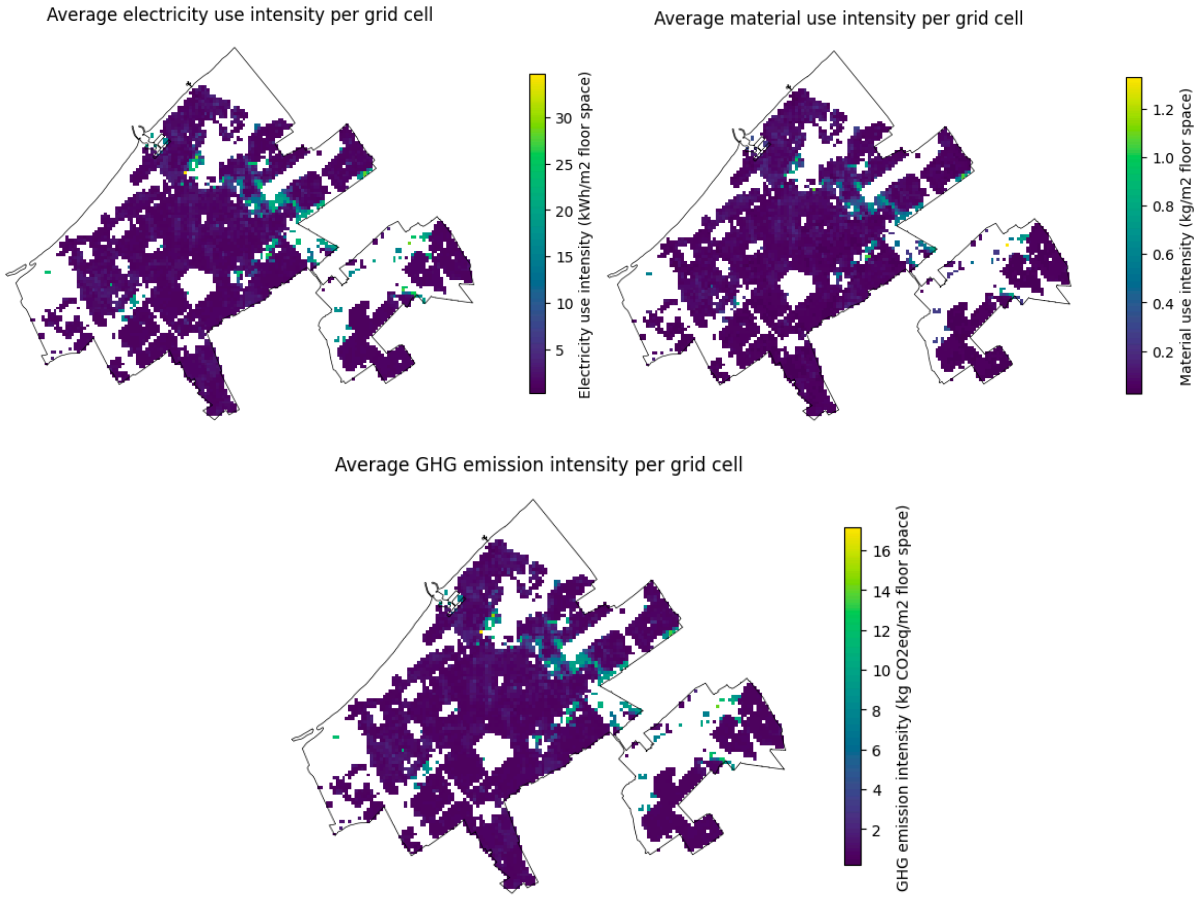

Figure 134: Spatial distribution of environmental impacts of cooling in the Status Quo (2020) scenario.

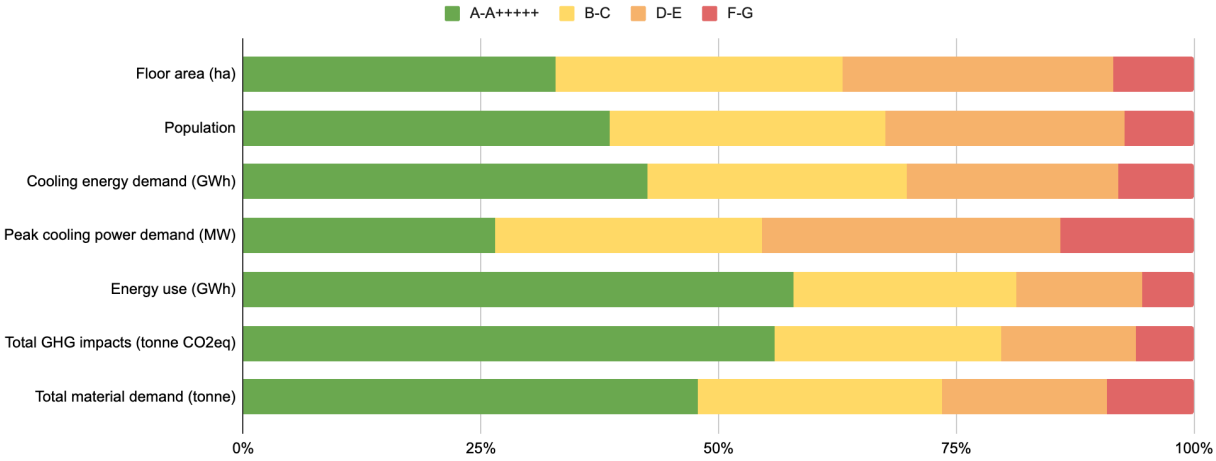

Figure 135: Contribution analysis of energy label classes across key impact metrics in the Status Quo (2020) scenario.

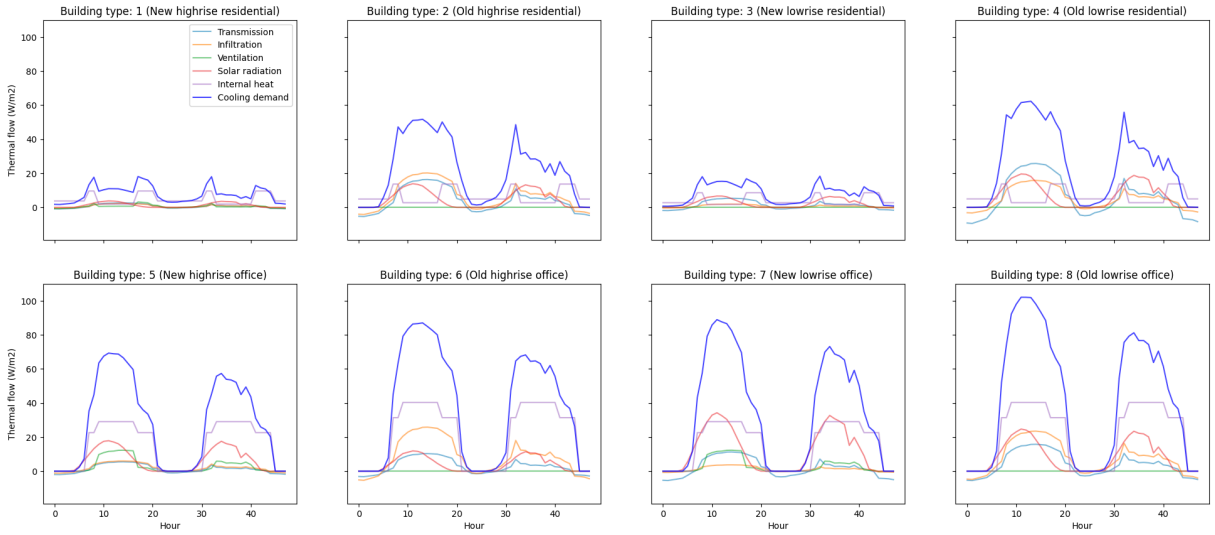

Figure 136: Thermal flows for varying building types during a heatwave, 2030 scenario.

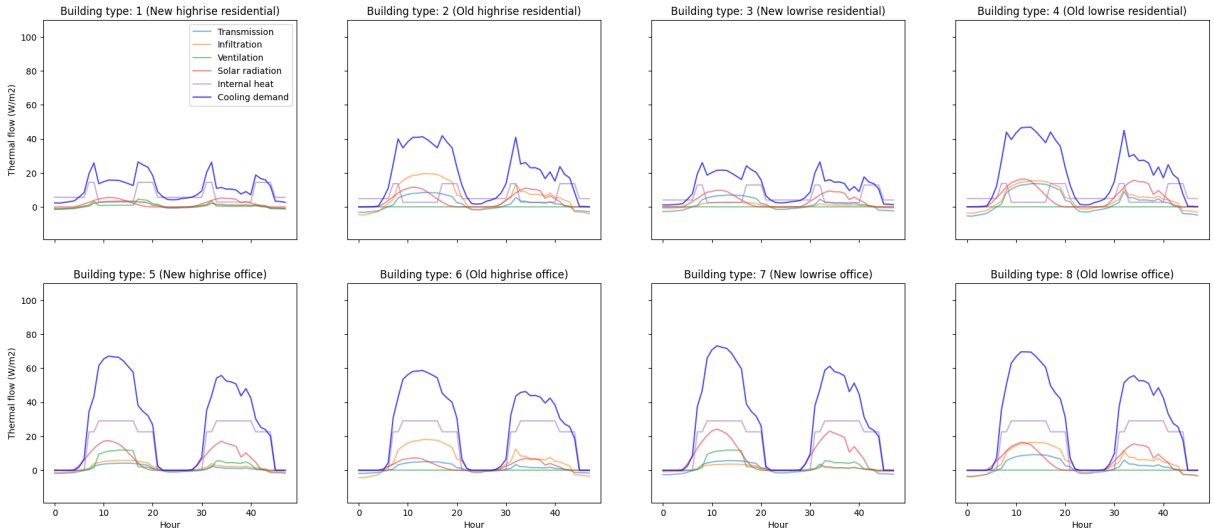

Figure 137: Thermal flows for varying building types during a heatwave, 2050-L scenario.

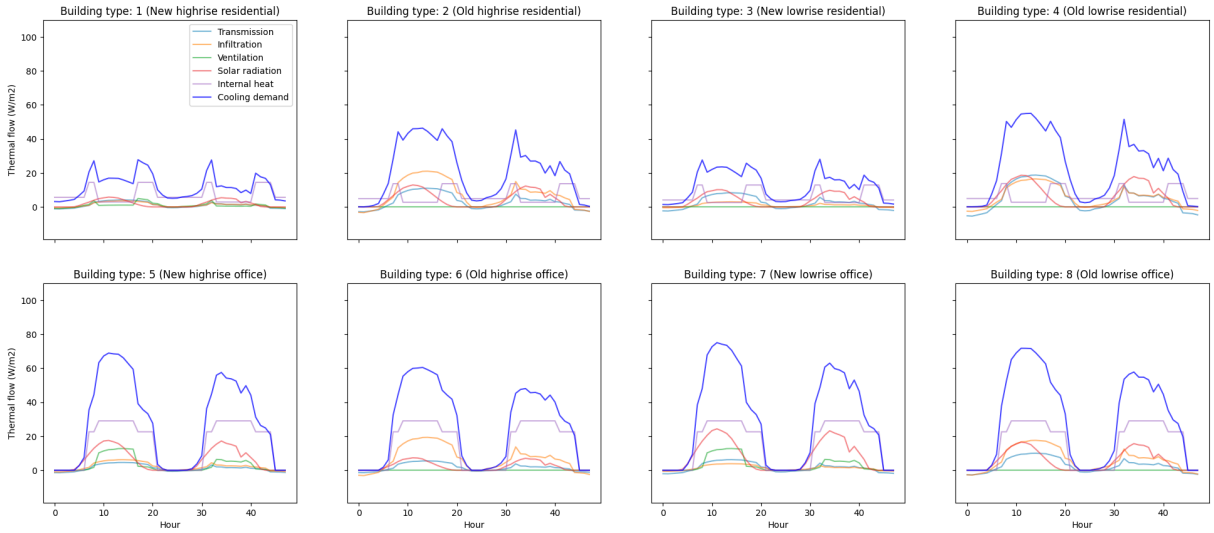

Figure 138: Thermal flows for varying building types during a heatwave, 2050 M scenario.

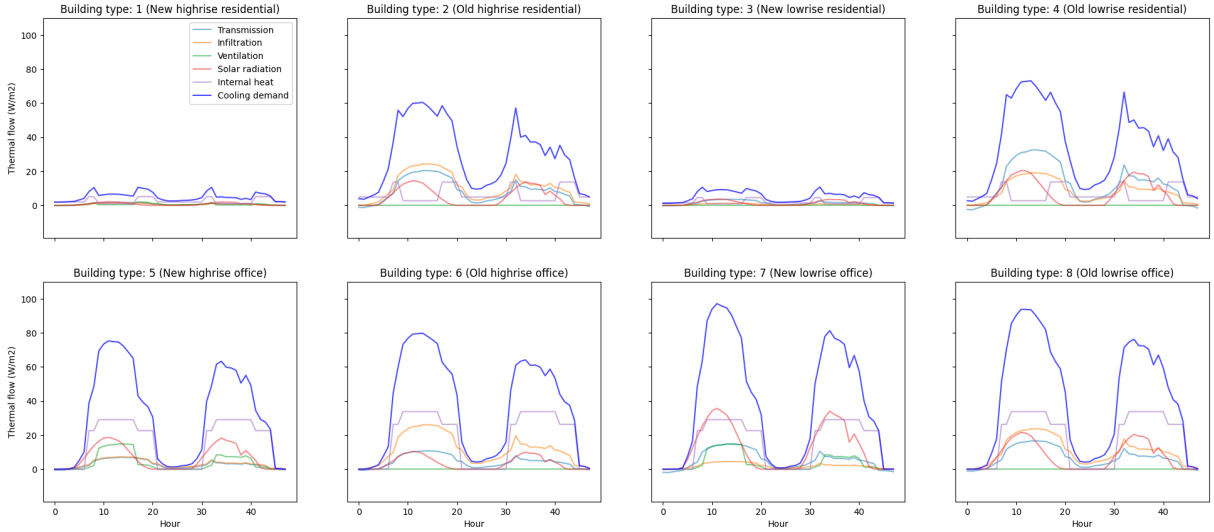

Figure 139: Thermal flows for varying building types during a heatwave, 2050-H scenario.

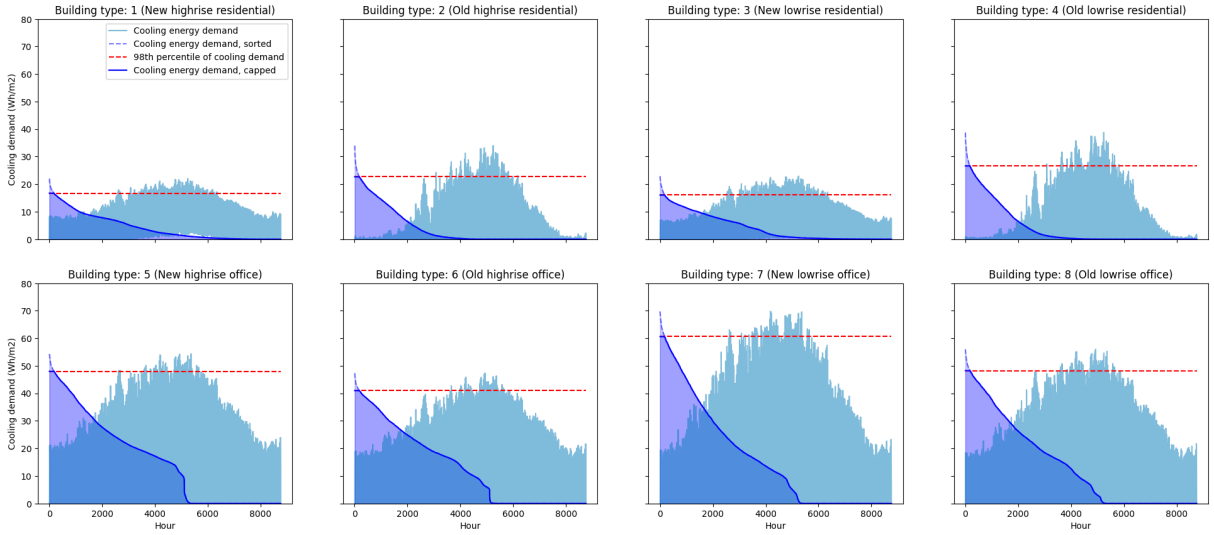

Figure 140: Annual cooling demand load for varying building types, 2030 scenario.

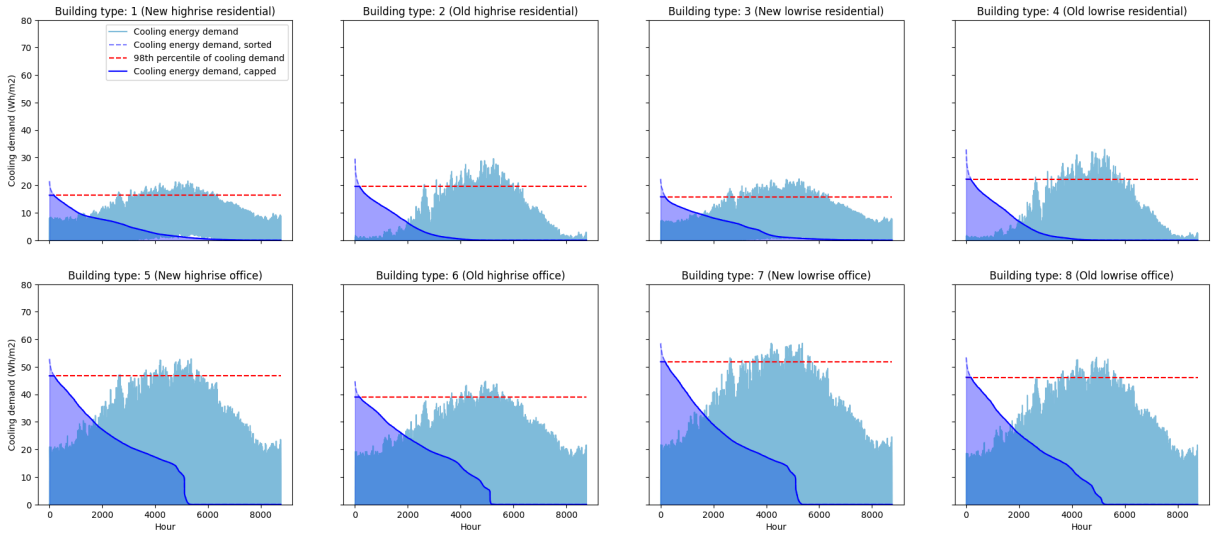

Figure 141: Annual cooling demand load for varying building types, 2050-L scenario.

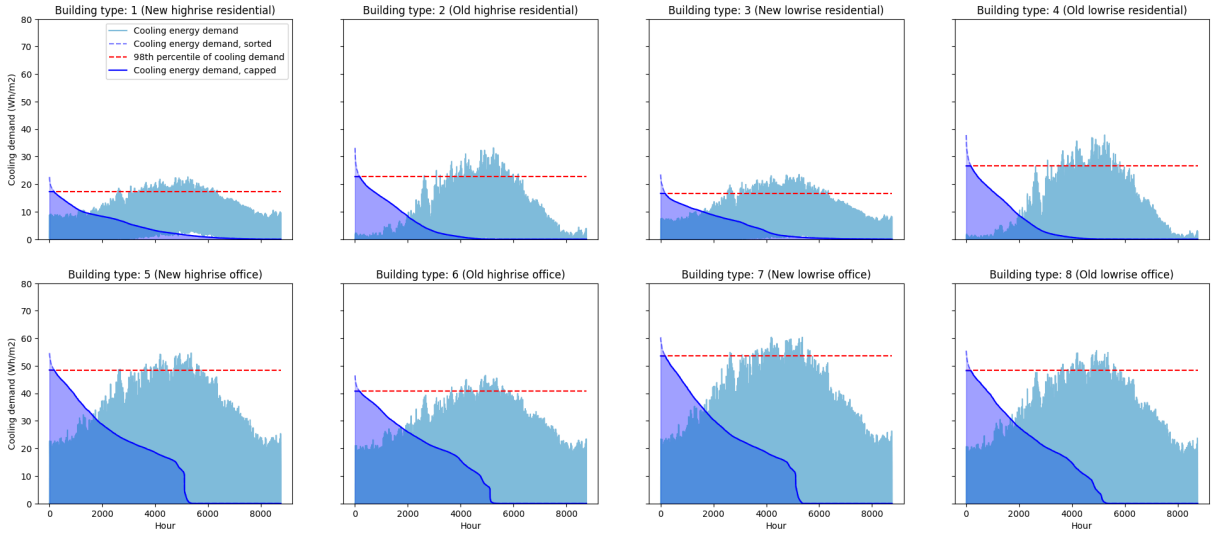

Figure 142: Annual cooling demand load for varying building types, 2050 M scenario.

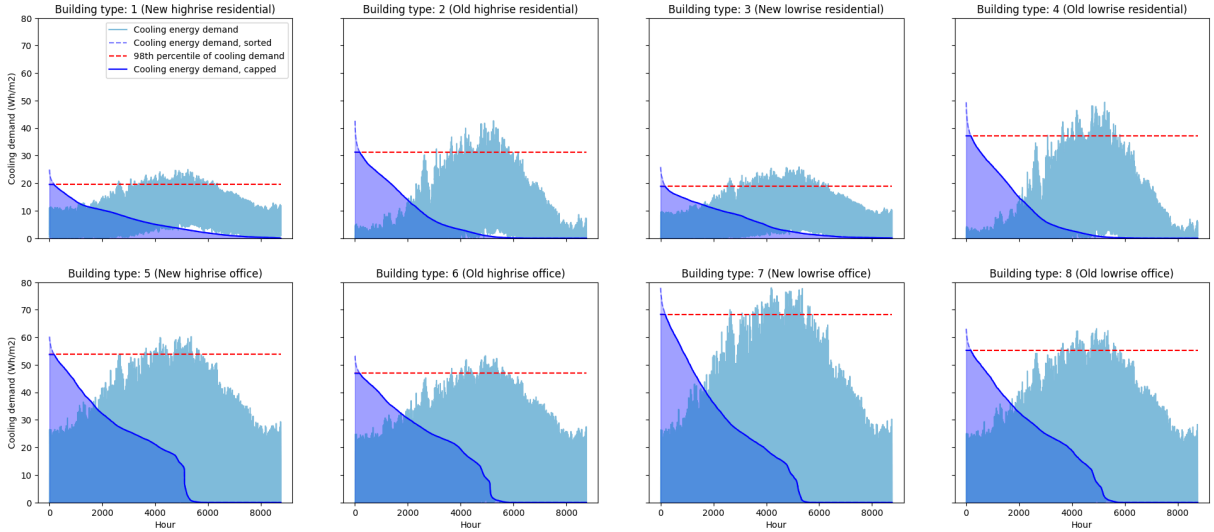

Figure 143: Annual cooling demand load for varying building types, 2050-H scenario.

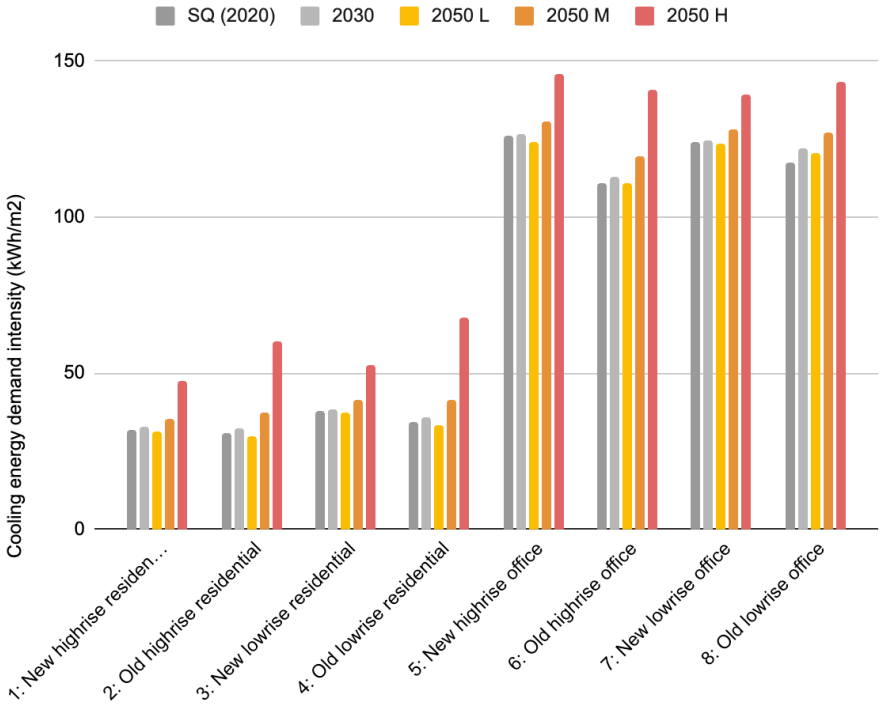

Figure 144: Cooling energy demand intensity (capped) per building type, across scenarios.

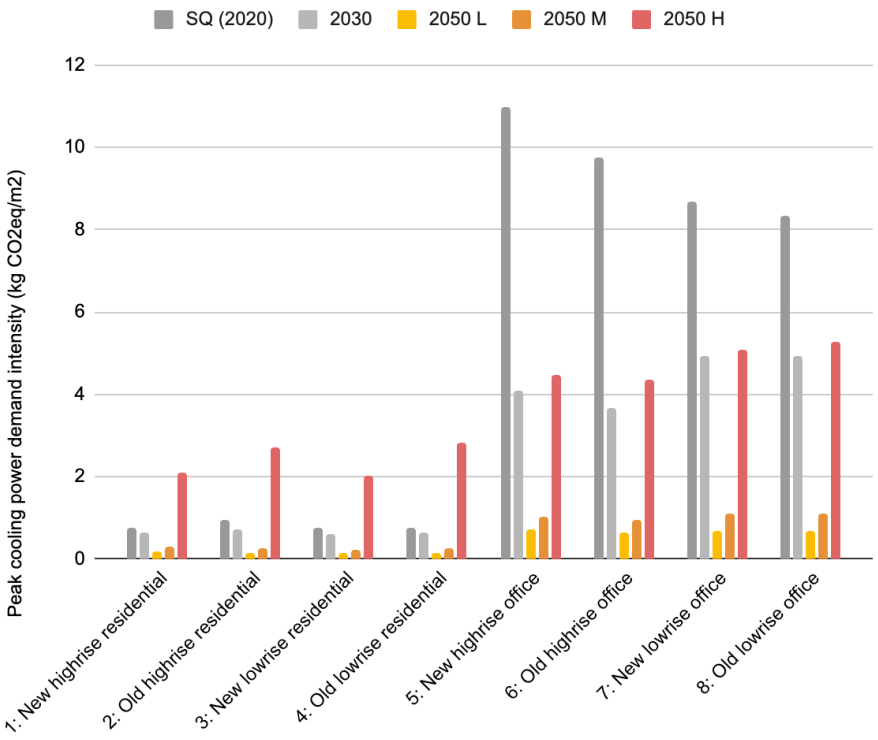

Figure 145: Peak cooling power demand intensity (capped) per building type, across scenarios.

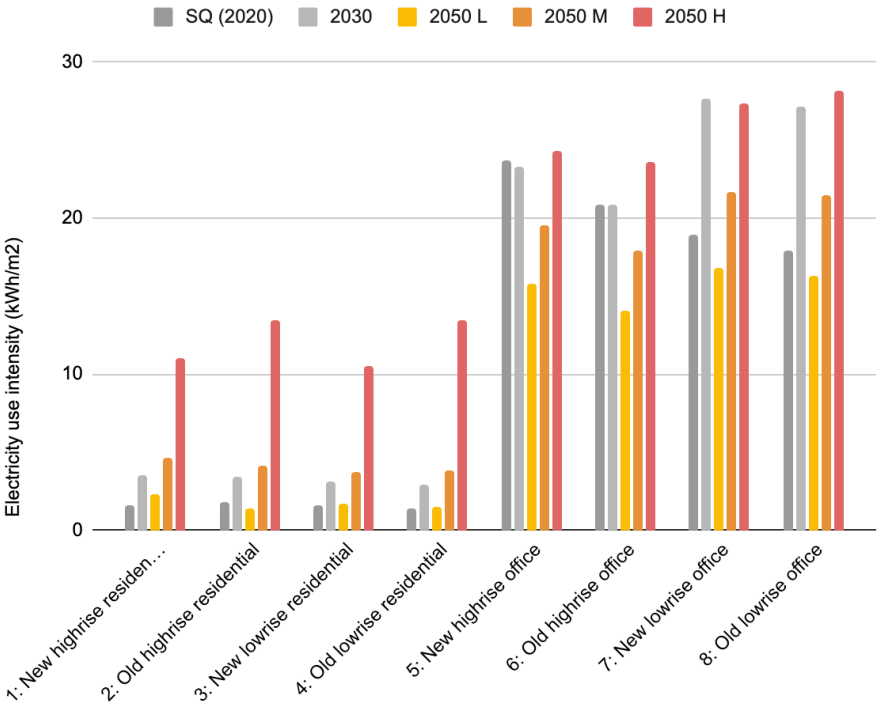

Figure 146: Electricity use intensity per building type, across scenarios.

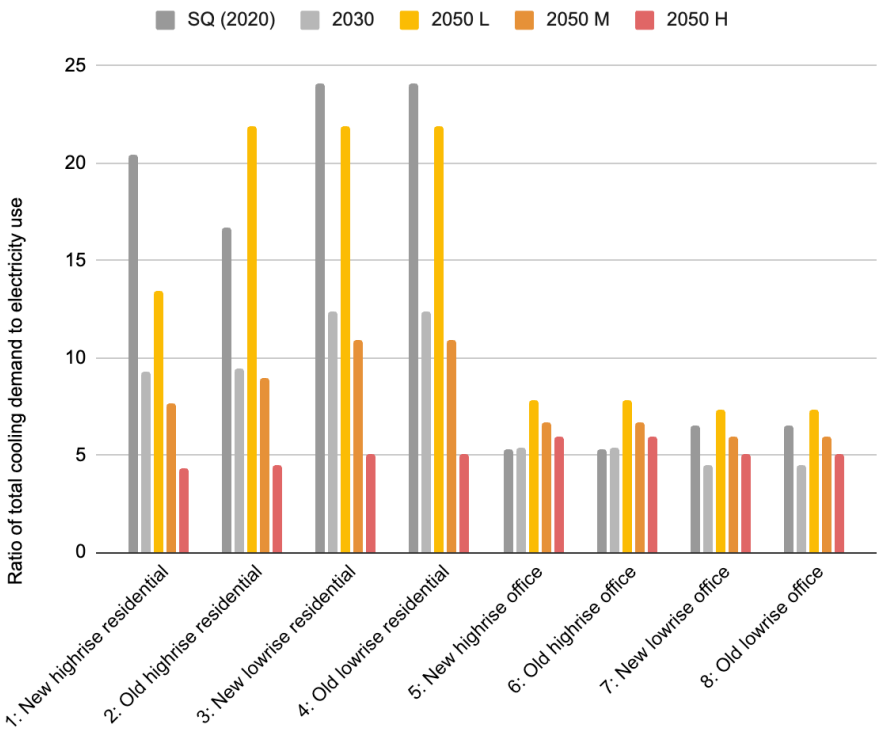

Figure 147: Ratio of total cooling demand to electricity use (effective SEER) per building type, across scenarios.

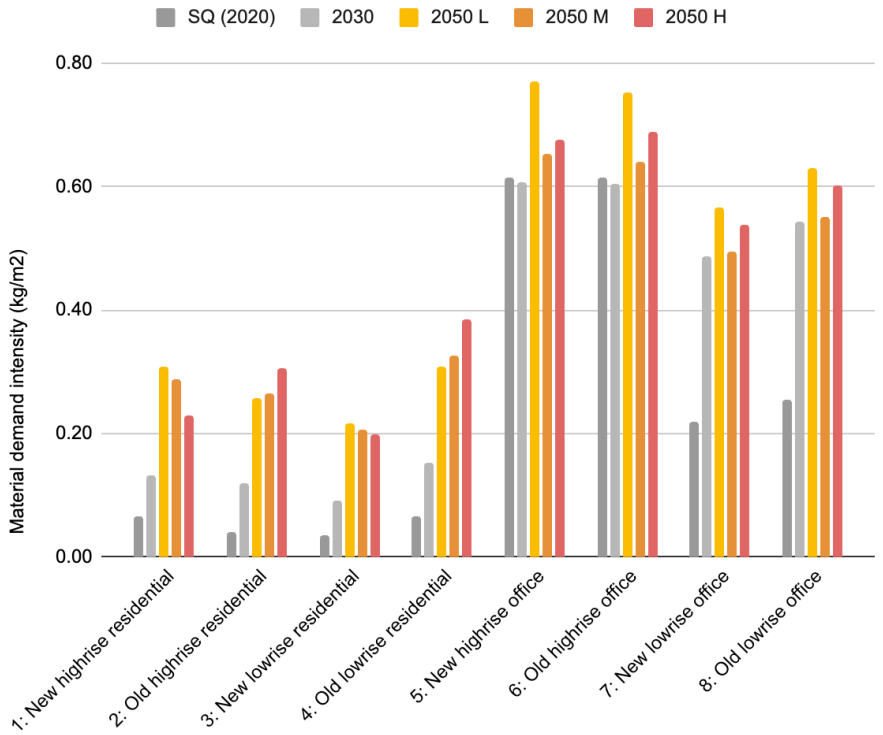

Figure 148: Material demand use intensities per building type, across scenarios.

Table 76: Annualized material demand and related environmental impact metrics of the modeled cooling equipment stock for all scenarios.

Scenario	Material demand (tonne)	ADP (kg Sb-eq)	CSI (kt Si-eq)
SQ (2020)	232	58	365
2030	356	92	576
2050-L	627	164	1,022
2050-M	684	181	1,128
2050-H	824	218	1,361

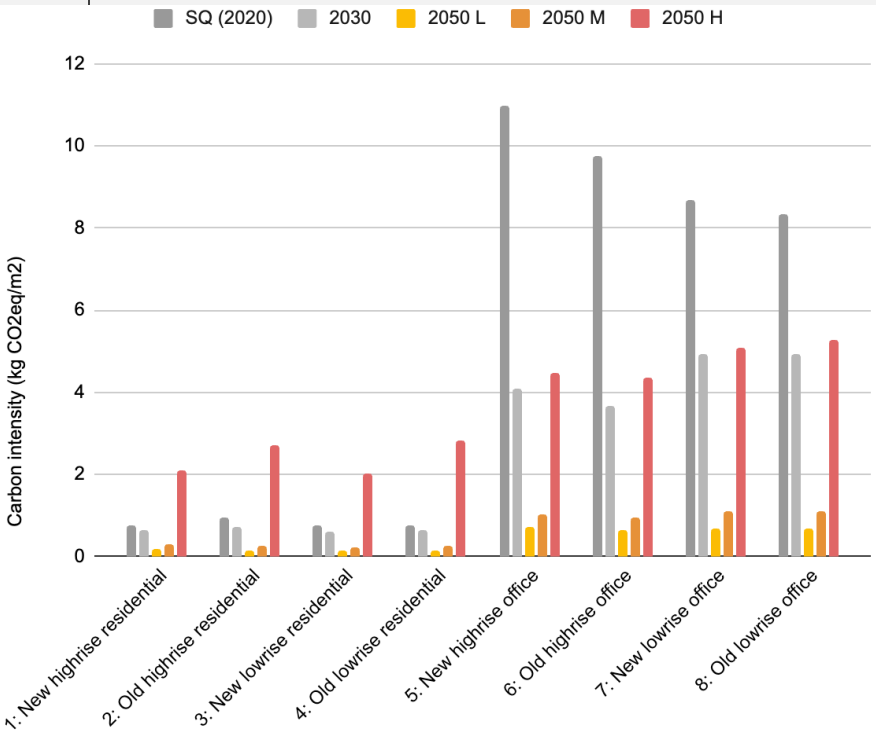

Figure 149: GHG emission demand intensities per building type, across scenarios.

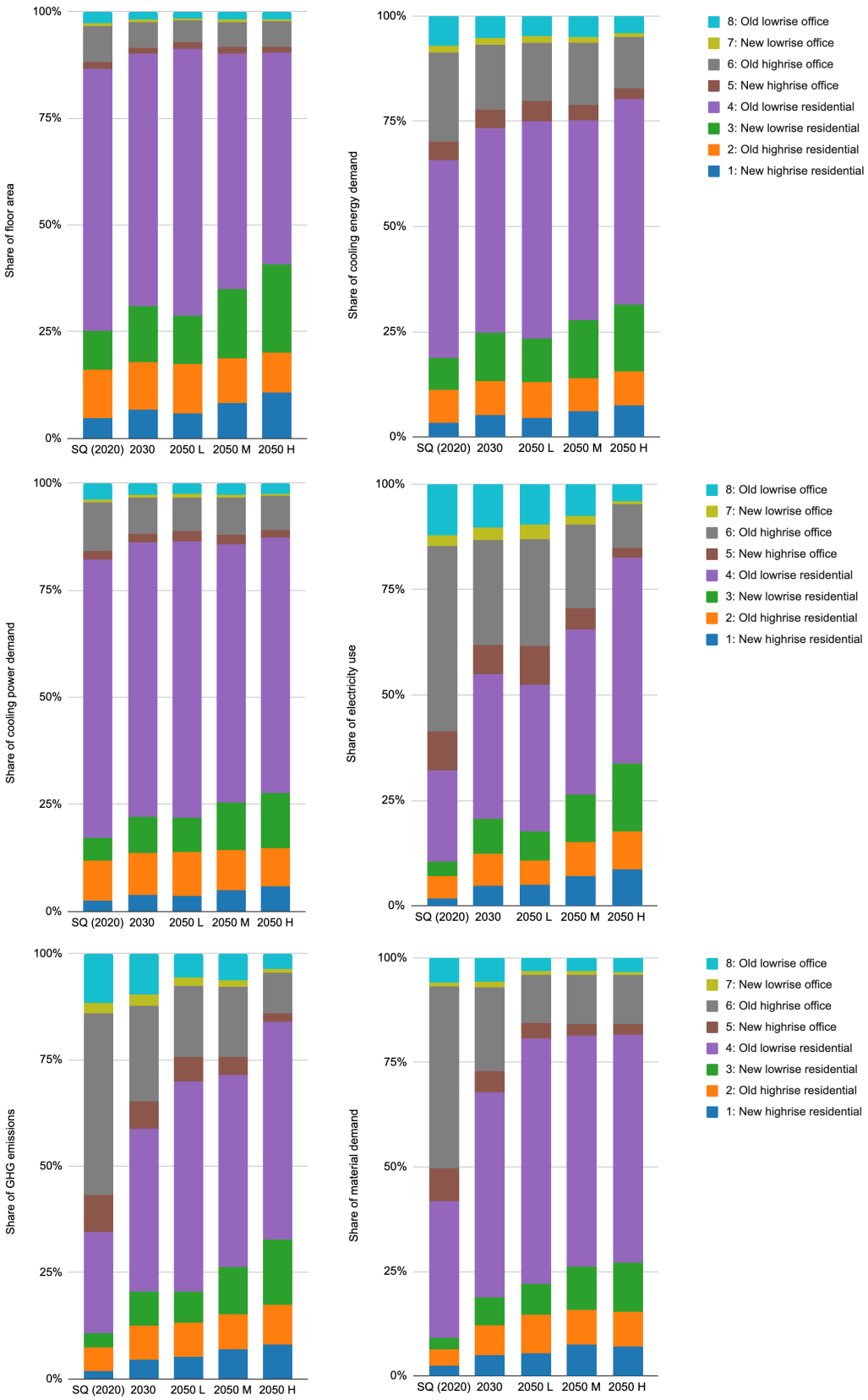

Figure 150: Relative share of building types in floor space and key impact metrics, across scenarios.

Appendix R Detailed Extrapolation Results

This appendix presents the cooling demand and environmental impact for three building stock sets, for each scenario:

- The results for the building stock with energy label data, i.e., the base building subset for which the cooling demand model was used to calculate impacts.
- Extrapolations of the impacts over the building stock lacking energy label data.
- The overall cumulative impacts for the entire residential and office building stock of The Hague.

Table 77: Extrapolation of cooling demand and environmental impact metrics for the residential and office building stock of The Hague.

Building subset	Scenario	Floor area (ha)	Cooling energy demand (GWh)	Peak cooling power demand (MW)	Electricity use (GWh)	GHG emissions (kt CO2-eq)	Material demand (kt)
RO buildings with energy label data (base CDM results)	SQ (2020)	2,478	1,118	1,431	101	48.8	3.00
	2030	2,571	1,127	1,307	129	25.1	4.67
	2050-L	2,429	987	1,030	67	4.74	8.00
	2050-M	2,746	1,334	1,266	148	9.32	8.94
	2050-H	3,062	2,111	1,685	419	83.6	10.7
Buildings without energy label	SQ (2020)	611	280	200	24	11.7	0.693
	2030	629	280	190	32	6.20	1.14
	2050-L	595	245	156	16	1.16	1.95
	2050-M	670	332	197	36	2.27	2,178
	2050-H	743	524	272	102	20.5	2.63
Total residential and office building stock of The Hague	SQ (2020)	3,089	1,398	1,631	125	60.5	3.70
	2030	3,200	1,408	1,497	161	31.3	5.82
	2050-L	3,024	1,232	1,186	83	5.90	9.94
	2050-M	3,415	1,665	1,462	184	11.6	11.1
	2050-H	3,805	2,635	1,956	521	104	13.3